UNIVERSITE DE VERSAILLES SAINT-QUENTIN-EN-YVELINES

CENTRE DE RECHERCHES EN ÉCONOMIE-ÉCOLOGIQUE, ÉCO-INNOVATION ET INGÉNIERIE DU DÉVELOPPEMENT SOUTENABLE (REEDS)

THÈSE DE DOCTORAT

présentée par

Elizaveta KUZNETSOVA

pour l'obtention du

GRADE DE DOCTEUR

DISCIPLINE / SPECIALITE : Eco-innovation

Thèse effectuée sous l'accord de collaboration avec la Chaire Sciences des Systèmes et Défis Énergétique (SSDE), Fondation Européenne pour les Énergies de Demain - Électricité de France (EDF) à l'Ecole Centrale Paris et Supelec, FRANCE

MICROGRID AGENT-BASED MODELLING AND OPTIMIZATION UNDER UNCERTAINTY

soutenue le : 5 Mars 2014

devant un jury composé de :

M. Antonello MONTI, RWTH Aachen University (Rapporteur)

M. Philippe DESSANTE, Supelec (Rapporteur)

Mme. Laetitia ANDRIEU, EDF (Examinateur)

M. Michel MINOUX, Université Paris - 6 (Examinateur)

M. Enrico ZIO, Ecole Centrale Paris / Supelec (Directeur de thèse)

ACKNOWLEDGMENTS

First and foremost, I would like to thank my former PhD supervisor Pr. Keith Culver who convinced me to start this research project and guided me through the first stages. I am grateful to him for introducing me to Pr. Enrico Zio, who became for the last three years my mentor, my motivator and, I hope, my friend. I would like to express my sincere gratitude to Pr. Zio for the continuous support for my PhD research work, for his patience, motivation, enthusiasm, and immense knowledge. Without his guidance, this PhD dissertation would not have materialized. I could not have imagined having a better advisor and mentor for my PhD research.

Besides my supervisor, I would like to thank my PhD thesis committee, president of the jury, Prof. Emeritus Michel Minoux, referees, Pr. Antonello Monti, Assis. Prof. Philippe Dessante, and the industrial representative, Dr Laetitia Andrieu, for their encouragement, insightful comments, and hard questions.

In addition, I received the generous support from my co-supervisors, Dr Carlos Ruiz and Assis. Prof. Yan-Fu Li, who gave me good advices and invaluable support on both an academic and a personal level for which I am extremely grateful.

My sincere thanks also goes to Pr. Graham Ault and Dr. Keith Bell, for offering me the opportunity to spend three months in the Institute for Energy and Environment of University of Strathclyde (Scotland) as a visiting researcher, to work with their research team and to share their experience and knowledge in terms of renewable energy.

I would like to acknowledge Econoving International Chair of University of Versailles Saint-Quentin-en-Yvelines for the financial support, as well as the “Programme Gare” project, of the National Society of French Railways (SNCF) and Econoving International Chair of University of Versailles Saint-Quentin-en-Yvelines, for the collaboration helping in understanding the energy management problematic in France and in developing of relevant case studies.

I offer my sincerest gratitude for technical and administrative support of Laboratory of Industrial Engineering of Ecole Centrale Paris, especially to the head of laboratory Pr. Jean-Claude Bocquet, for their hearty welcome and extremely pleasant working environment.

I thank all my fellow colleagues from the Laboratory of Industrial Engineering of Ecole Centrale Paris for the stimulating discussions and for all the fun we have had in the last three years.

Last but not least, I would like to thank my family: my sister Anastasia Ryzhikova and my mother Olga Kuznetsova for supporting me during all my life. My special acknowledge goes to my husband Adrien Gonzalez, who was my first supporter during my PhD, attentive listener and interested interlocutor.

Special dedication:

To my grandfather, Lev Sedov, who gave me the taste of Engineering

ABSTRACT

This thesis concerns the energy management of electricity microgrids. The scientific contribution follows two directions: *(i)* modelling individual intelligence in energy management under uncertainty and *(ii)* microgrid energy management integrating diverse actors with conflicting objectives. Agent-Based Modelling (ABM) is used to describe the dynamics of microgrid actors operating under limited access to information, and operational and environmental uncertainties. The approaches considered to model individual intelligence in this thesis, Reinforcement Learning and Robust Optimization, provide each agent with the capability of making decision, adapting to the stochastic environment and interacting with other agents. The modelling frameworks developed have been tested on urban microgrids integrating different energy consumers, sources of renewable energy and storage facilities, for optimal energy management in terms of reliability and economic indicators under operational and environmental uncertainty, and components failures.

Keywords: Smartgrids, microgrid, agent-based model, uncertainty, reinforcement learning, robust optimization.

RESUMÉ

Le travail de recherche est axé sur la gestion de l'énergie dans les micro réseaux électriques. La contribution scientifique est ici basée sur: (i) des approches de modélisation d'intelligence individuelle pour la gestion d'énergie sous incertitudes et (ii) la gestion de l'énergie dans un micro réseau intégrant différents acteurs avec des objectifs conflictuels. Les acteurs de micro réseaux, opérant sous un accès limité aux informations et en présence d'incertitudes opérationnelles et environnementales, sont modélisés par une approche orientée agent (Agent-Based Modelling). Les approches considérées pour la modélisation de l'intelligence individuelle dans cette thèse, i.e. l'apprentissage par renforcement (Reinforcement Learning) et l'optimisation robuste (Robust Optimization), attribuent à chaque agent des capacités de prise de décision, d'adaptation à leur environnement stochastique et d'interactions avec d'autres agents. Les méthodes de modélisation développées ont été testées sur des micro réseaux urbains impliquant différents consommateurs d'énergie, des sources d'énergie renouvelable et des moyens de stockage, afin d'optimiser la gestion de l'énergie en termes de fiabilité et des aspects économiques, sous incertitudes opérationnelle, environnementale et de défaillances des composants.

Mots clés: Réseaux intelligents (Smartgrids), micro réseau, approche orientée agent, incertitude, apprentissage par renforcement, optimisation robuste

CONTENTS

Part I

Part II

Paper I

E. Kuznetsova, C. Ruiz, Y. F. Li, E. Zio, G. Ault, and K. Bell, "Reinforcement learning for microgrid energy management," Energy, vol. 59, pp. 133–146, 2013.

Paper II

E. Kuznetsova, Y.-F. Li, C. Ruiz, and E. Zio, "An integrated framework of agent-based modelling and robust optimization for microgrid energy management," Applied Energy, vol. 129, pp. 70 – 88, 2014.

Paper III

E. Kuznetsova, Y.-F. Li, C. Ruiz, and E. Zio, "Analysis of robust optimization for decentralized microgrid energy management under uncertainty," Submitted to Electrical Power and Energy Systems, pp. 1 – 46, 2013.

ACRONYMS

ABM	Agent-Based Modelling
DSCS	Dynamic, Stochastic, Computational and Scalable technologies
CI	Computational Intelligence
RL	Reinforcement Learning
PI	Prediction Interval
NN	Neural Network
NSGA-II	Non-dominated Sorting Genetic Algorithm
RO	Robust Optimization
ISO	Independent System Operator
MIS	Market Information System
TS	Train Station
D	District or local community
WPP	Wind Power Plant

NOMENCLATURE

t time step *(h)*,

F_t^{pas} passengers flow through TS at time *t (number/h)*,

s_t average solar irradiation at time *t* (W/m^2),

E_t^l energy required for inside and outside lighting in the TS at time *t (kWh)*,

E_t^{elev} energy required for passengers lifting in the TS at time *t (kWh)*,

E_t^{elec} energy required for electronic equipment in the TS at time *t (kWh)*,

E_t^{TS} total hourly required energy in the TS at time *t (kWh)*,

P_t^{PV} available energy output from the PV generators installed in the TS at time *t (kWh)*,

S_t^{TS} portion of energy purchased from the external grid by the TS (*kWh),*

L_t^{TS} portion of energy sold to the external grid by the TS *(kWh)*,

V_t^{PV} portion of energy sold to the D and generated by the PV panels of the TS *(kWh),*

R_t^{TS} and R_{t-1}^{TS} energy levels in the TS battery at time *t* and *t-1 (kWh),*

$R^{TS,stor}$ energy portion that the TS battery is capable of charging or discharging during time *t (kWh)*,

$\delta_t^{TS,ch}$ and $\delta_t^{TS,dis}$ binary variables which model that the TS battery can either only be charged or discharged at time *t*,

$R^{TS,max}$ the maximum TS battery charge *(kWh)*,

T time period considered for the optimization *(h)*,

α^{TS} total costs for TS for time period *T (€)*,

c_t^p and c_t^s average hourly costs of purchasing and selling one *kWh* from the external grid, respectively, at time *t* (*€/kWh*),

c_t^D average hourly cost per *kWh* from the bilateral contract agreed with D at time *t (€/kWh),*

β coefficients defining the minimum amount of energy to be sold to D by TS,

$\tilde{E}_t^D$ expected energy demand for D at time step *t*, predicted by TS (*kWh*),

$\hat{E}_t^{TS}$ level of uncertainty in TS energy demand quantified for the robust optimization at time *t (kWh)*,

$E_t^{TS,ub}$ and $E_t^{TS,lb}$ upper and lower prediction bounds of TS energy demand at time *t*, respectively *(kWh)*,

τ simulation time period composed of *Ns* time steps of one hour *(h)*,

time step *(h)*,

D_t consumer load over the time interval *(Wh)*,

P_t electricity market price at time *t (\$/Wh)*,

P_t^{wt} available power output from the wind generator over the time interval Δt *(Wh)*,

R_t level of battery storage at time *t (Wh)*,

λ, μ failure and repair transition rates at normal wind speed conditions *(h^{-1})*,

λ', μ' failure and repair transition rates at extreme wind speed conditions *(h^{1})*,

i, *n*, *p* indexes of system states,

s_t^i system state of index *i* at time *t*,

a_t^j action at time *t*,

l index of generic scenario composed of $[s_t^i,\ s_{t+1}^n,\ s_{t+2}^p]$ system states at time steps *t*, *t+1* and *t+2*,

$Scenario_t^l$ generic scenario of index *l* at time *t*,

A_t^j sequence of actions of index *j* composed of $[a_t, a_{t+1}, a_{t+2}]$ at time steps *t*, *t+1* and *t+2*,

$r(s_t^i, a_t^j)$ reward value received as the result of taking action a_t^j in state s_t^i at time *t*,

$Q(s_t^i, a_t^j)$ value function of the state-action pair (s_t^i, a_t^j),

$r(Scenario_t^l, A_t^j)$ total discounted truncated reward for the sequence of actions A_t^j performed under the $Scenario_t^l$,

γ discounted factor taking values within the range of [0,1],

α learning rate taking values between 0 and 1,

J_i set of coefficients, which are subject to uncertainty, in row *i* of the matrix A,

a_{ij} expected value of the parameter,

$\hat{a}_{ij}$ uncertainty interval width of the uncertain parameter

η_{ij} random variable associated with the uncertain data $\tilde{a}_{ij}$,

Γ_i parameter, taking its values in the interval $[0, |J_i|]$, used to adjust the level of robustness of the proposed solution,

p_{ij}, y_j and z_i RO variables forced to be greater than or equal to zero,

z_t^{Power}, z_t^{Cost}, z_t^{Micro}, $p_t^{P_t^{PV}}$, $p_t^{E_t^{TS}}$, $p_t^{c_t^p}$, $p_t^{c_t^s}$, $p_t^{c_t^D}$, $y_t^{P_t^{PV}}$, $y_t^{E_t^{TS}}$, $y_t^{c_t^p}$, $y_t^{c_t^s}$ and $y_t^{c_t^D}$ RO variables in the methodological application forced to be greater than or equal to zero,

x_t^{n+1} and x_t^{n+2} auxiliary RO variables forced to be equal to one,

Γ_t^{Power} and Γ_t^{Cost} level of uncertainty considered in each optimization model of the methodological application ,

$\hat{E}_t^{TS}$ uncertainty in energy demand of TS,

$E_t^{TS,ub}$ and $E_t^{TS,lb}$ upper and lower prediction bounds of energy demand at time *t*, respectively *(kWh)*.

1. INTRODUCTION

The research of the present PhD thesis consists in the methodological development of modelling and optimization solutions for the novel concept of intelligent electricity grids, the so-called Smart grids, and in particular their deployment for the integration of distributed generation in city grids. The introduction to the research is presented below as follows. Section 1.1 recalls the major challenges of conventional electricity grids, in particular related to the diversification and massif integration of distributed generation sources into down-stream electricity grids. The Smart grids paradigm for addressing these challenges is introduced in Section 1.2. Section 1.3 provides the statement of the research problems in the context of Smart grids and maps the methods applied to find the responses. Finally, Section 1.4 presents the structure of the thesis.

1.1. Research motivations

1.1.2. Challenges in conventional power grids

Current energy production is largely reliant on fossil fuels, up to 69%[1] in the global energy mix [1], with implications on global greenhouse gas emissions exacerbating the effects of climate change, contributing 41% of global GHG emissions[2] [2]. The reliance on nearing depletion fossil fuels resources [3], [4] as a single source of energy production is unsustainable as the growing global population demands more energy, predicted to rise of 49% until 2035 [5].

The main criticality of current energy systems lies in their conventional centralized architecture. Environmental issues and the increase of energy demand are challenging the traditional ways of energy generation and distribution systems, whose architecture is organized in a strong hierarchical infrastructure with only few centralized electricity transmission channels from energy producers to load consumers under unidirectional power flow and vertical control and operation. This centralized hierarchical structure is widely used in the design of engineering systems and presents a relatively transparent system organization with clearly identifiable elements of topology, purpose and control which supply organizational advantages and facilitate system monitoring, fault detection and correction [6]. Undoubtedly, the current electricity architecture defines clearly the

[1] Accounts for coal (40%), natural gas (24%) and liquid fuels (5%) in 2010
[2] For electricity and heat generation in 2010

authority domain and the role for each actor on the energy market, as well as operation and interaction modes between the diverse elements.

The major vulnerability of centralized architecture electricity grids comes from their scale-free organization standing on a limited number of highly connected nodes of production sources and few unidirectional transmission channels through which cascading failure propagation may occur in the absence of bypass transmission [7]–[9].

1.1.3. Diversification and integration of distributed energy sources and related challenges

The energetic and environmental challenges of the 21st century drive the development and adoption of new energy sources for meeting several success criteria [10], [11]. The 'low carbon', ideally renewable, energy sources are fostered for improving the environmental performance of the energy industry while overcoming resource scarcity and meeting the increasing demand. At the same time, diversity of energy sources is expected to contribute to the resilience of energy systems.

The most widely used renewable energies at present can be divided into two major groups: hydropower systems and other renewable energies, e.g. solar, wind, geothermal, biomass and ocean (in majority wave and tidal power) energy production systems. The total renewable share of world electricity generation represents 21% [1]. Currently hydropower, including small and micro hydro-systems, is the dominant means of low carbon energy production with the share of 81% from total world renewable electricity generation in 2010 [1]. The second largest renewable generation is represented by wind power with the share of 8% from total world renewable electricity generation in 2010 [1]. Other experimental renewable energies, such as osmotic or salinity gradient power [12] and microbial fuel cell [13], are beginning to become available, although the technology is less developed and deployment is limited.

On the other hand, global installed capacity of renewable energy has grown very rapidly – up to 31.7% growth for wind power [14], up to 50% for PV solar energy [15], up to 50% for wave and tidal power [16] and up to 20% for geothermal energy between 2005 and 2010 [17].

Moreover, the current expansion of the renewable power capacity is driven by new energy policies and local incentives offered in order to face the energetic and environmental challenges of the 21st

century. Thus, the Renewable Energy Directive[3] sets a target of a 20% share of renewable energy to be achieved by 2020 [18] and the European Council counts on renewable energy generation playing a major role in achieving the long-term objective of 80-95% CO2 emissions reduction by 2050, with the 20% target likely to be achieved and even surpassed by 2020 [18].

The exploitation of renewable resources poses a new set of technological challenges to conventional transmission and distribution grids. Besides the availability of the renewable energy sources, which imposes geographical constraints on generation, local weather conditions and seasonal changes give them a character of 'intermittency' in contrast to the 'always-on' fossil or nuclear generation. The intermittent characteristic causes problems for their efficient and reliable management and calls for supplemental electricity generation to avoid power grid unreliability and instability in the presence of large-scale integration of renewable energy sources. This can lead to considerable increases in the cost of electricity. The intermittency of solar and wind energy makes them unsuited for base-load and peak demand without high-capacity energy storage systems to feed the electricity grid during peak demand. The forecasting error for energy generation from wind farms is up to 29% for 48 hours in advance depending on different forecasting models [19]. Based on these uncertainties, renewable energies need a large margin of backup electricity generation capacity, e.g., up to 3:1 wind to fossil fuel ratio in order to ensure power demand [20].

1.2. Smart grids – intelligent infrastructures

The paradigm to address the challenges of renewable energies integration in the distribution grids is the implementation of new emerging intelligent infrastructures, i.e., Smart grids, which are expected to improve coordination of energy generation by diverse energy sources, transmission and distribution efficiency to meet increasing demand, protection and resilience against vulnerabilities of aging and failing components, natural disasters and human attacks. At regional, national and world levels, Smart grid research, development and demonstration are showing the possibility of creating interconnections among energy infrastructure elements, such as producers

3 Directive 2009/28/EC Directive 2009/28/EC of the European Parliament and of the Council of 23 April 2009 on the promotion of the use of energy from renewable sources and amending and subsequently repealing Directives 2001/77/EC and 2003/30/EC.

and consumers, with intelligent management of the electricity balance in the grid [21]. According to [22], Smart grids are expected to reduce up to 5 – 9 % of GHG emissions on their own and up to 18 % reduction of GHG emissions may be possible via further enhancement of Smart grids with complementary technologies. Eventually, Smart grids can offer a substantial contribution to the development of renewable energy systems for responding to increased demand with improved efficiency and resilience against anticipated effects of climate change.

Current Smart grids concept definitions mainly focus on the final intelligent characteristics of the grids, rather than on means and strategies by which these characteristics could be achieved [23]–[26]. Smart grids solutions in the United States are focused mainly on reinforcement of power systems reliability for avoiding large electricity blackouts by means of improved fault localization and isolation capability [26], [27]. Smart grids in Western Europe are looked at within the actual power infrastructure portfolio for accommodating large volumes of renewable sources together with inflexible power sources, e.g. nuclear power plants, for efficient management and use of electricity power inside competitive markets and reduction of conventional electricity [28].

As a further challenge, Smart grids will need to enable integration and management of the unconventional micro generation plants (small wind farms, heat pumps, storage facilities etc.) and consumption loads (electrical vehicles), which were not accounted for in the original power infrastructure design and whose wide penetration could affect in unforeseen ways the operation of the power system.

Finally, Smart grids imply the integration of different innovative technologies into an engineered complex system of interconnected networks. Chapter 2 provides the analysis of such system from the point of view of complexity characteristics.

1.3. Current developments and thesis orientation

This Section narrows the discussion about intelligent infrastructure of Smart grids through the analysis of features expected from their integration and operation. To illustrate the development of Smart grids technologies for efficient energy management a short review of recent works is provided in this section.

The intelligent features expected from the Smart grids were anticipated and stated at the stage of the early development of the intelligent energy infrastructures concept by the USA Congress in 2007 [29]. The basic functions of these intelligent infrastructures, recalled by [30], are follows:

- increase transmission and distribution efficiencies;
- ensure protection and resilience against vulnerabilities;
- dynamic management of energy generation sources;
- hold self-healing capabilities;
- adaptive learning and evolution;
- fault tolerance and attacks resistance.

Since this first statement about Smart grids features, the list has been enlarged or updated based on the specificities of interested country, i.e., geographical location, electricity grids architecture, legislation etc. However, the backbone of the key features of Smart grids was kept unchanged and selected by different research institutions and industrial companies as the guidance for the progressive development of new engineering approaches able to address these features. By analysing these basic Smart grids features, the parallel can be done between Smart grids and complex system. Indeed, some of the discussed features, e.g., dynamic behaviour, dynamic learning and evolution, self-healing, are the characteristics proper to complex systems. In order to build the overall view on the Smart grids giving the reason to the developments done in this thesis, Chapter 2 provides the characterization of electricity Smart grids as complex systems.

The increase of Smart grids complexity traduced in the diversification of grid actors, their interconnections and objectives, as well as their operational environment, drives the development of energy management domain. On the one hand, this development enlarged the boundary of energy management domain by embracing new disciplines and approaches for efficient energy management, e.g. demand-side management concept, first introduced in 1977 at [31], founds his application at the era of Smart grids with the development of information and communication technologies. On the other hand, the individual disciplines, such as forecasting, became the strong research pillars requiring the specific expertise for the development of the cutting edge approaches. These forecasting approaches must ensure the support to the energy management domain, e.g., by providing the reliable forecast of renewable energy production for different terms.

Figure 1 presents the simplified cartography of energy management domain with its major pillars and interconnections, exemplified by the latest developments.

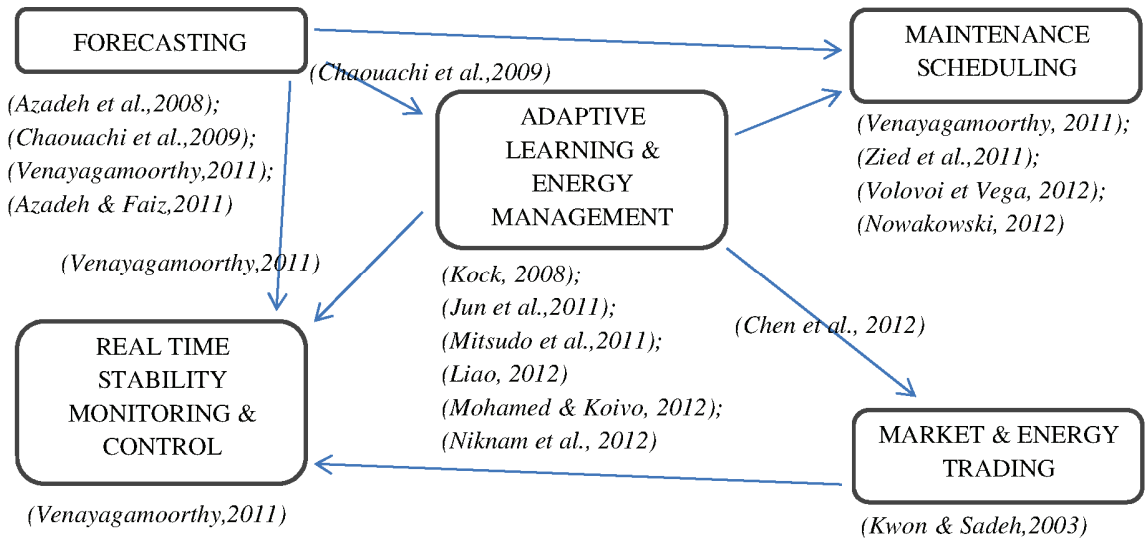

Figure 1. Cartography of energy management disciplines.

In this view, the recent developments in energy management domain contribute to the specific pillars, e.g., forecasting and adaptive learning, but also investigation of joint areas and their interconnections. The exemplification and analysis of the energy management approaches is done below.

Most existing works focus on the development of methods of optimization to achieve the largest benefits from the operation of microgrids involving various distributed generation sources, i.e., wind turbines, photovoltaic (PV) panels, fuel cells, micro turbines, consumption units and battery storages. The optimization goals of the benefits of operation are mathematically translated in objective functions accounting for the various system performance parameters, e.g., operation, maintenance, fuel consumption and GHG emission costs etc. Physical constraints limit the feasible solutions in terms of power flow constraints, minimum and maximum on/off time of power generators, real power generation capacity, energy storage limits etc. The optimal solutions are usually considered on a 24-hours energy management horizon. The input data for the case studies used to demonstrate the different optimization methods, e.g., solar irradiation, wind speed and load values, are real measurements or data from forecasting models.

Microgrid energy management requires the development of models accounting for various parameters, e.g., (i) power generation sources, (ii) power flow constraints and (iii) different pricing scenarios for electricity purchase/selling, emissions, fuel, operation and maintenance costs. Table 1 summarizes the analysis of some recent developments in the area of the microgrid energy management, indicating the main focus and contribution, and highlighting advantages and limitations. General limitations of these modelling developments are:

- Limited number of uncertainties accounted in the models of the individual components of the microgrid.
- Forecasting of point estimates of the uncertain variables.
- Failures of power generators and electrical lines not always accounted for.
- Global optimization of the microgrid, not accounting for the different interests of the individual microgrid actors.
- No account for possible management and utilization agreements among microgrid actors.

In this view, the critical open issues of the current developments in the area of intelligent energy management are related to the weak treatment of uncertainties, technical failures of power generators and electrical lines and interests of the individual microgrid actors. This thesis focus on the addressing these limitations through the development of a framework for modelling dynamic interactions between grids stakeholders and optimal energy management, whereby the different stakeholders can establish their profitable and efficient strategies of use of the local renewable generators and storage facilities in dynamically changing environments under uncertainty. The detailed focus of the thesis shared between two domains, i.e., modelling and optimization is done in Chapter 2. Supported by the justification issued from the detailed analysis of the Smart grids complexity, Chapter 2 provides the delimitation of the research area and introduces the research methods used to address thesis focus.

Table 1. Comparative analysis of existing approaches for microgrid energy management.

Approach	Main focus & contribution	Advantages and Limitations
1. Multiobjective intelligent energy management for a microgrid [29]	- Short- term forecasting: Artificial Neural Network Ensemble (24 h ahead for solar power generation, 1 h ahead for wind power generation and load) - Multiobjective optimization (two objective functions account for costs of emissions, maintenance and installations, price of purchased electricity and cost of fuel consumption + constraints of optimal power flow): fuzzy-logic based expert system allows safe operation of the battery, minimization of operation cost and gaseous emissions.	Limitations: - No accounting for mechanical failures of power generators. - No dynamic test of the prediction and optimization framework during long time period (no particular learning features holding by the algorithm) Advantages: - Accounting for various generation sources (wind, solar, fuel cell, storage) - Accounting for different charging strategies, which could affect performance of the battery and will provide the need for supplementary maintenance - 24 hours simulation of real conditions operation
2. Environmental economic dispatch of Smart Microgrid containing distributed generation system [30]	- Optimization "environmental protection and economic dispatch" (one objective function accounts for costs of the power generation, fuel, operation and maintenance, emission + constraints of optimal power flow): Chaotic Quantum Evolution Algorithm (based on evolutionary algorithm).	Limitations: - Only 24 hours summer and winter scenarios were tested. No dynamic dispatch of energy generation sources. - Comparison of improvements with the case when all electricity power is supplied from the external grid Advantages: - Accounting for various generation sources (wind, solar, water cell, fuel cell, gas turbine, micro gas turbine)
3. System modelling and online optimal management of microgrid using Mash adaptive direct search [31], [32]	- Optimization (objective function accounts for technical performance of supply options, locally available energy resources, load demand characteristics, environmental, start-up costs, daily purchased-sold power tariffs, operation and maintenance costs + constraints of power flow & min off/on time): Mesh Adaptive Direct Search (output is the optimal configuration of the microgrid).	Limitations: - Data about wind speed and solar radiation is taken for 24 hours (real measured data) Advantages: - Accounting for various generation sources (wind, solar, micro turbine, fuel cell, diesel generator) - Testing different scenarios: cover microgrid electricity demand with generated electricity with renewables or sell all to the external grid, variation of electricity purchase tariffs, etc.
4. Probabilistic energy and operation management of a microgrid [33]	- Optimization (objective function accounts for fuel, start-up and shut-down costs + power balance, real power generation capacity, spinning reserve and energy storage limits): Gravitational Search Algorithm	Limitations: - 24 hours input data generated by a Neural Network-based prediction model. Advantages: - Accounting for various generation sources (micro turbine, fuel cell, solar, wind turbine and battery)

1.4. Structure of the thesis

The thesis is composed of two parts. Part I, subdivided in four chapters, introduces and addresses the challenges related to Smart grids design and implementation, and illustrates the methodological approaches developed and applied in this Ph. D. work. Part II presents the collection of three selected papers published or submitted for publication as a result of the research work and to which the reader is invited to refer for further details. Table 2 summarizes the thesis structure and the relationships established between the thesis chapters of Part I and the selected papers of Part II.

Chapter 2 is devoted to the detailed analysis and discussion of the electricity grids characterization from the point of view of complex systems. The analysis of Smart grids complexity serves the foundation for the thesis focus. Chapter 3 deals with the subject of energy management in multi-agent environments, specifically introduces the Agent-based Modelling (ABM) paradigm and its application for energy management, and introduces the multi-layered agent architecture. Chapter 4 presents the modelling approaches for describing the intelligence of the individual agents involved in energy management under stochastic environments.

Paper 1 presents a 2 steps-ahead Reinforcement Learning (RL) algorithm for microgrid energy management. A multi-criteria decision-making framework is used by an individual consumer to learn the stochastic environment and make use of the experience to select optimal energy management actions.

Paper 2 contains the exemplification of the integrated microgrid energy management framework for the optimization of individual objectives of microgrid stakeholders. The system is described by ABM, in which each player is modelled as an individual agent aiming at a particular goal under the uncertain operational and environmental parameters, and failures of the renewable power generators. The operational and environmental uncertain parameters are represented in terms of Prediction Intervals (PIs) estimated by a Non-dominated Sorting Genetic Algorithm (NSGA-II) – trained Neural Network (NN) and each agent seeks optimal goal-directed actions planning by Robust Optimization (RO).

Paper 3 presents the analysis of RO in a decentralized microgrid under uncertainty. The focus is on “extreme” conditions predicted to require robust management decisions for reducing service

and operation problems versus expected conditions that can be handled without resorting to robust solutions, which are typically more expensive and constraining.

Table 2. Structure of the thesis.

Topic	Part I Chapter	Part II Paper(s)
Analysis of Smart grid complexity	2	-
Energy management in multi-agents environment	3	2, 3
Individual intelligence for energy management in stochastic environments	4	1, 2, 3

Figure 2 provides a pictorial view of the flow of the thesis, and the issues and methodological approaches considered for optimal energy management.

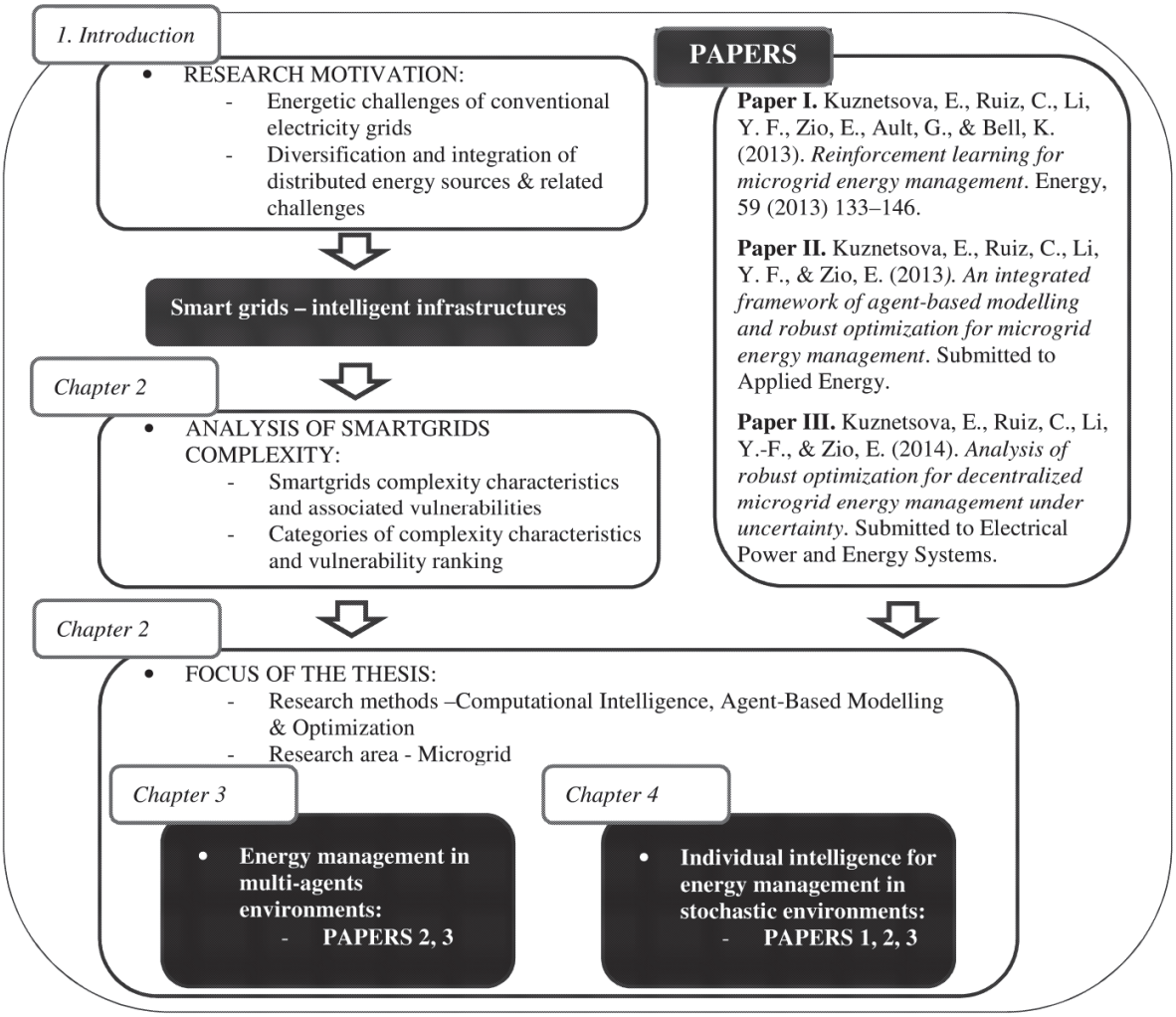

Figure 2. Pictorial view of the flow of the thesis, and the issues and methodological approaches for optimal energy management.

2. ANALYSIS OF SMART GRIDS COMPLEXITY

Sections 2.1 and 2.2 of this chapter are devoted to the characterization of electricity Smart grids as complex systems. This provides the foundation for the thesis focus, as presented in Section 2.3, identifying the research methods and delimiting the area of research.

2.1. Characteristics of complexity and associated vulnerability in Smart grids

The framework of analysis adopted for the characterization of Smart grids complexity and the related vulnerabilities, is similar to that used for other engineered complex systems, e.g. transportation infrastructures, telecommunication systems. These systems are characterized by a large number of elements with complex interconnections, nonlinear and discontinuous operations, and the involvement of multiple actors. Further, uncertainties typically exist in the characterization of the system elements and their interconnections [32]. As a result, the modelling and analysis of such systems by reductionist methods are likely to fail, and holistic approaches are needed [33].

To facilitate the understanding of the type of analysis performed, an analogy is drawn with the complex system of Internet. Initiated in 1969 in the United States as a military project [34], the Internet has become pervasive in our lives: it penetrates our offices, houses and public spaces, supported by the increasing use of personal computing devices. Today, the Internet is a global platform for commercial and social interactions, used regularly by 20% of the world's population already in 2008 [35]. Using widespread and standard engineering services with easy access to information, communication and data sharing, the Internet increases the efficiency of economic activities and considerably increases social interactions [35]. Its evolution continuously demands creation of new policy frameworks, to "encourage innovation, growth and change, and develop appropriate governance that does not stifle creativity or affects the openness of the Internet" [35]. As a backbone and enabler of convergence across multiple fields (engineering, social, economic, finance and policies), the Internet is a good example of a complex engineered system.

The Internet is particularly relevant as reference complex system in our exploration of Smart grids complexity: in a sense, the Smart grid concept may be regarded as a kind of 'Internet of Energy.' Indeed, while resorting to Internet itself as the basis of connection between the various elements

of the energy grid, the Smart grid concept additionally borrows from the Internet the way of conceiving the energy grid: Smart grids, just like the Internet, aim at creating a global, interconnected network of energy actors, while at the same time going further by monitoring, managing and optimizing energy flows.

To investigate the complexity characteristics of Smart grids, this section recalls classical concepts of complex systems, from the point of view of both topological and behavioural properties (Figure 3). In the analysis done, potential vulnerabilities arising from the complexity characteristics of Smart grids are highlighted.

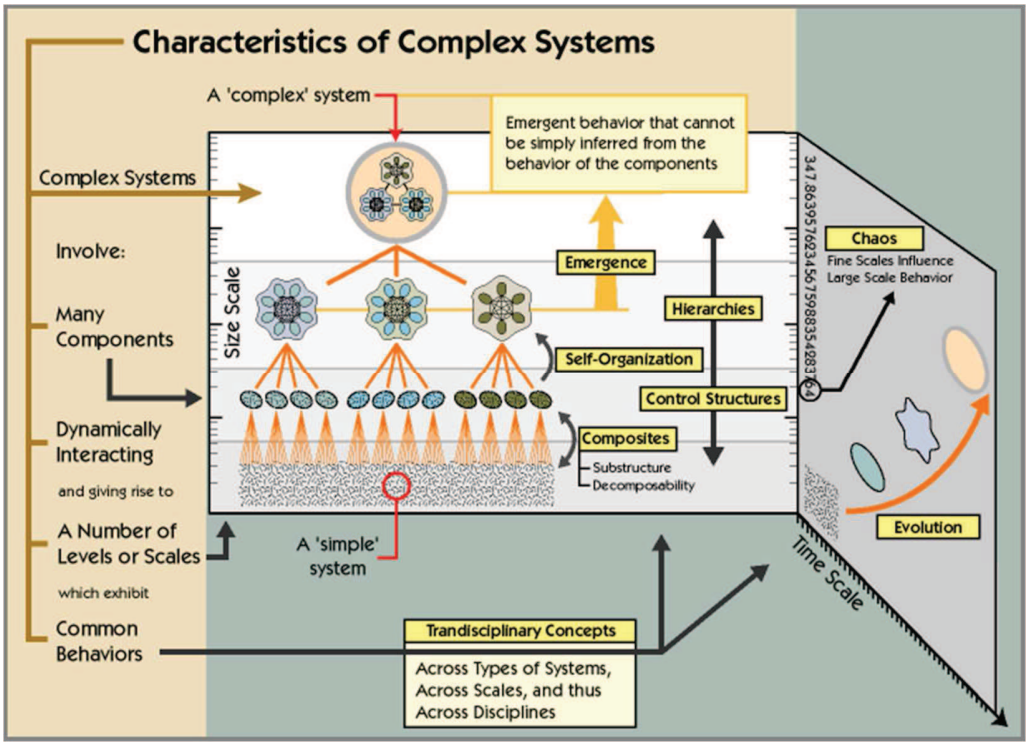

Figure 3 Characteristics of complex systems [36].

a) Architecture

System architecture is the core characteristic defining the topological and/or logic structure linking the elements of a system through their interrelations. For example, a common architectural structure is that of hierarchical organization, like it is found in the ecological, taxonomic, genealogical and somatic organization of biological systems.

System architecture provides the backbone for system behavioural features such as adaptive learning, emergence and evolution. For example, the adaptive and evolutionary mechanisms of organisms of biological systems that attempts to maintain or increase their fitness in the face of changing environmental conditions, are driven by the hierarchical structural-interactive architecture [37].

Complex engineered systems, such as the Internet, manifest pronounced hierarchical structuring with highly connected nodes of "isolated sub-systems, forming a mantle-like mass of peer-connected nodes" [38].

On top of the presence of hierarchical interdependencies in complex engineered systems, the overall structure itself and the wiring of the different elements in it are very complex to model. Various empirical and theoretical approaches analyse the structure of these complex networks by graph theory, at different levels of abstraction of the physical system, e.g., unweighted graphs for pure topological characterization, weighted graphs for attributing physical meaning to the connections, planar graphs to account for physical constraints. A taxonomy based on the nodes connectivity distribution distinguishes free-scale (inhomogeneous) networks, and small-world and random (homogeneous) networks [39].

In view of the above, the architecture of Smart grid systems is considered relevant and needs careful consideration for its influence on system evolution and adaptation. System architecture not only lays down the topological map of the system structure, but also allows taking into account the differences between its elements and connections, which are heterogeneous physically, functionally and in role.

As is highlighted in the introduction, the architecture of the traditional electricity grid is organized in a strong centralized hierarchical infrastructure (Figure 4 a) characterized by unidirectional power flow and vertical control and operation. The major vulnerability of electricity grids architecture comes from their scale-free organization standing on a limited number of highly connected nodes of production sources and few unidirectional transmission channels through which cascading failure propagation may occur in the absence of bypass transmission [7]–[9]. Smart grids design is likely to implement a structure with more homogeneous connected nodes (Figure 4 b), capable to reroute power supply and isolate undamaged lines [8].

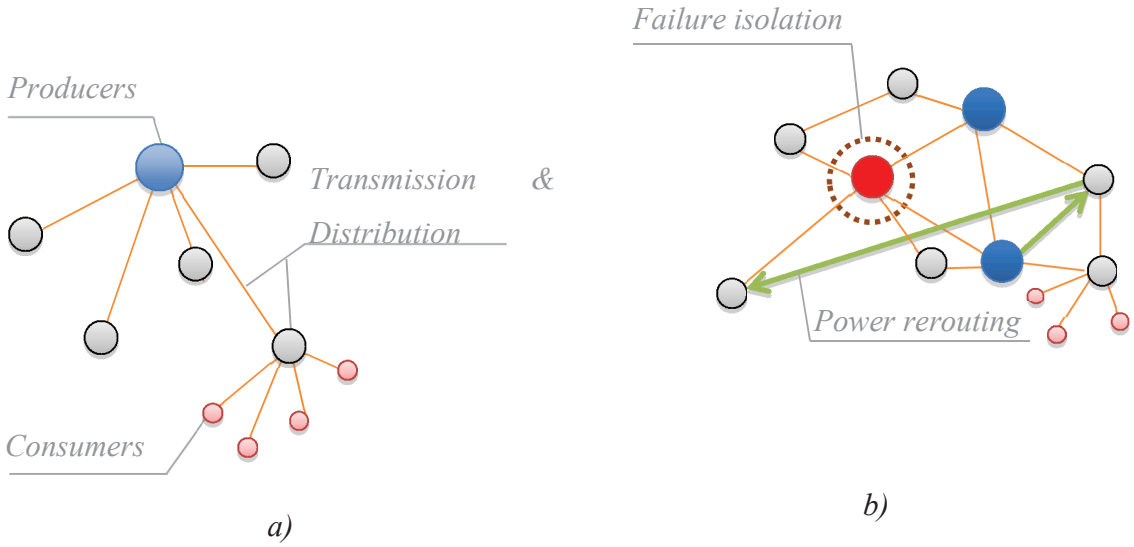

Figure 4 Structures of electricity grids: a) Centralized hierarchical structure; b) Failure isolation in homogeneously distributed networks.

b) Heterogeneity of elements and connections

Heterogeneity refers to the differences in the elements, their interconnections and roles within the system hierarchical organization, often with high-connected core elements and low-connected periphery nodes. Heterogeneity is strong in current electricity systems, with architectures in the form of hierarchical trees where production facilities are connected by centralized high-voltage transmission systems, to transformation substations linked, in their turn, to final consumers by distribution branches. Notably, Smart grid systems aim at evolving towards more decentralized architectures, with a more homogeneous distribution of heterogeneous production sources of different nature and size, including renewable energies. These will need to penetrate the network at all levels, homogeneously. The arising grid pattern forms a sort of neural or vascular system, manifesting in some conditions structured into self-similarities [40].

In any case, the strong heterogeneity of the elements and connections in current electricity grids, which will serve the foundation for the future Smart grids, translate into high sensitivity to direct attacks [7], [41]. This high vulnerability to direct targeted attacks of scale-free networks can be limited by allocating supplemental connections and elements for a more homogeneously distributed architecture. Indeed, the tolerance of homogeneous networks is similar for random failures or direct attacks to nodes and connections, independent of the network size [42].

c) Self-similarities

Self-similarities are complex system structures also called fractals and described as "a rough or fragmented geometric shape that can be split into parts, each of which is (at least approximately) a reduced-size copy of the whole" [43]. Where self-similarities are present in a complex system, they lead to similar properties at all hierarchical levels, similar complexities at different scales without a unique characteristic size for their structures. Assertion of the existence of a fractal structure in a given complex system depends on the possibility of ascribing to that structure specific dimensionless numbers indicating the nature of self-similarity in the structure or behaviour in the complex system [44]. The dimensionless quantification of a fractal structure provides fractals with the property of scalability.

The principle of fractal structuring of veins, characterized by an efficient mechanism of blood distribution with minimum structure and shortest path, was borrowed to study the optimal design of the Internet network [45]. A further structural analogy can be found in the extension of the Internet concept onto Smart grid networks. The Smart grid concept exhibits fractal structuring insofar as a particular Smart grid may contain an ‘energy automation network’ for ‘positive energy building’ inside district Smart grids, district Smart grids inside city Smart grids and so forth. Here, the ‘energy automation network’ constitutes the mini Smart grid network, involving consumers, local renewable energy producers, transportation and storage facilities. Smart grids for ‘positive energy building’ manifest clear periodical self-similarities, with district Smart grids included in energy flows management with respect to day and season energy demand fluctuations. Certainly, self-similarities appear as an evident characteristic of Smart grids system structuring.

Looking at fractal properties for engineering and non-engineering complex systems, it appears that it is not the presence of self-similarities, but rather their absence which may render Smart grids vulnerable [45]–[48]. For example, there are nearly no fractals in the current scale-free architecture of electricity grids connected with energy production to form the core production sub-system. In this setting, a direct attack on a production hub may result in the failure of the core production sub-system [48]. For this reason, Smart grids are likely to seek fractal architectures, where consumers are regrouped around distributed production sources without strong connections with other production hubs.

d) Self-organization and decomposability

Two other characteristics related to the structure of engineered systems are *decomposability* and *self-organization.* The former relates to the divisibility of the system structure into subsystems and into further separate elementary elements. Electricity grids seem to exhibit a structural property of decomposability, especially evident within the fractal patterns envisioned for future Smart grids structures.

Self-organization refers mostly to the behavioural feature of a complex system capable of re-organizing its isolated elements and subsystems into coherent patterns without intervention from external influences or a central authority. For example, the open system of the Internet, affected by a continuous growth in the number of components and by technologies evolution, tends to self-organize into stable patterns through the creation of particular niches of services or user 'coalitions.' Such flexibility allows the Internet to adapt continuously to changes in the local environment, while maintaining coherence of structure and reliability of service [49]. In this sense, self-organization constitutes mostly an adaptive and evolution property of complex dynamic systems, spontaneously emerging from the interactions of the different system components. In this view, the possibility that Smart grids will possess such complexity will depend on the level of autonomy of the system from other systems, and the number and dynamics of Smart grids users. For the moment, the role and involvement of consumers in the mechanisms of the electricity network management are not clearly defined, but the potential for failure-resilient self-organization, responsible for other properties such as emergence, adaptive learning and evolution, is ripe for exploitation.

By enabling 'disassembly' of a complex system into its subsystems and their components, decomposability allows understanding and categorization of system elements. Low decomposability implies potential vulnerability as the system is characterized by massive elements with limited capacity for adaptation and evolution in response to nearly emerging challenges. On the other hand, high decomposability translates into a large number of components, connections and interrelations, which may make the system difficult to control, and thus vulnerable. Another situation of vulnerability may arise from significant variations of decomposability level across the Smart grid, resulting in system stiffness and possible instabilities.

The impact of the self-organization process is significant in systems without central authority. In this view, the self-organization in Smart grids may turn into vulnerability depending on the extent and type of active involvement of the users without strong enough centralized control.

e) Emergence

Induced by the complex non-linear interconnections between the separate system elements, subsystems and fractals at a micro level, emergence is a property of complex systems, which appears only at a macro level manifesting itself by the arising of novel and coherent structures, patterns and behavioural properties [50]. Mainly due to self-organization processes, emergent behaviour appears more evident in complex dynamic systems without a clear central authority, where some even small local changes evolve into unpredictable forms of high-level organization and behaviour. In the case of the Internet, social bookmarking or tagging leads to an emergent effect in which information resources are re-organized according to users priorities. Social networks are not only used for networking with friends, but are also exploited for gathering and communicating relevant users information, or coordinating system-wide actions of entire segments of population. Electricity grids have also shown emergent behaviour in the past, where local failures have evolved into unexpected cascade failure patterns with transnational, cross-industry effects. In this sense, Smart grids are also expected to be characterized by an emergent behaviour, also in connection to the above mentioned self-organization mechanisms of complex systems and depending on the extent and type of the active involvement of users in the energy management process.

A situation in which a large amount of information is exchanged within technologies at a period of high electricity demand can lead to a vulnerable condition of the system, similar to Internet networks and information traffic congestion [51]. This emergent behaviour could be driven by small changes in users behaviour and result in grid dysfunction. However, emergence can also offer opportunities to find resilient solutions in the recombination of evolved structures and processes, renewal of system components and new connection trajectories to satisfy demands [8]. For Smart grids, one could imagine using the bookmarking mechanism to make social participation more visible and involve people in energy infrastructure design and operation by communication of their major expectations and needs, as well as to take into account their feedback during system updates. In this view, an emergence process driven in reasonable proportion between social

participation and central authority can make Smart grids more resilient to environmental changes without losing the functional capacity.

f) Adaptive learning

Adaptive learning allows a system to adjust its architecture and behaviour into a stable coherent pattern under external pressures, using long-term memory experience feedback to anticipate future unfavourable changes in system functioning. This adaptation process is made possible by a set of internal mechanisms, named detectors and effectors [36]. The system collects the information on acting external pressures through the detectors. Then, effectors, such as locomotion, communication, manipulation and expulsion, actively change the state of certain components, subsystems and/or their interrelations to keep the system in equilibrium under the acting external forces. Feedback mechanisms play an indispensable role for the anticipation of future changes in support of system equilibrium. The dynamic feedback and learning process provides changes in time to the system components and their interrelations through the successive consideration and evaluation of external and internal factors [36]. In complex engineered systems like the Internet, the adaptive learning process partly relies on the ability of self-organization driven by local changes. As the Smart grid concept strongly relies on a system of intelligent and sustainable management of power flows, adaptive learning mechanisms are expected to be a central feature of design, operation and control.

Adaptive learning is a challenge-response property which results from the trade-off between consumer involvement and control by the central authority in the energy management process. On one side, intense consumer involvement can initiate chaotic behaviour in the electrical system; on the opposite side, strong control by the central authority renders the system rigid, missing opportunities for service efficiency and for exercising system resilience and adaptation capacity. This raises the uncertainty regarding the extent of adaptive learning in Smart grids, as well as on the suitable functioning of its mechanism.

g) Evolution and growth mechanisms

When the external pressures applied to a system exceed ‘critical values’ beyond which adaptive learning mechanisms are inefficient, the system is forced to evolve. In the absence of a central authority governing system changes, the evolutionary process resembles natural selection in biological systems resulting in the consequent disappearance of elements associated with low

adaptive fitness. The Internet, for example, is the product of the evolution of its constitutive software and hardware technologies, information and communication services and applications, and also faces the creation of new ways of use, such as e-commerce. Unlike biological systems, complex engineered systems are exposed also to constant growth of user portfolios. Future Smart grid complex systems will both evolve in the way typical of analogous biological systems and also incorporate unanticipated new elements.

Smart grids may be exposed to vulnerabilities emerging from the growth mechanisms of the system. Restricted by technical constraints and transmission capacity, the extension of current electricity grids is done by preferential attachment, whereby highly connected nodes attract new links. This is a typical mechanism of growth of complex networks [52], [53]. The result of this particular mechanism of growth is that it reinforces the 'scale-free' nature of electrical systems and, as a consequence, makes them vulnerable to direct attacks and propagation of cascading failures. This means that the electricity system growth must be carefully monitored in order to anticipate possible critical decision points at which infrastructure development must be steered in a preferred direction. In this sense, the resilient mechanism for electricity infrastructure growth is likely to be based on the repulsion process between the hubs at all length scales, when the hubs prefer to grow by connections to less-connected nodes [48]. On the other hand, user involvement in the energy management process may cause drastic shifts in system evolution, leading to unexpected events and system vulnerabilities.

h) Chaos

Chaos theory is used to describe and explain various processes occurring in complex systems, e.g. earth atmosphere and aerodynamics processes [54], [55], chemical processes [56] and information and communication processes [51]. In these processes, chaos is used to characterize the capacity of non-linear dynamic systems to produce an unpredictable change in large-scale behaviour or a sudden shift in system pattern, in response to fine-scale changes in initial conditions [54]. Hence, the well-known aphorism, that butterfly wings flapping can cause a tornado [57].

Engineered chaotic systems are characterized by high sensitivity to changes, but also by mixing and periodicity. These two last properties are mainly responsible for the formation of complex fractal structures as a manifestation of chaotic properties within a complex system. On the other hand, the fractal structure resulting in 'positive energy building' within Smart grids is more a man-

made structuring aimed at facilitating electricity flows management than an emerging result of chaotic evolution. However, even if Smart grids patterns will be mainly characterized by 'artificial' structuring, some periodic daily or seasonal self-similarities, for example in energy consumption behaviour between building and district Smart grids, are likely to arise in manifestation of chaotic behavioural patterns.

The extent of system exposure to chaos is related to the level of influence of the controlling central authority. In the case of Smart grids, chaos may arise mainly after the integration process, due to the influence of system-affecting non-engineering factors which are difficult to forecast and control, including social acceptance and participation. Given the nature of these factors, modelling scenarios of chaotic behaviour at the design stage is a challenging forecasting problem of multidisciplinary nature, since realistically the major interrelations among elements arise after system implementation.

i) Multidisciplinary relations

Multidisciplinary relations are an integral part of engineered complex systems. Smart grids in particular involve a number of engineering and non-engineering disciplines for defining the successful implementation of new energy systems, e.g. by creation of necessary legislative frameworks for technologies use, finding adequate finance models for innovative projects elaboration, providing incentive support and elaboration of standards, and securing social acceptance and participation.

The nature and dynamics of multidisciplinary relations which will affect the Smart grids life cycle are difficult to forecast and control, and the related uncertainties may hide potential vulnerabilities.

j) Vague boundaries

Through the integration process, complex engineered systems become open systems interacting with the environment. Their multiple relations with non-engineering domains and with other engineered systems result in difficulties of boundary definition. Necessarily, then, the modelling of the complex system limits depends on the observer's scope of analysis rather than being an intrinsic property of the system. In some associated analyses of analogous systems, other organizational categories are proposed.

Imprecise definition of Smart grid boundaries at the design stage driven by 'preconceived' engineering views on current energy challenges can result in losses of information about the patterns of interconnections with influencing non-technical factors, and their possible underestimation. Even in the case of well-engineered, smart electricity management, vulnerabilities in Smart grid systems can arise if relevant influencing factors are neglected, e.g. social involvement and participation in the design and operation processes.

k) Self-healing and attacks resistance

As discussed above, Smart grids potentially exhibit a number of topological and behavioural characteristics typical of complex systems. In addition, they are intended to have specific characteristics arguably conceived as core to the Smart grids concept: according to a popular vision of 'intelligent electricity grids', they will possess a range of additional properties such as *self-healing* and *resistance* to external natural disasters and human attacks [23]–[25], [58]. These two particular characteristics are related to adaptive learning and evolutionary mechanisms. However, to mark their importance for the Smart grid concept we will consider these properties apart.

These two properties were underlined as specific Smart grids characteristics within adaptive learning and are considered as challenge-response characteristics. In the case of their strong influence, the adaptive learning property will dominate the evolution process and obstruct system upgrades, which will be restrictive for Smart grids development. Therefore, these properties must be considered carefully.

2.2. Taxonomy of Smart grids complexity characteristics and vulnerability ranking

2.2.1. Categories of Smart grids complexity

In the context of complex systems, although the structural backbones are created by the engineers who develop the constituent components of the system, the connections of such components within the systems are not necessarily all 'designed.' In many instances, undersigned or even undesired connections 'emerge' from system evolution for meeting the demand under given operation constraints [59].

Complex systems can be said to evolve from the design blueprints to complex structures and behaviours through *engineering, updating* and *integration* processes. At the *engineering process*

level, elements are assembled by design to provide optimal, consistent and reliable operation, as well as functional safety [59]. In general, this is achieved with engineered systems which may be *complicated* but not yet *complex* [59]. The engineering process is usually organized by hierarchical methods in top-down approaches, managed on a linear timeline organization [32]. In principle, the final product of such process could be reduced to pieces and reassembled, without losing its function. Vulnerability may arise in these systems, particularly from designed defects due to calculation errors or simplifications during the design process.

As the system 'lives', its *updating* and *integration* occurs by insertion of new technology and extension of capacity to meet service demands with the required performance. This creates a need for connection between the engineering of the system and the ever-changing domains of society, economy, legislation and politics, which determine service demands and generate constraints. In virtue of this connection, the originally complicated engineered system becomes complex with hallmarks of adaptation, self-organization and emergent behaviour, which constitute opportunities but pose also vulnerabilities, mostly due to unforeseen complications during the integration process [59].

In the next section, each characteristic identified in Section 2.1, is analysed from the point of view of Smart grids and allocated to groups enabling identification of primary sources of system vulnerability related to the processes of *engineering, updating* and *integration*.

2.2.2. Ranking of Smart grids complexity characteristics

In order to explore and explain the complexity of Smart grids, this section maps the characteristics of complexity discussed previously into three major categories – *inherent*, *challenge-response* and *acquired* characteristics (Table 3). These categories are defined in relation to the three processes of *engineering*, *updating* and *integration* of complex engineered systems. The first *inherent* category contains characteristics of Smart grid systems designed at the *engineering* process level. Properties such as the heterogeneity of elements and connections, as well as system architecture, are considered as inherent characteristics of system complexity amenable to control and, therefore, of minimum uncertainty impact on Smart grid functioning. The second category includes *challenge-response* characteristics. Inspired by the underlying Smart grids strategy of a flexible and transparent energy management concept for the reinforcement of electricity infrastructure reliability [60], these characteristics result from the continuous *updating* process in response to the

evolution of the challenges to the Smart grid function. In this context, adaptive learning and self-healing are desirable prospective characteristics for effective challenge-response by smart electricity infrastructures. Due to the uncertain and somewhat unpredictable evolving environment, the challenge-response properties of Smart grids could not be guaranteed through design process, and their achievement is a challenge itself. Eventually, the third category of acquired characteristics includes self-organization, emergence and chaos which arise as a consequence of the *integration* of the system in the complex socio-economical environment which drives its functioning. This category regroups the major sources of uncertainty on the functioning of Smart grids.

Table 3. Categorization of Smart grids complexity characteristics

Smart grids complexity characteristics		
Inherent (engineering)	**Challenge-response** (updating)	**Acquired** (integration)
Architecture	Adaptive learning	Vague boundaries
Heterogeneity	Evolution and growth	Self-organization
Self-similarities	Self-healing	Emergence
Decomposability	Attack resistance	Chaos
		Multidisciplinary relations

Note that this categorization may not be exclusive as some characteristics could be mapped into more than one category. For example, evolution could be considered as both a challenge-response and acquired characteristic. On the one hand, this property can provide Smart grids the challenge-response characteristic needed for flexibility in handling the uncertain stresses upon the system. On the other hand, evolution may have uncertain negative effects on Smart grids functioning resulting in increasing of vulnerabilities and incapability to correctly respond to challenges of electricity demand. This may occur under specified conditions: as in the next section, characteristics such as adaptive learning, evolution and growth can not only produce a positive impact on the Smart grid functioning, but can also turn into vulnerabilities in the absence of a central authority.

In this respect, not only the uncertain properties of the acquired category, but also inherent complex system characteristics could become vulnerability sources. For example, topological properties of Smart grids could induce behavioural vulnerability by facilitating disturbance propagation within the network of connections, giving rise to cascading processes which would impair system

functioning. This leads to the need of identifying sources of potential vulnerability within the system characteristics and of ranking them according to their impact on Smart grids development and functioning.

Most of the complexity characteristics discussed in Section 2.1 are candidate sources of Smart grid system vulnerability. Their ranking with respect to their potential impact on the most valuable system resources and functionalities of electrical network is an objective of vulnerability assessment, because it can guide allocation and protection at the design and operation phases. However, at this stage of development of the Smart grid concept, ranking vulnerabilities by the importance of their expected impact would be an helplessly abstract exercise. A preliminary qualitative ranking could follow the categorization of Smart grids complexity characteristics of Table 3 and their mapping into inherent, challenge-response and acquired categories, each of them related to the engineering, updating and integration processes of Smart grids as complex engineered systems. The engineering process can be regarded as providing the designer with full control of a given Smart grids topological and behavioural properties. In this view, in this first category the characteristics manifesting vulnerabilities could be subordinated and their consequences reduced. In the updating process, the level of designer involvement is lower and the vulnerabilities to which Smart grids may be exposed are more difficult to control and avoid, without intervening on the associated influencing environments, e.g. the social and economic contexts. The second category regroups vulnerabilities of more unforeseen character than at the engineering stage. The last category expresses the most uncertain characteristics of Smart grids, capable of producing echo effects in different contexts, with consequences which are difficult to predict. For this reason, these characteristics are considered to have large potential of leading to vulnerable states of Smart grid systems.

2.3. Focus of the thesis

The analysis of Smart grids complexity done in this section, creates the foundation for the focus of the thesis, with the identification of appropriate research methods for the delimited research area.

As discussed in the previous sections, the energetic and environmental challenges of the 21st century compel the transformation of the conventional centrally managed energy systems,

incorporating large fossil-fuel plants, into new energy systems characterized by multiple small-scale schemes integrating non-conventional energy generation. This will transform the conventional centralized grids of passive one-way bulk energy systems to complex Smart grid infrastructures consisting of multiple bi-directional energy clients. The analysis performed in Sections 2.1 and 2.2 shows the potential vulnerability of this transformation due to the particular Smart grid characteristics of complexity: regarded as the enablers for clean, renewable, local generated energy, Smart grids become highly complex systems that could be difficult to optimize and vulnerable to instability. This calls for a paradigm shift in the development of the intelligent technologies for Smart grids, which must allow the dynamic optimization of current operation and the incorporation of dynamic gateways for alternative sources of energy production and storage [30].

This thesis brings contributions in modelling and optimization within the problematic of microgrid energy management by taking into account uncertainties, dynamics, communication, multiple actors with various goals and their interactions. The thesis developments will directly contribute to address a range of bottlenecks, identified based on the review of existing research works, presented in Section 1.3. Under this view, in this section the detailed focus of research, the problem addressed and the research methods used in this thesis are highlighted.

2.3.1. Research methods

Smart grids systemic studies have been mainly focused on the challenge-response characteristics of such intelligent grids, rather than on the means and strategies by which these characteristics can be obtained [23]–[26]. Through the detailed analysis of the system challenge-response properties, various researchers have dedicated their efforts to the development of intelligent approaches [61]–[63] classified by [30] under the category of Dynamic, Stochastic, Computational and Scalable (DSCS) technologies. The development of these DSCS technologies is required for Smart grids in order to achieve the desired challenge-response characteristics, i.e., the ability to monitor, forecast, plan, learn, understand complexity, share understanding across neighbouring areas, schedule, make decisions and take appropriate actions to ensure stability, reliability and efficiency of electricity grids [30]. Therefore, Smart grids could be designed by awarding different types of Computational Intelligence (CI) to electricity grids actors, which will become capable for sense-making, decision-making and adaptation, and by adding collaborations not only vertically between

different hierarchical levels, but also horizontally [30]. These connections will bring more homogenous distribution of grid actors connections inside the system by decreasing the number of super nodes and, therefore, reducing system vulnerability to direct attacks.

The need of development of the intelligent technologies is confirmed by the opinions of key international research organizations and industrial companies working on the CI approaches for Smart grids capable of providing the response to question on how to assign the property of autonomy to individual agents of electricity grids without undermining overall grid efficiency [30], [64]. To decrease hierarchical dependency and local vulnerability, different types of CI, i.e. forecasting [30], [65]–[67], adaptive learning [68]–[70], maintenance scheduling [30], [71]–[73], market and energy trading [74] and voltage stability monitoring and real-time stability assessment [30], could be implemented to reinforce the distributed intelligence of individual grid actors.

In this context, the present thesis aims at contributing methods and frameworks of analysis for energy management by the individual stakeholder as well as by multiple stakeholders, accounting for different sources of uncertainty. The energy management methods and frameworks address the Smart grid concept by combining CI technologies capable of capturing the stochasticity of the environment and enabling adequate decisions of energy strategy, learning from feedbacks and adapting to the changing environment under uncertainty.

By taking into account the peculiarities of Smart grid infrastructures, some methods regarded as suitable have been described and analysed in [75]. Among these, the ABM has been regarded capable of providing an accurate representation of complex dynamic systems and of simulating challenge-response and acquired characteristics of Smart grids, such as adaptive learning, self-organization, adaptation etc. [76]–[81]. However, the integration of physical models for the representation of engineering and non-engineering factors with their complex relations, must be rendered computationally feasible in order to represent realistically the complex behaviours of large-scale systems in reasonable times [33]. The accurate representation of multiple components and connections in multiple agents appears to be a complicated task, with a large number of parameters whose values need to be determined on the basis of data and information that may be unavailable for some components and connections. It is therefore expected that for Smart grids, the ABM approach can be used for studying specific, geographically limited areas [33].

The research contained in the thesis, then, falls within the exploitation of existing computational methods of ABM for providing not only the autonomy of decision-making individual agents, but also the intelligent adaptation to complex, uncertain and changing environments. The following section specifies the research of this thesis.

2.3.2. Research area

The selection of the research (application) area for the current thesis is driven by two important conditions for the successful development of the underlying engineering concepts, namely the developed approach must hold the properties of *scalability* and *transferability*.

By embracing the concept of fractals or self-similarities in the Smart grid system architecture, the thesis focus has been put on the elementary fractal, i.e., the *microgrid*, integrating different energy consumption and production sources, as well as storage facilities, under strategies of energy management, which can be similar at different scales of building, district, city. This is a challenging problem, as increased penetration of electricity distribution grids (low voltage) by new unconventional micro generation sources, not accounted for during power infrastructure design, can lead to unforeseen situations and vulnerable emerging properties for sustainable electricity management. In this view, the consideration of the microgrid as the fractal of extended Smart grid systems allows considering and testing DSCS technologies, *scalable* to Smart grids of large size.

Furthermore, the management strategies of aggregation of renewable power plants with high capacity depend mainly on regulatory and economic mechanisms, topology and technical constraints of electricity grids, and diversity and flexibility of generation portfolio [82], [83]. The interoperability problem of the European grids exists due to variations in renewable energy input states, as different national grids operate using different voltage levels. In Greece, for example, mid-sized wind farms are, consistent with their energy production, connected to a high-voltage network [21]. By contrast, in Denmark, a large number of decentralized production units are connected directly to distribution grids. In France, the integration of production units is ensured with both distribution and transmission grids [21]. For this reason, the research of this thesis considers the general case of renewables sources penetration in low and medium voltage distribution systems, i.e. *microgrid*, for developing a *transferable* energy management framework, which could be successfully applied in different technical, economical and regulatory contexts.

In this context, the research performed during the PhD has been aimed at developing simulation / optimization frameworks capable of describing the dynamic interactions among microgrid actors and embedding algorithms of CI for energy management in *microgrids*. The underlying objective of the optimization is to establish profitable and efficient strategies for use of local renewable generators and storage facilities in dynamically changing and uncertain environments.

3. ENERGY MANAGEMENT IN MULTI-AGENTS ENVIRONMENTS

This chapter addresses the subject of energy management in multi-agent environments. Section 3.1 discusses the ABM paradigm adopted in this PhD work to treat the subject and exemplifies its application in the domain of energy management. Section 3.2 introduces the particular multi-layered agent architecture considered in this work. Section 3.3 provides contributions of this thesis work by presenting the exemplification of the applicative contributions, retrieved from the scientific papers of Part II, and by summarizing the overall methodological and applicative contributions.

Chapter 3 provides also the references to Part II. Paper 2 illustrates the application of the proposed multi-layered energy management framework to achieve the energy management goals of the individual agents in a microgrid system. Paper 3 adopts the optimization framework developed in Paper 2 and evaluates its performance under different levels of uncertainty in the operational and environmental conditions.

3.1. Agent-Based Modelling (ABM) for microgrid energy management

According to the definition of [84], multi-agent systems are systems composed of multiple interacting computing elements, known as *agents*, capable of performing *autonomous actions* in order to satisfy their design objectives and of *interacting* with other agents in form of cooperation, coordination, negotiation, etc. To explore these particular properties the ABM approach is widely used for different applications. In the domain of energy management, ABM is used for describing dynamics of the individual goal-oriented decision-making of different stakeholders and the interactions among individual intelligent decision makers (the agents) acting on electricity grid system [76], [77]. The most widespread application of this modelling approach concerns the bidding strategies among individual agents, who want to increase their immediate profits through mutual negotiations, and the modelling of the energy market dynamics [78]–[81].

Figure 5 shows an example scheme of typical interactions among agents in an ABM of an electricity market [85]. The generation companies interact with the central Independent System Operator (ISO) by submitting bids to the pool market, receiving bidding results, and conducting

the dispatches specified by the ISO. The generation companies could also negotiate directly with the customer companies for long-term bilateral contracts, which must be approved by the ISO. The interactions between customer companies and the ISO are performed in a similar way. Among these interactions, customer and generation companies aim to achieve their objectives, i.e., reduce the expenses for customer companies and increase the revenues for generation companies. These objectives are achieved under the approval of the ISO holding control and monitoring functions. Finally, the transmission companies deliver transmission information to the Market Information System (MIS) and implement the transmission schedules determined by the ISO. At the physical system level, transmission lines transmit electricity directly from generators to customers. As it can be observed in this application, the ABM restricts the decision freedom of the individual agents, whose optimal operation is monitored by the ISO.

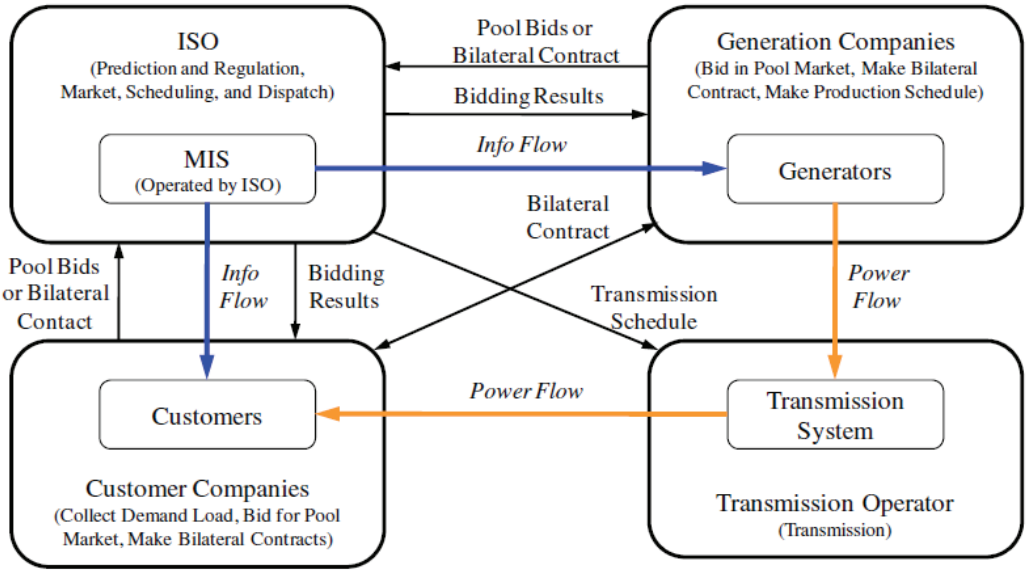

Figure 5. Example of scheme of interactions among agents in the ABM of electricity markets.

Recent studies show possible extensions of ABM to consider more complex interactions in the energy management of hybrid renewable energy generation systems [69], [77]. In these works, the long-term goals are focused on the efficient use of electricity within microgrids, e.g., the optimal scheduling of a battery to locally store the electricity generated by renewable sources and reuse it during periods of high electricity demand [69]. However, the decision framework is commonly developed under typical deterministic conditions, e.g., those of a typical day in summer.

3.2. Multi-layered architecture for energy management

As it was highlighted above, ABM enables to represent complex interactions by assigning to the individual agents particular decision-making heuristic techniques, learning rules or adaptive processes and interaction frameworks with their environment. The architecture must allow an individual microgrid agent to: (i) capture the nature of the stochastic environment, (ii) take the adequate decision about the actions to perform and (iii) interact with other agents and with the non-agent environment. By taking this into account the multi-layered agent architecture is applied. Figure 6 presents a generalized multi-layered architecture used by an individual agent for its energy management, similar to the one in [69]. The architecture of an individual agent is divided into three specific layers, each one responsible for a particular task. For each time step, the agent captures the situation of the non-agent environment using the behavioural model of the reactor layer. The information about the eventual changes is transmitted to the planning mechanism, which performs the local planning by using the feedback obtained from other agents during previous interactions and cumulated by the learning and evaluation mechanisms. By using the social model for cooperation, agents interact with each other by sending their own parameters to the related agents, by asking for cooperation, and by getting global decision and information from the related agents. Further, each agent makes the final decision about the optimal action to be taken based on the other agents replies, which may switch its states and step into a new continuous control cycle; the signal about the action to be taken is transmitted to the behaviour layer where it is implemented. In this view, the information is transmitted from the bottom to the top while the control orders flow is transmitted from the top to the bottom across all three layers.

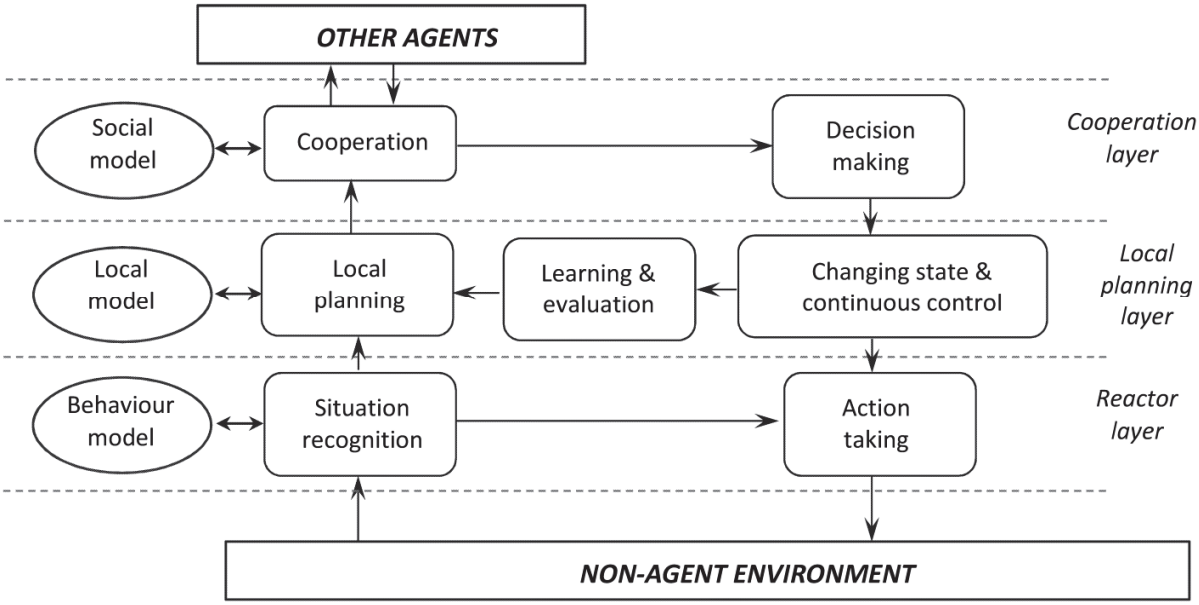

Figure 6. Generalized multi-layered architecture of an individual agent.

Inspired by the particular abilities of an intelligent agent, the multi-layered architecture has been also used for microgrid energy management by combining it with Artificial Intelligence (AI) techniques jointly with linear programming-based, multi-objective optimization models [86]. Figure 7 illustrates the procedure used for the integration of the multi-layered management framework in the operation timeline. This integration is divided into three stages:

(1) *prediction* of the uncertain operational and environmental parameters for the particular duration of the planning horizon;

(2) planning of the scheduling actions by taking into account the particular optimization goals to be achieved for the prediction horizon;

(3) *implementation* of the optimized scheduling actions under real operational and environmental conditions.

It is important to highlight, that the *implementation* of scheduled actions can be done for periods shorter than the considered prediction and planning horizons (one hour-ahead is considered in this PhD work): this gives the decision-makers the possibility to 'shift' the prediction horizon and readjust their planning actions according to their goals.

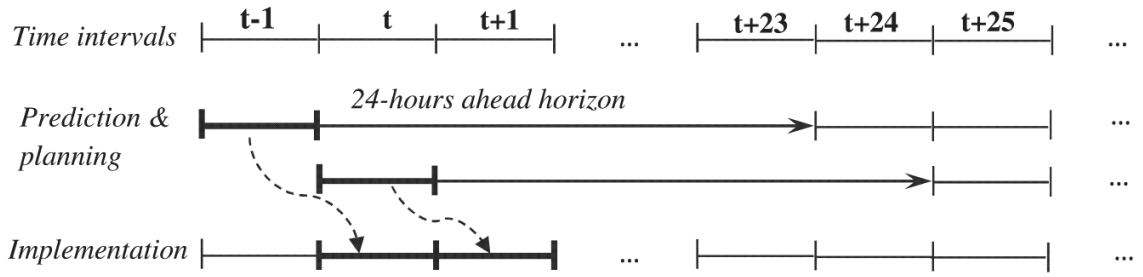

Figure 7. Example of the multi-layered management framework integration in the operation timeline [87].

3.3. Methodological and applicative contributions

This section maps the contributions of this thesis work. Section 3.3.1 illustrates the application of ABM approach for the energy management through the representation of the typical microgrid agent. Section 3.3.2 maps the methodological and applicative contributions of the thesis in relation with Part II.

3.3.1. Exemplification of applicative contributions

This section presents the typical microgrid agent and its operational environment defined through the environmental and operational conditions. These definitions are translated in mathematical formulation providing the specific information about agents objectives, constraints and energy balance equations.

a) Model of the individual agent

For exemplification, a typical microgrid agent has been retrieved from the Paper 2 of Part II [87]. This paper discusses the research done within the project on energy performance of a middle-size train station (TS) and its environment in the Paris region [88]. In this view, this middle-size TS has been selected to illustrate a typical microgrid agent. Specifically, the goal of TS is to decrease its electricity expenses while satisfying its demand. To achieve this, the TS strategy includes the integration of renewable generators, i.e., photovoltaic (PV) panels [89], [90], and energy exchanges with the local community or district (D) to increase the power flexibility of the microgrid. In addition, we assume that TS had the capacity to store electricity in batteries.

Therefore, the model of the individual agent includes the models of the TS energy consumption, production and battery scheduling.

The energy consumption of the TS is divided in two groups: (i) variable energy consumption of lifting, lighting and heating equipment, which depends on the operational and environmental variables (e.g., solar irradiation, passengers flow etc.) and (ii) fixed energy consumption of other equipment, such as ticket control and vending machines, which are constantly plugged to the power network.

Based on the energy consumption modelling and the findings of the project [88], the major energy consumption in the TS is due to lighting, lifting and other electronic and heating equipment, in a ratio of about 50%, 25% and 25%, respectively, of the total main building energy consumption without auxiliary buildings and activities. Energy consumption related to the heating of the TS offices was neglected. The total hourly required energy E_t^{TS} *(kWh)* at time *t* is approximated with eq. (1) below, representing the three main types of equipment units, i.e., inside and outside lighting E_t^l *(kWh)*, passengers lifts by escalators and elevators E_t^{elev} *(kWh)* and electronic equipment E_t^{elec} *(kWh)*:

$$E_t^{TS} = E_t^{elev}\left(F_t^{pas}\right) + E_t^l(r_t) + E_t^{elec} \qquad \forall t \qquad (1)$$

where r_t is the solar radiation *(W/m² or lx)* and F_t^{pas} is the passengers flow in the TS (pas/h). The power required by the elevator equipment E_t^{elev} is calculated as the sum of variable E_t^{var} and stand by E_t^{fix} power [91]. The variable energy consumption of the escalator is related to the transported passengers F_t^{pas}:

$$E_t^{var} = (F_t^{pas} \cdot g \cdot r_e \cdot m_p \cdot k_{wf})/3600000 \qquad \forall t \qquad (2)$$

where g = 9.81 m/s², r_e is the vertical rise of the escalator *(m)*, m_p is the average weight of passenger *(kg)* and k_{wf} is the walking factor, which is defined as the ratio of the time that passengers actually spend on the escalator to the time that they would spend if no walking took place [91]. Division by 3600000 is introduced to convert the final results from units of joules *(J)* to *kWh*.

The fixed power E_t^{fix} is related to the power consumed by the unloaded escalator and depends on the particular technical features of the escalator, such as the type of gear box, step chain bearing

and guidance system. The work [91] presents a correlation with the height of escalator rise r_e, as dominant factor to qualify the different escalator designs:

$$E_t^{fix} = a \cdot r_e + b \qquad \forall t \tag{3}$$

where *a* and *b* are coefficients depending on the technical features of the escalator. To select the coefficients values the escalators were assumed to have following technical features: ball bearing step chain guidance and involute gearbox [91].

The electrical energy E_t^l required by the lighting equipment depends on its design and on the control systems and requirements of illumination standard setup adopted for the TS (e.g., EN13272:2001 UK) and urban areas [92]. Finally, the electronic equipment that is constantly plugged into the grid are the ticket vending and control machines, and food and drinks distributors, with assumed required fixe amount of hourly energy [93], [94].

The total energy produced by PV P_t^{PV} *(kWh)* at time *t* is the sum of the outputs P_t^{PVi} of several individual PV panels at time step *t*. Taking into account the solar irradiation, whose model is described in the next section, the ambient temperature and the characteristics of the module, the electricity output from one solar generation unit can be evaluated using the following set of equations used in [95], [96]. The technical parameters of the solar generation units can be retrieved from available industrial specifications [96].

The battery allows to store electricity generated by PV or exported from the external grid. The set of eqs. (4) - (8) governs the energy flow dynamics of the storage in the TS:

$$R_t^{TS} = R_{t-1}^{TS} + \delta_t^{TS,ch} \cdot R^{TS,stor} - \delta_t^{TS,dis} \cdot R^{TS,stor} \qquad \forall t \tag{4}$$

$$\delta_t^{TS,ch} + \delta_t^{TS,dis} \leq 1 \qquad \forall t \tag{5}$$

$$0 \leq \delta_t^{TS,ch} \leq 1 \qquad \forall t \tag{6}$$

$$0 \leq \delta_t^{TS,dis} \leq 1 \qquad \forall t \tag{7}$$

$$0 \leq R_t^{TS} \leq R^{TS,max} \qquad \forall t \tag{8}$$

where R_t^{TS} and R_{t-1}^{TS} are the energy levels in the battery at time *t* and *t-1 (kWh)*; $R^{TS,stor}$ is the energy portion that the battery is capable of charging or discharging during time *t (kWh)*, and $\delta_t^{TS,ch}$

and $\delta_t^{TS,dis}$ are the binary variables which can take values either 0 or 1 model indicating that the battery can either only be charged or discharged at time *t*, and $R^{TS,max}$ is the maximum battery charge *(kWh)*. The battery is assumed to have constant charging and discharging speeds, and no performance degradations or losses are considered.

b) Environmental and operational conditions

A set of the environmental and operational conditions impacts TS energy consumption, production and strategy for battery scheduling. This section presents the specific environmental and operational conditions influencing TS operation and provides their models.

The solar irradiation s_t *(W/m²)* at time *t* affects the amount of energy required by the consumers, e.g., the inside and outside lighting of the TS, and also the energy output of PV panels. Different approaches have been proposed to model the behaviour of solar irradiation, e.g., probability density functions (PDFs), times series [97] and artificial NN [98]. In the present work, we use the beta distribution, a sufficiently flexible two-parameter distribution that can fit well the empirical data under different conditions [96], [97], [99]. We use Beta distribution to model solar irradiation as in [100] for simplicity given that the focus of the work is not to model the fluctuations and make accurate predictions of solar irradiation, but to illustrate an optimization framework capable of handling this aspect. In the application of the papers 2 and 3 of Part II [87], [101], the average hourly solar irradiation data from [95] has been used to estimate the beta parameters.

The passenger flow F_t^{pas} *(number/h)* through TS at time *t* is the most important factor influencing the energy consumption of the lifting equipment, i.e., elevators and escalators. The passengers' flow is provided by the TS operator, who takes in-situ real time records of the passengers flow during the opening periods of the TS , i.e., from 5 a.m. to 1 a.m. of the next day, with a time step of one hour. The typical passengers flow in the TS during week day and week day and week end is presented in Figure 8. The two characteristic peaks during the working days related to the periods of high affluence of passengers going to work and coming back home can be noticed. The passengers' flow during the week-end days is almost constant throughout the day, at a level which is around 15% of that of peak during working days.

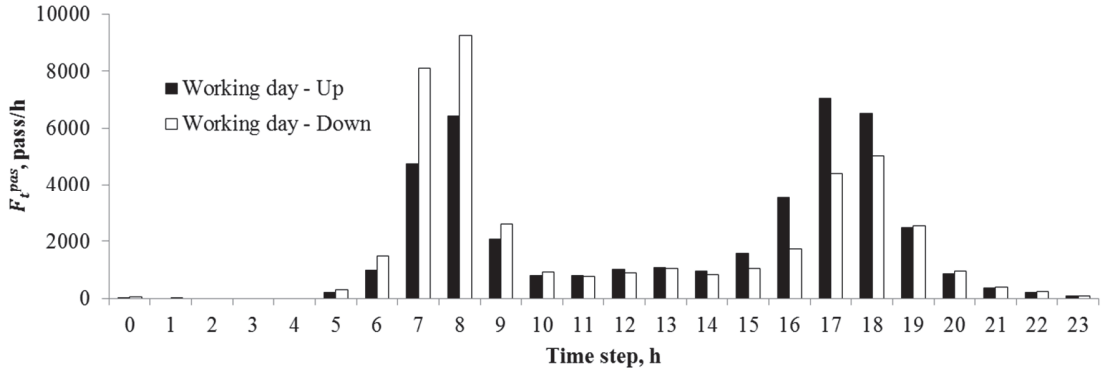

a)

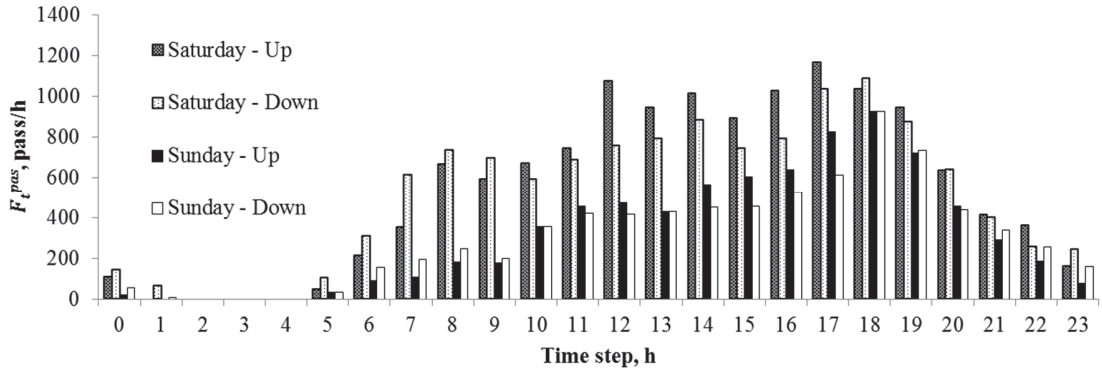

b)

Figure 8. Up and down passenger flow through the TS: a) working days; b) Saturday and Sunday.

Another key variables are the electricity prices affecting TS expenses and revenues. In the paper 2 of Part II [87], the market electricity price c_t^p (€/kWh) is assumed variable in a way similar to the trend of the wholesale market price in France [102] lead to hourly electricity market prices higher during working days than during weekends, which is situation is typical for most electricity systems. However, in countries with strong electricity markets, which include producers, consumers and transmission companies, the correlation between electricity consumption and price decreases significantly. Moreover, the electricity price of the individual regional market can be highly affected by other factors, e.g., fuel availability and transmission constraints. In this view, the existing speculations in the fuel markets can artificially increase the electricity price during the periods of low electricity demand (the case of some regions in UK). In addition, it was assumed

that the grid offers fixed electricity price c_t^s *(€/kWh)* to purchase the energy from the TS. The electricity price c_t^D *(€/kWh)* is the price offered to TS by the local community D to purchase the energy.

c) Microgrid agent objectives

In order to formulate agent energy management problem, the TS agent is represented as 'open systems' that continuously interact with other agents and the external grid through energy exchanges at time *t* (Figure 9).

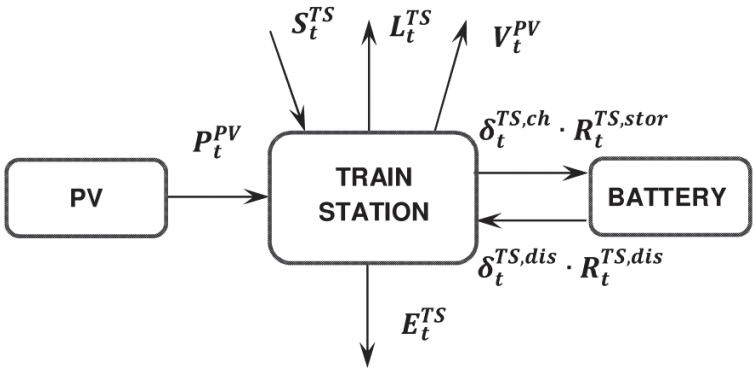

Figure 9. . Input and output energy flows for the TS agent.

By taking into account the portions of energy exchanged between the agents (TS and D) and the external grid, the objective functions to be minimize can be formulated in terms of expenses for energy purchase minus revenues for energy sale for the time period *T*:

$$\alpha^{TS} = \sum_{t=0}^{T}(c_t^p \cdot S_t^{TS} - c_t^s \cdot L_t^{TS} - c_t^D \cdot V_t^{PV}) \qquad \forall t \qquad (9)$$

where α^{TS} *(€)* is the total costs for TS for time periods of duration *T*, c_t^p and c_t^s ($€kWh$) are average hourly prices of purchasing and selling one *kWh* from/to the external grid, respectively, and c_t^D *(€kWh)* is the average hourly price of one *kWh* from the bilateral contract agreed with D, L_t^{TS} *(kWh)* is the energy portion sold to the external grid, S_t^{TS} *(kWh)* is the energy portion purchased from the external grid, V_t^{PV} *(kWh)* is the energy portion sold to the D and generated by the PV panels.

The energy optimization problems for the TS is formulated as follows.

Optimization problem - TS

Minimize $\boldsymbol{\alpha^{TS}}$

s.t.

$$E_t^{TS} + L_t^{TS} + \delta_t^{TS,ch} \cdot R^{TS,stor} - \delta_t^{TS,dis} \cdot R^{TS,stor} + V_t^{PV} \leq P_t^{PV} + S_t^{TS} \qquad \forall t \qquad (10)$$

$$\sum_{t=0}^{T} (c_t^p \cdot S_t^{TS} - c_t^s \cdot L_t^{TS} - c_t^D \cdot V_t^{PV}) \leq \alpha^{TS} \qquad (11)$$

$$L_t^{TS} + V_t^{PV} \leq P_t^{PV} \qquad \forall t \qquad (12)$$

$$\begin{cases} \beta \cdot \tilde{E}_t^D \leq V_t^{PV}, & if\ P_t^{PV} \geq \beta \cdot \tilde{E}_t^D \\ 0 \leq V_t^{PV}, & otherwise \end{cases} \qquad \forall t \qquad (13)$$

$$R_t^{TS} \leq R_{t-1}^{TS} + \delta_t^{TS,ch} \cdot R^{TS,stor} - \delta_t^{TS,dis} \cdot R^{TS,stor} \qquad \forall t \qquad (14)$$

$$\delta_t^{TS,ch} + \delta_t^{TS,dis} \leq 1 \qquad \forall t \qquad (15)$$

$$0 \leq \delta_t^{TS,ch} \leq 1 \qquad \forall t \qquad (16)$$

$$0 \leq \delta_t^{TS,dis} \leq 1 \qquad \forall t \qquad (17)$$

$$0 \leq R_t^{TS} \leq R^{TS,max} \qquad \forall t \qquad (18)$$

$$S_t^{TS} \geq 0 \qquad \forall t \qquad (19)$$

$$L_t^{TS} \geq 0 \qquad \forall t \qquad (20)$$

where β is the coefficient defining the minimum amount of energy to be sold to D by TS, $\tilde{E}_t^D$ (kWh) is the expected energy demand for D at time step *t*, predicted by TS. The optimization problems account for the energy balance eqs. (10), (12), and the costs eqs. (11). The batteries charging and discharging dynamics is formulated with eqs. (14) - (18) and eqs.(19) and (20) are the decision variables constraints. The coefficient β in eq. (13) increases the regularity of energy exchanges between the microgrid agents, by imposing the minimum amount of energy that TS must supply to the D under conditions of availability of wind and solar energy outputs and promoting the local energy exchanges among the microgrid agents. The energy management decisions are done by using the communication and energy exchanges protocols. The communication protocol developed in this thesis is presented Paper 2 and 3 of Part II [87], [101].

After clear statement of the energy management problem, microgrid agent uses different prediction, communication and optimization modules to address its optimization objectives. In order to improve agent confidence in energy management decisions and ensure system reliability against uncertainties, the multi-layered agent architecture, described in Section 3.2, has been integrated with different CI modules giving to the TS the capabilities of:

- capturing and prediction environmental and operational conditions, e.g., Markov chain model [100] and NSGA-II – trained NN [87], [99];
- performing local planning and decision-making, e.g. RL [100] and RO [87], [99];
- communicating and exchanging with other microgrid agents, e.g. agents communication protocol [87], [99];
- learning and evaluation , e.g. RL [100].

The detailed description of these CI modules is done in scientific papers 1 – 3 of Part II [87], [101], [103].

3.3.2. Methodological and applicative contributions

In this PhD thesis work, the coordination procedures for the microgrid energy management are done in a decentralized manner through the local planning and the direct negotiation among the agents, similar to [69], [81]. To facilitate the agents communication, an additional agent called ISO, inspired from [85], has been introduced in the model to assist the communications between the microgrid agents. The developed ABM framework has been shown to be flexible and modular, and is capable of accommodating more complex models of the individual agents, e.g., the refinement of the time step to account for shorter-term variations. The specific communication and decision-making scheme developed for the microgrid operation allows an efficient energy management among the microgrid agents: on the one hand, it increases the revenues of renewable generators by deciding their most profitable energy strategy; on the other hand, it encourages the purchase of emissions-free and less expensive energy by the microgrid consumers. A detailed description of the ABM of the individual components of the microgrid and the of agent interaction framework is presented in Papers 2 and 3 of Part II [87], [101].

If compared with the limitations of the modelling developments summarized in Section 1.3, the main contributions of this thesis work, in terms of the modelling and optimization frameworks,

must be considered jointly with the intelligence models developed for the microgrid agents. The benefit gained with this joint development lies in the consideration of the individual intelligent agent as an autonomous decision-making entity that accounts for its individual objectives. By doing so, the global optimization of the ABM of the microgrid is achieved through the joint consideration of all the optimization problems of the individual agents. In this view, the present thesis work makes a relevant contribution to the development and implementation of the ABM and optimization framework, by developing, implementing and evaluating different approaches to model the individual intelligences of the microgrid agents, i.e., RO and RL.

The developed optimization frameworks for the microgrid energy management are capable of explicitly considering the uncertainty associated to the stochasticity of operational and environmental conditions, as well as the mechanical failures of the renewable generators. The uncertainty related to the predictions of the energy quantities and the information communicated by the agents is also accounted. For more details, the reader is referred to Papers 2 and 3 of Part II [87], [101].

The reader is referred to Chapter 4 for a methodological description of the approaches considered to model the agents intelligences and to Papers 1, 2 and 3 of Part II for their application [87], [101], [103].

4. INDIVIDUAL INTELLIGENCE FOR ENERGY MANAGEMENT IN STOCHASTIC ENVIRONMENTS

In this chapter, the approaches considered to model the individual agents intelligences that are incorporated in the framework developed in this thesis are presented in details. Section 4.1 introduces the RL algorithm, which allows learning from a stochastic environment and making use of the experience to select optimal energy management actions. Section 4.2 presents the formulation of the RO problem that accounts for the uncertainty. Each section includes the exemplification of the applicative contributions, retrieved from the scientific papers of Part II. Section 3.3 summarizes the overall methodological and applicative contributions done in terms of microgrid energy management based on RL and RO.

Chapter 4 gives also the references to Part II that provides the exemplification of the individual intelligence approaches developed and implemented. Paper 1 shows the application of the 2 steps-ahead RL algorithm to plan the consumer energy management actions in a microgrid with a stochastic environment. Papers 2 and 3 illustrate the application of the RO framework for the optimization of the individual objectives of the microgrid stakeholders under uncertainty.

4.1. Reinforcement learning (RL)

This section introduces and exemplifies the problem statement for the microgrid energy management and presents the optimization approach used to address the problem statement. The section also presents the example of results for the specific case study of the microgrid energy management.

4.1.1. Problem statement

By taking into account the limitations of current developments in terms of energy management, identified in Section 1.3, and the research focus, stated in Section 2.3, this thesis work aims to bring contributions in the microgrid energy management by addressing several optimization challenges. In this view, the following aspects are taken into account:

- individual agents objectives,
- agent-environment interaction;

- uncertainties.

The example of microgrid energy management, explored in Paper 1 of Part II [103], is considered here to illustrate this problem statement. In this paper we focus on a simple urban microgrid involving a consumer with inelastic load D_t, a transformer, providing electricity power from the external grid as well as information about the electricity market price P_t, a renewable generator with available power output P_t^{wt} and a storage facility with a level of battery charge R_t, where the subscript t is used to indicate time (Figure 10). The consumer has the possibility to control the storage and renewable generator, and thus, can decide to purchase all electricity from the external grid or cover partly its demand by using the electricity produced by the local renewable generator. For this, the consumer can store electricity when the renewable resource is available and discharge the storage when needed. The model is kept purposely simple, but sufficiently comprehensive in the properties relevant to the study of the RL paradigm, selected to address energy management challenges.

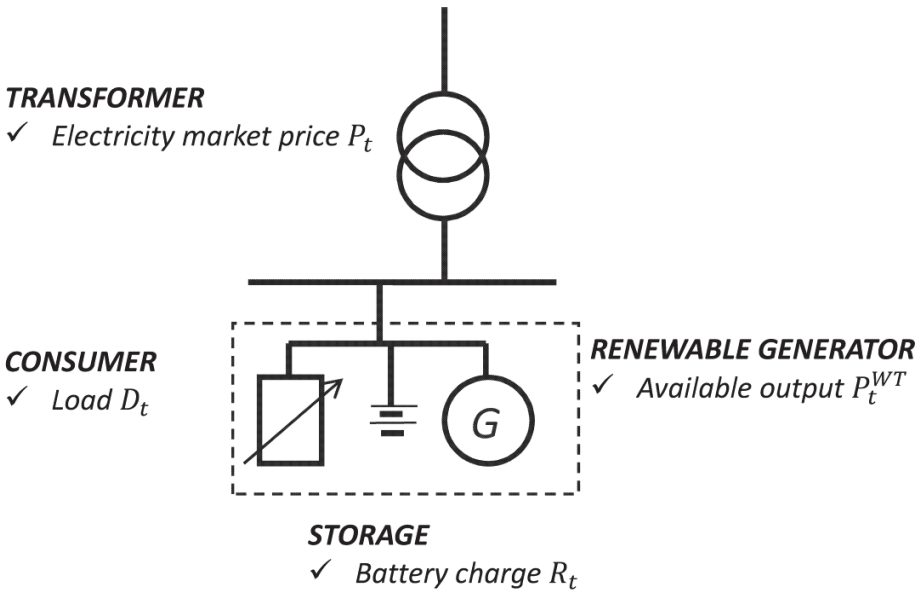

Figure 10. Architecture of the considered microgrid.

For the considered case, the consumer strategy is driven by the optimization of a numerical reward, which quantifies two goals or decision-making criteria. These goals are: i) increasing the utilization rate of the battery during high electricity demand (so as to decrease the electricity purchase from the external grid) and ii) increasing the utilization rate of the wind turbine for local

use (so as to increase the consumer independence from the external grid). The optimization of the numerical reward is achieved through the choice of the action $a_t^j = [a^0, a^1]$ of battery scheduling. Since the battery cannot be charged and discharged at the same time, only one of these actions can be selected and performed at any time step *t*: this makes the two criteria conflicting and for this reason, the consumer aims at increasing its performance by selecting an optimal sequence of actions for an energy management planning horizon.

The decisions for the optimal energy management must be done under several uncertainties. In Paper 1 of Part II [103], these uncertainties are related to the variability of energy output P_t^{wt} from the wind generator, affected by the availability of the wind source and the random mechanical failures of the wind generator components [104], [105]. Markov chain modelling framework is adopted to describe the dynamics of stochastic transition among different levels of wind speed conditions and mechanical states (Figure 11). This approach is used to model natural processes, including synthetic generation of hourly wind speed time series [106], [107].

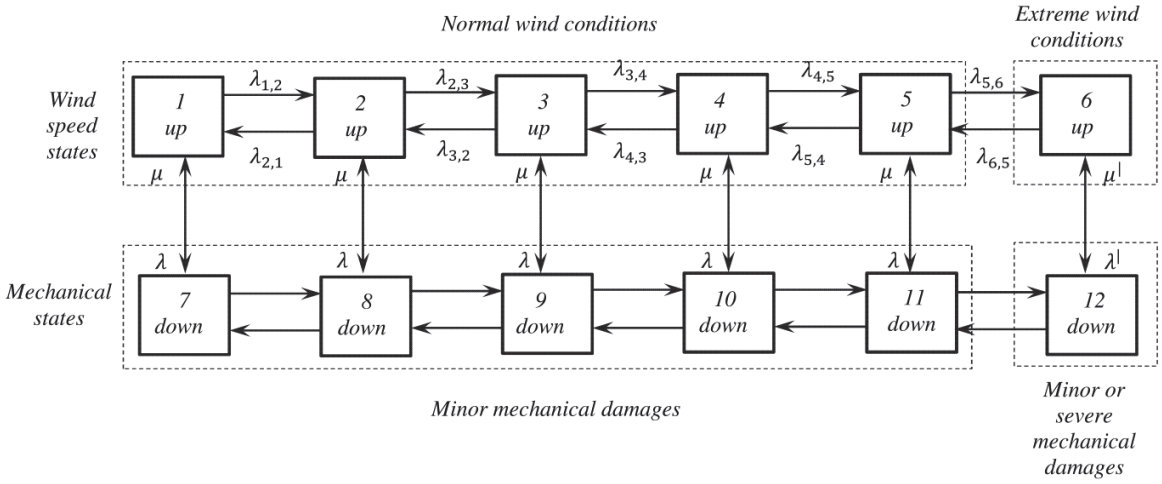

Figure 11. Markov chain model for wind generation.

The transition rates are calculated based on the principle of frequency balance between any two states, presented in [108]. As input data for the transition rates calculation, the wind speed data with one hour time step from [109] is used. Based on the various references [108], [110]–[113]. The correlation between wind speed intensity and severity of occurred failures is taken into account with Markov chain model.

We adopt an ABM framework to implement the decision-making heuristics, learning rules and adaptive processes of interactions with the environment [84]. Specifically, the consumer is presented in the form of an individual agent who evolves by interacting with its environment defined through the available wind power output P_t^{wt}, the load D_t and the level of battery charge R_t. The decisions linked to these interactions are driven by the particular goals of the consumer and are implemented in the form of battery scheduling actions, following a process of RL presented in details in Section 4.1.2. By so doing, we implement intelligence directly into the consumer's behaviour, so that he can decide and act in its own interests without implication of additional management actors, such as the facilitator used for energy management in electricity grids with multiple distributed generations [69].

4.1.2. RL algorithm

An optimization framework that is based on RL is characterized by a learning process that is based on rewards or penalties on actions taken in response to environmental dynamics [114], [115]. In a deterministic setting, this method allows to find the optimal set of actions for a given environmental state whereas in a stochastic setting, it is capable of accounting for the uncertainties in the exploration of the environment [115].

As highlighted in [114] "the most important feature distinguishing RL from other types of learning is that it uses training information that evaluates the actions taken rather than instructs by giving correct actions." This optimization method uses the combination of an instructive feedback, indicating the correct action to be taken, and an evaluative one, which assess random unforeseen actions.

The Q-learning method has shown to achieve excellent performance in the dynamic power management of embedded systems by minimizing power consumptions [116], [117]. First introduced in 1989 [118], Q-learning is widely applied as a RL algorithm that makes use of an action-value function to evaluate the utility of the performed action. This can be formulated as follows:

$$Q\left(s_t^i, a_t^j\right) \leftarrow Q\left(s_t^i, a_t^j\right) + \alpha\left(r\left(s_t^i, a_t^j\right) - Q\left(s_t^i, a_t^j\right)\right) \quad (21)$$

where $Q(s_t^i, a_t^j)$ is the value function of the state-action pair (s_t^i, a_t^j), $0 < \alpha < 1$ is the learning rate, and $r(s_t^i, a_t^j)$ is the reward value received as the result of taking action a_t^j in state s_t^i at time *t*.

A reward function $r(s_t^i, a_t^j)$ is used to define the goal of the RL [114]; the corresponding reward value in response to a performed action quantifies the benefit of this action at the current state. When evaluating the return corresponding to a sequence of actions, the discounted parameter γ is introduced to bound the total return as follows:

$$r_t = r_{t+1} + \gamma r_{t+2} + \gamma^2 r_{t+3} + \cdots = \sum_{k=1}^{\infty} \gamma^k r_{t+k+1} \tag{22}$$

The discount rate $0 < \gamma < 1$ is used to 'weigh' the values of the reward functions that are expected to be obtained after performing the sequence of actions at successive times *t+1*, *t+2*, *t+3* etc. Discounting describes that rewards arriving further in the future are worth less.

The trade-off between exploitation and exploration is usually ensured by using an ε-greedy action selection approach [114]. For each time step *t*, each agent generates a random parameter $0 < \xi < 1$. If $\xi < \varepsilon$, which is the fixed probability of the random action selection for each time step, then a random action is selected. Otherwise, the agent performs the action a_t^j with the highest value $Q(s_t^i, a_t^j)$ for state s_t^i, from history records that are usually stored in matrix form:

$$\begin{array}{c} \\ s^0 \\ \vdots \\ \boldsymbol{s^i} \\ \vdots \\ s^n \end{array} \begin{array}{c} \begin{array}{ccccc} a^0 & \cdots & \boldsymbol{a^j} & \cdots & a^m \end{array} \\ \begin{bmatrix} Q^{0,0} & \cdots & Q^{0,j} & \cdots & Q^{0,m} \\ \vdots & & & & \vdots \\ Q^{i,0} & \ddots & \boldsymbol{Q^{i,j}} & \ddots & Q^{i,m} \\ \vdots & & & & \vdots \\ Q^{n,0} & \cdots & Q^{n,j} & \cdots & Q^{n,m} \end{bmatrix} \end{array} \tag{23}$$

By using eq. (21), the Q-value of each action a_t^j for each state s_t^i automatically converges to its maximum Q*-value by following the optimal policy of actions selection [119].

The simplified architecture of a RL [114], illustrated in Figure 12, is widely used in the domain of agent learning [115]. *Agents* interact with their *environment* by receiving signals about states and rewards. On its turn, the environment receives from the agents signals about the performed actions. To exemplify this interaction we use the previous notation. At time step *t*, each agent receives the information about the environment state, denoted as s_t^i. By taking into account this information,

each agent selects and performs action a_t^j, which updates the environment state to s_{t+1}^p at time step *t+1*. Based on this update, each agent receives a reward, which evaluates the benefit of this update from the point of view of the agent objective. Here, the dotted line denotes the time horizon of a single time step *t*, with the new state and reward signals after action a_t^j has been performed.

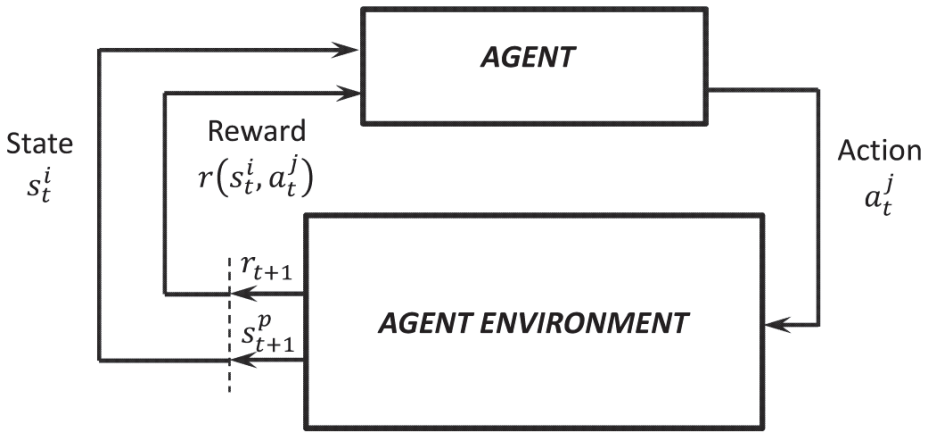

Figure 12. Simplified architecture of the RL mechanism [114].

This approach has also been applied to develop a comprehensive and beneficial demand response model for energy pricing [81]: a retail energy provider exploits Q-learning to define the optimal real time pricing considering different aspects such as price caps and customer responses. The Q-learning method can be coupled with other approaches, e.g., leading to genetic-based fuzzy Q-learning [120] and Metropolis Criterion-based fuzzy Q-learning [121] for intelligent energy management.

4.1.3. Results exemplification

The RL algorithm is used in Paper 1 of Part II [103] to model the consumer's adaptation to a dynamically changing environment by performing actions of battery scheduling. The synthetized form of the algorithm is presented below:

1. Initialize to 0 the Q-values of all possible actions sequences for each scenario and set time t=0.

2. a) For time t, identify the values of load D_t and available wind power output P_t^{WT}, and make the forecast of available wind power output P_{t+1}^{WT}, P_{t+2}^{WT} and load D_{t+1}, D_{t+2} for 2

steps-ahead. Identify $Scenario_t^l = [s_t^i; s_{t+1}^n; s_{t+2}^p]$, *the forecasted states of wind conditions for the local generation, simulated with the Markov chain model.*

b) Based on identified $Scenario_t^l$ *and battery charge* R_t *at time step t, define all possible actions sequences of battery scheduling for 2 steps ahead.*

c) Apply the policy for selection of sequence of actions.

d) Perform the selected sequence A_t^j *under real system conditions, simulated using the Markov chain model for real wind conditions. Update the value of the sequence performed.*

3. *Move to time step t+3; repeat step 2.*

Note that the uncertainty in load is not accounted here, as the consumer is assumed to hold a perfect knowledge about its own consumption.

The diagram of the algorithm and simulation scheme for forecasted and real wind speed conditions is presented in Figure 13.

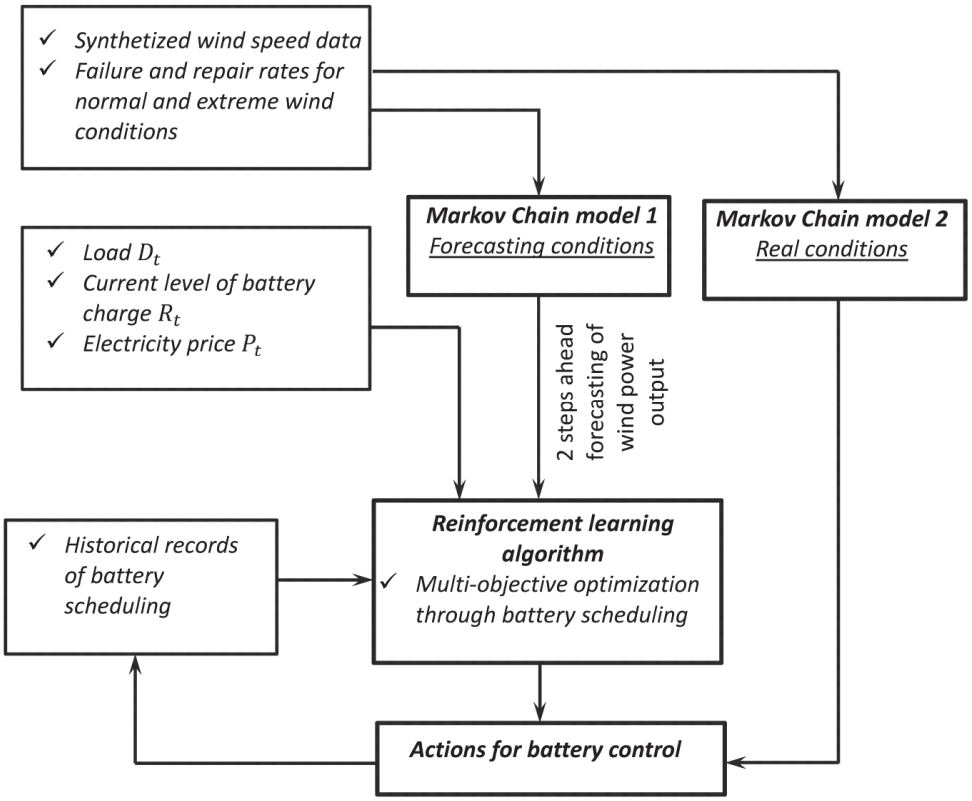

a)

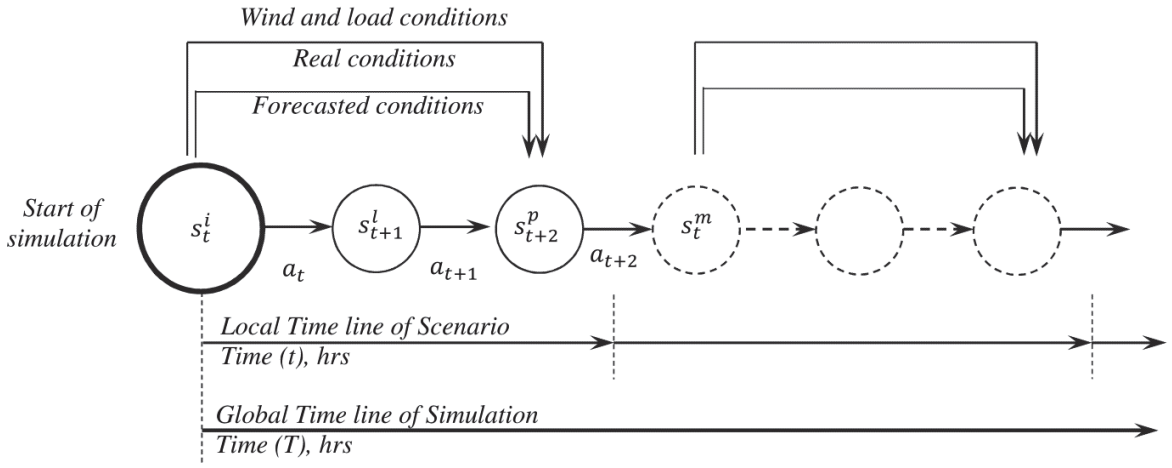

b)

Figure 13. The RL algorithm: a) Structure of the battery scheduling algorithm; b) Simulation scheme for forecasted and real wind speed conditions.

As it can be seen from Figure 13, forecasted and real wind speed state evolutions are modeled with two identical Markov chain models. The first Markov chain model generates the forecasts of wind speed conditions, which are used to identify the 2 steps-ahead scenario and select the actions sequence for battery scheduling. The second Markov chain models real wind speed conditions, starting from the same state as the forecasted conditions, under which the selected actions sequence will be performed.

As described previously, the learning process is achieved through the selection of sequences of actions for 2 steps-ahead scenarios. Firstly, the continuous repetition of similar scenarios with random selection of sequence of actions allows to define the maximum Q*-values of all sequences. Secondly, the selection of a high-valued sequence of actions allows to perform the sequence of actions for battery scheduling most adapted to each scenario. However, the repeated occurrence of similar scenarios, for the definition of the maximum Q*-value, is considerably affected by the stochasticity of the wind power output P_t^{WT}. In other words, the efficiency of the learning process depends on the rate of occurrence of similar scenarios. The learning process can be illustrated with the learning trend (Figure 14) providing the occurrence rate of new scenarios and scenarios with more than a threshold number, after which the optimal actions are already identified (here threshold is fixed to 16 repetitions of the same scenario). On the one hand, Figure 14 shows the

fast decrease of the occurrence of new scenarios during the simulation. After 10 years, the proportion of new scenarios represents less than 1.5% of the total number of scenarios occurred annually. The number of scenarios with more than 16 occurrences rises to 87% in the last year of simulation: this large number of scenarios occurrences (16) allows identifying the action sequences of highest Q*-value for battery scheduling.

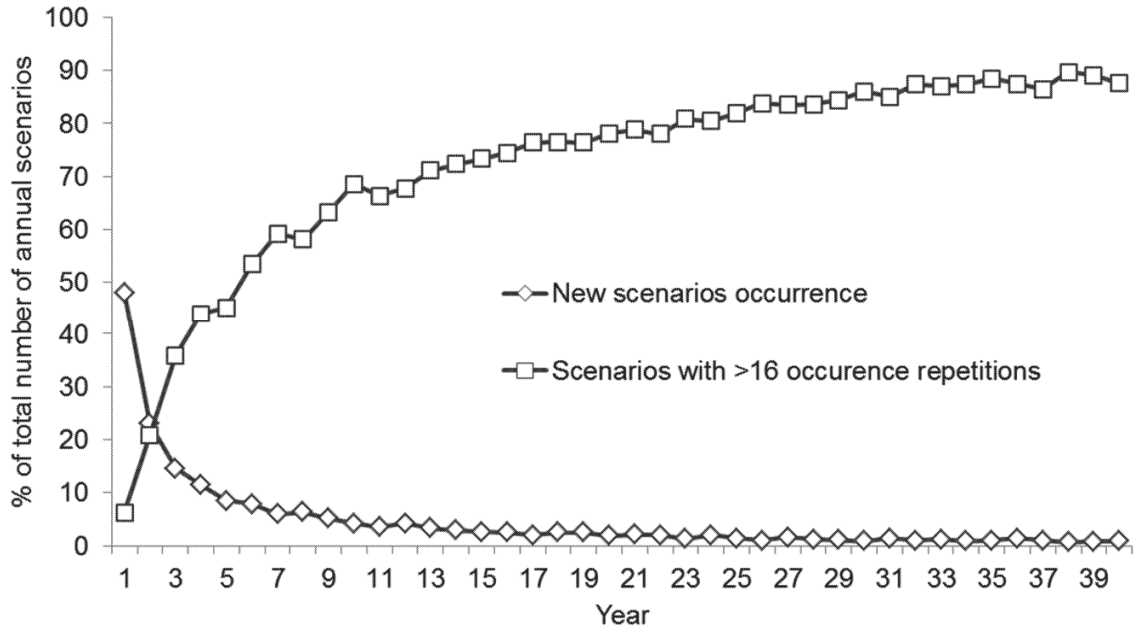

Figure 14. Trend of new scenarios occurrence and scenarios with more than 16 occurrence repetitions.

In this view, Figure 14 represents the learning (or training) period for the RL algorithm during which the optimal actions can be identified for different scenarios. This training period can be illustrated by several indicators evaluating the level of consumer goals achievement. One of them is the cumulative annual expenses of microgrid consumer for the power purchase from the external grid E^{av}, which shows the progressive decrease during the learning period (Figure 15). This gives the evidence of the continuous improvements brought by the RL.

Figure 15. The annual cumulative expenses of consumer E^{av}.

According to the results of Paper 1 of Part II [103], the trained RL algorithm can accomplish an average improvement of 12.88% E^{av} in comparison with the case when the consumer does not have precise goals to follow in the selection of an optimal sequence of actions. It also provides the support tool for the daily energy management with battery scheduling, illustrated in Figure 16 for a day of operation.

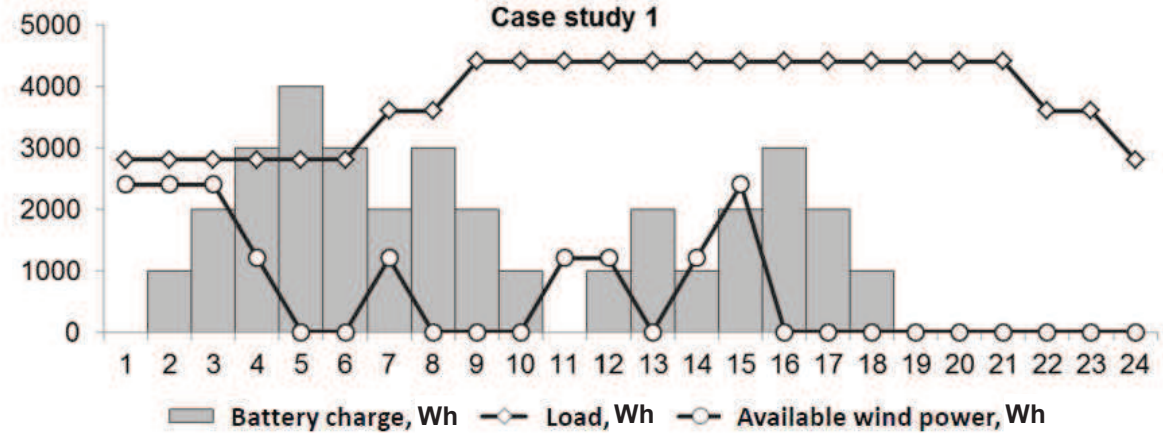

Figure 16. Example of battery scheduling process for a day of operation.

For more details regarding the definition the RL feature for case study used of problem statement exemplification (Section 4.1.1), the extended sensitivity and results analysis the interested reader can refer to Paper 1 of Part II [103].

4.2. Robust optimization (RO)

This section presents the extended problem statement in comparison with the developments done in Section 4.1 and exemplified in Paper 1 of Part II [103]. Similar to Section 4.1 this section presents the optimization algorithm used to tackle the energy management problem and the example of results for the specific case study of the microgrid energy management.

4.2.1. Problem statement

Microgrid energy management with the RL algorithm presented and exemplified in Section 4.1 brings several major contributions to the research focus of the thesis, mapped in Section 2.3, e.g., explicitly accounts for the individual microgrid agents objectives and perform energy management under uncertain renewable energy generation and mechanical failures. However, few major limitations need to be highlighted and addressed with further development. These limitations, mainly related to the specificity of the RL algorithm and the way it tackle the uncertain parameters, are the follows:

- The increase of parameters characterised the operational state of microgrid system or the duration of planning scenario drives the increase of problem complexity, e.g., extend of the learning period for optimal action identification and decrease the computational tractability of the optimization problem.
- RL needs time to gain knowledge in order to identify the optimal actions to take for the specific scenario.
- The uncertain parameters are estimated as the point predictions, which do not always allow the reliability margin for the energy management decision.

In this view, a range of developments must be done to address these limitations allowing the optimal and efficient energy management in the multi-agent microgrid under different environmental and operational uncertainties. The example of such microgrid case study, is retrieved from the Papers 2 and 3 of Part II [87], [101] (Figure 17).

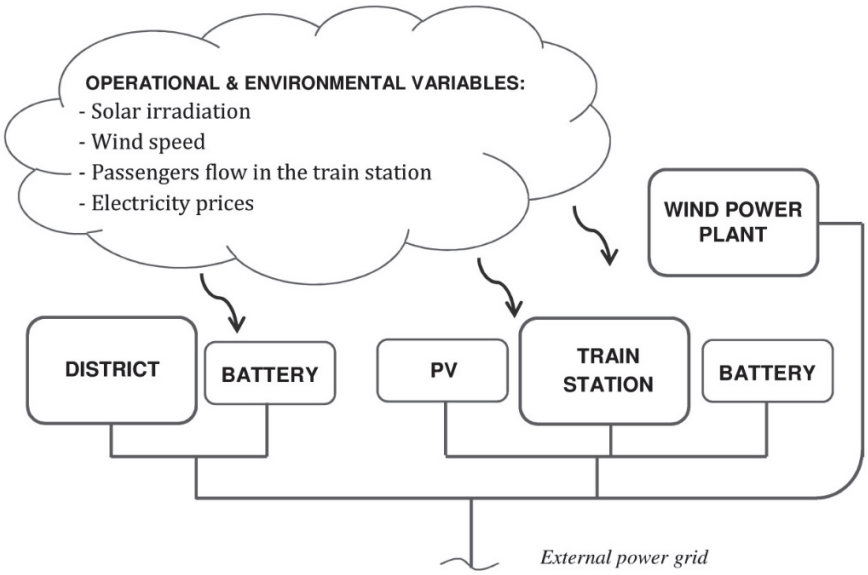

Figure 17. Scheme of the reference microgrid.

This reference system includes a middle-size TS, which can play the role of power producer and consumer, the surrounding D with residences and small businesses, and a small urban wind power plant (WPP). The goal of TS is to decrease its electricity expenses while satisfying its demand. To achieve this, the TS strategy includes the integration of renewable generators and energy exchanges with the local community to increase the power flexibility of the microgrid. Photovoltaic panels (PV) have been shown to be an adapted and efficient technology for its implementation on large commercial, public buildings and transportation hubs [89], [90]. For the energy exchanges with local community, we consider only the possibility of exchange between the TS and the D. This is done to keep the model simple but also complete in order to properly illustrate the optimization analysis.

The goal of WPP is to increase its revenues from selling the electricity to the external grid and to the D. The latter is considered only as an energy consumer, with the goal of decreasing its electricity purchase from the external grid by prioritizing the purchase of electricity from local sources, i.e., the TS and the WPP. In addition, we assume that the TS and the D have the capacity to store electricity in batteries.

As the additional goals are the improvement of overall system reliability and the efficient use of locally installed renewable generators and storage.

The microgrid agents decisions about the optimal energy management strategies, as well as the global reliability of the microgrid, are affected by the uncertain parameters, such as energy outputs from renewable generators P_t^{PV} and P_t^{WPP}, energy demands of the consumers E_t^{TS} and E_t^{D}, and electricity prices c_t^{p}, c_t^{s} and c_t^{D}. In addition, the technical failures of renewable generators are accounted for.

To tackle the limitations of the previous work, where the uncertain parameters are accounted as the point predictions, here the uncertain parameters are quantified in terms of PIs estimated by a NSGA-II – trained NN [122]. These PIs are optimized both in terms of coverage probability (CP) and PI width (PIW). For this purpose, a multi-objective NSGA-II is implemented to find the optimal parameters (weights and biases) of the NN. By using NSGA-II, Pareto-optimal solution sets, including several non-dominated solutions with respect to the two objectives (CP and PIW), are generated. The example of Pareto front of PIs for TS energy demand E_t^{TS} is depicted in Figure 18. From this Pareto front different solutions can be selected and used in the energy management by RO, differing in interval widths and coverage probability.

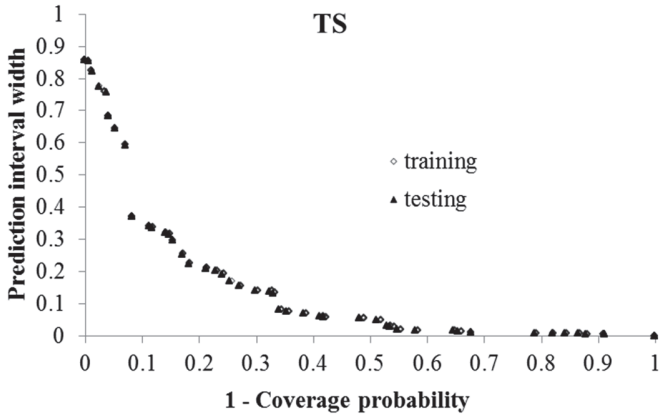

Figure 18 Pareto fronts of PIs for E_t^{TS}.

The microgrid agents are represented as the individual agents following their energy management objectives by taking into account their interactions with other microgrid agents. For more details about models of individual agents, their operational environment and the communication protocol they are using, the interested reader is invited to refer to Papers 2 and 3 of Part II [87], [101].

4.2.2. RO algorithm

This section discusses some of the optimization techniques that have been specifically designed in this PhD work to account for the variability and randomness of the operational and environmental parameters. Optimization approaches for this have been progressively developed and extended over the last years. Fuzzy mathematical programming models and their extensions have been successfully applied for the optimal management of hybrid energy systems [123], [124]. Stochastic programming, where the uncertain parameters are accounted for by probability distributions and interval programming models [125], [126], have been used to deal with different sources of uncertainty in different frameworks, e.g., economic-energy scenarios planning [127], design of renewable systems for community energy management [128] and water quality and waste management [129], [130].

In this PhD thesis, RO has been adopted as the framework for achieving optimal actions scheduling strategies under uncertainty.

For explanation purposes, consider a nominal linear optimization problem (eq. (24)), where uncertainty affects only the elements in matrix **A** whereas the objective function **c** is not subject to uncertainty:

$$\begin{aligned} &\text{maximize} && \boldsymbol{c'x} \\ &\text{subject to} && Ax \leq b \\ & && 1 \leq x \leq u \end{aligned} \tag{24}$$

This formal problem was analysed in [131] with the aim of constructing a solution that is feasible for any data belonging to a convex set. The formulation considers a particular row *i* of the matrix **A** where J_i represents the set of coefficients in row *i* that are subject to uncertainty. To account for the uncertainty in each entry $\tilde{a}_{ij}, j \in J_i$, it is modelled as a symmetric and bounded variable $\tilde{a}_{ij} \in \left[a_{ij} - \hat{a}_{ij}, a_{ij} + \hat{a}_{ij}\right]$, where a_{ij} represents the expected value of the parameter and $\hat{a}_{ij}$ is its uncertainty interval width. The resulting robust counterpart of problem eq. (24) is:

$$\begin{aligned} &\text{maximize} && \boldsymbol{c'x} \\ &\text{subject to} && \textstyle\sum_j a_{ij}\, x_j + \sum_{j \in J_i} \hat{a}_{ij}\, y_j \leq b_i, \qquad \forall i \end{aligned} \tag{25}$$

$$-y_j \le x_j \le y_j \qquad \forall j$$

$$1 \le x \le u$$

$$y \ge 0$$

Note that if x^* is an optimal solution, $y_j = |x_j^*|$, then:

$$\sum_j a_{ij}\, x_j + \sum_{j \in J_i} \hat{a}_{ij}\, |x_j^*|, \le b_i, \qquad \forall i \tag{26}$$

It has been shown [126] that for any possible realization $\tilde{a}_{ij}$ of the uncertain data, the solution remains feasible and 'robust':

$$\sum_j \tilde{a}_{ij}\, x_j{}^* = \sum_j a_{ij} x_j^* + \sum_{j \in J_i} \eta_{ij} \hat{a}_{ij}\, x_j^* \le \sum_j a_{ij} x_j^* + \sum_{j \in J_i} \hat{a}_{ij}\, |x_j^*| \le b_i, \qquad \forall i \tag{27}$$

where $\eta_{ij} = (\tilde{a}_{ij} - a_{ij})/\hat{a}_{ij}$ is the random variable associated with the uncertain data $\tilde{a}_{ij}$, which obeys an unknown but symmetric distribution, and takes values in $[-1, 1]$. In this view, for every i^{th} constraint, the term $\sum_{j \in J_i} \hat{a}_{ij}\, |x_j^*|$ gives the necessary protection of the constraint by managing a gap between $\sum_j a_{ij} x_j^*$ and b_i [126].

This formulation of the optimization problem allows obtaining conservative solutions that ensure the robustness of the model. Following developments have been focused on relaxing the level of conservatism introduced by the robust problem [132]–[135].

The RO formulation adopted in this PhD thesis work has been originally proposed in [126] and allows to linearly formulate the robust counterpart of an optimization problem for different levels of conservatism in the solution. In other words, the new formulation is able to accommodate the parameters uncertainty in the data uncertainty set U without excessively affecting the objective function. By considering the formulation in [131], [126] introduces for every *i* a parameter Γ_i, not necessary integer, that takes values in the interval $[0, |J_i|]$. The role of this new parameter Γ_i is to adjust the level of robustness of the proposed solution; the goal is to derive solutions that guarantee that up to $\lfloor \Gamma_i \rfloor$ of these coefficients are allowed to change, and one coefficient a_{ij} changes by $(\Gamma_i - \lfloor \Gamma_i \rfloor)\hat{a}_{ij}$. By doing so, [126] assumes that nature will be restricted in its behaviour in that only a subset of the coefficients will change in order to adversely affect the solution. Finally, the proposed discrete optimization problem allows the robust solution to be feasible with a very high

probability even if more than $\lfloor \Gamma_i \rfloor$ change. Here below, the resulting linear formulation of the robust counterpart problem in [126] is presented:

$$
\begin{aligned}
&\text{maximize} && c'x \\
&\text{subject to} && \textstyle\sum_j a_{ij}\, x_j + z_i \Gamma_i + \sum_{j \in J_i} p_{ij} \le b_i, && \forall i \\
& && z_i + p_{ij} \ge \hat{a}_{ij} y_j, && \forall i, j \in J_i \\
& && -y_j \le x_j \le y_j && \forall j \\
& && l_j \le x_j \le u_j && \forall j \\
& && p_{ij} \ge 0, && \forall i, j \in J_i \\
& && y_j \ge 0 && \forall j \\
& && z_i \ge 0 && \forall i
\end{aligned}
\tag{28}
$$

where matrix A coefficient $\tilde{a}_{ij}$ is again considered an uncertain parameter varying in the interval $\left[a_{ij} - \hat{a}_{ij}, a_{ij} + \hat{a}_{ij}\right]$, p_{ij}, y_j and z_i are the RO variables which are forced to be greater than or equal to zero, Γ_i defines the level of uncertainty considered in the optimization model (a value of zero corresponds to the deterministic problem) and b_i is a deterministic parameter. As it can be observed, for every *i*, a parameter Γ_i is introduced taking its values within the interval $[0, |J_i|]$; the role of this parameter is to adjust the level of conservatism of the solution [126].

This technique has been recently used for optimal energy system planning under uncertainties related to: the power output of renewable generators [136], production costs [137], electricity demand [138] and their combination [139], [140]. Similarly, the uncertainties can be quantified by probability levels [136]–[138] or by probability bounds on constraint violation [139].

4.2.3. Results exemplification

Using the RO approach described above, the energy management problem for each agent can be reformulated in order to tackle different environmental and operational uncertainty. The optimization problem of TS, presented in Section 3.3.1, is used to illustrate the RO formulation.

TS

Minimize $\boldsymbol{\alpha^{TS}}$

s.t.

$$-S_t^{TS} + L_t^{TS} + \delta_t^{TS,ch} \cdot R^{TS,stor} - \delta_t^{TS,dis} \cdot R^{TS,stor} + V_t^{PV} - P_t^{PV} \cdot x_t^{n+1} + E_t^{TS} \cdot x_t^{n+2} + z_t^{Power} \cdot \Gamma_t^{Power} + p_t^{P_t^{PV}} + p_t^{E_t^{TS}} \leq 0 \qquad \forall t \tag{29}$$

$$z_t^{Power} + p_t^{P_t^{PV}} \geq \hat{P}_t^{PV} \cdot y_t^{P_t^{PV}},\ z_t^{Power} + p_t^{E_t^{TS}} \geq \hat{E}_t^{TS} \cdot y_t^{E_t^{TS}} \qquad \forall t \tag{30}$$

$$-y_t^{P_t^{PV}} \leq x_t^{n+1} \leq y_t^{P_t^{PV}}, -y_t^{E_t^{TS}} \leq x_t^{n+2} \leq y_t^{E_t^{TS}} \qquad \forall t \tag{31}$$

$$L_t^{TS} + V_t^{PV} - P_t^{PV} \cdot x_t^{n+1} + z_t^{Micro} \cdot \Gamma_t^{Micro} + p_t^{P_t^{PV}} \leq 0 \qquad \forall t \tag{32}$$

$$z_t^{Micro} + p_t^{P_t^{PV}} \geq \hat{P}_t^{PV} \cdot y_t^{P_t^{PV}} \qquad \forall t \tag{33}$$

$$\sum_{t=0}^{T} (c_t^p \cdot S_t^{TS} - c_t^s \cdot L_t^{TS} - c_t^D \cdot V_t^{PV}) + \sum_{t=0}^{T} \left(z_t^{Cost} \cdot \Gamma_t^{Cost} + p_t^{c_t^p} + p_t^{c_t^s} + p_t^{c_t^D} \right) \leq \alpha^{TS} \tag{34}$$

$$z_t^{Cost} + p_t^{c_t^p} \geq \hat{c}_t^p \cdot y_t^{c_t^p}, z_t^{Cost} + p_t^{c_t^s} \geq \hat{c}_t^s \cdot y_t^{c_t^s}, z_t^{Cost} + p_t^{c_t^D} \geq \hat{c}_t^D \cdot y_t^{c_t^D} \qquad \forall t \tag{35}$$

$$-y_t^{c_t^p} \leq S_t^{TS} \leq y_t^{c_t^p}, -y_t^{c_t^s} \leq L_t^{TS} \leq y_t^{c_t^s}, -y_t^{c_t^D} \leq V_t^{PV} \leq y_t^{c_t^D} \qquad \forall t \tag{36}$$

$$S_t^{TS} \geq 0, L_t^{TS} \geq 0, V_t^{PV} \geq 0 \qquad \forall t \tag{37}$$

$$\begin{cases} \beta \cdot \tilde{E}_t^D \leq V_t^{PV}, & if\ P_t^{PV} \geq \beta \cdot \tilde{E}_t^D \\ 0 \leq V_t^{PV}, & otherwise \end{cases} \qquad \forall t \tag{38}$$

$$R_t^{TS} \leq R_{t-1}^{TS} + \delta_t^{TS,ch} \cdot R^{TS,stor} - \delta_t^{TS,dis} \cdot R^{TS,stor} \qquad \forall t \tag{39}$$

$$\delta_t^{TS,ch} + \delta_t^{TS,dis} \leq 1 \qquad \forall t \tag{40}$$

$$0 \leq \delta_t^{TS,ch} \leq 1, 0 \leq \delta_t^{TS,dis} \leq 1 \qquad \forall t \tag{41}$$

$$0 \leq R_t^{TS} \leq R^{TS,max}, \qquad \forall t \tag{42}$$

where z_t^{Power}, z_t^{Cost}, z_t^{Micro}, $p_t^{P_t^{PV}}$, $p_t^{E_t^{TS}}$, $p_t^{c_t^p}$, $p_t^{c_t^s}$, $p_t^{c_t^D}$, $y_t^{P_t^{PV}}$, $y_t^{E_t^{TS}}$, $y_t^{c_t^p}$, $y_t^{c_t^s}$ and $y_t^{c_t^D}$ are the RO variables which are forced to be greater than or equal to zero, x_t^{n+1} and x_t^{n+2} are auxiliary variables that are forced to be equal to one. Γ_t^{Power} and Γ_t^{Cost} define the level of uncertainty considered in

each optimization model (a zero value corresponds to the deterministic problem) and are such that $0 \leq \Gamma_t^{Power} \leq 2$ and $0 \leq \Gamma_t^{Cost} \leq 3$ for the TS. As mentioned earlier, the objective function to be optimized for TS is cost for energy purchase. The optimization problems account for the energy balance eqs. (29) and (32), and the costs eq. (34). The batteries charging and discharging dynamics is formulated with eqs. (39) - (42). Eq. (37) presents the decision variables constraints.

Note that the RO presents the advantage that it represents the uncertainty related to the variations of the operational or environmental conditions in terms of PIs without making any assumption about the probabilistic distribution of the uncertainty. For example, for the TS in the robust formulation the level of uncertainty $\hat{E}_t^{TS}$ is calculated as $\hat{E}_t^{TS} = (E_t^{TS,ub} - E_t^{TS,lb})/2$, where $E_t^{TS,ub}$ and $E_t^{TS,lb}$ *(kWh)* are the upper and lower prediction bounds at time *t*, respectively. In this work, we take the mean of the PI as point estimate of the wind energy output E_t^{TS} in eq. (29).

Figure 19 illustrates the structure of the control algorithm and operation procedure of the microgrid. The outputs from the models of the individual components are used to forecast the energy demands of the TS and D, the wind power output of the WPP, as well as the energy prices. These forecasted quantities are used by the RO for the decision making strategy for each agent, identified by using the RO approach, is based on the goal of cost functions minimization for the D and TS, and revenues function maximization for the WPP. These goals are achieved through the strategic battery scheduling and the selection of the optimal energy exchanges between the microgrid agents and the upstream electricity grid. Since the battery cannot be charged and discharged at the same time, only one of these actions can be executed at time *t*. Thus, the consumer aims at optimizing its decision-making strategy on a time horizon of 24 time steps, each of one hour duration.

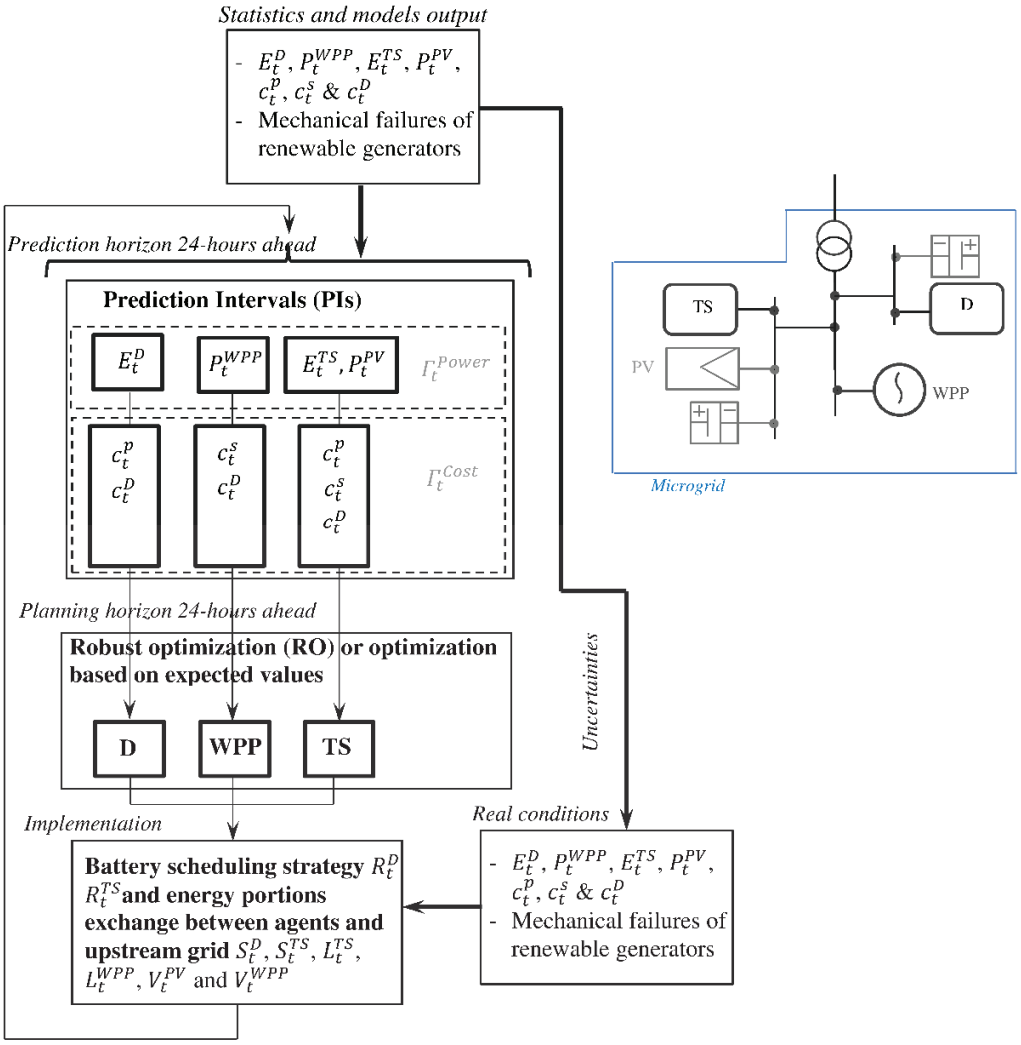

a)

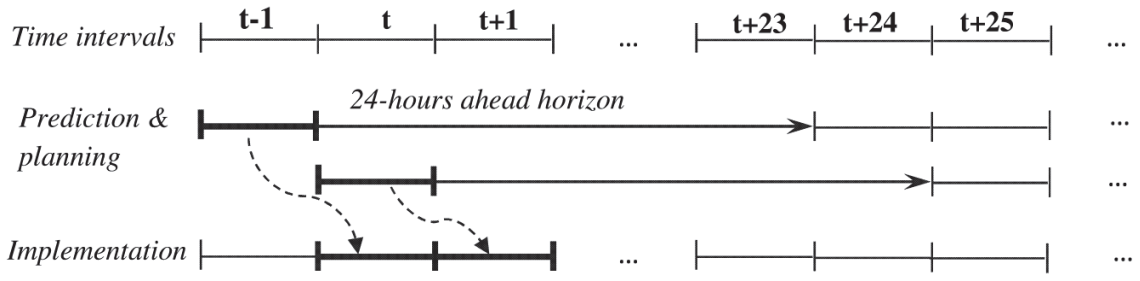

b)

Figure 19. Integrated framework: a) Structure of the control algorithm; b) Operation procedure.

To make the final decision about energy management strategy, microgrid agents uses communication protocol developed and specified in Paper 2 of Part II [87]. For more details the interested reader is invited to refer to Papers 2 and 3 of Part II [87], [101].

The example of energy management for the TS within one working day was selected to illustrate the results obtained with RO. Figure 20 gives an example of the variation of the energy management decision variables for the TS, as a function of their input parameters. As it can be observed, the TS tends to charge the battery (i.e., R_t^{TS} increases) during the periods of lower prices and lower energy demand in order to discharge it during the periods of peak prices and higher consumption levels, in order to decrease its expenses. This is possible because the lower electricity prices c_t^p, especially during the night period, allow the TS to increase the amount of energy imported from the external grid S_t^{TS}, which is used to charge the battery. According to the formulation of the optimization problem, i.e., eq. (32), the available PV energy output P_t^{PV} is used to sell the energy to the D (i.e., V_t^{PV}) and the external grid (i.e., L_t^{TS}). Note that the optimization problem could be reformulated to allow the TS to use the available energy output P_t^{PV} to charge the battery.

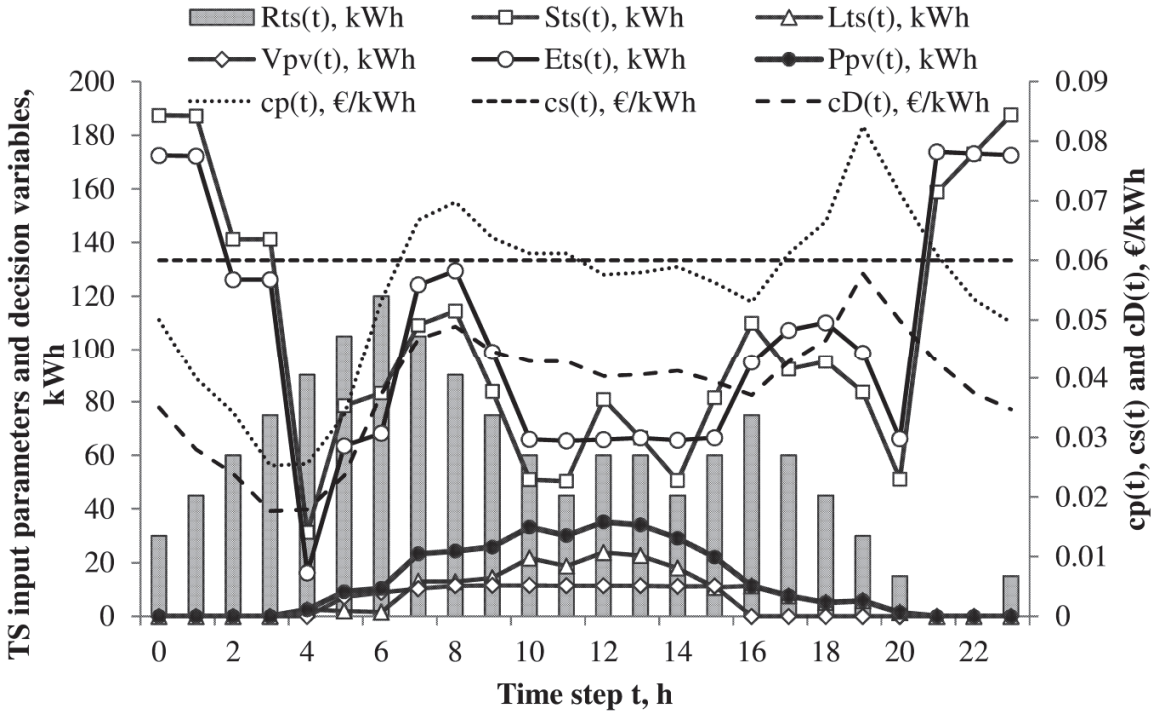

Figure 20. Energy management for TS.

In this view, RO allows the efficient management of energy portions exchanged between microgrid agents and the external grid, as well as battery scheduling strategies, depending on the uncertain environmental and operational variables. It also provides the optimistic results regarding the system reliability improvements, evaluated with classical reliability indicators, i.e., Loss of Load Expectation (LOLE), used to characterize the probability of unsatisfied electricity demand, and Loss of Expected Energy (LOEE), used to quantify the expected amount of energy losses for the simulation period τ.

Table 4 provides the results for microgrid system reliability using different optimization techniques, i.e., optimization based on expected values (point predictions) and RO based on PIs. For the RO two different sets of PIs with different CP were selected. As it can be noticed the RO based on the PIs gives more reliable results in terms of decrease of LOLE and LOEE indicators. Moreover, by comparing the RO based on PIs with 56% and 96% CPs, the RO based on PIs with high CP provides the significant increase of system reliability.

Table 4. Microgrid system reliability using different optimization techniques.

#	**Expected values**	**PIs with CP = 56%**	**PIs with CP = 96%**
LOLE, h/τ	0.2568	0.0048	0.002
LOEE, kWh/τ	1.3834	0.0485	0.0202

The exhaustive presentation and analysis of results, as well as comparison with existent optimization frameworks, is provided in Papers 2 and 3 of Part II [87], [101].

4.3. Methodological and applicative contributions

This section presents the methodological and applicative contributions of the work thesis in terms of microgrid energy management frameworks based on RL and RO, described in Sections 4.1 and 4.2, respectively.

4.3.1. RL

In this PhD thesis work, the RL framework is extended to a multi-criteria decision-making one considering 2 steps-ahead planning scenarios. The proposed framework is exemplified on a urban microgrid that connects through a transformer to the external grid and that involves an energy consumer, a locally installed wind turbine and a battery storage. This is a purposely simple microgrid architecture, but also sufficiently comprehensive to explore the efficiency of the proposed RL framework. A detailed description of the different models for the individual components, and several tests performed on the developed RL framework are presented in Paper 1 of Part II [103].

The original contributions of this PhD thesis work, with respect to the general limitations of the current modelling developments summarized in Section 1.3, are highlighted below.

The consumer is represented as an individual intelligent agent equipped with RL capabilities that, by a gradual trial-and-error decision-making process, is guided towards an optimal long term energy management. In other words, the individual intelligence of the RL framework is implemented directly into the consumer's behaviour, so that he/she can decide and act to his/her own interests without implication of additional management actors. Thus, the developed RL for the medium-term planning allows deriving the optimal microgrid energy management by selecting the appropriate sequence of actions for each operational scenario in a stochastic environment.

In this view, another contribution of this work lies in the possibility to account and to learn from the stochastic environment to identify the optimal management actions to be taken. Contrary to the frameworks in [141], [142], analysed in Section 1.3, where the optimization algorithms are applied to a deterministic optimization, the proposed modelling framework is capable of accounting for uncertainty, e.g., variability of renewable generation and failures of the power generators. Additionally, the optimization framework gives the possibility to reduce the uncertainties related to forecasting errors and to identify the optimal actions for long-term planning.

Moreover, the optimization framework based on RL is analysed through a comprehensive sensitivity analysis aimed at understanding the role of the learning parameters underpinning in the optimization process. This analysis allows improving the learning procedure and thus, achieving the energy management objectives more efficiently.

The reader is referred to Paper 1 of Part II [103] for more details. A summary of the main results obtained in these applications is given in Chapter 5.

4.3.2. RO

In this PhD thesis work, RO is applied for the individual energy management of the microgrid stakeholders under operational and environmental uncertain parameters as well as failures of the microgrid components, i.e., failures of renewable generators and electrical lines. The optimization framework is developed, implemented and tested on a reference microgrid system including a middle-size TS, which can play the role of a power producer and consumer, a surrounding D, and a small urban WPP. The reliability analysis performed for the energy scheduling under different levels of wind power output uncertainty shows a significant improvement of the reliability indicators with a decrease of the energy imbalances, i.e., shortage and surplus, for the case of RO based on PIs estimation in comparison with the results that can be obtained by optimization based on estimated expected values. The detailed presentation of the models of the individual components of the microgrid and an analysis of the RO framework performance is presented in Papers 2 and 3 of Part II [87], [101].

Regarding the limitations of the modelling developments summarized in Section 1.3, the original contributions of this PhD thesis work are as follows.

The developed RO framework for microgrid energy management considers the uncertainty associated to the stochasticity of operational and environmental conditions and failures of microgrid components; moreover, the uncertainties related to the predictions of energy quantities and the information communicated by the agents are also accounted for.

As in the previous case of RL, the RO is implemented with respect to each individual agent allowing microgrid energy management via the optimization of the objective functions of the individual agents, which are considered as autonomous decision-making entities with their individual objectives.

An additional original contribution of this PhD thesis work in the domain of energy management, lies in the way uncertainty is accounted for, as presented in Papers 2 and 3 of Part II [87], [101]. The novel implementation of PIs estimation by a NSGA-II - trained NN is proposed to define the bounds of uncertain parameters variation for input to the RO. In comparison with other works,

where the uncertain parameters are described by assumed probability levels [136]–[138] or probability bounds of constraint violation [139], the proposed framework allows each microgrid agent to regulate its conservatism under different uncertain parameters by setting and selecting the appropriate PIs width from the available solutions: the level of RO conservatism in the solution can be raised, for example, by increasing the width of the PIs associated to the renewable energy output from the generators. The reader is referred to Paper 2 of Part II [87] for more details.

Also, the thorough analysis performed on the RO framework provides insight and indications for identifying the level of uncertainty existing in the problem setting, which performs RO versus a (simpler) optimization based on expected values of the uncertain parameters. In this view, the PhD thesis work contributes to the exploration and understanding of the effects of the level of RO conservatism onto the microgrid performance. As expected, the RO framework is found to improve the reliability of the microgrid operation by selecting energy management actions that are optimal under the worst realization of the uncertainty conditions; however, this is done at the cost of possible lower revenues for the energy generators and higher expenses for the energy consumers than those that could be obtained by optimizing over the expected values of the uncertain parameters. In this view, the analysis proposed in Paper 3 of Part II [101] investigates and shows the influence of uncertainty on the microgrid performance and proposes a methodology to identify the level of uncertainty in the operational and environmental conditions for which RO performs better than optimization based on expected values. This analysis, and its findings, can assist the decision-makers in selecting their preferred microgrid energy management actions that provide an adequate trade-off between system reliability and economic performance. For more details, the reader is referred to Paper 3 of Part II [101].

A summary of the main conclusions obtained from these studies is synthetized in Chapter 5.

5. CONCLUSIONS AND PERSPECTIVES

The research contained in the PhD thesis here presented, is contributing to the advancements of the Smart grid concept by developing a framework for modelling dynamic interactions between grids stakeholders within optimal energy management. By exemplification on microgrid systems, seen as the representative elementary fractal dimension, the developed framework allows the different stakeholders to establish their profitable and efficient energy strategies in the management of the local renewable generators and storage facilities by exchanges with other stakeholders, in a dynamically changing environment under uncertainty.

Agent – Based Modelling (ABM) has been adopted in this research to accurately represent the complex dynamic elements and their interactions within a decision making context of individual agents that need to adapt to complex, uncertain and changing environments. The focus on the elementary fractal of the *microgrid* dimension allows for properties of scalability and transferability of the developed and implemented modelling / optimization frameworks.

The main contributions in the domain of microgrid energy management in multi-agents environments, presented in Papers 2 and 3 of Part II [87], [101], are:

- The microgrid energy management is achieved not through the optimization of the overall energy flows in the microgrid, e.g., like in [136]–[138], [143], but by the optimization of the objective functions of the individual agents considered as autonomous decision-making entities that account for their individual objectives.
- The proposed agent-based optimization framework is flexible and modular, and capable of accommodating more complex models of individual agents, e.g., to account for variations of charging and discharging efficiencies and energy losses due to battery degradation, and the refinement of the time step to account for shorter-term variations.

The original contributions in the domain of optimization techniques, i.e., RL and RO, for microgrid energy management are:

- Contrary to energy management frameworks such as [141], [142], where the optimization algorithms are applied to a deterministic power output, the proposed modelling and optimization framework is capable of accounting for generation uncertainty. For this

purpose, two Markov chain models are used in Paper 1 of Part II [103] to capture the differences in the forecasted and real wind power outputs by describing the dynamics of stochastic transitions among different levels of wind speed conditions and mechanical states. In Papers 2 and 3 of Part II [87], [101], the uncertainties are quantified by PIs and integrated in the RO.

- The RO based on data-driven estimated PIs for the quantification of the uncertain parameters, shown in Papers 2 and 3 of Part II [87], [101] and the extension of the RL framework to multi-criteria decision-making used to plan the energy management actions for consumer in Paper 1 of Part II [103] are applied to energy management for the first time.
- The performance of RO and RL are demonstrated by comparison with other optimization approaches. RO provides optimistic results in comparison with Fuzzy – NN and methods based on the Probabilistic Choice in Paper 2 of Part II [87]. The RL algorithm demonstrates the improvements in the strategy of microgrid operation with respect to the defined rewards in Paper 1 of Part II [103].
- A detailed sensitivity analysis is provided for both RO and RL. The optimization framework of RL is analysed through a comprehensive sensitivity analysis aimed at understanding the role of the learning parameters in Paper 1 of Part 2 [103]. This analysis allows improving the learning process and thus, the energy management objectives. Through the exploration of RO, an analysis framework is established to provide a way of identifying the level of uncertainty in operational and environmental conditions which preferably requires RO versus optimization based on expected values in Paper 3 of Part II [101].

Different research directions can be considered to extend the work developed in this thesis. The first direction aims at the extension and the improvement of the developed simulation / optimization frameworks. Indeed, the need to obtain a computationally tractable model and the limited available data guided to the range of assumptions considered in this thesis in order to build the models of the individual components. One of the major limitations is the one hour sampling time considered in the modelling / optimization frameworks. Guided by the need to catch major trends and test the performance of energy management frameworks, the future work must be

focused on the refinement of the time step in order to capture more accurately fluctuations of the microgrid environmental and operational conditions, i.e., energy prices, loads and renewable energy outputs form the power generators. This is a relevant development for energy optimization of small residential microgrids, where the short-term fluctuations in the individual loads and energy outputs from renewable generators can be significant within the hour and, as a consequence, also the decisions for optimal actions of energy management.

A perspective direction of future research focuses on the development of energy management frameworks that combine simultaneously RO and RL. On the one hand, RO allows a linear formulation of the robust counterpart of the optimization problem for different levels of conservatism in the solution, which can be adjusted by means of the PIW. Thus, the RO framework improves the reliability of the microgrid operation by selecting energy management actions that are optimal under the worst realization of the set uncertainty conditions. However, as it is highlighted in Section 4.2, this is done at the cost of possible lower revenues for the energy generators and higher expenses for the energy consumers than those that could be obtained by optimizing over the expected values of the uncertain parameters. On the other hand, RL allows identifying appropriate strategies for specific scenarios by reducing the uncertainties related to forecasting errors; but the optimal actions are eventually identified based on point predictions using the knowledge gathered during the training period. In this view, a promising development can be aimed at the combination of the two optimization techniques, whereby RL can be integrated as a supporting tool for RO in order to improve the economic indicators.

Finally, the application and testing of the developed frameworks on real microgrids seems a worthwhile line of future research, now that a number of actual real microgrid initiatives are becoming available.

REFERENCES

[1] EIA, “International Energy Outlook 2013,” 2013.

[2] IEA, “CO2 Emissions from Fuel Combustion. Highlights,” 2012.

[3] W. Nel and C. Cooper, “Implications of fossil fuel constraints on economic growth and global warming,” *Energy Policy*, vol. 37, no. 1, pp. 166–180, Jan. 2009.

[4] S. Shafiee and E. Topal, “When will fossil fuel reserves be diminished?,” *Energy Policy*, vol. 37, no. 1, pp. 181–189, Jan. 2009.

[5] EIA, “International Energy Outlook 2010,” 2010.

[6] H. H. Pattee, *Hierarchy theory — the challenge of complex systems*. New York: George Braziller, 1973.

[7] E. Zio, “From complexity science to reliability efficiency: A new way of looking at complex network systems and critical infrastructures,” *Int. J. Crit. Infrastructures*, vol. 3, no. 3/4, p. 488, 2007.

[8] M. Rosas I Casals, “Topological complexity of the electricity transmission network. Implications in the sustainability paradigm,” Universitat Politècnica de Catalunya, 2009.

[9] P. Hines, S. Blumsack, E. Cotilla Sanchez, and C. Barrows, “The topological and electrical structure of power grids,” in *2010 43rd Hawaii International Conference on System Sciences (HICSS)*, 2010, pp. 1 – 10.

[10] J. C. Glenn, T. J. Gordon, and E. Florescu, “2009 State of the Future,” 2009.

[11] B. J. Owen, “The planet ’s future : Climate change ' will cause civilisation to collapse ',” *The Independent*, London, 2009.

[12] W. Moskwa, “Norway opens world ’s first osmotic power plant,” 2009. [Online]. Available: http://www.reuters.com/article/idUSTRE5AN20Q20091124. [Accessed: 22-Sep-2010].

[13] Microbial Fuel Cells, “Microbial Fuel Cells,” 2008. [Online]. Available: http://www.microbialfuelcell.org/www/. [Accessed: 22-Sep-2010].

[14] WWEA, “World Wind Energy Report 2009,” Bonn, Germany, 2010.

[15] IEA, “Technology Roadmap Solar photovoltaic energy,” 2010.

[16] World Water, “World Wave and Tidal Market,” 2008. [Online]. Available: http://www.waterlink-international.com/news/id379-World_Wave_and_Tidal_Market.html. [Accessed: 22-Sep-2010].

[17] B. A. Holm, L. Blodgett, D. Jennejohn, and K. Gawell, “Geothermal Energy : International Market Update,” 2010.

[18] Policy Department A: Economic and Scientific, “European Renewable Energy Network,” Brussels, European Union, 2012.

[19] G. Giebel, P. Sørensen, and H. Holttinen, “Further Developping Europe’s Power Market for Large Scale Integration of Wind Power. Forecast error of aggregated wind power,” 2007.

[20] B. K. Sovacool, “The intermittency of wind, solar, and renewable electricity generators: Technical barrier or rhetorical excuse?,” *Util. Policy*, vol. 17, no. 3–4, pp. 288–296, Sep. 2009.

[21] T. Hammons, “Integrating renewable energy sources into European grids,” *Int. J. Electr. Power Energy Syst.*, vol. 30, no. 8, pp. 462–475, Oct. 2008.

[22] M. Jung and P. Yeung, “Connecting smart grid and climate change,” 2009.

REFERENCES

[23] A. Battaglini, J. Lilliestam, A. Haas, and A. Patt, "Development of SuperSmart Grids for a more efficient utilisation of electricity from renewable sources," *J. Clean. Prod.*, vol. 17, no. 10, pp. 911–918, Jul. 2009.

[24] W. Breuer, D. Povh, D. Retzmann, C. Urbanke, and M. Weinhold, "Prospects of Smart Grid Technologies for a Sustainable and Secure Power Supply," in *World Energy Council*, 2007.

[25] D. P. Chassin, "What Can the Smart Grid Do for You? And What Can You Do for the Smart Grid?," *Electr. J.*, vol. 23, no. 5, pp. 57–63, Jun. 2010.

[26] D. Coll-Mayor, M. Paget, and E. Lightner, "Future intelligent power grids: Analysis of the vision in the European Union and the United States," *Energy Policy*, vol. 35, no. 4, pp. 2453–2465, Apr. 2007.

[27] B. K. Sovacool, "Rejecting renewables: The socio-technical impediments to renewable electricity in the United States," *Energy Policy*, vol. 37, no. 11, pp. 4500–4513, Nov. 2009.

[28] K. Bell, "Climate change drivers for a single and smart EU grid," in *Wind Energy*, 2009, pp. 1–10.

[29] "Energy Independence and Security Act of 2007," Washington, USA, 2007.

[30] G. K. Venayagamoorthy, "Dynamic, stochastic, computational and scalable technologies for Smart Grids," *IEEE Comput. Intell. Mag.*, pp. 22 – 35, 2011.

[31] A. B. Lovins, "The Most Important Issue We ' ve Ever Published," *Foreign Aff.*, vol. 6, no. 20, 1977.

[32] W. B. Rouse, "Engineering complex systems: Implications for research in systems engineering," *IEEE Trans. Syst. Man Cybern. Part C (Applications Rev.*, vol. 33, no. 2, pp. 154–156, May 2003.

[33] W. Kroger and E. Zio, "Vulnerable Systems," *Springer*, 2011.

[34] J. Ryan, *A History of the Internet and the Digital Future*. Reaktion Books, 2010.

[35] OECD, "The future of the internet economy," *Policy Br.*, Apr. 2008.

[36] NESCI, "Visualizing complex system science (CSS)," *New England Complex Systems Institute*, 2005. [Online]. Available: www.necsi.org/projects/mclemens/viscss.html. [Accessed: 30-Nov-2010].

[37] H. Nederbragt, "Hierarchical organization of biological systems and the structure of adaptation in evolution and tumorigenesis.," *J. Theor. Biol.*, vol. 184, no. 2, pp. 149–56, Jan. 1997.

[38] G.-R. Duncan, "Mapping the Internet," *Technology Review*, 2007. [Online]. Available: http://www.technologyreview.com/printer_friendly_article.aspx?id=18944. [Accessed: 09-Dec-2010].

[39] M. Barth, "Spatial networks," *Networks*, pp. 1–86, 2010.

[40] L. F. Agnati, F. Baluska, P. W. Barlow, and D. Guidolin, "Three explanatory instruments in biology," *Commun. Integr. Biol.*, vol. 2, no. 6, pp. 552–563, 2009.

[41] P. Crucitti, "Efficiency of scale-free networks: error and attack tolerance," *Phys. A Stat. Mech. its Appl.*, vol. 320, pp. 622–642, Mar. 2003.

[42] M. Rosas-Casals, S. Valverde, and R. V. Solé, "Topological vulnerability of the european power grid under errors and attacks," *Int. J. Bifurc. Chaos*, vol. 17, no. 07, p. 2465, 2007.

[43] B. B. Mandelbrot, *The fractal geometry of nature*. W.H. Freeman and Company, 1982.

[44] R. Prud'homme, "Dimensionless Numbers and Similarity," in *Flows of Reactive Fluids*, vol. 94, Birkhäuser Boston, 2010, pp. 97–108.

[45] G. Caldarelli, R. Marchetti, and L. Pietronero, "The fractal properties of Internet," *Europhys. Lett.*, vol. 52, no. 4, pp. 386–391, Nov. 2000.

[46] a L. Goldberger and B. J. West, “Fractals in physiology and medicine.,” *Yale J. Biol. Med.*, vol. 60, no. 5, pp. 421–35, 1987.
[47] J. R. Krummel, R. H. Gardner, G. Sugihara, R. V. O. Neill, P. R. Coleman, and N. Mar, “Landscape patterns in a disturbed environment,” *Oikos*, vol. 48, no. 3, pp. 321–324, 2008.
[48] C. Song, S. Havlin, and H. A. Makse, “Origins of fractality in the growth of complex networks,” *Nat. Phys.*, vol. 2, no. 4, pp. 275–281, Apr. 2006.
[49] I. Granic, “The self-organization of the Internet and changing modes of thought,” *New Ideas Psychol.*, vol. 18, no. 1, pp. 93–107, Apr. 2000.
[50] J. Goldstein, “Emergence as a construct: History and issues,” *Emergence*, vol. 1, no. 1, pp. 49–72, Mar. 1999.
[51] L. Chen, X. Wang, and Z. Han, “Controlling chaos in Internet congestion control model,” *Chaos, Solitons & Fractals*, vol. 21, no. 1, pp. 81–91, Jul. 2004.
[52] S. Boccaletti, V. Latora, Y. Moreno, M. Chavez, and D. Hwang, “Complex networks: Structure and dynamics,” *Phys. Rep.*, vol. 424, no. 4–5, pp. 175–308, Feb. 2006.
[53] A. Barabasi, R. Albert, and H. Jeong, “Scale-free characteristics of random networks: the topology of the world-wide web,” *Phys. A Stat. Mech. its Appl.*, vol. 281, no. 1–4, pp. 69–77, Jun. 2000.
[54] A. C. W. Baas, “Chaos, fractals and self-organization in coastal geomorphology : simulating dune landscapes in vegetated environments,” *Geomorphology*, vol. 48, pp. 309 – 328, 2002.
[55] W. M. Macek, “Chaos and multifractals in the solar wind,” *Adv. Sp. Res.*, vol. 46, no. 4, pp. 526–531, Aug. 2010.
[56] J. Lee, “Applications of chaos and fractals in process systems engineering,” *J. Process Control*, vol. 6, no. 2–3, pp. 71–87, Jun. 1996.
[57] H. Lorenz, “Strange attractors in a multisector business cycle model,” *J. Econ. Behav.* , vol. 8, no. 3, pp. 397–411, Sep. 1987.
[58] P. Fox-Penner, “Smart Power. Climate change, the Smart Grid and the Future of Electric Utilities,” Island Press, Ed. Washington, 2010, pp. 1 – 344.
[59] J. M. Ottino, “Engineering complex systems,” *Nature*, vol. 427, no. 6973, p. 399, Jan. 2004.
[60] R. Hledik, “How Green Is the Smart Grid?,” *Electr. J.*, vol. 22, no. 3, pp. 29–41, Apr. 2009.
[61] H. Borsenberger, P. Dessante, and G. Sandou, “Unit Commitment with Production Cost Uncertainty : A Recourse Programming Method,” *J. Energy Power Eng.*, vol. 5, pp. 164–172, 2011.
[62] V. K. Garg, T. S. Jayram, and B. Narayanaswamy, “Online Optimization with Dynamic Temporal Uncertainty: Incorporating Short Term Predictions for Renewable Integration in Intelligent Energy Systems,” in *Proceedings of the Twenty-Seventh AAAI Conference on Artificial Intelligence*, 2013, no. i, pp. 1291–1297.
[63] A. Benigni, J. Liu, A. Helmedag, W. Li, C. Molitor, B. Schäfer, and A. Monti, “An Advanced Real-Time Simulation Laboratory for Future Grid Studies : Current State and Future Development,” in *Complexity in Engineering (COMPENG)*, 2012, pp. 1 – 6.
[64] S. D. J. McArthur, P. C. Taylor, G. W. Ault, J. E. King, D. Athanasiadis, V. D. Alimisis, and M. Czaplewski, “The Autonomic Power System - Network operation and control beyond smart grids,” in *International Conference and Exhibition on Innovative Smart Grid Technologies (ISGT Europe), 2012 3rd IEEE PES*, 2012, pp. 1–7.
[65] A. Azadeh, S. Ghaderi, and S. Sohrabkhani, “Annual electricity consumption forecasting by neural network in high energy consuming industrial sectors,” *Energy Convers. Manag.*, vol. 49, no. 8, pp. 2272–2278, Aug. 2008.

[66] A. Chaouachi, R. M. Kamel, R. Ichikawa, H. Hayashi, and K. Nagasaka, "Neural network ensemble-based solar power generation short-term forecasting," *Eng. Technol.*, vol. 54, pp. 54–59, 2009.

[67] A. Azadeh and Z. S. Faiz, "A meta-heuristic framework for forecasting household electricity consumption," *Appl. Soft Comput.*, vol. 11, no. 1, pp. 614–620, Jan. 2011.

[68] M. Kock, "Computational intelligence for communication and cooperation guidance in adaptive e-learning systems," in *16th Workshop on Adaptivity and User Modeling in Interactive Systems*, 2008, pp. 32–34.

[69] Z. Jun, L. Junfeng, W. Jie, and H. W. Ngan, "A multi-agent solution to energy management in hybrid renewable energy generation system," *Renew. Energy*, vol. 36, no. 5, pp. 1352–1363, May 2011.

[70] K. Mitsudo, T. Kanno, and K. Furuta, "Institutional design of product recall based on multi-agent simulation," in *Advances in Safety, Reliability and Risk Management*, 2012, vol. 2009, pp. 2781–2788.

[71] H. Zied, D. Sofiene, and R. Nidhal, "An optimal maintenance / production planning for a manufacturing system under random failure rate and a subcontracting constraint," in *2011 International Conference on Industrial Engineering and Operations Management*, 2011, pp. 1185–1190.

[72] V. Volovoi and R. V. Vega, "Combined representation of coupling effects in maintenance processes of complex engineering systems," in *Advances in Safety, Reliability and Risk Management*, 2012, pp. 824–831.

[73] T. Nowakowski, "Developments of time dependencies modelling concepts," in *Advances in Safety, Reliability and Risk Management*, 2012, pp. 832–838.

[74] O. B. Kwon and N. Sadeh, "Applying case-based reasoning and multi-agent intelligent system to context-aware comparative shopping," *Decis. Support Syst.*, vol. 37, pp. 199 – 213, Feb. 2003.

[75] E. Kuznetsova, K. Culver, and E. Zio, "Complexity and vulnerability of Smartgrid systems," in *European Safety and Reliability Conference (ESREL 2011)*, 2011, pp. 1–8.

[76] A. G. De Muro, J. Jimeno, and J. Anduaga, "Architecture of a microgrid energy management system," *Eur. Trans. Electr. Power*, vol. 21, pp. 1142–1158, 2011.

[77] M. H. Colson, C. M. Nehrir, and R. W. Gunderson, "Multi-agent Microgrid Power Management," in *18th IFAC World Congress*, 2011, pp. 3678–3683.

[78] P. P. Reddy and M. M. Veloso, "Strategy Learning for Autonomous Agents in Smart Grid Markets," in *Twenty-Second International Joint Conference on Artificial Intelligence*, 2005, pp. 1446–1451.

[79] T. Krause, E. Beck, R. Cherkaoui, A. Germond, G. Andersson, and D. Ernst, "A comparison of Nash equilibria analysis and agent-based modelling for power markets," *Int. J. Electr. Power Energy Syst.*, vol. 28, no. 9, pp. 599–607, Nov. 2006.

[80] A. Weidlich and D. Veit, "A critical survey of agent-based wholesale electricity market models," *Energy Econ.*, vol. 30, no. 4, pp. 1728–1759, Jul. 2008.

[81] S. Yousefi, M. P. Moghaddam, and V. J. Majd, "Optimal real time pricing in an agent-based retail market using a comprehensive demand response model," *Energy*, vol. 36, no. 9, pp. 5716–5727, Sep. 2011.

[82] C. Kieny, N. Hadjsaïd, B. Raison, Y. Besanger, R. Caire, D. Roye, O. Devaux, and G. Malarange, "Distribution grid security management with high DG penetration rate:

Situation in France and some future trends," *Power Energy Soc. Gen. Meet. - Convers. Deliv. Electr. Energy 21st Century, 2008 IEEE*, pp. 1–6, 2008.

[83] S. C. E. Jupe and P. C. Taylor, "Distributed generation output control for network power flow management," *IET Renew. Power Gener.*, vol. 3, no. 4, p. 371, 2009.

[84] M. Wooldridge, *An introduction to multiagent systems*. United Kingdom: John Wiley and Sons Ltd., 2002, pp. 1–460.

[85] Z. Zhi, C. Wai Kin, and C. Joe H, "Agent-based simulation of electricity markets : a survey of tools," *Artif. Intell. Rev.*, vol. 28, pp. 305–342, 2009.

[86] A. Chaouachi, R. M. Kamel, R. Andoulsi, and K. Nagasaka, "Multiobjective Intelligent Energy Management for a Microgrid," *IEEE Trans. Ind. Electron.*, vol. 60, no. 4, pp. 1688 – 1699, 2013.

[87] E. Kuznetsova, Y.-F. Li, C. Ruiz, and E. Zio, "An integrated framework of agent-based modelling and robust optimization for microgrid energy management," *Appl. Energy*, vol. 129, pp. 70 – 88, 2014.

[88] Econoving, "Programme Gare," *Econoving*, 2011. [Online]. Available: http://www.econoving.uvsq.fr/econoving/langue-fr/recherche/projets/programme-gare/programme-gare-236018.kjsp. [Accessed: 13-Feb-2013].

[89] European Commission, "Photovoltaic Solar Energy Best Practice Stroies," 2002.

[90] E. Fischer and C. Lo, "Back to the future : Top trends in railway station design," *railway-technology.com*, 2011. [Online]. Available: http://www.railway-technology.com/features/featureback-to-the-future-top-trends-in-railway-station-design. [Accessed: 24-Sep-2013].

[91] L. Al-Sharif, "Modelling of escalator energy consumption," *Energy Build.*, vol. 43, no. 6, pp. 1382–1391, Jun. 2011.

[92] Ademe, "Eclairage public: routier, urban, grands espaces, illuminations et cadre de vie," 2002.

[93] Safety Time Inc., "Automatic Fare Collection System," 2010.

[94] B. Roux Dit Riche, "Les distributeurs automatiques devront réduire leur consommation d ' énergie," *Cleantech Republic*, 2011. [Online]. Available: http://www.cleantechrepublic.com/2009/06/09/les-distributeurs-automatiques-devront-reduire-leur-consommation-denergie/. [Accessed: 12-Apr-2011].

[95] F. A. Mohamed and H. N. Koivo, "System modelling and online optimal management of MicroGrid using mesh adaptive direct search," *Int. J. Electr. Power Energy Syst.*, vol. 32, no. 5, pp. 398–407, 2010.

[96] Y. M. Atwa, M. M. A. Salama, and R. Seethapathy, "Optimal renewable resources mix for distribution system energy loss minimization," *IEEE Trans. Power Syst.*, vol. 25, no. 1, pp. 360–370, 2010.

[97] F. Y. Ettoumi, A. Mefti, A. Adane, and M. Y. Bouroubi, "Statistical analysis of solar measurements in Algeria using beta distributions," *Renew. Energy*, vol. 26, pp. 47–67, 2002.

[98] L. Martin, L. F. Zarzalejo, J. Polo, A. Navarro, R. Marchante, and M. Cony, "Prediction of global solar irradiance based on time series analysis: Application to solar thermal power plants energy production planning," *Sol. Energy*, vol. 84, pp. 1772–1781, 2010.

[99] M. Y. Sulaiman, W. M. H. Oo, and M. A. Wahab, "Application of beta distribution model to Malaysian sunshine data," *Renew. Energy*, vol. 18, pp. 573–579, 1999.

[100] S. Mohammadi, B. Mozafari, S. Solimani, and T. Niknam, "An Adaptive Modified Firefly Optimisation Algorithm based on Hong's Point Estimate Method to optimal operation management in a microgrid with consideration of uncertainties," *Energy*, vol. 51, pp. 339–348, Mar. 2013.

[101] E. Kuznetsova, Y.-F. Li, C. Ruiz, and E. Zio, "Analysis of robust optimization for decentralized microgrid energy management under uncertainty," *Submitt. to Electr. Power Energy Syst.*, pp. 1 – 46, 2013.

[102] EEX, "Hour Contracts - France," *European Energy Exchange*, 2013. [Online]. Available: http://www.eex.com/en/Market Data/Trading Data/Power/Hour Contracts | Spot Hourly Auction/spot-hours-table/2013-02-14/FRANCE. [Accessed: 13-Feb-2013].

[103] E. Kuznetsova, C. Ruiz, Y. F. Li, E. Zio, G. Ault, and K. Bell, "Reinforcement learning for microgrid energy management," *Energy*, vol. 59, pp. 133–146, 2013.

[104] N. Dalili, A. Edrisy, and R. Carriveau, "A review of surface engineering issues critical to wind turbine performance," *Renew. Sustain. Energy Rev.*, vol. 13, pp. 428–438, 2009.

[105] Y. F. Li and E. Zio, "A multi-state power model for adequacy assessment of distributed generation via universal generating function," *Reliab. Eng. Syst. Saf.*, vol. 106, pp. 28–36, 2012.

[106] A. Shamshad, M. Bawadi, W. Wanhussin, T. Majid, and S. Sanusi, "First and second order Markov chain models for synthetic generation of wind speed time series," *Energy*, vol. 30, no. 5, pp. 693–708, Apr. 2005.

[107] L. Fawcett and D. Walshaw, "Markov chain models for extreme wind speeds," *Environmetrics*, vol. 17, no. 8, pp. 795–809, Dec. 2006.

[108] F. C. Sayas and R. N. Allan, "Generation availability assessment of wind farms," in *IEE Proc.-Gener. Transm. Distrib.*, 1996, pp. 507–518.

[109] D. C. Hill, D. Mcmillan, K. R. W. Bell, and D. Infield, "Application of auto-regressive models to UK wind speed data for power system impact studies," *IEEE Trans. Sustain. Energy*, vol. 3, no. 1, 2012.

[110] R. N. Clark and R. G. Davis, "Performance of an Enertech 44 during 11 years of operation," in *Proceedings of the AWEA Wind-Power'93 Conference*, 1993, pp. 204–212.

[111] S. Faulstich, P. Lyding, and B. Hahn, "Component reliability ranking with respect to WT concept and external environmental conditions," Kassel, Germany, 2006.

[112] L. Duenas-Osorio, "Unavailability of wind turbines due to wind-induced accelerations," *Eng. Struct.*, vol. 30, no. 4, pp. 885–893, Apr. 2008.

[113] P. Tavner, "SUPERGEN Wind 2011 General Assembly," in *SUPERGEN Wind 2011 General Assembly*, 2011, no. March.

[114] R. S. Sutton and A. G. Barto, *Reinforcement learning : An introduction*. London, England: The MIT Press., 2005, pp. 1–398.

[115] L. Panait and S. Luke, "Cooperative Multi-Agent Learning : The State of the Art," *Auton. Agent. Multi. Agent. Syst.*, vol. 11, no. 3, pp. 387 – 434, 2005.

[116] V. L. Prabha and E. C. Monie, "Hardware Architecture of Reinforcement Learning Scheme for Dynamic Power Management in Embedded Systems," *EURASIP J. Embed. Syst.*, pp. 1–6, 2007.

[117] Y. Tan, W. Liu, and Q. Qiu, "Adaptive Power Management Using Reinforcement Learning," in *International Conference on Computer-Aided Design (ICCAD'09)*, 2009, pp. 1 – 7.

[118] C. J. C. H. Watkins, "Learning from delayed rewards," King's College, 1989.

[119] E. R. Gomes and R. Kowalczyk, "Dynamic analysis of multiagent Q-learning with e-greedy exploration," in *26th International Conference on Machine Learning*, 2009.
[120] L. Xin, Z. Chuanzhi, Z. Peng, and Y. Haibin, "Genetic based fuzzy Q-learning energy management for smart grid," *Control Conference (CCC), 2012 31st Chinese*. pp. 6924–6927, 2012.
[121] X. Li, C. Zang, W. Liu, P. Zeng, and H. Yu, "Metropolis Criterion Based Fuzzy Q-Learning Energy Management for Smart Grids," *TELKOMNIKA*, vol. 10, no. 8, pp. 1956–1962, 2012.
[122] R. Ak, Y. F. Li, V. Vitelli, and E. Zio, "Multi-objective Generic Algorithm Optimization of a Neural Network for Estimating Wind Speed Prediction Intervals," *Submitt. to Appl. Soft Comput.*, 2013.
[123] J. Lagorse, M. G. Simoes, and A. Miraoui, "A Multiagent Fuzzy-Logic-Based Energy Management of Hybrid Systems," *Ind. Appl. IEEE Trans.*, vol. 45, no. 6, pp. 2123–2129, 2009.
[124] J. Solano Martínez, R. I. John, D. Hissel, and M.-C. Péra, "A survey-based type-2 fuzzy logic system for energy management in hybrid electrical vehicles," *Inf. Sci. (Ny).*, vol. 190, pp. 192–207, May 2012.
[125] A. Ben-Tal and A. Nemirovski, "Robust solutions of uncertain linear programs," *Oper. Res. Lett.*, vol. 25, no. 1, pp. 1–13, Aug. 1999.
[126] D. Bertsimas and M. Sim, "The Price of Robustness," *Oper. Res.*, vol. 52, no. 1, pp. 35–53, 2004.
[127] V. Krey, D. Martinsen, and H.-J. Wagner, "Effects of stochastic energy prices on long-term energy-economic scenarios," *Energy*, vol. 32, no. 12, pp. 2340–2349, Dec. 2007.
[128] Y. P. Cai, G. H. Huang, Z. F. Yang, Q. G. Lin, and Q. Tan, "Community-scale renewable energy systems planning under uncertainty—An interval chance-constrained programming approach," *Renew. Sustain. Energy Rev.*, vol. 13, no. 4, pp. 721–735, May 2009.
[129] M. Liu, "An Interval-parameter Fuzzy Robust Nonlinear Programming Model for Water Quality Management," *J. Water Resour. Prot.*, vol. 05, no. 01, pp. 12–16, 2013.
[130] Y. Li and G. Huang, "Robust interval quadratic programming and its application to waste management under uncertainty," *Environ. Syst. Res.*, vol. 1, no. 1, p. 7, 2012.
[131] A. L. Soyster, "Convex Programming with Set-Inclusive Constraints and Applications to Inexact Linear Programming," *Oper. Res.*, vol. 21, no. 5, pp. 1154–1157, Sep. 1973.
[132] L. El Ghaoui and H. Lebret, "Robust Solutions to Least-Squares Problems with Uncertain Data," *SIAM J. Matrix Anal. Appl.*, vol. 18, no. 4, pp. 1035–1064, Oct. 1997.
[133] L. El Ghaoui, F. Oustry, and H. Lebret, "Robust Solutions to Uncertain Semidefinite Programs," *SIAM J. Optim.*, vol. 9, no. 1, pp. 33–52, Jan. 1998.
[134] A. Ben-Tal and A. Nemirovski, "Robust solutions of Linear Programming problems contaminated with uncertain data," *Math. Program.*, vol. 88, no. 3, pp. 411–424, Sep. 2000.
[135] A. Ben-Tal and A. Nemirovski, "Robust Convex Optimization," *Math. Oper. Res.*, vol. 23, no. 4, pp. 769 – 805, 1998.
[136] A. Parisio, C. Del Vecchio, and A. Vaccaro, "Electrical Power and Energy Systems A robust optimization approach to energy hub management," *Int. J. Electr. Power Energy Syst.*, vol. 42, no. 1, pp. 98–104, 2012.
[137] C. Chen, Y. P. Li, G. H. Huang, and Y. F. Li, "A robust optimization method for planning regional-scale electric power systems and managing carbon dioxide," *Electr. Power Energy Syst.*, vol. 40, pp. 70–84, 2012.

[138] C. Chen, Y. P. Li, G. H. Huang, and Y. Zhu, “An inexact robust nonlinear optimization method for energy systems planning under uncertainty,” *Renew. Energy*, vol. 47, pp. 55–66, 2012.

[139] C. Dong, G. H. Huang, Y. P. Cai, and Y. Liu, “Robust planning of energy management systems with environmental and constraint-conservative considerations under multiple uncertainties,” *Energy Convers. Manag.*, vol. 65, pp. 471–486, 2013.

[140] T. Niknam, R. Azizipanah-Abarghooee, and M. R. Narimani, “An efficient scenario-based stochastic programming framework for multi-objective optimal micro-grid operation,” *Appl. Energy*, pp. 455 – 470, Jul. 2012.

[141] F. A. Mohamed and H. N. Koivo, “System Modelling and Online Optimal Management of MicroGrid with Battery Storage,” *Int. J. Electr. Power Energy Syst.*, vol. 32, no. 5, pp. 398–407, 2010.

[142] C. M. Colson, M. H. Nehrir, and S. A. Pourmousavi, “Towards Real-time Microgrid Power Management using Computational Intelligence Methods,” in *2010 IEEE Power and Energy Society General Meeting*, 2010, pp. 1–8.

[143] T. Niknam, R. Azizipanah-Abarghooee, and M. R. Narimani, “An efficient scenario-based stochastic programming framework for multi-objective optimal micro-grid operation,” *Appl. Energy*, vol. 99, pp. 455–470, Nov. 2012.

Paper 1

Reinforcement learning for microgrid energy management

Elizaveta Kuznetsova, Yan Fu Li, Carlos Ruiz, Enrico Zio, Graham Ault and Keith Bell

Energy vol. 59, pp. 133–146, 2013

Reinforcement learning for microgrid energy management

Elizaveta Kuznetsova[1,2], Yan Fu Li[2], Carlos Ruiz[2,3], Enrico Zio[2,4] Graham Ault[5], Keith Bell[5]

[1] ECONOVING International Chair in Eco-Innovation, REEDS International Centre for Research in Ecological Economics, Eco-Innovation and Tool Development for Sustainability, University of Versailles Saint Quentin-en-Yvelines, 5-7 Boulevard d'Alembert, bâtiment d'Alembert - room A301, 78047 Guyancourt, France
[2] Chair on Systems Science and the Energetic Challenge, European Foundation for New Energy-Electricité de France, Ecole Centrale Paris, Grande Voie des Vignes 92295 Châtenay-Malabry, Supelec, 91190 Gif-sur-Yvette, France.
[3]Department of Statistics, Universidad Carlos III de Madrid, Avda. de la Universidad, 30, 28911-Leganes (Madrid), Spain (current affiliation)
[4] Dipartimento di Energia, Politecnico di Milano, Via Lambruschini 4, 20156 Milano, Italy
[5] Institute for Energy and Environment, University of Strathclyde, Royal College Building, 204 George Street, Glasgow, G1 1XW, Scotland

ABSTRACT

We consider a microgrid for energy distribution, with a local consumer, a renewable generator (wind turbine) and a storage facility (battery), connected to the external grid via a transformer. We propose a 2 steps-ahead reinforcement learning algorithm to plan the battery scheduling, which plays a key role in the achievement of the consumer goals. The underlying framework is one of multi-criteria decision-making by an individual consumer who has the goals of increasing the utilization rate of the battery during high electricity demand (so as to decrease the electricity purchase from the external grid) and increasing the utilization rate of the wind turbine for local use (so as to increase the consumer independence from the external grid). Predictions of available wind power feed the reinforcement learning algorithm for selecting the optimal battery scheduling actions. The embedded learning mechanism allows to enhance the consumer knowledge about the optimal actions for battery scheduling under different time-dependent environmental conditions. The developed framework gives the capability to intelligent consumers to learn the stochastic environment and make use of the experience to select optimal energy management actions.

Keywords: Smartgrids, microgrids, Markov chain model, reinforcement learning, sensitivity analysis

NOMENCLATURE

t	time step *(h)*,
Δt	time step interval *(h)*,
D_t	consumer load over the time interval Δt *(Wh)*,
P_t	electricity market price at time *t (\$/Wh)*,
P_t^{wt}	available power output from the wind generator over the time interval Δt *(Wh)*,
R_t	level of battery storage at time *t (Wh)*,
$\lambda_{y,z}$	transition rate between wind speed states *y* and *z* (h^{-1}),
λ, μ	failure and repair transition rates at normal wind speed conditions (h^{-1}),
λ', μ'	failure and repair transition rates at extreme wind speed conditions (h^{1}),
D^{peak}	maximum annual peak of load *(Wh)*,
r_d^{peak}, r_w^{peak}	daily and weekly peaks of power demand, respectively *(%)*,
r_h^{peak}	hourly peak defined for working days and weekends *(%)*,
R_t, R_{t-1}	levels of the energy stored in the battery at time *t* and *t-1* (*Wh*),
$R_t^{stor,discharge}$	power flowing between the battery and the consumer at time *t* (*Wh*),
$R_t^{stor,charge}$	power flowing between the wind generator and the battery at time *t* (*Wh*),
i, n, p	indexes of system states,
s_t^i	system state of index *i* at time *t*,
l	index of generic scenario composed of $[s_t^i,\ s_{t+1}^n,\ s_{t+2}^p]$ system states at time steps *t*, *t+1* and *t+2*,
$Scenario_t^l$	generic scenario of index *l* at time *t*,
a_t	action at time *t*, which can take value of a^0 for the battery discharging or a^1 for the battery charging,
j	index of sequence of actions,

A_t^j	sequence of actions of index *j* composed of $[a_t, a_{t+1}, a_{t+2}]$ at time steps *t*, *t+1* and *t+2*,
$f_t(a_t)$	reward function at time *t* for action a_t,
k	weight coefficient for the reward function $f_t(a_t)$,
$r(Scenario_t^l, A_t^j)$	total discounted truncated reward for the sequence of actions A_t^j performed under the $Scenario_t^l$,
γ	discounted factor taking values within the range of [0,1],
p	number of occurrences of the $Scenario_t^l$,
$Q\left(Scenario_t^l, A_t^j\right)_p$	Q-value of the sequence of actions A_t^j performed under the $Scenario_t^l$ of *p-th* occurrence,
α	learning rate taking values between 0 and 1,
$p^{Scenario_t^l}$	burn in period of the $Scenario_t^l$.

1. INTRODUCTION

Renewable energies are promising solutions to the energetic and environmental challenges of the 21st century [1], [2]. Their integration into the existing grids generates technical and social challenges related to their efficient and secure management. The paradigm to address these challenges is the implementation of Smartgrids, which are expected to contribute to energy efficiency in decentralized networks by the adequate management of production and consumption [3], [4].

Under this perspective, on the one hand, a closer location of generation and consumption sources tends to increase service quality from the consumer's point of view, by decreasing transmission losses and the time needed to manage fault restoration and congestions. On the other hand, energy management issues related to the emergence of a large number of microgrids arise with possible conflicting requirements and limited communications between different agents of the microgrids, which calls for the implementation of distributed intelligent techniques [5]. This is the reason why the need for detailed exploration of smart energy management frameworks within microgrids has been pointed out in various works [6–8] aimed at optimal operation of microgrids [9–11]. The development of such frameworks relies on models of the energy system that properly account for its multi-level dynamic behaviour.

One approach to model energy distributed systems is that of agent-based modelling [5], [12], [13]. In studies related to Smart electricity grids, the agent-based approach is used to simulate and analyse the interactions between individual intelligent decision-makers. The most widespread application of this modelling approach concerns the bidding strategies between individual agents and energy market dynamics [14–18]. In all case studies of energy markets, individual agents tend to increase their immediate profits through mutual negotiations. Recent studies show the extension of the agent-based approach to model more complex interactions for energy management in hybrid renewable energy generation [19], [20]. Here the long-term goals are focused on the efficient use of the electricity within microgrids, e.g., the planning of battery scheduling to store the locally generated electricity from renewable sources and reuse it during periods of high electricity demand [20]. However, the decision framework has been tested under deterministic conditions of a typical day in summer: the electricity demand, and wind speed and

solar irradiation to model power output from the wind turbine and photovoltaic panel, respectively.

In this paper, we look at one consumer (which can be seen as an agent) and we develop a scheme of optimization of its energy management objectives based on reinforcement learning. The aim for the consumer is to establish profitable and efficient strategies of energy use in constantly changing environments. The originality of the work lies in the particular structuring of the intelligent framework used by the consumer for energy management, which integrates two blocks: a forecasting step, in view of the stochasticity of the wind speed conditions, and an optimization, adaptive task for finding the strategy of battery scheduling optimal with respect to the consumer goals.

The optimization framework is based on reinforcement learning by the so called Q-learning method. This method drives the learning on the basis of rewards or penalties evaluated on a sequence of actions taken in response to the environment dynamics [21], [22]. In a deterministic setting, the method allows to find the most promising set of actions for the given environment state, whereas in a stochastic setting it is capable of accounting for the uncertainties in the exploration of the environment [22]. The Q-learning method has been shown to achieve excellent performance in dynamic power management of embedded systems, by minimizing power consumptions [23], [24]. The approach has also been applied to develop a comprehensive and beneficial demand response model for energy pricing [18]: a retail energy provider exploits Q-learning to define the optimal real time pricing considering different aspects such as price caps and customer responses. The Q-learning method can be coupled with other approaches, e.g., leading to genetic-based fuzzy Q-learning [25] and Metropolis Criterion-based fuzzy Q-learning [26] for intelligent energy management.

In the work here presented, we extend the framework of reinforcement learning to multi-criteria decision-making on medium-term (2 steps-ahead) scenarios. The medium-term planning allows identifying appropriate subsequent charging and discharging actions for specific scenarios, by reducing the uncertainties related to forecasting errors, and identifying optimal actions for long-term planning. To test the optimization framework, a range of assumptions are made:

- The time step for the energy system optimization is set to be one hour.

- The selection of the individual components models was guided by the need to keep these models simple, but physically meaningful, in order to test the performance of the reinforcement learning algorithm. In this view, we do not account for power losses over time t, and neither consider the charging and discharging efficiencies in the model of the battery storage.
- The number of discretization states of the stochastic variables relevant to the problem is relatively small but sufficient for not losing major trends. This is to obtain a computationally tractable model for testing the reinforcement learning algorithm and analyse its sensitivity with respect to some of the main parameters.

The rest of the paper is organized as follows. Section 2 presents the modelling framework, gives the details of the simulation model of the wind power generator, accounting for wind speed stochasticity and random mechanical failures, and illustrates the models of the other physical components constituting the microgrid. Section 3 provides the detailed framework of consumer energy management with reinforcement learning. The sensitivity analysis to the learning parameters is presented in details in Section 4. In Section 5, the simulation results on the available wind power output and the performance of the microgrid system are presented and analysed. Section 6 provides the analysis and recommendations regarding the Q-learning optimization framework in comparison with other energy optimization approached. The last section draws general conclusions and suggests possible improvements to learning efficiency and extensions of the modelling framework.

2. THE MODEL OF THE MICROGRID AND ITS PHYSICAL COMPONENTS

Strategies for renewable sources integration can be driven by diverse criteria and constraints, such as regulatory and economic mechanisms, topology and technical constraints of electricity grids, and diversity and flexibility of generation portfolio [27], [28]. We focus on a simple urban microgrid involving a consumer with inelastic load D_t, a transformer, providing electricity power from the external grid as well as information about the electricity market price P_t, a renewable generator with available power output P_t^{wt} and a storage facility with a level of battery charge R_t. The subscript t is used to indicate time. The architecture of the considered microgrid is

shown in Figure 1. The consumer has the possibility to control the storage and renewable generator, and thus, can decide to purchase all electricity from the external grid or cover partly its demand by using the electricity produced by the local renewable generator. For this, the consumer can store electricity when the renewable resource is available and discharge the storage when needed. The model is kept purposely simple, but sufficiently comprehensive in the properties relevant to the study of the reinforcement learning paradigm in the context of interest.

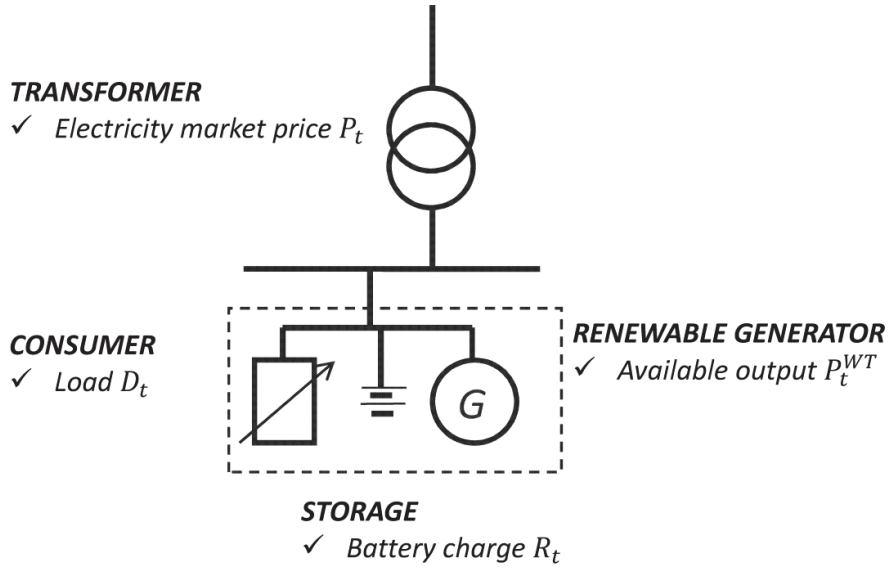

Figure 1. Architecture of the considered microgrid.

We adopt an agent-based modelling framework to implement the decision-making heuristics, learning rules and adaptive processes of interactions with the environment [29]. Specifically, the consumer is presented in the form of an individual agent who evolves by interacting with the influencing variables of the environment - the available wind power output P_t^{wt}, the load D_t and the level of battery charge R_t. The actions linked to these interactions are driven by the particular goals of the consumer and are implemented in the form of battery scheduling, following a process of reinforcement learning presented in details in Section 3. By so doing, we implement intelligence directly into the consumer's behaviour, so that he can decide and act in its own interests without implication of additional management actors, such as the facilitator used for energy management in electricity grids with multiple distributed generations [20].

The external grid imposes technical constraints to the microgrid, such as voltage and current limits of the network, and sets the market electricity price P_t. The former are the technical

requirements for ensuring the reliable and optimal management of the power flow inside the grid [30]. For simplicity, in this paper we consider no losses and no technical constraints on the lines and generators capacities. The electricity price is assumed to be constant and equal to one *$* per *Wh* for all time step intervals.

The rest of this section presents in detail the models of the wind generator, the load and the battery storage.

2.1. Model of the wind generator

The amount of electricity output P_t^{wt} from the wind generator depends on the availability of the wind source and the random mechanical failures of the wind generator components [31], [32]. In this paper, we adopt a Markov chain modelling framework to describe the dynamics of stochastic transition among different levels of wind speed conditions and mechanical states (Figure 2). This approach is used to model natural processes, including synthetic generation of hourly wind speed time series [33], [34]. Research on wind generator modelling shows the necessity for an adequate discretization of the wind speed, with a small discrete state width of few m/s [35], [36]. We set this width to 3 m/s, which results in an adequate resolution for the planning of the battery scheduling.

The transition rates (Table 1) are calculated based on the principle of frequency balance between any two states, presented in [37]. As input data for the transition rates calculation, the wind speed data with one hour time step from [38] is used. The site for wind speed data is representative of an urban location equipped with a wind generator of capacity factor of about 13%, i.e. the ratio between the actual wind power output and the potential wind power output if the wind turbine operates constantly at its nominal capacity.

Table 1. Transition rates between wind speed states.

Transition rates between wind speed states (occurrence per year)		
$\lambda_{1,2} = 1418$	$\lambda_{2,3} = 2199$	$\lambda_{3,4} = 1835$
$\lambda_{2,1} = 1797$	$\lambda_{3,2} = 2031$	$\lambda_{4,3} = 2249$
$\lambda_{4,5} = 1633$	$\lambda_{5,6} = 1268$	
$\lambda_{5,4} = 2625$	$\lambda_{6,5} = 2191$	

The correlation between the wind speed and the mechanical states of the wind turbine has been discussed and studied in various references [37], [39–42]. Analyses based on real data collected from installed wind turbines show increased number of failure occurrences and severity during the phase which precedes the cut-off of the wind turbine. To take this phenomenon into account, the Markov chain relates the mechanical states to normal and extreme levels of wind speed (Figure 2). The states 1 – 5 represent normal wind speed conditions for the generator operation (up), with only potential minor damages occurring to the equipment at rate λ represented by transitions to the down states 7 - 11. State 6 (up) describes extreme wind speed operational conditions (before the cut-off), which can lead to minor or severe damage of the wind turbine (down state 12) occurring at a failure rate λ' higher than the one for normal operational conditions ($\lambda' > \lambda$). Therefore, states 1 – 6 represent the working conditions (up) of wind generator and states 7 – 12 represent the failure states (down). We consider that after a repair, the wind turbine resets to its operation at one of the reachable states of wind speed 1 – 6 in an "as good as new" mechanical state [43].

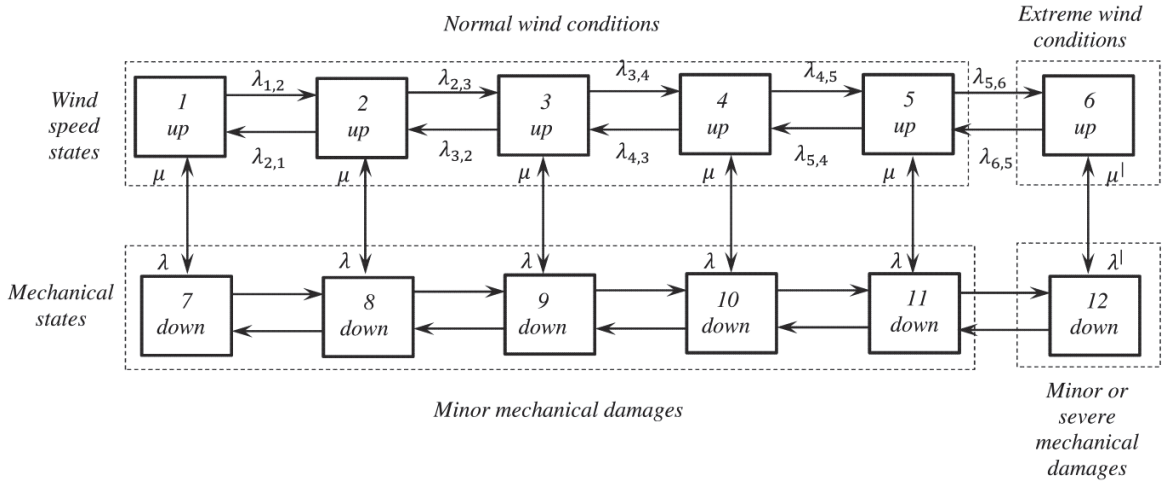

Figure 2. Markov chain model for wind generation.

The failure and repair transition rates in normal and extreme wind conditions are presented in Table 2, taken from [37]. The Mean Time to Failure (MTTF) and Mean Time to Repair (MTTR) for normal wind speed conditions are 2183 and 97 h, respectively. The Mean Time to Failure (MTTF) and Mean Time to Repair (MTTR) for the extreme wind speed conditions are 364 and 364 h, respectively. It is seen that during normal wind speed conditions, failures occur relatively rarely and cause minor damage to the wind generator, which can be repaired in relatively short

time (97 h). During extreme wind conditions, the wind generator suffers additional stress, which gives a shorter MTTF and failures requiring longer time for repair (364 h). Finally, we note that the values of Table 2 are comparable with those of other references (e.g., [44]).

Table 2. Failure and repair rates of wind turbine.

Transition rates (occ./year)	Wind speed conditions	
	Normal	Extreme
To failure	4	24
To repair	90	24

2.2. Model of load

To simulate the load of the consumer, a top-down approach based on available statistical collections of electricity consumption has been used [45]:

$$D_t = D^{peak} \cdot r_w^{peak} \cdot r_d^{peak} \cdot r_h^{peak} \quad (1)$$

where r_h^{peak} is the hourly peak defined for working days and weekends *(%)*, r_d^{peak} and r_w^{peak} are the daily and weekly peaks of power demand *(%)* and D^{peak} is the maximum hourly peak of power demand over a year *(Wh)*.

2.3. Model of battery storage

A simplified model of battery storage dynamics is adopted by implementing a discrete time system for the power flow dynamics over the time step interval Δt :

$$R_t = R_{t-1} + R_t^{stor,charge} - R_t^{stor,discharge} \quad (2)$$

where R_t and R_{t-1} are the levels of the energy stored in the battery at time *t* and *t-1 (Wh)*, $R_t^{stor,discharge}$ and $R_t^{stor,charge}$ are the power flows over time step interval Δt between battery and consumer and wind generator and battery *(Wh)*, respectively.

3. MODELLING OF THE CONSUMER AGENT

As introduced in Section 2, the consumer is modelled as an individual agent who makes use of particular heuristics for its decision-making, action-taking and adaptation to external conditions.

This section presents the reinforcement learning algorithm used by the consumer to interact, adapt and take decisions towards its goals defined in the form of reward functions, and taking into account a dynamically changing environment characterized by the available wind power output P_t^{wt}, the load D_t and the level of battery charge R_t. The section starts with a general introduction to the framework of reinforcement learning algorithm and continues with detailed descriptions of particular features and parameters of the algorithm specifically developed.

3.1. Reinforcement learning algorithm

The reinforcement learning algorithm is used here to model the consumer's adaptation to a dynamically changing environment by performing actions of battery scheduling. The synthetized form of the algorithm is presented below:

1. Initialize to 0 the Q-values of all possible actions sequences for each scenario and set time t=0.

2. a) For time t, identify the values of load D_t and available wind power output P_t^{WT}, and make the forecast of available wind power output P_{t+1}^{WT}, P_{t+2}^{WT} and load D_{t+1}, D_{t+2} for 2 steps-ahead. Identify $Scenario_t^l = [s_t^i; s_{t+1}^n; s_{t+2}^p]$, the forecasted states of wind conditions for the local generation, simulated with the Markov chain model.

b) Based on identified $Scenario_t^l$ and battery charge R_t at time step t, define all possible actions sequences of battery scheduling for 2 steps ahead.

c) Apply the policy for selection of sequence of actions.

d) Perform the selected sequence A_t^j under real system conditions, simulated using the Markov chain model for real wind conditions. Update the value of the sequence performed.

3. Move to time step t+3; repeat step 2.

The description of specific learning features in the algorithm, such as the Q-values and $Scenario_t^l$, is presented in details in the next subsections. Note that the uncertainty in load is not accounted here, as the consumer is assumed to hold a perfect knowledge about its own consumption.

The diagram of the algorithm and simulation scheme for forecasted and real wind speed conditions is presented in Figure 3.

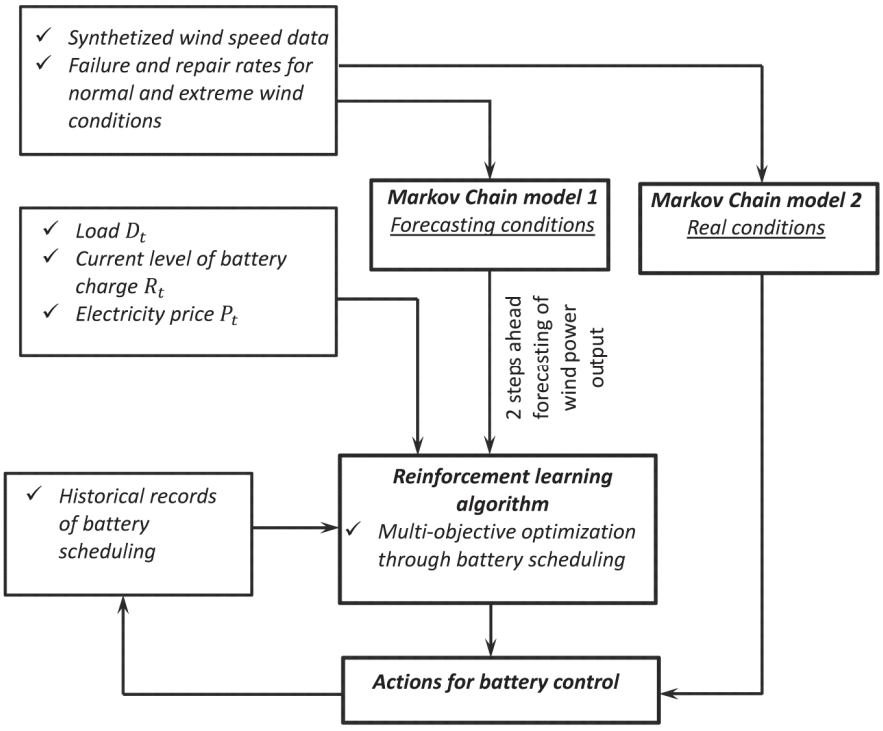

a)

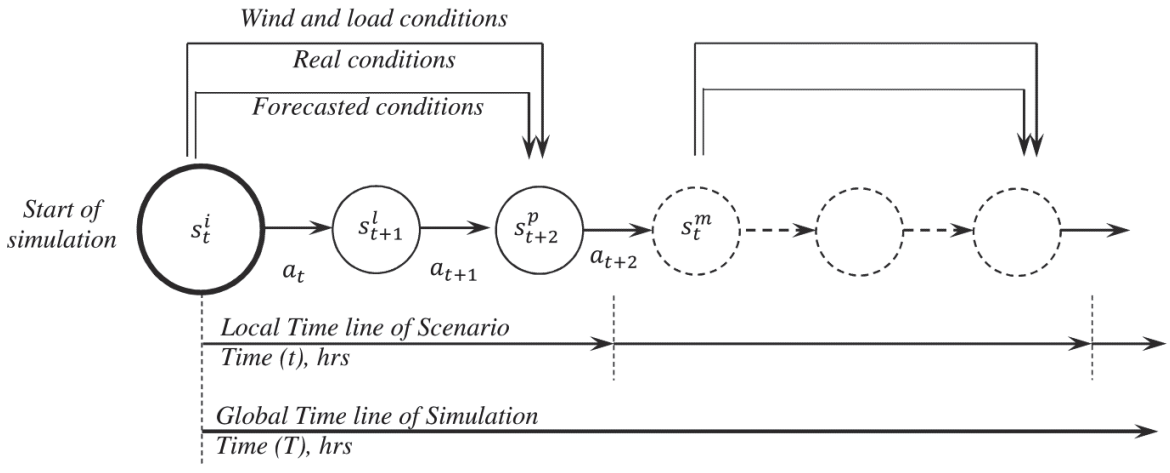

b)

Figure 3. The reinforcement learning algorithm: a) Structure of the battery scheduling algorithm; b) Simulation scheme for forecasted and real wind speed conditions.

As it can be seen from Figure 3, forecasted and real wind speed state evolutions are modelled with two identical Markov chain models. The first Markov chain model generates the forecasts of wind speed conditions, which are used to identify the 2 steps-ahead scenario and select the actions sequence for battery scheduling. The second Markov chain models real wind speed conditions, starting from the same state as the forecasted conditions, under which the selected actions sequence will be performed. Note that the noise in the forecasted wind power output for 2 steps-ahead is automatically accounted for by the stochasticity of the Markov chain model.

3.2. Definition of scenarios and actions for battery scheduling

Available wind power output and consumer load are the two variables defining the dynamic environment of the consumer. The values of these two variables at time step *t* define the system state $s_t^i = [D_t; P_t^{WT}]$. The actual (initial) states at time *t* and the future states at the next two time steps *t+1* and *t+2* define the generic $Scenario_t^l = [s_t^i; s_{t+1}^n; s_{t+2}^p]$, where *i*, *n*, *p* are indexes of system states and *l* is the scenario index. Furthermore, the level of battery charge R_t at time step *t* for $Scenario_t^l$ must also be considered.

Note that the number of possible scenarios grows exponentially with the number of time steps in the generic scenario. The consideration of a 2 steps-ahead scenario represents a good trade-off between the appropriate representation of the dynamics and the computational tractability of the model. Indeed, the 'profit' from the battery scheduling process increases with the extension of the forecasting and planning horizons, which allows to identify the appropriate subsequent charging and discharging actions; however, the increase of this horizon entails the increase of uncertainties related to forecasting errors and difficulties to identify the appropriate subsequent actions for the long-term planning. Then for tractability reasons, the duration of scenarios is limited to 2 steps-ahead.

At time step *t*, the decision must be made about the actions to take at times *t*, *t+1* and *t+2*. The 2 steps-ahead sequence of three actions decided at time *t* for battery scheduling in the scenario is denoted as $A_t^j = [a_t, a_{t+1}, a_{t+2}]$. At each time step *t*, action a_t can assume 'values' $a_t = a^0$ or $a_t = a^1$, where action a^0 corresponds to covering part of the consumer electricity demand by discharging the battery, whereas action a^1 consists in purchasing all the electricity demanded by

the consumer from the external grid while charging the battery. In this view, two options for action a_t, two for a_{t+1} and two for a_{t+2} provide the total of possible sequences of actions for each scenario, which is equal to eight. Figure 4 illustrates the possible sequences of actions for battery scheduling starting by the state R^3 defined using a decision tree diagram by considering four possible states of a battery charge $R_t = [R^0, R^1, R^2, R^3, R^4, R^5, R^6]$ at time *t*, where R^0 and R^6 are respectively the minimum and maximum possible levels of battery charge.

Note that the battery scheduling is a continuous process, where the final level of battery charge R_{t+2} for one scenario becomes the initial level of battery charge R_t for the subsequent scenario and so on.

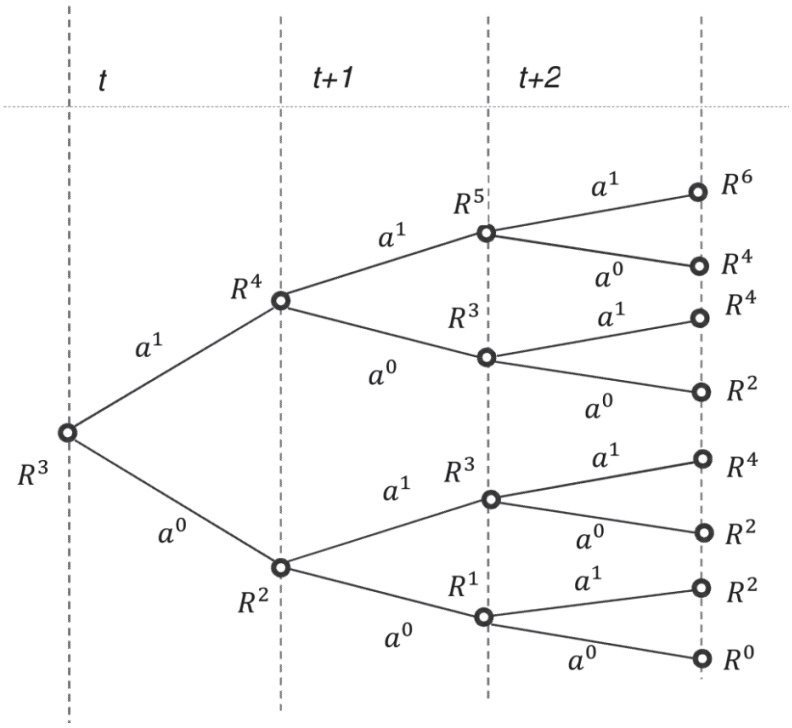

Figure 4. Tree diagram for battery scheduling.

It is important to underline that for the research presented in this paper only the possibility to charge the battery from the wind turbine is considered. However, in practice the battery can be charged also by purchasing the electricity from the external grid during the periods of low electricity price, while the electricity produced by the wind turbine can be injected to the grid in exchange of remuneration (periods of high electricity price). However, since in this paper the electricity price is assumed to be constant, we focus on the development of the learning

algorithm for the efficient management of the microgrid through the coupling battery – wind turbine.

3.3. Reward functions and actions for battery scheduling

The derivation of the consumer optimal battery scheduling within 2 steps-ahead scenarios is based on reinforcement learning. This is a process of action-reward dynamics, driven by quantitative performance indicators which evaluate the action or sequence of actions undertaken and feedback the value to adjust future scheduling decisions [21].

For the considered case, the consumer strategy is driven by the optimization of a numerical reward, which quantifies two goals or decision-making criteria. These are: i) increasing the utilization rate of the battery during high electricity demand (so as to decrease the electricity purchase from the external grid) and ii) increasing the utilization rate of the wind turbine for local use (so as to increase the consumer independence from the external grid). The optimization of the numerical reward is achieved through the choice of the actions a^0 and a^1 of battery scheduling. Since the battery cannot be charged and discharged at the same time, only one of these actions can be selected and performed at any time step *t*: this makes the two criteria conflicting and for this reason, the consumer aims at increasing its performance by selecting an optimal sequence of actions for a 2-steps ahead time period.

The reward function from the undertaken actions is defined as follows:

$$f_t(a_t) = \begin{cases} \frac{P_t^{wt}}{D_t}\left(D_t - R_t^{stor,discharge}\right), & if\ a_t = a^0 \\ k \cdot \left(P_t^{wt} - R_t^{stor,charge}\right), & if\ a_t = a^1\ \&\ P_t^{wt} > 0 \\ 0, & if\ a_t = a^1\ \&\ P_t^{wt} = 0 \end{cases} \quad (3)$$

where k is a weight coefficient for the reward function $f_t(a_t)$ when $a_t = a^1$, $R_t^{stor,discharge}$ and $R_t^{stor,charge}$ are the amounts of electricity *(Wh)* that the battery is capable of discharging and charging during one hour, respectively. Observe that by increasing the value of the weight coefficient k the value of reward obtained after action a^1 increases in comparison with the reward obtained after action a^0, which makes action a^1 more likely to be performed. The detailed analysis of the influence of the weight k is given in Subsection 4.1. For equally

weighted reward functions ($k = 1$), both reward functions can vary in the same range of values between 0 and 5500.

As indicated previously, the successful scheduling of the battery, and thus the increase of the microgrid performance with respect to the consumer goals, is done by considering 2 steps-ahead scenarios, by forecasting the load and the available wind power output in 2 time steps ahead. This information is used to select the optimal sequence of actions A_t^j for the entire scenario, then performed to maximize the set of reward functions calculated by eq. (3).

Note that if action a_t is taken and reward function $f_t(a_t)$ is calculated by taking into account only one time step, undesired situations may occur. For example, the selection of action a^0 to discharge the battery, instead of action a^1 to charge the battery, seems optimal in case of high electricity demand and low wind power output at time step *t*. However, this discharging action at time step *t* deprives the available charge of the battery and does not allow to use it at the next time steps *t+1* and *t+2*, when wind power output may be unavailable. This is avoided if actions are planned with 2 steps-ahead scenarios, and this is the reason why we consider such planning horizon.

In this view, the aim of the algorithm is to maximize not only the immediate reward at the current time *t* by means of action a_t, but also the rewards of the future states at time steps *t+1* and *t+2* by means of the sequence of actions A_t^j. To allow this, the total discounted truncated reward $r(Scenario_t^l, A_t^j)$ from future actions is calculated as [46]:

$$r\left(Scenario_t^l, A_t^j\right) = \gamma^0 \cdot f_t(a_t) + \gamma^1 \cdot f_{t+1}(a_{t+1}) + \gamma^2 \cdot f_{t+2}(a_{t+2}) \quad (4)$$

where $f_t(a_t)$, $f_{t+1}(a_{t+1})$ and $f_{t+2}(a_{t+2})$ are the reward functions from the actions a_t, a_{t+1} and a_{t+2} undertaken at time steps *t*, *t+1* and *t+2*, respectively. The most common method to 'weigh' values of reward functions at time step *t* is by using the power law, where γ represents the discounted factor taking values within the range of [0,1] and the exponent of γ corresponds to the number of time steps in the $Scenario_t^l$. The action a_t, undertaken at time *t*, is considered to be more important, and thus, more valuable with reward function $f_t(a_t)$ taken with maximum weight. Every subsequent reward function in the $Scenario_t^l$ has smaller weight than the precedent, so that the algorithm is able to determine the present values of the future reward

functions. Observe that if γ is equal to zero, only the reward function $f_t(a_t)$ is accounted for in the total truncated reward $r\left(Scenario_t^l, A_t^j\right)$; while if γ is slightly less than one, the total truncated reward will take into account the values of the future reward functions. Following the practice of [46], the discounted rate is here considered to take a value slightly less than one, specifically $\gamma = 0.8$. Still, observe that this method allows the calculation of the total truncated reward, prioritizing the reward function obtained from the first action a_t, which is more robust because less affected by the possible forecasting errors.

3.4. Evaluation of actions for battery scheduling

In this paper, to obtain the optimal actions for battery scheduling, we adopt the Q-learning algorithm for which the reward $r(Scenario_t^l, A_t^j)$, calculated with eq. 5, is used to iteratively update the value Q of the sequence of actions A_t^j at the p-th occurrence of the $Scenario_t^l$ [21]:

$$Q\left(Scenario_t^l, A_t^j\right)_p = Q\left(Scenario_t^l, A_t^j\right)_{p-1} + \alpha\left[r\left(Scenario_t^l, A_t^j\right)_p - Q\left(Scenario_t^l, A_t^j\right)_{p-1}\right] \quad (5)$$

where α is the learning rate whose value is between 0 and 1. The influence of the learning rate coefficient on the learning process is discussed in Subsection 4.3. By using this approach, the Q-value of each sequence of actions for a scenario will be automatically updated by eq. (5) until it converges to its maximum Q*-value. For a particular scenario, the sequence of actions holding the highest Q*-value among other sequences of actions will be the optimal sequence for that scenario.

The identification of Q*-values is done by the following procedure of sequence selection:

- The algorithm starts by setting all Q-values of possible sequences of actions equal to zero.
- When the $Scenario_t^l$ occurs, a sequence of actions is selected randomly, actions are performed and its associated Q-value is calculated.
- The random selection of sequence of actions for the $Scenario_t^l$ continues until all Q-values converge to maximum Q*-values. The durations of this convergence step, called burn in period $p^{Scenario_t^l}$, is measured by the number of occurrences of the same $Scenario_t^l$ and is discussed in Subsection 4.3.

- After the Q*-values for all possible sequences of actions for $Scenario_t^l$ are identified, the sequence of actions with highest Q*-value is performed at the future occurrences of $Scenario_t^l$.

The sequence selection and updating of Q-values procedures are applied identically for all scenarios. Obviously, the sequence of actions with highest Q*-value will be identified faster for frequently occurred scenarios than for rarely repeated scenarios, whose sequence of actions will be mostly selected at random. Then, the learning efficiency is highly dependent on the rate of occurrence of the possible different scenarios. This aspect is treated in Subsection 5.2.

Note that if the real environmental conditions do not allow performing the planned optimal sequence, for example because of unavailability of wind, a penalty could be applied to the reward to strengthen the learning. However, in this work we focus on planning errors due to inefficiency of the forecasting model, so that incorrect actions are not penalized.

4. SENSITIVITY ANALYSIS OF LEARNING PARAMETERS

To understand the role of the learning parameters, i.e. the weight coefficient k, the discounted rate γ and the learning rate α and set their values, a crude sensitivity analysis is performed on two case study scenarios, whose characteristics are reported in Table 3. The choice of the two scenarios has been made with the goal of representing two opposite situations: Scenario 1 is characterized by low wind power output and medium and high values of load, whereas Scenario 2 is characterized by high wind power output and low load. The initial charge of the battery at time *t* is 3000 W in both cases. Based on values of forecasted wind power output at time steps *t*, *t+1* and *t+2* and on the initial battery charge at time *t*, eight sequences of actions for battery scheduling are possible for these scenarios.

Table 3. Case study scenarios for sensitivity analysis.

Scenario 1 with initial battery charge $R_t = 3000\ Wh$			
Parameters	*Time steps*		
	t	*t+1*	*t+2*
Wind power output (P_t^{wt}), Wh	*1200*	*1200*	*1200*
Load (D_t), Wh	*4400*	*5200*	*5200*
Scenario 2 with initial battery charge $R_t = 3000\ Wh$			
Parameters	*Time steps*		
	t	*t+1*	*t+2*
Wind power output (P_t^{wt}), Wh	*6000*	*4800*	*4800*
Load (D_t), Wh	*2800*	*2800*	*2800*
Possible sequences of actions $[a_t, a_{t+1}, a_{t+2}]$	a^0	a^0	a^0
	a^0	a^0	a^1
	a^0	a^1	a^0
	a^0	a^1	a^1
	a^1	a^0	a^0
	a^1	a^0	a^1
	a^1	a^1	a^0
	a^1	a^1	a^1

In the following subsections, the influence of the learning parameters k, γ and α on the reinforcement learning algorithm is analysed.

4.1. Weight coefficient k of the reward function $f_t(a^1)$

4.1.1. Possible values of the weight k

At each time step *t*, the consumer makes a choice between actions a^0 and a^1 by considering the respective reward function values $f_t(a^0)$ and $f_t(a^1)$ and the optimization goals of discharging the electricity from the battery during periods of high load and charging it during periods of available wind power output (cf. Subsection 3.2). Considering this, the possible scenarios can be divided into three groups, depending on which of the following conditions is met:

- $f_t(a^0) > f_t(a^1)$, for the states of high loads and low wind power outputs, so as to increase the utilization rate of the battery during high electricity demand;
- $f_t(a^0) < f_t(a^1)$, for the states of low loads and high wind power outputs, so as to increase the utilization rate of the wind turbine;
- $f_t(a^0) = f_t(a^1)$, for particular states where both actions a^0 and a^1 are equally valuable.

The competition between $f_t(a^0)$ and $f_t(a^1)$ depends on the weight coefficient k applied to f_t. Figure 5 shows the values of reward functions $f_t(a^0)$, grey-coloured surface, and $f_t(a^1)$, white-coloured surface, in the three dimensional coordinate system defined by the following axes: load *(Wh)*, wind power output *(Wh)* and value of reward function. The three-dimensional plots of $f_t(a^0)$ and $f_t(a^1)$ are drawn using eq. (3) for different discretized values of load and wind power output. Such representation of the reward function for different levels of load and wind power output gives a comprehensive illustration of the preferences between actions a^0 and a^1 for different states depending on the weight coefficient k.

For this paper, three values of the weight coefficient were considered in representation of different preference situations, as explained below:

- $k = 1$, which weighs equally $f_t\ (a^0)$ and $f_t(a^1)$ and, thus, prioritizes the use of the wind turbine during the three states (round points in Figure 5 *a*) corresponding to maximum wind power output and minimum load.
- $k = \begin{cases} 2^{1200/P_t^{wt}}, & if\ P_t^{wt} > 0 \\ 0, & if\ P_t^{wt} = 0 \end{cases}$ which weighs differently depending on the available wind power output and, thus, prioritizes the use of the wind turbine during particular states of the wind power output and load (round points in Figure 5 b);
- $k = 6$ which overweighs $f_t(a^1)$ and, thus, leads to charging the battery at all times *t* of available wind power output (Figure 5 c).

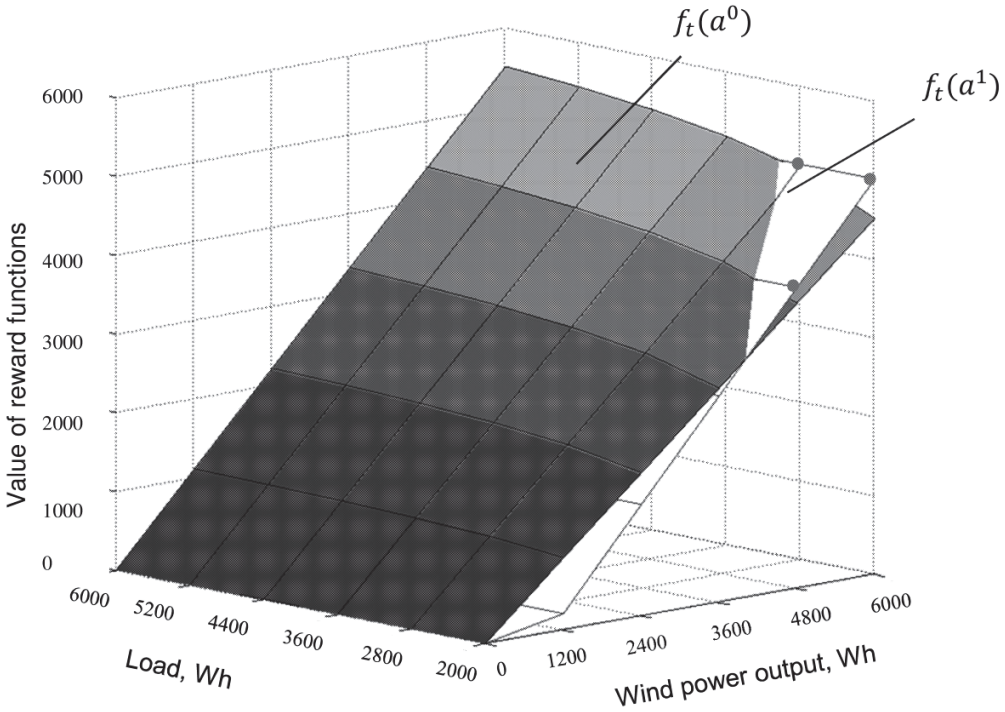
$f_t(a^0)$
$f_t(a^1)$
Value of reward functions
6000
5000
4000
3000
2000
1000
0
6000 5200 4400 3600 2800 2000
Load, Wh
0 1200 2400 3600 4800 6000
Wind power output, Wh

a)

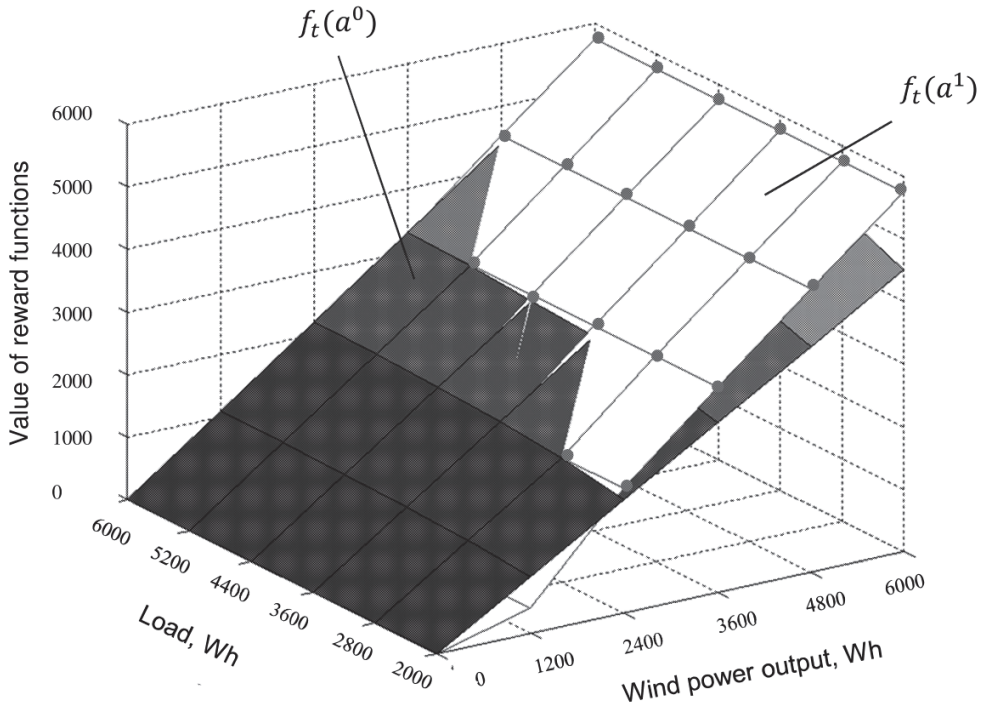
$f_t(a^0)$
$f_t(a^1)$
Value of reward functions
6000
5000
4000
3000
2000
1000
0
6000 5200 4400 3600 2800 2000
Load, Wh
0 1200 2400 3600 4800 6000
Wind power output, Wh

b)

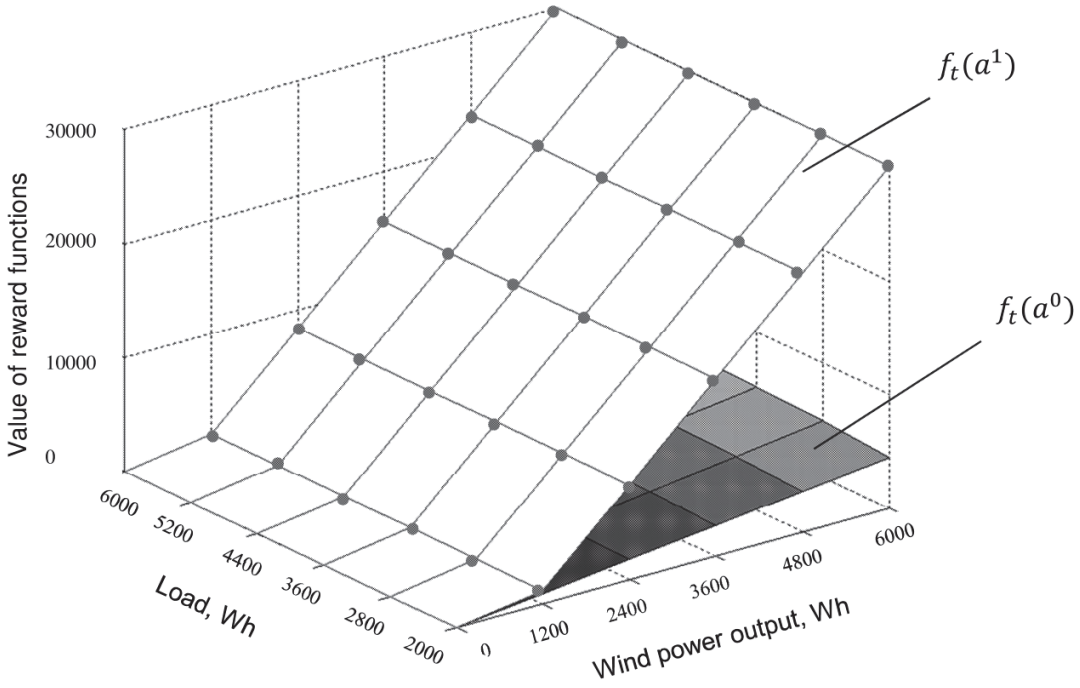

c)

Figure 5. $f_t(a^0)$ *and* $f_t(a^1)$ *as functions of load* D_t *and wind power output* P_t^{wt} *for different weight coefficient values: a)* $k = 1$*; b)* $k = 2^{1200/P_t^{wt}}$*; c)* $k = 6$.

As it can be seen from Figure 5, the intersection of the two surfaces $f_t(a^0)$ and $f_t(a^1)$ falls outside the grey points representing the system states: this indicates that for the considered data and scenarios, the selected weight values cannot lead to the case $f_t(a^0) = f_t(a^1)$.

4.1.2. Influence of the weight **k** *on the optimal sequence of actions*

As expected, the value of the weight coefficient *k* influences the calculations of the final Q*-values. A large *k* increases the value of the reward function $f_t(a^1)$ from action a^1, leading to the fact that the sequences containing actions a^1 hold the highest Q*-values. Then, the optimality of the action sequences based on the highest Q*-value, leads to performing sequences where actions a^1 are dominantly present. On the contrary, low *k* values favour actions a^0, and this is reflected in the calculation of the Q*-values which are highest for the sequences containing actions a^0.

Table 4 shows the optimal action sequences of highest Q*-values, for the two case study scenarios of Table 3 and the three different values of the weight coefficient *k*. The discounted rate γ and α are taken equal to 0.8 and 0.6, respectively.

Table 4. Optimal action sequences for case study Scenarios 1 and 2, and the three different weight coefficient values.

Value of weight coefficient *k*	Scenario 1	Scenario 2
1	$[a^0,a^0,a^0]$	$[a^1,a^1,a^1]$
$2^{1200/P_t^{wt}}$	$[a^0,a^0,a^0]$	$[a^1,a^1,a^1]$
6	$[a^1,a^1,a^1]$	$[a^1,a^1,a^1]$

It is seen that using a weight coefficient $k = 1$ favours the discharge of the battery through the sequence of actions $[a^0,a^0,a^0]$ for the Scenario 1 of high load and low wind power output, whereas the sequence of action $[a^1,a^1,a^1]$ is optimal for Scenario 2 of high wind power output and low load. As for the case of $k = 1$, also the variable weight coefficient $k = 2^{1200/P_t^{wt}}$ leads to the same two optimal action sequences for the two scenarios.

On the contrary, the large value of the weight coefficient $k = 6$ leads to the same optimal sequence of actions $[a^1,a^1,a^1]$ for the two scenarios.

Based on the findings of the crude sensitivity analysis, the following guidelines can be provided for the choice of the value of the weight coefficient *k* in our case. On the one hand, the situation of zero wind speed is relevant in an urban area, such as the assumed location for our microgrid; on the other hand, the information about availability of wind becomes less reliable for scenarios that go beyond 2 steps ahead in the future. Then, if we were to take a value of the weight coefficient $k = 1$ or $k = 2^{1200/P_t^{wt}}$ the following situation would occur for case study Scenario 1: the sequence of actions $[a^0,a^0,a^0]$ is selected and the battery is discharged even in presence of sufficient wind power output (Table 4); this sequence of actions is indeed profitable for the particular case study scenario, but it does not take into account the potential absence of wind of the subsequent scenario. For long term benefits, it is, then, more reasonable to take a large value of the weight coefficient ($k = 6$), to favour action a^1 and, thus, profit from all available wind power output to maintain the charge in the battery.

4.2. Discounted rate γ

The discounted rate γ contributes to determining the values of future reward functions using eq. (3). Therefore, it plays an important role in the calculation of Q*-values and the consequent definition of the optimal sequence of actions. The sequences of actions holding highest Q*-values for on different values of γ and $k = 6$, $\alpha = 0.6$ are shown in Table 5. The optimal sequence turns out to be the same for the two considered scenarios.

Table 5. Sequences of actions with highest Q-value depending on different values of discounted rate.*

Value of discounted rate γ	Scenario 1 / Scenario 2
0	$[a^1,a^1,a^1]$, $[a^1,a^1,a^0]$, $[a^1,a^0,a^1]$, $[a^1,a^0,a^0]$
0.2	$[a^1,a^1,a^1]$
0.4	$[a^1,a^1,a^1]$
0.6	$[a^1,a^1,a^1]$
0.8	$[a^1,a^1,a^1]$
1	$[a^1,a^1,a^1]$

As it can be observed, the sequence of actions $[a^1,a^1,a^1]$ holds the highest Q*-value for all values of the discounted rate. For discounted rate $\gamma = 0$, values of actions undertaken at time steps *t+1* and *t+2* are neglected and only the first action at time step *t* is valuable; in other words for $\gamma = 0$, the sequences of actions $[a^1,a^1,a^1]$, $[a^1,a^1,a^0]$, $[a^1,a^0,a^1]$ and $[a^1,a^0,a^0]$ are all equally valuable. Furthermore, γ values in the range 0.2 - 1 do not influence the sequence of actions with highest Q*-value. Based on this, and as anticipated earlier, following the practice of [42] the discounted rate γ is taken equal to a value slightly less than one, i.e. $\gamma = 0.8$.

4.3. Learning rate $\boldsymbol{\alpha}$

The value of the learning rate α influences the speed of convergence to Q*-values but not to the final highest Q*-values. Figure 6 illustrates the convergence of action sequence $[a^1,a^1,a^1]$ for Scenario 1 for different values of the learning rate $\alpha = [0.2, 0.4, 0.6, 0.8,1]$. The convergence is calculated analytically by using eq. (5). The values of γ and k are 0.8 and 6, respectively. Similar convergence behaviour is observed for the other action sequences.

From Figure 6, it can be observed that a higher value of α leads to updating $Q\left(Scenario_t^l, A_t^j\right)_p$ to a higher value after the occurrence of $Scenario_t^l$, so that the convergence to Q*-values is more rapid. A value of α close to zero reduces the update of the Q-values, and, thus, slows down convergence. On the other hand, the use of a low value of the learning rate is justified in some cases, especially because it modulates new coming rewards that must be considered with precaution. In our case, the value of the learning rate has been set to $\alpha = 1$.

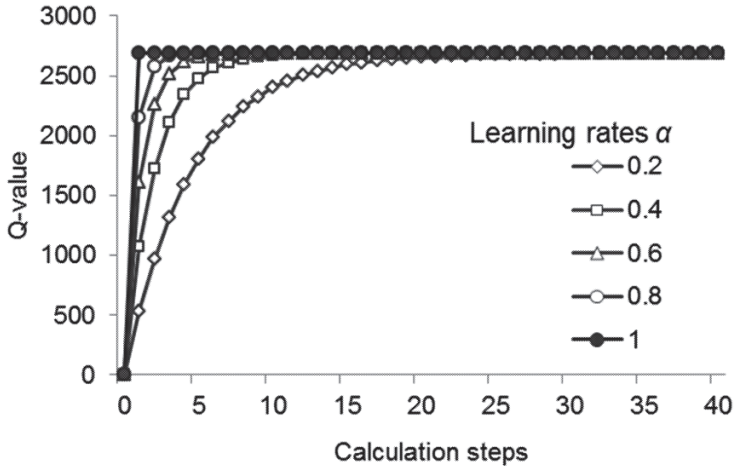

Figure 6. Convergence of Q-values of sequences of actions $[a^1,a^1,a^1]$ depending on different learning rates α.

It seems important to recall that each scenario allows performing up to five possible sequences of actions, while the updating process is done only for one specific sequence of actions for the scenario of occurrence. Thus, the real duration of the burn-in period $p^{Scenario_t^l}$ for defining the Q*-values on randomly selected sequences is longer than the burn-in period calculated analytically. Indeed, convergence to the maximum Q*-values of all sequences of actions is obtained already after 11 occurrences of the case study scenarios. Based on these findings, we set the duration of the burn-in period for each scenario to $p^{Scenario_t^l} = 16$ occurrences of the same scenario: then, the sequence of actions holding the highest Q*-value for a given scenario will be performed every time that scenario occurs.

5. SIMULATION RESULTS AND ANALYSIS

This section summarizes the simulation results obtained with the reinforcement learning algorithm and the framework defined through the sensitivity analysis, illustrated in the previous section. For computational tractability, the values of the wind power output P_t, load D_t and energy level in the battey R_t are discretized in six equally sized states, as anticipated.

The power output from the wind generator is calculated from the wind speed states 1 – 6 of the Markov chain (Figure 2), assuming linear relationship [47]:

$$P_t^{wt} = \begin{cases} 0, & if\ v < v_{ci} \\ P^r \cdot \dfrac{(v_t - v^{ci})}{(v^r - v^{ci})} \cdot \Delta t, & if\ v_{ci} \le v < v_r \\ P^r \cdot \Delta t, & if\ v_r \le v < v_{co} \\ 0, & if\ v > v_{co} \end{cases} \quad (6)$$

where v_t is the working wind speed *(m/s)* at time step *t* of 1 hour, v^{ci}, v^r and v^{co} are the cut-in, rated and cut-off wind speeds *(m/s)*, respectively, and P^r is the rated power of the wind turbine *(W)*.

We have assumed the wind power output to be proportional to the rated power of the wind generator as done in other research [47–49]. We are aware that this does not allow taking into account the nonlinearities of the wind power output, especially near cut-in and cut-off wind speeds. However, for the purpose of our work we think that this approximation is sufficient, although other functional dependencies (e.g., quadratic or cubic) between power output and wind speed can be used. In the case of a non-linear function, the discretization intervals between possible wind power outputs will not be equal.

The specifications of the wind turbine considered for the simulation are summarized in Table 6.

Table 6. Parameters of the wind turbine.

Parameters	P^r	v_{ci}	v_r	v_{co}
Values	6000 W	3 m/s	12 m/s	20 m/s

Wind power output over time step interval Δt is, then, [0, 1200, 2400, 3600, 4800, 6000] *Wh*, depending on the wind speed state. By considering the annual hourly peak and minimum loads as *6000 Wh* and *2000 Wh*, respectively, over time step interval Δt the load is also discretized into [2000, 2800, 3600, 4400, 5200, 6000] *Wh*. The amounts of power flowing between the battery

and the consumer $R_t^{stor,discharge}$ and between the wind generator and the battery $R_t^{stor,charge}$ over time step interval Δt, are considered to be constant for each time *t* and equal to *1000 Wh*. In addition, no performance degradations or losses are considered and the simultaneous charging and discharging of the battery is not allowed. By assuming the maximum capacity of the battery to be *6000 Wh*, the discretization states of the energy level in the battery are [0, 1000, 2000, 3000, 4000, 5000, 6000] *Wh*.

Subsection 5.1 presents the results of the available wind power output obtained with the Markov chain model of Subsection 2.1 and provides a comparison with results obtained analytically. Subsection 5.2 discusses the efficiency of the reinforcement learning algorithm. The 40 years simulation run is used to train the reinforcement learning algorithm. Once the algorithm is trained, and thus capable of identifying the optimal sequence of actions for most occurred scenarios, it can be used by the consumer to identify the optimal strategy for the battery scheduling on a daily basis. The training evolution is followed through the improvement of the performance indicators V0, V1 and E introduced in Subsection 5.3. The daily simulation of the battery scheduling process with the trained algorithm is presented and the performance of the trained algorithm is analysed. All numerical results presented in this section were obtained with the values of the parameters set as a result of the sensitivity analysis performed in Section 4.

5.1. Available wind power output

This subsection presents the results of wind power output calculated with the Markov chain model presented in Subsection 2.1. The probabilities of different states of wind power output are compared with analysed results. The duration of the simulation is 40 years. An example of curve of yearly cumulated available wind power output obtained with the Markov chain model is presented in Figure 7.

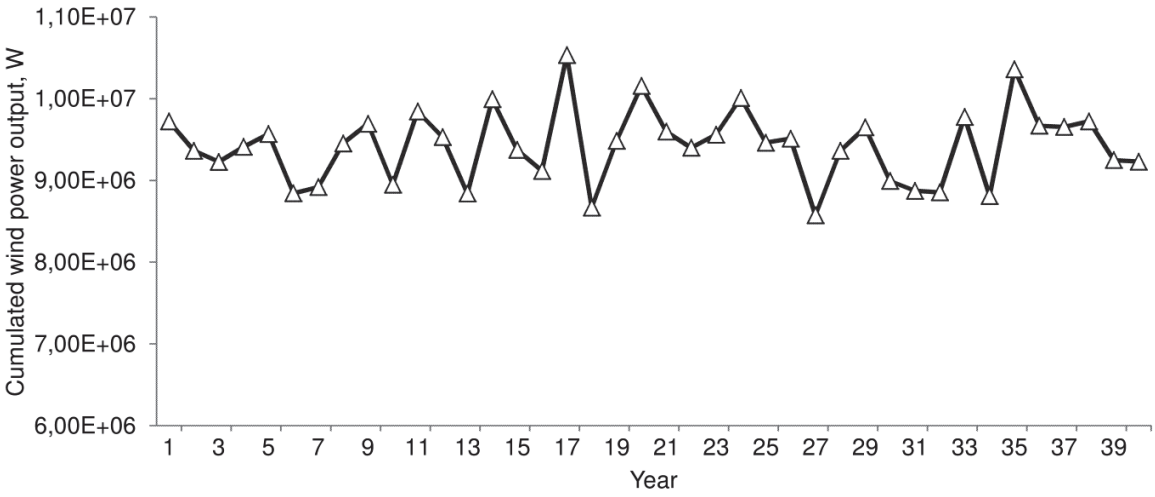

Figure 7. Cumulated annual available wind power output.

The 6 state probabilities of numerical wind power output compare well with the analytical values obtained solving the Markov chain model by the method of eigen-vectors (Figure 8) [50].

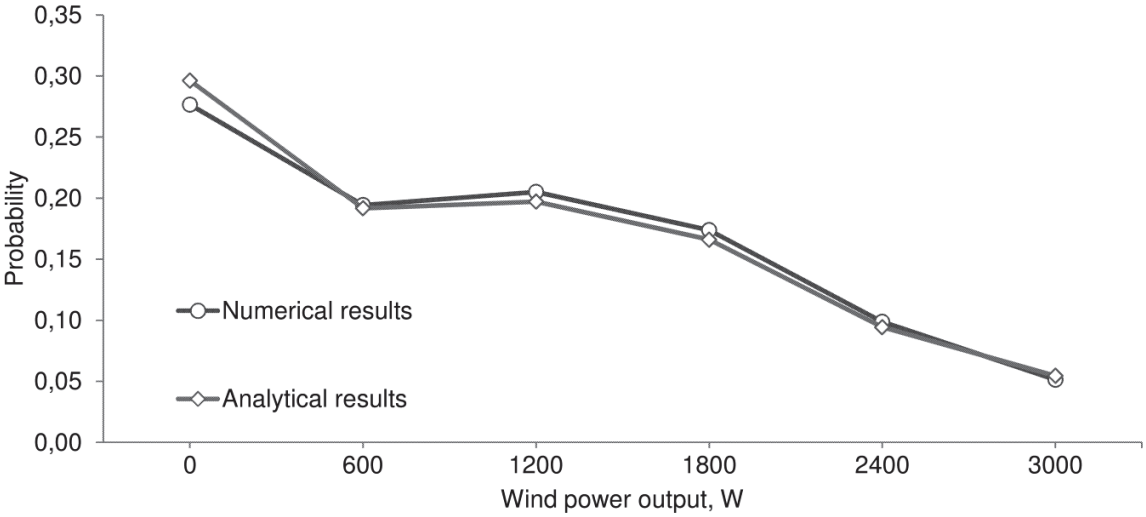

Figure 8. Probability of wind output states.

5.2. Analysis of the efficiency of the reinforcement learning algorithm

As described in Section 3, the learning process is achieved through the selection of sequences of actions for 2 steps-ahead scenarios. Firstly, the continuous repetition of similar scenarios with random selection of sequence of actions allows to define the maximum Q*-values of all

sequences. Secondly, the selection of a high-valued sequence of actions allows to perform the sequence of actions for battery scheduling most adapted to each scenario. However, the repeated occurrence of similar scenarios, for the definition of the maximum Q*-value, is considerably affected by the stochasticity of the wind power output P_t^{WT}. In other words, the efficiency of the learning process depends on the rate of occurrence of similar scenarios.

The purpose of this subsection is to illustrate and discuss the efficiency of the reinforcement learning algorithm. The learning trend is analysed by observing the increase of the occurrence rate of new scenarios and scenarios with more than 16 repetitions. Figure 9 illustrates the rate of first occurrence of new scenarios and of 'frequent' scenarios with more than 16 repetitions during each year. On the one hand, Figure 9 shows the fast decrease of the occurrence of new scenarios during the simulation. After 10 years, the proportion of new scenarios represents less than 1.5% of the total number of scenarios occurred annually. The number of scenarios with more than 16 occurrences rises to 87% in the last year of simulation: this large number of scenarios occurrences (16) allows identifying the action sequences of highest Q*-value for battery scheduling.

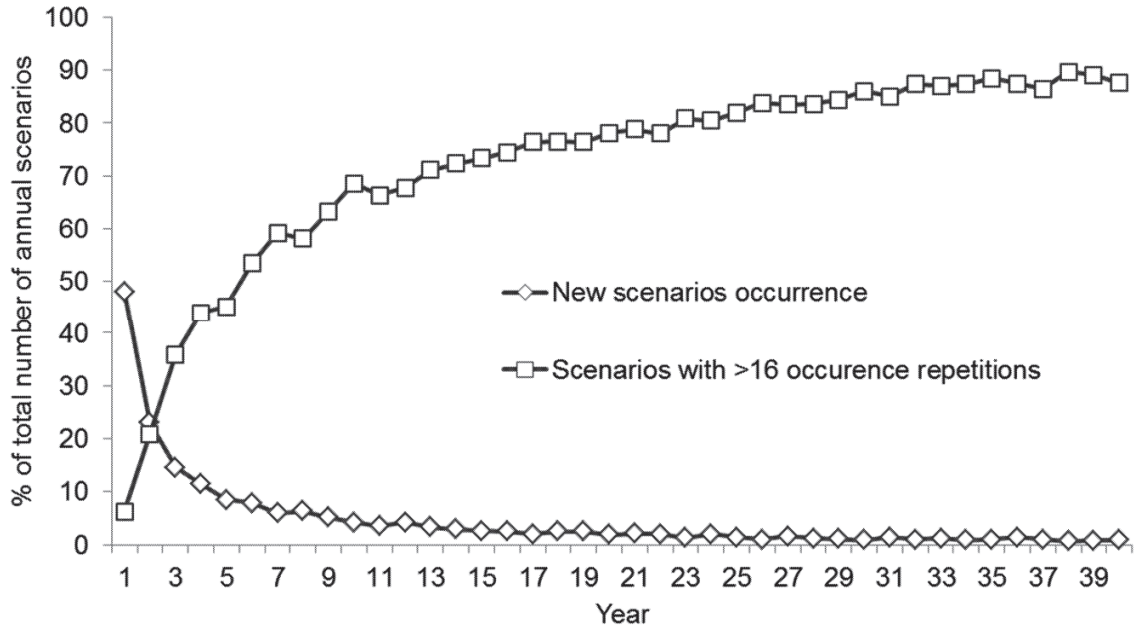

Figure 9. Trend of new scenarios occurrence and scenarios with more than 16 occurrence repetitions.

On the other hand, Figure 10 shows that the number of scenarios with low occurrences remains high throughout the simulation. For the 'rare' scenarios as optimal Q*-valued action sequence may not be identified, which could limit the performance of the reinforcement learning algorithm.

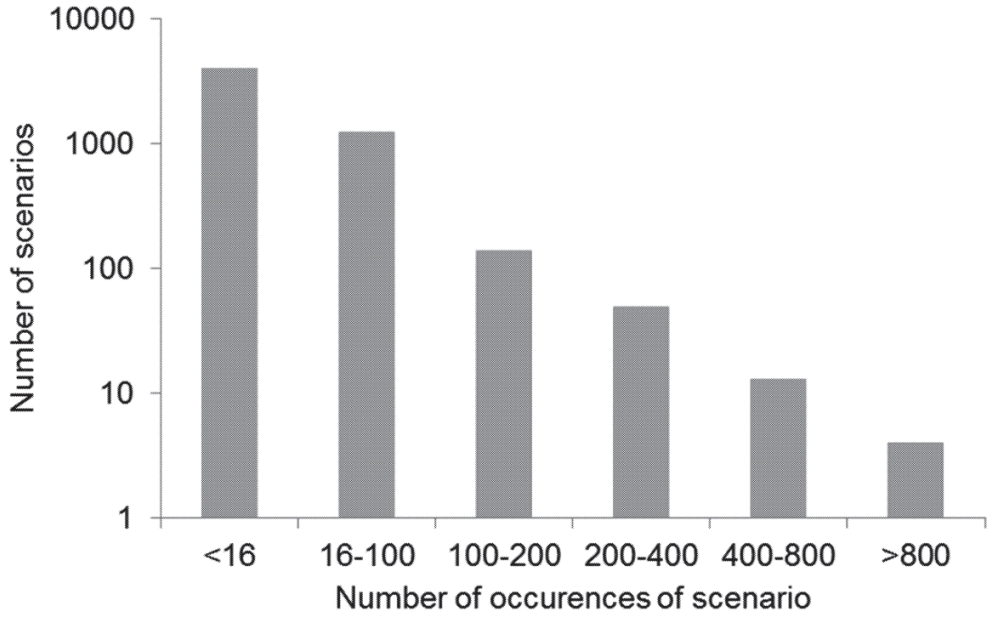

Figure 10. Classification of scenarios by the number of their occurrences.

5.3. Evaluation of the microgrid performance

The microgrid performance depends on the efficiency of the reinforcement learning algorithm. Usually the performance of the learning algorithm is analysed by representing the evolution of the Q-values of the actions [24], like in Subsection 4.3 (Figure 6), or the reward or penalty functions [23], [51]. It can be also evaluated by looking at the convergence of the relative percentage difference between the value of the optimization parameter, such as price, selected for time step interval Δt and its best value over the time period of analysis [18]. The performance is also illustrated by plotting the evolution of the values of other system parameters, such as price [18], [26], power [24] etc.

In this paper, three indicators V_0, V_1 and E are used to analyse the performance of the microgrid managed with the reinforcement learning:

$$V_0 = \frac{\sum R_t^{stor,discharge}}{\sum D_t} \tag{7}$$

$$V_1 = \frac{\sum R_t^{stor,charge}}{\sum P_t^{wt}} \tag{8}$$

$$E = \left(\sum D_t - \sum R_t^{stor,discharge}\right) \cdot P_t \tag{9}$$

where P_t is assumed constant and equal to one price unit per *W* for all time step intervals.

The increase of the utilization of electricity from the battery is estimated by V_0, which is defined as the ratio of the cumulative power used from the battery to the yearly cumulative load (eq. (7)). The increase of the utilization rate of the wind turbine is evaluated by V_1, which is defined as the ratio of the yearly cumulative power used from the wind generator to the yearly cumulative available wind power output (eq. (8)); obviously, the yearly cumulative power from the wind generator is equal to the yearly cumulative power from the battery during the year. Finally, parameter E indicates the cumulative annual expenses for the power purchase from the external grid (eq. (9)).

To evaluate the improvements of the performance indicators achieved by the application of the reinforcement learning for microgrid management under stochastic wind speed conditions, $N_s = 50$ independent simulation runs are executed. Each of these simulation runs generates a wind profile similar to the one depicted in Figure 7. The convergence of V_0 and V_1 is evaluated by using $\widehat{V_0}$ and $\widehat{V_1}$ estimators representing the floating average values of V_0 and V_1 through 50 independent simulation runs:

$$\widehat{V_0} = \frac{\sum_{j=1}^{N_s} V_0^j}{N_s} \tag{10}$$

$$\widehat{V_1} = \frac{\sum_{j=1}^{N_s} V_1^j}{N_s} \tag{11}$$

where V_0^j and V_1^j are the values of the two performance indicators in the *j-th* simulation run. For clarity of illustration, Figure 11 (a, b) shows the convergence of $\widehat{V_0}$ and $\widehat{V_1}$ for five randomly

selected years. Similar patterns of satisfactory stabilisation of $\widehat{V_0}$ and $\widehat{V_1}$ are observed for the other simulated years.

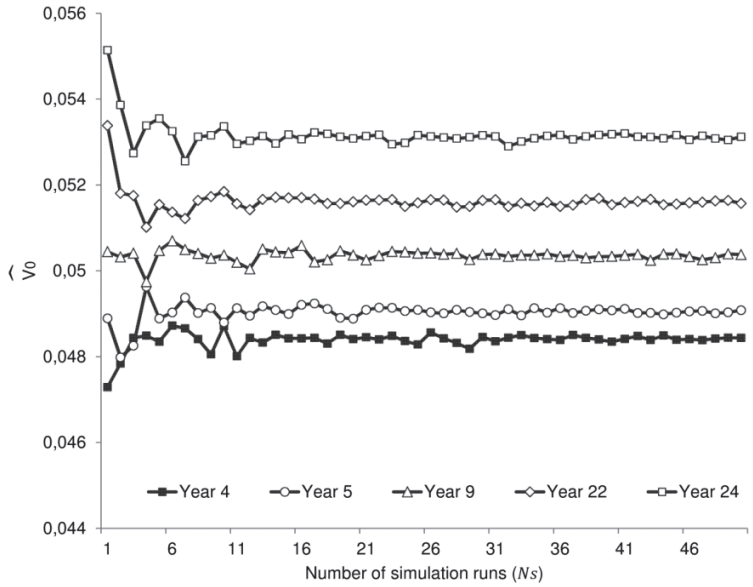

a)

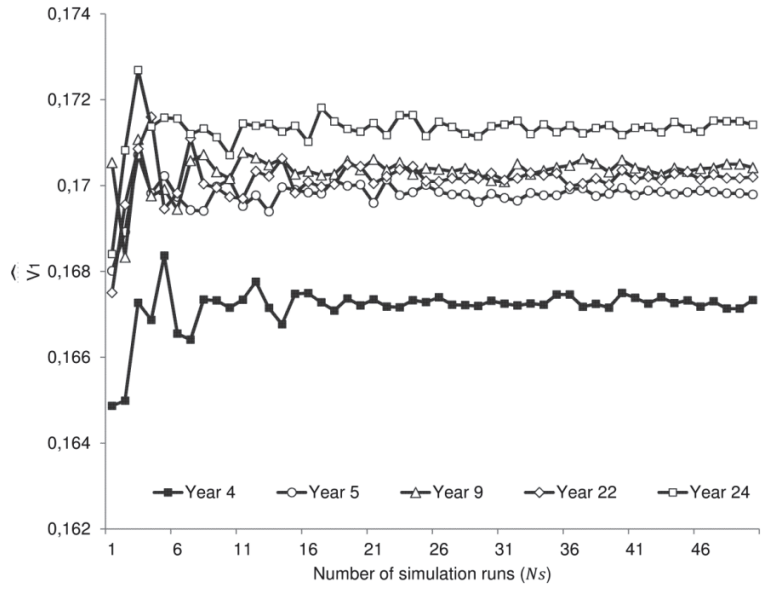

b)

Figure 11. Convergence of performance indicators: a) $\widehat{V_0}$; b) $\widehat{V_1}$.

To evaluate the performance of the microgrid achieved by reinforcement learning, the average values of the performance indicators V_0^{av}, V_1^{av} and E^{av} are calculated for each year from the results obtained in the 50 simulation runs. Figure 12 (a, b, c) illustrates the evolution of the average values V_0^{av}, V_1^{av} and E^{av} during the 40 years of simulation.

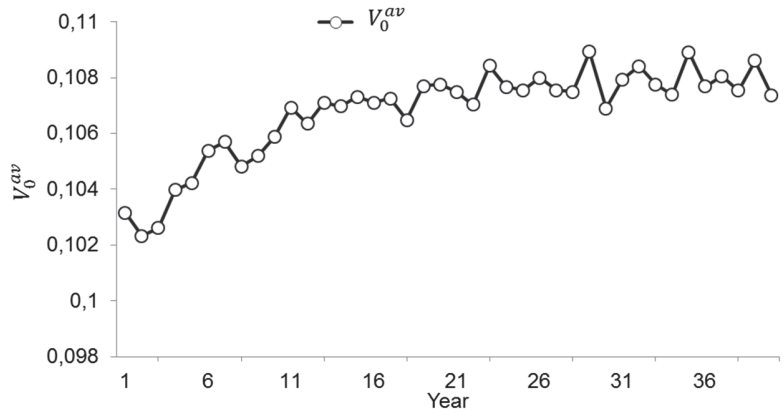

a)

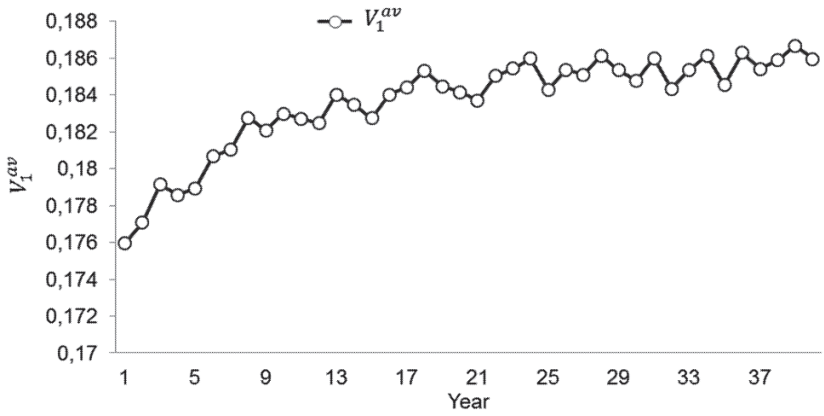

b)

c)

Figure 12. Average performance indicators: a) V_0^{av}; b) V_1^{av}; c) E^{av}.

As it can be observed from Figure 12 (a, b), the performance indicators show an increase in value. Following from these improvements, Figure 12 c shows the progressive decrease of the E^{av}. This gives the evidence of the continuous improvements brought by the reinforcement learning. Table 7 summarizes the improvements of the three performance indicators for two different cases. The first is set to favour the use of wind power to charge the battery during all times *t*, by using the weight coefficient $k = 6$; the second is set to favour the use of wind power only during particular states of wind power and load, by using the variable weight coefficient $k = 2^{1200/P_t^{wt}}$.

Table 7. Improvement of performance indicators for two different case studies.

		Case study 1. $k = 6$	Case study 2. $k = 2^{1200/P_t^{wt}}$
Average improvement of performance indicators after convergence	V0	3.93%	2.72%
	V1	5.37%	0.96%
	E	-0.47%(1)	-0.26%(1)

(1) Negative improvements indicate a decrease in annual expenses for electricity purchase.

It is important to highlight that the average improvements in Table 7 are related to the 40-years training period of the reinforcement learning algorithm and do not represent the ultimate profit in terms of performance indicators which can be achieved by the consumer in the daily operation. The training of the learning algorithm is done for the identification of optimal sequences of

actions for the different scenarios that may occur: the optimal actions are, then, applied by the consumer to perform profitable battery scheduling when the different scenarios occur.

As it can be seen from the results of Table 7, it is more valuable for the consumer to adopt the strategy illustrated by the case study 1 with weight coefficient $k = 6$. This conclusion is confirmed by Figure 13 (a, b), which represents an example of battery scheduling during one random day. The case study with weight coefficient $k = 6$, allows profiting from the available wind power output to increase the battery charge, which will, then, be used by the consumer during the periods of unavailability of wind power output.

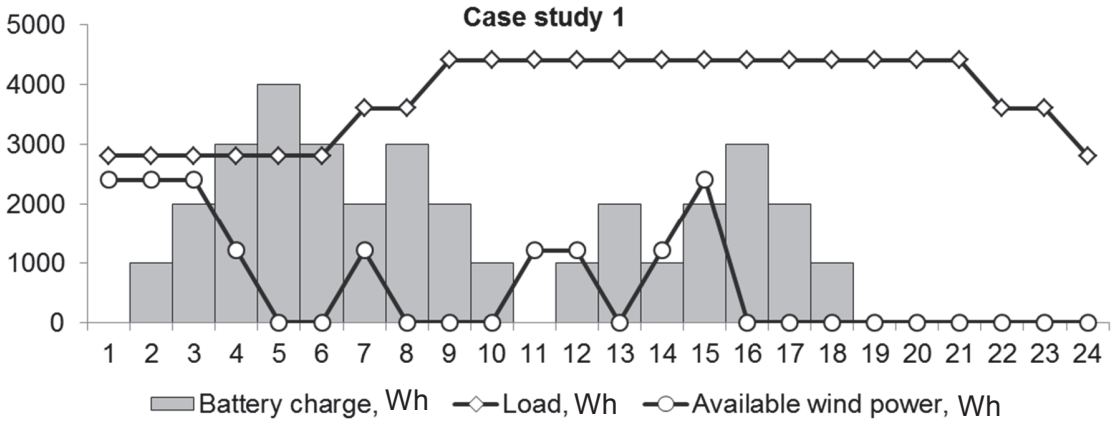

a)

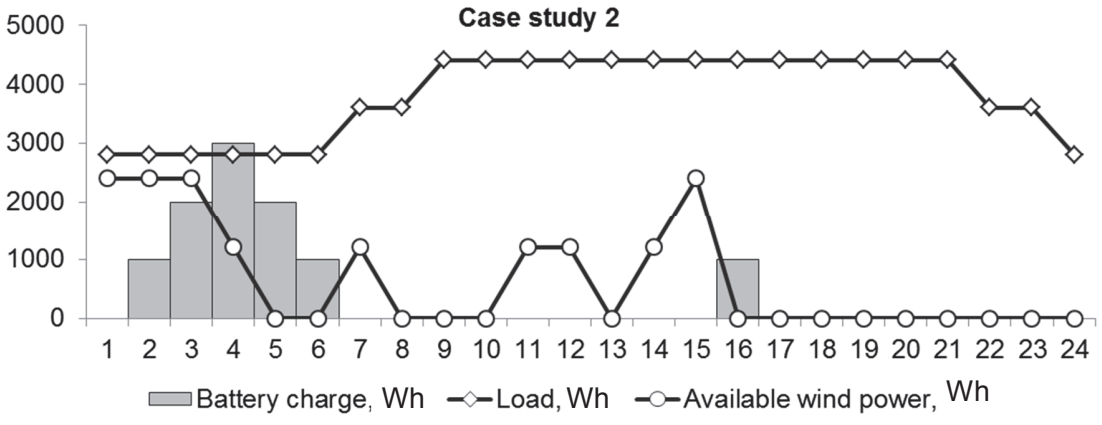

b)

Figure 13. Example of battery scheduling process for a day of operation: a) Case study 1; b) Case study 2.

Eventually, the trained reinforcement learning algorithm with weight coefficient $k = 6$ accomplishes an average improvement of 9.39%, 9.41% and 12.88% for V_0^{av}, V_1^{av} and E^{av}, respectively, regarding the case when the consumer does not have precise goals to follow in the selection of an optimal sequence of actions.

6. DISCUSSION

In this section, we provide a qualitative comparison between the developed reinforcement learning algorithm and other optimization approaches. The comparison leads us to conclude that the approach proposed in the present work is promising for optimal energy management of a microgrid through battery scheduling. Similar to our study, references [52–54] propose different methods for the energy management of microgrids with few energy generation sources, loads and storage facilities. For instance, a multi-objective optimization by fuzzy logic expert systems is presented in [54] and other classical and heuristic algorithms are used in [52], [53]. In these works, efforts are made for capturing most physical phenomena that influence the renewable power generation [53], [54] and complex optimization objective functions are considered to account for several goals including cost of environmental externalities [52]. The optimization frameworks developed in these references provide promising results and are capable of handling several optimization variables characterizing different generation technologies, loads and storage units within the microgrid.

This paper presents a Q-learning based optimization framework for selecting the optimal set of actions under possible scenarios. The original contributions of this paper are:

- The microgrid energy management is done for the benefit of the consumer, i.e., to maximize her or his personal objectives. The consumer is represented as an individual intelligent agent equipped with reinforcement learning capabilities that, by a gradual trial-and-error decision-making process, guide her or him towards optimal long term energy management.
- Contrary to the frameworks in [52], [53], where the optimization algorithms are applied to a deterministic power output, the proposed modelling framework is capable of accounting for generation uncertainty. For this, two Markov chain models are used to capture the differences in the forecasted and the real wind power outputs by describing

the dynamics of stochastic transition among different levels of wind speed conditions and mechanical states.

- The optimization framework of reinforcement learning is analysed through a comprehensive sensitivity analysis aimed at understanding the role of the learning parameters. This analysis allows improving the learning process and, thus, the energy management objectives.

We should indicate that the purposely simple model presented in this paper is the first elementary step to the implementation of a more complete agent-based model of the microgrid, in which multiple energy generators and consumers can be represented as individual intelligent agents with conflicting energy management objectives and limited access to information.

In the case study presented, our choice to have one hour sampling time is guided by the need of simplifying the models of the individual components. The objective of our work is not to capture fluctuations of load, wind power output and power flow of the battery storage within one hour, but to catch major trends and test the performance of the reinforcement learning algorithm for the long-term energy management.

The model describing the power flow through the battery does not integrate power losses over time t, and the charging and discharging efficiencies depending on the level of the energy stored. In our research the choice of the battery model was guided by the need to keep the models of individual components simple, but physically meaningful, in order to test the performance of the reinforcement learning algorithm.

In addition, the discretization of relevant stochastic variables was done roughly to keep the modelling of the individual components simple enough to allow concentrating on testing the performance of the reinforcement learning algorithm and its sensitivity to some main parameters. In this view, it was important to reduce the number of states of variables and, therefore the number of operational scenarios in order to obtain a model that is computationally treatable, especially for the purpose of the sensitivity analysis of Section 4.

Encouraged by the results of the performance indicators V0, V1 and E, the proposed architecture of reinforcement learning can be upscaled to integrate more complete models of individual

components with more refined discretization states. Moreover, the time step can be refined to take into account short-term fluctuations.

7. CONCLUSIONS

We have extended a framework of reinforcement learning for autonomous multi-state and multi-criteria decision-making in medium-term scenarios of energy storage management in a microgrid system. A simulation model has been developed to represent the dynamic interactions between the consumer agent and its environment, with a reinforcement learning for reward optimization by battery scheduling. Uncertainties in the power available from the wind generator, due to the stochastic nature of the wind source and the random mechanical failures of the wind generator components, are accounted for. To evaluate the performance of the learning algorithm, three indicators have been introduced.

The results obtained on a case study demonstrate the improvements in the strategy of microgrid operation with respect to the defined rewards.

The proposed framework gives to the intelligent consumer the ability to explore and understand the stochastic environment, and reuse this experience for selecting the optimal energy management actions.

Future work will focus on (i) the refinement of the agent-models of the individual components, (ii) the improvement of the forecasting and learning capabilities and (iii) the extension to multiple agents integrating diverse renewable generators and several intelligent consumers with conflicting requirements for electricity supply, limited access to information about the power available and limited communication capabilities within the microgrid.

ACKNOWLEDGEMENTS

The authors wish to thank the anonymous referees for their scrupulous review work and the comments provided to us, which have helped improving the paper significantly.

REFERENCES

[1] J. C. Glenn, T. J. Gordon, and E. Florescu, "2009 State of the Future," 2009.

[2] B. J. Owen, "The planet 's future : Climate change ' will cause civilisation to collapse '," *The Independent*, London, 2009.

[3] M. Jung and P. Yeung, "Connecting smart grid and climate change," 2009.

[4] R. Hledik, "How Green Is the Smart Grid?," *The Electricity Journal*, vol. 22, no. 3, pp. 29–41, Apr. 2009.

[5] N. D. Hatziargyriou, *European Transactions on Electrical Power. Special Issue: Microgrids and Energy Management*, no. December 2010. 2011, pp. 1139–1342.

[6] F. Katiraei and M. R. Iravani, "Power Management Strategies for a Microgrid With Multiple Distributed Generation Units," *Power Systems, IEEE Transactions on*, vol. 21, no. 4. pp. 1821–1831, 2006.

[7] J. M. Carrasco, L. G. Franquelo, J. T. Bialasiewicz, E. Galvan, R. C. P. Guisado, M. A. M. Prats, J. I. Leon, and N. Moreno-Alfonso, "Power-Electronic Systems for the Grid Integration of Renewable Energy Sources: A Survey," *Industrial Electronics, IEEE Transactions on*, vol. 53, no. 4. pp. 1002–1016, 2006.

[8] M. Manfren, P. Caputo, and G. Costa, "Paradigm shift in urban energy systems through distributed generation: Methods and models," *Applied Energy*, vol. 88, no. 4, pp. 1032–1048, Apr. 2011.

[9] C. Chen, S. Duan, T. Cai, B. Liu, and G. Hu, "Smart energy management system for optimal microgrid economic operation," *Renewable Power Generation, IET*, vol. 5, no. 3. pp. 258–267, 2011.

[10] T. Niknam, R. Azizipanah-Abarghooee, and M. R. Narimani, "An efficient scenario-based stochastic programming framework for multi-objective optimal micro-grid operation," *Applied Energy*, Jul. 2012.

[11] T. Niknam, F. Golestaneh, and A. Malekpour, "Probabilistic energy and operation management of a microgrid containing wind/photovoltaic/fuel cell generation and energy storage devices based on point estimate method and self-adaptive gravitational search algorithm," *Energy*, vol. 43, no. 1, pp. 427–437, Jul. 2012.

[12] T. Ma and Y. Nakamori, "Modeling technological change in energy systems – From optimization to agent-based modeling," *Energy*, vol. 34, no. 7, pp. 873–879, 2009.

[13] E. Kuznetsova, K. Culver, and E. Zio, "Complexity and vulnerability of Smartgrid systems," in *Advances in Safety, Reliability and Risk Management, European Safety and Reliability Conference (ESREL 2011)*, 2011, pp. 2474–2482.

[14] P. P. Reddy and M. M. Veloso, "Strategy Learning for Autonomous Agents in Smart Grid Markets," in *Twenty-Second International Joint Conference on Artificial Intelligence*, 2005, pp. 1446–1451.

[15] T. Krause, E. Beck, R. Cherkaoui, A. Germond, G. Andersson, and D. Ernst, "A comparison of Nash equilibria analysis and agent-based modelling for power markets," *International Journal of Electrical Power & Energy Systems*, vol. 28, no. 9, pp. 599–607, Nov. 2006.

[16] A. Weidlich and D. Veit, "A critical survey of agent-based wholesale electricity market models," *Energy Economics*, vol. 30, no. 4, pp. 1728–1759, Jul. 2008.

[17] R. W. Lincoln, "Learning to Trade Power," University of Strathclyde, 2011.

[18] S. Yousefi, M. P. Moghaddam, and V. J. Majd, "Optimal real time pricing in an agent-based retail market using a comprehensive demand response model," *Energy*, vol. 36, no. 9, pp. 5716–5727, Sep. 2011.

[19] M. H. Colson, C. M. Nehrir, and R. W. Gunderson, "Multi-agent Microgrid Power Management," in *18th IFAC World Congress*, 2011, pp. 3678–3683.

[20] Z. Jun, L. Junfeng, W. Jie, and H. W. Ngan, "A multi-agent solution to energy management in hybrid renewable energy generation system," *Renew. Energ.*, vol. 36, no. 5, pp. 1352–1363, May 2011.

[21] R. S. Sutton and A. G. Barto, *Reinforcement learning : An introduction*. London, England: The MIT Press., 2005, pp. 1–398.

[22] L. Panait and S. Luke, "Cooperative Multi-Agent Learning : The State of the Art," *Autonomous Agents and Multi-Agent Systems*, vol. 11, no. 3, pp. 387 – 434, 2005.

[23] V. L. Prabha and E. C. Monie, "Hardware Architecture of Reinforcement Learning Scheme for Dynamic Power Management in Embedded Systems," *EURASIP Journal on Embedded Systems*, pp. 1–6, 2007.

[24] Y. Tan, "Adaptive Power Management Using Reinforcement Learning," in *International Conference on Computer-Aided Design (ICCAD'09)*, 2009.

[25] L. Xin, Z. Chuanzhi, Z. Peng, and Y. Haibin, "Genetic based fuzzy Q-learning energy management for smart grid," *Control Conference (CCC), 2012 31st Chinese*. pp. 6924–6927, 2012.

[26] X. Li, C. Zang, W. Liu, P. Zeng, and H. Yu, "Metropolis Criterion Based Fuzzy Q-Learning Energy Management for Smart Grids," *TELKOMNIKA*, vol. 10, no. 8, pp. 1956–1962, 2012.

[27] C. Kieny, N. Hadjsaïd, B. Raison, Y. Besanger, R. Caire, D. Roye, O. Devaux, and G. Malarange, "Distribution grid security management with high DG penetration rate: Situation in France and some future trends," *Power and Energy Society General Meeting - Conversion and Delivery of Electrical Energy in the 21st Century, 2008 IEEE*, pp. 1–6, 2008.

[28] S. C. E. Jupe and P. C. Taylor, "Distributed generation output control for network power flow management," *IET Renewable Power Generation*, vol. 3, no. 4, p. 371, 2009.

[29] M. Wooldridge, *An introduction to multiagent systems*. United Kingdom: John Wiley and Sons Ltd., 2009, pp. 1–460.

[30] M. J. Dolan, E. M. Davidson, J. R. Mcdonald, and G. W. Ault, "Techniques for managing power flows in active distribution networks within thermal constraints," in *20 th International Conference on Electricity Distribution*, 2009, no. 0736, pp. 8–11.

[31] N. Dalili, A. Edrisy, and R. Carriveau, "A review of surface engineering issues critical to wind turbine performance," *Renew. and Sustain. Energy Rev.*, vol. 13, pp. 428–438, 2009.

[32] Y. F. Li and E. Zio, "A multi-state power model for adequacy assessment of distributed generation via universal generating function," *Reliability Engineering and Systems Safety*, vol. 106, pp. 28–36, 2012.

[33] A. Shamshad, M. Bawadi, W. Wanhussin, T. Majid, and S. Sanusi, "First and second order Markov chain models for synthetic generation of wind speed time series," *Energy*, vol. 30, no. 5, pp. 693–708, Apr. 2005.

[34] L. Fawcett and D. Walshaw, "Markov chain models for extreme wind speeds," *Environmetrics*, vol. 17, no. 8, pp. 795–809, Dec. 2006.

[35] A. Shamshad, W. M. A. Wan Hussin, M. A. Bawadi, and S. A. Mohd Sanusi, "First and second order Markov Chain models for synthetic generation of wind speed time series," *Energy*, vol. 30, no. 5, pp. 693–708, Apr. 2005.

[36] G. Papaefthymiou and B. Klockl, "MCMC for Wind Power Simulation," *IEEE Transactions on energy conversion*, vol. 23, no. 1, pp. 234–240, 2008.

[37] F. C. Sayas and R. N. Allan, "Generation availability assessment of wind farms," in *IEE Proc.-Gener. Transm. Distrib.*, 1996, pp. 507–518.

[38] D. C. Hill, D. Mcmillan, K. R. W. Bell, and D. Infield, "Application of auto-regressive models to UK wind speed data for power system impact studies," *IEEE Trans. on Sustain. Energy*, vol. 3, no. 1, 2012.

[39] R. N. Clark and R. G. Davis, "Performance of an Enertech 44 during 11 years of operation," in *Proceedings of the AWEA Wind-Power'93 Conference*, 1993, pp. 204–212.

[40] S. Faulstich, P. Lyding, and B. Hahn, "Component reliability ranking with respect to WT concept and external environmental conditions," Kassel, Germany, 2006.
[41] L. Duenas-Osorio, "Unavailability of wind turbines due to wind-induced accelerations," *Engineering Structures*, vol. 30, no. 4, pp. 885–893, Apr. 2008.
[42] P. Tavner, "SUPERGEN Wind 2011 General Assembly," in *SUPERGEN Wind 2011 General Assembly*, 2011, no. March.
[43] D. M. Louit, R. Pascual, and A. K. S. Jardine, "A practical procedure for the selection of time-to-failure models based on the assessment of trends in maintenance data," *Reliability Engineering & System Safety*, vol. 94, no. 10, pp. 1618–1628, Oct. 2009.
[44] R. Karki and R. Billinton, "Reliability/cost implications of PV and wind energy utilization in small isolated power systems," *IEEE Trans. on Energy Convers.*, vol. 16, no. 4, pp. 368–373, 2001.
[45] C. Fong, S. Haddad, and D. Patton, "The IEEE reliability test system - 1996," *IEEE Trans. on Power Syst.*, vol. 14, no. 3, 1999.
[46] C. J. C. H. Watkins, "Learning from delayed rewards," King's College, 1989.
[47] S. Roy, "Market constrained optimal planning for wind energy conversion systems over multiple installation sites," *Energy Conversion, IEEE Transactions on*, vol. 17, no. 1, pp. 124–129, 2002.
[48] J. Hetzer, D. C. Yu, and K. Bhattarai, "An economic dispatch model incorporating wind power," *IEEE Trans. on Energy Convers.*, vol. 23, no. 2, pp. 603–611, 2008.
[49] Y. M. Atwa, M. M. A. Salama, and R. Seethapathy, "Optimal renewable resources mix for distribution system energy loss minimization," *IEEE Trans. on Power Syst.*, vol. 25, no. 1, pp. 360–370, 2010.
[50] E. Zio, "Markov Reliability and Availability Analysis," in *Computational Methods for Reliability and Risk Analysis*, Imperial C., 2009, p. 364.
[51] M. Mahvi and M. M. Ardehali, "Optimal bidding strategy in a competitive electricity market based on agent-based approach and numerical sensitivity analysis," *Energy*, vol. 36, no. 11, pp. 6367–6374, 2011.
[52] F. A. Mohamed and H. N. Koivo, "System Modelling and Online Optimal Management of MicroGrid with Battery Storage," *International Journal on Electrical Power and Energy Systems*, vol. 32, no. 5, pp. 398–407, 2010.
[53] C. M. Colson, M. H. Nehrir, and S. A. Pourmousavi, "Towards Real-time Microgrid Power Management using Computational Intelligence Methods," *IEEE*, pp. 1–8, 2010.
[54] A. Chaouachi, R. M. Kamel, R. Andoulsi, and K. Nagasaka, "Multiobjective Intelligent Energy Management for a Microgrid," *IEEE Transactions on Industrial Electronics*, vol. 60, no. 4, pp. 1688 – 1699, 2013.

Paper 2

An integrated framework of agent-based modelling and robust optimization for microgrid energy management

Elizaveta Kuznetsova, Yan Fu Li, Carlos Ruiz and Enrico Zio

Applied Energy vol. 129, pp. 70 – 88, 2014

An integrated framework of agent-based modelling and robust optimization for microgrid energy management

Elizaveta Kuznetsova[1,2], Yan-Fu Li[2], Carlos Ruiz[3], Enrico Zio[2,4]

[1] ECONOVING International Chair in Eco-Innovation, REEDS International Centre for Research in Ecological Economics, Eco-Innovation and Tool Development for Sustainability, University of Versailles Saint Quentin-en-Yvelines, 5-7 Boulevard d'Alembert, bâtiment d'Alembert - room A301, 78047 Guyancourt, France.
[2] Chair on Systems Science and the Energetic Challenge, European Foundation for New Energy-Electricité de France, Ecole Centrale Paris, Grande Voie des Vignes 92295 Châtenay-Malabry, Supelec, 91190 Gif-sur-Yvette, France.
[3] Department of Statistics, Universidad Carlos III de Madrid, Avda. de la Universidad, 30, 28911-Leganes (Madrid), Spain.
[4] Dipartimento di Energia, Politecnico di Milano, Via Lambruschini 4, 20156 Milano, Italy.

ABSTRACT

A microgrid energy management framework for the optimization of individual objectives of microgrid stakeholders is proposed. The framework is exemplified by way of a microgrid that is connected to an external grid via a transformer and includes the following players: a middle-size train station with integrated photovoltaic power production system, a small energy production plant composed of urban wind turbines, and a surrounding district including residences and small businesses. The system is described by Agent-Based Modelling (ABM), in which each player is modelled as an individual agent aiming at a particular goal, (i) decreasing its expenses for power purchase or (ii) increasing its revenues from power selling. The context in which the agents operate is uncertain due to the stochasticity of operational and environmental parameters, and the technical failures of the renewable power generators. The uncertain operational and environmental parameters of the microgrid are quantified in terms of Prediction Intervals (PIs) by a Non-dominated Sorting Genetic Algorithm (NSGA-II) – trained Neural Network (NN). Under these uncertainties, each agent is seeking for optimal goal-directed actions planning by Robust Optimization (RO). The developed framework is shown to lead to an increase in system performance, evaluated in terms of typical reliability (adequacy) indicators for energy systems, such as Loss of Load Expectation (LOLE) and Loss of Expected Energy (LOEE), in comparison with optimal planning based on expected values of the uncertain parameters.

Keywords: microgrid, agent-based model, uncertain scenarios, system reliability, robust optimization, power imbalance.

NOMENCLATURE

t time step *(h)*,

F_t^{pas} passengers flow through TS at time *t (number/h)*,

s_t average solar irradiation at time *t (W/m²)*,

v_t average wind speed at time *t (m/s)*,

E_t^l energy required for inside and outside lighting in the TS at time *t (kWh)*,

E_t^{elev} energy required for passengers lifting in the TS at time *t (kWh)*,

E_t^{elec} energy required for electronic equipment in the TS at time *t (kWh)*,

E_t^{TS} total hourly required energy in the TS at time *t (kWh)*,

E_t^D total hourly required energy in the D at time *t (kWh)*,

P_t^{PV} available energy output from the PV generators installed in the TS at time *t (kWh)*,

P_t^{WPP} available energy output from the WPP at time *t (kWh)*,

S_t^{TS} and S_t^D portions of energy purchased from the external grid by the TS and D, respectively (*kWh),*

L_t^{TS} and L_t^{WPP} portions of energy sold to the external grid by the TS and WPP, respectively *(kWh)*,

V_t^{PV} and V_t^{WPP} portions of energy sold to the district and generated by the PV panels of the TS and WPP, respectively *(kWh),*

R_t^{TS} and R_{t-1}^{TS} energy levels in the TS battery at time *t* and *t-1 (kWh),*

R_t^D and R_{t-1}^D energy levels in the D battery at time *t* and *t-1 (kWh),*

$R^{TS,stor}$ energy portion that the TS battery is capable of charging or discharging during time *t (kWh)*,

$R^{D,stor}$ energy portion that the D battery is capable of charging or discharging during time *t (kWh)*,

$\delta_t^{TS,ch}$ and $\delta_t^{TS,dis}$ binary variables which model that the TS battery can either only be charged or discharged at time *t*,

$\delta_t^{D,ch}$ and $\delta_t^{D,dis}$ binary variables which model that the D battery can either only be charged or discharged at time *t*,

$R^{TS,max}$ the maximum TS battery charge *(kWh)*,

$R^{D,max}$ the maximum D battery charge *(kWh)*,

T time period considered for the optimization *(h)*,

α^{TS} and α^{D} total costs for TS and D, respectively, for time period *T (€)*,

α^{WPP} total revenue for WPP for time period *T (€),*

c_t^p and c_t^s average hourly costs of purchasing and selling one *kWh* from the external grid, respectively, at time *t* (*€/kWh*),

c_t^D average hourly cost per *kWh* from the bilateral contract agreed with D at time *t (€/kWh),*

β and γ coefficients defining the minimum amount of energy to be sold to D by TS and WPP, respectively,

$\tilde{E}_t^D$ expected energy demand for D (for the moment, considered without uncertainty) at time step *t*, predicted by TS and WPP (*kWh*),

$\tilde{V}_t^{PV}$ and $\tilde{V}_t^{WPP}$ energy portions, which TS and WPP are ready to sell to D at time step *t* (*kWh*),

$\hat{P}_t^{WPP}$ level of uncertainty in WPP energy output quantified for the robust optimization at time *t (kWh)*,

$P_t^{WPP,ub}$ and $P_t^{WPP,lb}$ upper and lower prediction bounds of WPP energy output at time *t*, respectively *(kWh)*,

τ simulation time period composed of *Ns* time steps of one hour *(h)*,

LOLE Loss of Load Expectation characterized the probability of unsatisfied electricity demand during τ *(t/τ)*,

LOEE Loss of Expected Energy quantified the expected amount of energy losses during τ *(kWh/τ)*,

P_t available capacity in the microgrid at time period *t (kWh)*,

E_t energy demand in the microgrid at time step *t* (*kWh)*,

$Pr_t(P_t < E_t)$ probability of loss of load at time step *t,*

$E_t - P_t$ energy portion that the system is not able to supply at time step *t* (*kWh)*,

$L_t^{WPP,c}$ and $V_t^{WPP,c}$ portions of energy contracted by the WPP to the external and microgrids, respectively *(kWh)*,

$L_t^{WPP,*}$ and $V_t^{WPP,*}$ actual portions of energy provided by the WPP to the external and microgrids, respectively *(kWh)*,

T_t^{WPP} imbalance cost generated by WPP at time step *t (€),*

$d_t^{WPP,*}$ energy imbalance generated by WPP at time step *t (kWh)*,

$c_t^{D,+}$ and $c_t^{D,-}$ imbalance prices for positive and negative imbalances, respectively, at time step *t (€/kWh)*,

γ performance ratio calculated over a simulation period of *Ns* hours by normalizing the actual revenue of the WPP by the revenue that would be obtained in the case of the perfect forecast.

1. INTRODUCTION

Renewable energies are promising solutions to the energetic and environmental challenges of the 21st century [1], [2]. Their integration into the existing grids generates technical and social challenges related to their efficient and secure management. The paradigm to address these challenges is the implementation of Smartgrids, which are expected to contribute to energy efficiency in decentralized networks by the adequate management of production and consumption [3], [4].

Under this perspective, on the one hand, a closer location of generation and consumption sources in microgrids tends to increase service quality from the consumer's point of view, by decreasing transmission losses and the time needed to manage fault restoration and congestions. On the other hand, energy management issues arise related to the emergence of microgrids with possible conflicting requirements and limited communications between different microgrids agents, which calls for the implementation of distributed intelligent techniques [5]. Hence, the need for the development of frameworks of energy management for microgrids, as pointed out in various works [6]–[8], for optimal microgrid operation [9]–[11].

An appropriate approach to model microgrids and the related individual goal-oriented decision-making for different types of microgrid actors, is that of Agent-Based Modelling (ABM) [12]–[14], which allows to analyse by simulation the interactions among individual intelligent decision makers (the agents). The most widespread application of this modelling approach concerns the bidding strategies among individual agents who want to increase their immediate profits through mutual negotiations, and the energy market dynamics [15]–[18]. Recent studies show the extension of the ABM approach to more complex interactions in the energy management of hybrid renewable energy generation systems [14], [19], [20]. In these works, the long-term goals are focused on the efficient use of electricity within microgrids, e.g., the planning of battery scheduling to locally store the electricity generated by renewable sources and reuse it during periods of high electricity demand [19]. However, the decision framework is commonly developed under deterministic typical conditions, e.g., those of a typical day in summer.

To account for the variability and randomness of the operational and environmental parameters of the energy systems, the optimization capable of tackling uncertainty has been progressively introduced [21]. Fuzzy mathematical programming models and their extensions have also been successfully applied for optimal management of hybrid energy systems [22], [23]. Stochastic programming models, where the uncertain parameters are accounted by probability and interval programming models, where the uncertainty is described by intervals [24], [25], have been used to deal with different sources of uncertainty in different optimization problems, e.g., economic-energy scenarios planning [26], design of renewable systems for community energy management [27] and water quality and waste management [28], [29].

In this paper, we present an original framework for microgrid energy management, where each agent is seeking for an optimal goal-directed action planning under power consumption, production and price uncertainties. The optimal scheduling strategy is achieved by using a Robust Optimization (RO) approach, which has been recently used for optimal energy system planning under uncertainties related to the power output of renewable generators [30], production costs [31], electricity demand [32], and their combination [10], [33], quantified by probability levels [30]–[32] or probability bounds of constraint violation [33]. The RO formulation adopted in this paper has been initially proposed in [25] and allows to linearly formulate the robust counterpart of an optimization problem for different levels of conservatism in the solution. Novelty of the research proposed lies in the way of quantifying the uncertainties by Prediction Intervals (PIs), integrated in the RO. The PIs for the uncertain parameters are obtained by a Non-dominated Sorting Genetic Algorithm (NSGA-II)-trained Neural Network (NN) [34], which gives lower and upper prediction bounds between which the uncertain value is expected to lie with a given confidence [34], [35].

The paper is organized as follows. Section 2 presents the motivation of the research, in particular with respect to the selection of the microgrid components in the reference system considered. Section 3 describes the models of the individual components. The uncertainties in the energy management parameters, presented in Section 4, are accounting in Section 5 presenting robust optimization, prediction and communication frameworks, respectively. Section 6 defines the performance indicators for the assessment of the system reliability and the impact of the prediction error. Section 7 shows an application with respect to the reference system. Eventually,

the last section draws some conclusions and gives an outlook on future research. Appendix presents the discussion on environmental and operational conditions.

2. RESEARCH MOTIVATION AND POSITIONING

The research presented in this paper is part of a project of study of the energy consumption and management of a middle-size train station in the Paris region, including the participation of a multidisciplinary team of academic and industrial actors [36]. The project is specifically focused on the evaluation of the energetic performance of a train station, as individual actor and as part of an energy distribution microgrid. The lookout vision of the railway, energy companies and local authorities is for the train station to become an active energy player in the power grid [37]. In view of the project, the reference system considered in this paper includes a middle-size train station (TS), which can play the role of power producer and consumer, the surrounding district (D) with residences and small businesses, and a small urban wind power plant (WPP) (Figure 1).

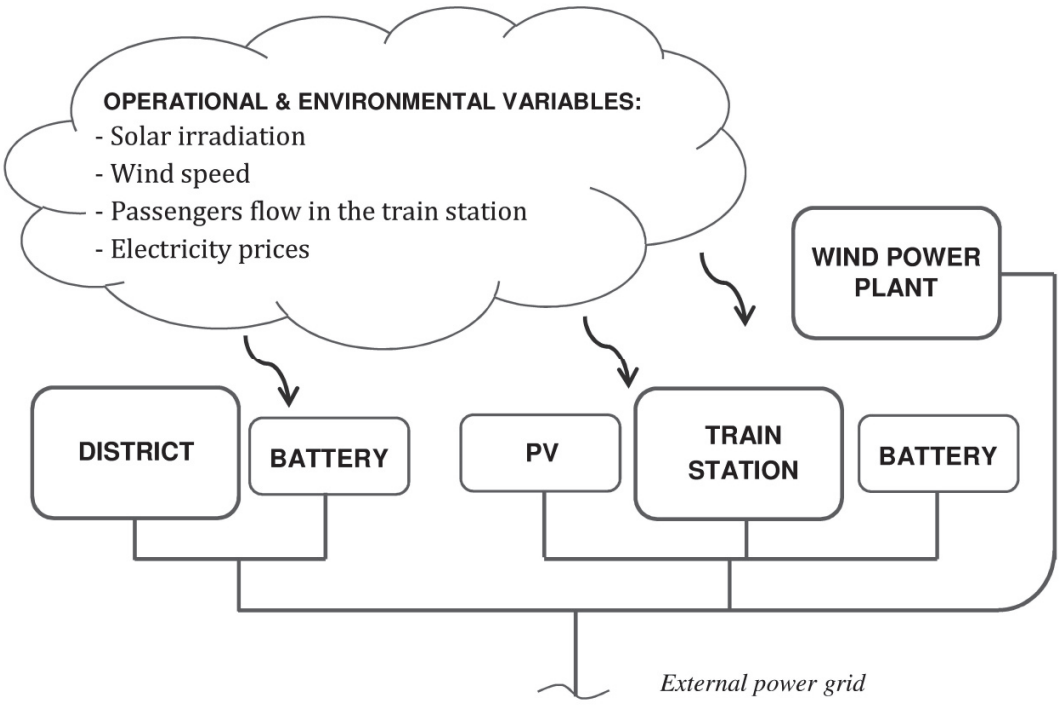

Figure 1. Scheme of the reference microgrid.

The case study considered in this paper is based on an on-going project of microgrid, whereby each system is considered an individual agent with its own strategy driven by specific

management objectives. Specifically, the goal of TS is to decrease its electricity expenses while satisfying its demand. To achieve this, the TS strategy includes the integration of renewable generators and energy exchanges with the local community to increase the power flexibility of the microgrid. Photovoltaic panels (PV) have been shown to be an adapted and efficient solution for implementation on large commercial, public buildings and transportation hubs [38], [39]. For the energy exchanges with local community, we consider only the possibility of exchange between TS and D to keep the modelling aspect sufficiently simple, but complete, for the purpose of illustration of the methods proposed. Future work includes the consideration of modelling the energy exchanges between the TS and the WPP.

The goal of WPP is to increase its revenues from sales of electricity to the external grid and to the local community D. This latter is considered only as an energy consumer, with the goal of decreasing its electricity purchase from the external grid by prioritizing the purchase of electricity from the local sources, i.e., TS and WPP. In addition, we assume that TS and D have the capacity to store electricity in batteries.

For our current D model, we assume that the effect of locally installed renewable generators, e.g., PV panels, can be neglected. The energy generated with PV panels is around 0.8% of the annual energy consumption in 2012 for the considered area [40]. The installation of domestic PV energy generators can be included in the future, under different market and legislation profiles [41]. On the other hand, we note also the fast development of electrical cars-hire services near the transportation hubs and residential areas [42], which can be an additional motivation for the integration of large-scale storage capability in the D and TS.

The original contributions of this paper are:

- The paper contributes to the development and analysis of microgrids with individual intelligent agents. The microgrid energy management is achieved not through the optimization of the overall energy flows in the microgrid, like in [30]–[32], [43], but by the optimization of the objective functions of the individual agents, considered as autonomous decision-making entities that account for their individual objectives.
  The framework of microgrid energy management considers the uncertainty associated to the predictions of the energy quantities of interest and the information communicated by the agents.

- The paper introduces in the microgrid energy management a novel approach for uncertainty quantification, i.e., PIs estimation with NSGA-II trained Neural Network (NN) to define the boundaries of the uncertain parameters variation which are used as the input for the RO. In comparison with other references, where the uncertain parameters were characterized by assumed probability levels [30]–[32] or probability bounds of constraint violation [33], the proposed framework allows each microgrid agent to regulate its conservatism under different uncertain parameters and select the appropriate width of the PIs from the available prediction solutions. For example, by increasing the width of the PIs associated to the renewable energy output, the uncertainty caused by the variability of the environmental conditions and, in some cases, the unavailability of the renewable energy output due to possible technical failures of the generator, can be accounted for conservatively.
- The paper presents a flexible, modular framework which can accommodate models of individual agents and different levels of complexity as needed, e.g., to account for the eventual variations of charging and discharging efficiencies and energy losses due to battery degradation, and/or short time steps to account for short-term variations.

By definition, microgrids are designed to operate in two modes: the grid-connected mode and the islanded mode. On the one hand, in the grid-connected mode, a microgrid can trade power with the upstream power grid to solve power imbalances within the microgrid. On the other hand, when the power imbalance occurs in the islanded mode, the decrease of total output of distributed generators, or load-shedding, which is an intentional load reduction, can be used to solve the power imbalances [44]. Note that the grid-connected mode is the most common one [11], [45], [46] and thus, we focus on this mode in this paper. Therefore, the power imbalances are accounted inside the microgrid and between the microgrid power producers and the upstream external grid. We do not consider active power control to improve the dispatch of distributed energy resources and provide loads balancing, but focus on the microgrid management at the more abstract level of the agents communication framework.

The optimization problem of the active and reactive power in the microgrid with distributed energy generators, consumers and storage facilities, is one of the core research subjects of the power system community. The problem is usually formulated as an optimal power flow (OPF)

problem that determines the optimal active and reactive powers to be produced or consumed by each element of the system, as well as the energy flows through the lines, so that the overall system costs are minimized. This is done by satisfying all the system technical constraints. The active power, which depends on the variation of the voltage phases, is generally the main focus on power prediction [47] and optimization problems [31]–[33], [48]–[51]. The research presented in this paper is focused on the RO of management strategies of energy systems, aiming to satisfy the energy demand-supply balance in presence of uncertainties. In the optimization problem, the objectives are formulated in terms of cost and revenue, as customary, and equations for the constraints (i.e., technical, environmental) are introduced. Similar to other research papers in the field, e.g., planning of energy management systems [52], [53] and planning of emissions trading and clean energy development [54], the voltage stability in the microgrid is not considered given the specific focus of the work. The optimization framework developed allows identifying the optimal energy management strategy for the particular microgrid configuration.

Eventually, in real life application the optimization is used by energy generation and transmission companies for the optimal short and long term decision-making in terms of energy generation sources management, choice of technologies and investment for grid upgrade and capacity expansion, maintenance planning, strategies for energy trading with other countries etc. The final decision-making of the optimal energy management applied to the particular grid configuration is done through the trade-off between the economically optimal energy planning, identified by solving the optimization problem, and system stability.

3. MODELS OF THE MICROGRID INDIVIDUAL AGENTS

This section presents the models of the different individual agents in the microgrid, describing their energy consumption, production and dynamic management of the batteries where in place.

3.1. Train station(TS)

The “heart” of the district is the middle size train station (TS) with the overall daily passenger flow of about 80,000 pas./day. The energy consumption of the TS is divided in two groups: (i) variable energy consumption of lifting, lighting and heating equipment, which depends on the

operational and environmental variables (e.g., solar irradiation, passengers flow etc.) and (ii) fixed energy consumption of other equipment, such as ticket control and vending machines, which are constantly plugged to the power network. The TS has the possibility to generate and store energy through the integrated PV panels and the battery, respectively.

3.1.1. Energy consumption

In this paper, only the energy consumption in the main passengers building, which includes the passengers' halls, tickets vending and controlling areas and accesses to platforms, is considered. According to the exploitation and construction standards, the energy used for the heating of the passengers areas is not available. Moreover, the heating of TS workers areas is performed by gas.

Based on the energy consumption modelling and the findings of the project [36], the major energy consumption in the TS is due to lighting, lifting and other electronic and heating equipment, in a ratio of about 50%, 25% and 25%, respectively, of the total main building energy consumption without auxiliary buildings and activities. Energy consumption related to the heating of the TS offices was neglected. The total hourly required energy E_t^{TS} *(kWh)* at time *t* is approximated with eq. (1) below, representing the three main types of equipment units, i.e., inside and outside lighting E_t^l *(kWh)*, passengers lifts by escalators and elevators E_t^{elev} *(kWh)* and electronic equipment E_t^{elec} *(kWh)*:

$$E_t^{TS} = E_t^{elev}\left(F_t^{pas}\right) + E_t^l(r_t) + E_t^{elec} \qquad \forall t \qquad (1)$$

where r_t is the solar radiation *(W/m² or lx)* and F_t^{pas} is the passengers flow in the TS (pas/h).

The power required by the elevator equipment E_t^{elev} is calculated as the sum of variable E_t^{var} and stand by E_t^{fix} power [55]. The variable energy consumption of the escalator is related to the transported passengers F_t^{pas}:

$$E_t^{var} = (F_t^{pas} \cdot g \cdot r_e \cdot m_p \cdot k_{wf})/3600000 \qquad \forall t \qquad (2)$$

where g = 9.81 m/s², r_e is the vertical rise of the escalator *(m)*, m_p is the average weight of passenger *(kg)* and k_{wf} is the walking factor, which is defined as the ratio of the time that passengers actually spend on the escalator to the time that they would spend if no walking took place [55]. Division by 3600000 is introduced to convert the final results from units of joules *(J)* to *kWh*.

The fixed power E_t^{fix} is related to the power consumed by the unloaded escalator and depends on the particular technical features of the escalator, such as the type of gear box, step chain bearing and guidance system. The work [55] presents a correlation with the height of escalator rise r_e, as dominant factor to qualify the different escalator designs:

$$E_t^{fix} = a \cdot r_e + b \qquad \forall t \qquad (3)$$

where *a* and *b* are coefficients depending on the technical features of the escalator. To select the coefficients values the escalators were assumed to have following technical features: ball bearing step chain guidance and involute gearbox [55].

The electrical energy E_t^l required by the lighting equipment depends on its design and on the control systems and requirements of illumination standard setup adopted for the TS (e.g., EN13272:2001 UK) and urban areas [56]. Therefore in the application, the activation of lighting to maintain the inside luminosity of the TS hall to be equal or higher than 75 *lux* will be considered for hours when the outside luminosity is less than 20 *lux*.

Finally, the electronic equipment that is constantly plugged into the grid are the ticket vending and control machines, and food and drinks distributors, with assumed required hourly energy 0.802, 0.752 and 0.206 *kWh*, respectively [57], [58].

3.1.2. Energy production

The total energy produced by PV P_t^{PV} *(kWh)* at time *t* is the sum of the outputs P_t^{PVi} of several individual PV panels at time step *t*. Taking into account the solar irradiation, whose model is described in Appendix, the ambient temperature and the characteristics of the module, the electricity output from one solar generation unit can be evaluated using the following set of equations used in [59], [60]. The technical parameters of the solar generation units can be retrieved from available industrial specifications. For the current study, we consider 500 solar modules with technical specifications from [60].

3.1.3. Battery storage

The set of eqs. (4) - (8) governs the energy flow dynamics of the battery storage in the TS:

$$R_t^{TS} = R_{t-1}^{TS} + \delta_t^{TS,ch} \cdot R^{TS,stor} - \delta_t^{TS,dis} \cdot R^{TS,stor} \qquad \forall t \qquad (4)$$

$$\delta_t^{TS,ch} + \delta_t^{TS,dis} \leq 1 \qquad \forall t \qquad (5)$$

$$0 \leq \delta_t^{TS,ch} \leq 1 \qquad \forall t \qquad (6)$$

$$0 \leq \delta_t^{TS,dis} \leq 1 \qquad \forall t \qquad (7)$$

$$0 \leq R_t^{TS} \leq R^{TS,max} \qquad \forall t \qquad (8)$$

where R_t^{TS} and R_{t-1}^{TS} are the energy levels in the battery at time *t* and *t-1 (kWh)*; $R^{TS,stor}$ is the energy portion that the battery is capable of charging or discharging during time *t (kWh)*, and $\delta_t^{TS,ch}$ and $\delta_t^{TS,dis}$ are the binary variables which can take values either 0 or 1 model indicating that the battery can either only be charged or discharged at time *t*, and $R^{TS,max}$ is the maximum battery charge *(kWh)*. The battery is assumed to have constant charging and discharging speeds, and no performance degradations or losses are considered.

Note that the eventual variations of charging and discharging efficiencies and energy losses due to the battery degradations are not accounted for in eq. (4) of the battery charging dynamics. This is done to simplify the battery model, considering the methodological aim of the paper: a more complex and complete model of the battery storage would not affect the way of performing the RO approach and its efficiency and it can be accounted for in future research.

3.2. Wind power plant (WPP)

We assume that a small wind power plant (WPP) is installed near the TS and the local community.

3.2.1. Energy production

The total energy produced by the WPP P_t^{WPP} *(kWh)* is assumed to be the sum of the individual outputs of all the wind turbines P_t^{WPPi} at time step *t*. As discussed in Appendix, the wind speed data form [61] is used to calculate the wind energy output from the individual wind turbine by the cubic correlation [62]. The total wind power output P_t^{WPP} is the uncertain variable and the prediction of its values are made by a NN trained by a NSGA-II [34], as described in Subsection 1.1.

3.3. District (D)

The local community or district (D) is constituted by residences and small businesses, such as shops and offices, situated around the TS. D is considered only as an energy consumer with an integrated battery, which allows storing energy during periods of low electricity price and discharging it during periods of high electricity price.

3.3.1. Energy consumption

To simulate the energy consumption of the D, we use the top-down approach based on available statistical collections of electricity consumptions [63]. We purposely decided to not divide the energy consumptions in the D and to consider it as the independent consumer to reduce the complexity of the model. In this view, the energy consumption for the D is formulated as follows:

$$E_t^D = E^{peak} \cdot r_w^{peak} \cdot r_d^{peak} \cdot r_h^{peak} \quad (9)$$

where r_h^{peak} is the hourly peak defined for working days and weekends (%), r_d^{peak} and r_w^{peak} are the daily and weekly peaks of power demand (%), and E^{peak} is the maximum hourly peak of power demand over a year (kWh).

3.3.2. Battery storage

The energy flow dynamics of the battery storage in D is formulated similarly to that of the TS battery (eqs. (4) – (8) in Subsection 3.1.3).

4. UNCERTAINTIES IN ENERGY MANAGEMENT

The expenses and revenues of each agent, and the global reliability of the microgrid are affected by uncertain parameters, such as energy outputs from renewable generators P_t^{PV} and P_t^{WPP}, energy demands of the consumers E_t^{TS} and E_t^D, and electricity prices c_t^p, c_t^s and c_t^D.

1.1.Energy output of renewable energy generators

The energy outputs from of the renewable generators are affected by the variability of the renewable sources of energy, i.e., wind for WPP and solar irradiation for PV.

As discussed in Subsection 3.2, the uncertainty related to the availability of the wind energy output P_t^{WPP} is accounted for in the form of the Prediction intervals (PIs) estimated by NSGA-II trained NN of [34].

In this study, the uncertainty related to the availability of the PV energy output P_t^{PV} is accounted for by intervals, whose lower and upper bounds are symmetric around the expected value of the PV energy output. The width of the intervals is selected to account for the variability of the PV energy output in the time period considered.

In this research, we have used the term 'technical failure' to represent all modes of failures of the wind turbine and the generator units. For the numerical application presented in this paper, the Mean Time To Failure (MTTF) and Mean Time To Repair (MTTR) of the wind power generation units have been taken equal to 1920 *h* and 25 *h*, respectively [64], accounting for all causes of wind turbines failures. The energy output from renewable generators is also affected by failures, which may lead to periods of production unavailability during the subsequent repairs. The technical unavailability of energy generation units can be caused by failures of different subassemblies. In this view, for wind power generation [65] we classify failures into two major categories depending on their causes: (i) mechanical components failures associated with the blades, gearbox, hydraulic unit, yaw unit and brake pad, and (ii) electrical and electronic components failures related to the control panel, capacitor panel and generator failures. The analysis of failures in the field shows that a wind farm usually experiences more failures due to mechanical components than failures due to electrical and electronic components (79% and 21% of failures over a lifetime period, respectively, are the values reported in [65]). Moreover, the loss of power generation due to mechanical components failure is higher than that of the electrical components failure to an extent up to 116% [65].

Technical failures of generation units of the same type are, for simplicity, assumed to be independent from each other: no common causes for failures are considered. Moreover, no particular reduction of energy production due to units degradation has been considered: only two states are possible, i.e., 100% of technical availability and 0% during the repair upon a failure. Failure and repair times are assumed to follow exponential distributions, considering the useful life of the components.

Failure times and repair durations are simulated by sampling with the inverse transform technique [66].

1.2.Energy demand

Also to estimate the PIs accounting for the variability of the energy demands E_t^{TS} and E_t^D, the NSGA-II trained NN of [34] is used.

1.3. Electricity prices

Similar to the PV energy output, the uncertainty related to the variability of electricity prices c_t^p, c_t^s and c_t^D is accounted for in the form of intervals, whose lower and upper bounds are symmetric around the expected value of each variable. The width of the intervals is selected to account for the fluctuations of these variables in the time period considered.

5. ENERGY SCHEDULING OPTIMIZATION

To formulate the power scheduling problem, the TS, WPP and D agents are represented as 'open systems' that continuously interact with each other through energy exchanges at time *t* (Figure 2 a, b, c).

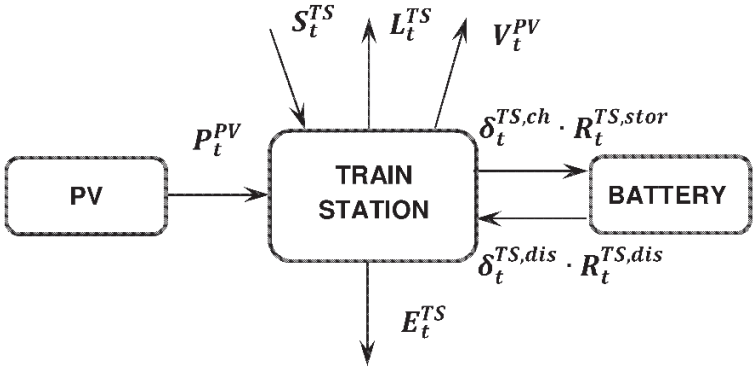

a)

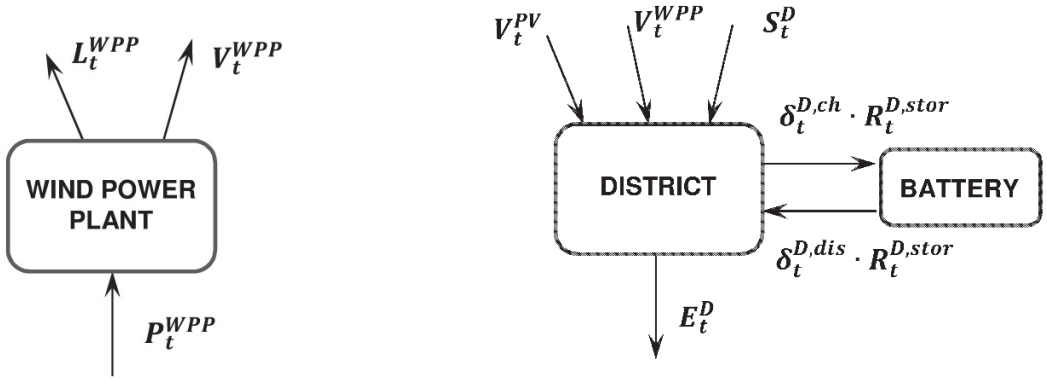

b) *c)*

Figure 2. Input and output energy flows for the agents: a) TS; b) WPP and c) D.

5.1. Robust optimization

The decision-making strategy for each agent, identified by using the RO, is based on the goals of cost functions minimization for the D and TS and revenues function maximization for the WPP [25].The approach adopted in this paper allows the linear formulation of the robust counterpart of an optimization problem. Based on the representations of Figure 2, the RO of energy scheduling for the TS, WPP and D, where the objective functions to be optimized are formulated in terms of costs for the TS (eq.(15)) and D (eq.(27)), and revenues for the WPP (eq.(39)), are posed as follows.

Train Station

Minimize $\boldsymbol{\alpha^{TS}}$

s.t.

$$-S_t^{TS} + L_t^{TS} + \delta_t^{TS,ch} \cdot R^{TS,stor} - \delta_t^{TS,dis} \cdot R^{TS,stor} + V_t^{PV} - P_t^{PV} \cdot x_t^{n+1} + E_t^{TS} \cdot x_t^{n+2} + z_t^{Power} \cdot \Gamma_t^{Power} + p_t^{P_t^{PV}} + p_t^{E_t^{TS}} \leq 0 \qquad \forall t \qquad (10)$$

$$z_t^{Power} + p_t^{P_t^{PV}} \geq \hat{P}_t^{PV} \cdot y_t^{P_t^{PV}},\ z_t^{Power} + p_t^{E_t^{TS}} \geq \hat{E}_t^{TS} \cdot y_t^{E_t^{TS}} \qquad \forall t \qquad (11)$$

$$-y_t^{P_t^{PV}} \leq x_t^{n+1} \leq y_t^{P_t^{PV}}, -y_t^{E_t^{TS}} \leq x_t^{n+2} \leq y_t^{E_t^{TS}} \qquad \forall t \qquad (12)$$

$$L_t^{TS} + V_t^{PV} - P_t^{PV} \cdot x_t^{n+1} + z_t^{Micro} \cdot \Gamma_t^{Micro} + p_t^{P_t^{PV}} \leq 0 \qquad \forall t \tag{13}$$

$$z_t^{Micro} + p_t^{P_t^{PV}} \geq \hat{P}_t^{PV} \cdot y_t^{P_t^{PV}} \qquad \forall t \tag{14}$$

$$\sum_{t=0}^{T} (c_t^p \cdot S_t^{TS} - c_t^s \cdot L_t^{TS} - c_t^D \cdot V_t^{PV}) + \sum_{t=0}^{T} \left(z_t^{Cost} \cdot \Gamma_t^{Cost} + p_t^{c_t^p} + p_t^{c_t^s} + p_t^{c_t^D} \right) \leq \alpha^{TS} \tag{15}$$

$$z_t^{Cost} + p_t^{c_t^p} \geq \hat{c}_t^p \cdot y_t^{c_t^p}, z_t^{Cost} + p_t^{c_t^s} \geq \hat{c}_t^s \cdot y_t^{c_t^s}, z_t^{Cost} + p_t^{c_t^D} \geq \hat{c}_t^D \cdot y_t^{c_t^D} \qquad \forall t \tag{16}$$

$$-y_t^{c_t^p} \leq S_t^{TS} \leq y_t^{c_t^p}, -y_t^{c_t^s} \leq L_t^{TS} \leq y_t^{c_t^s}, -y_t^{c_t^D} \leq V_t^{PV} \leq y_t^{c_t^D} \qquad \forall t \tag{17}$$

$$S_t^{TS} \geq 0, L_t^{TS} \geq 0, V_t^{PV} \geq 0 \qquad \forall t \tag{18}$$

$$\begin{cases} \beta \cdot \tilde{E}_t^D \leq V_t^{PV}, & if\ P_t^{PV} \geq \beta \cdot \tilde{E}_t^D \\ 0 \leq V_t^{PV}, & otherwise \end{cases} \qquad \forall t \tag{19}$$

$$R_t^{TS} \leq R_{t-1}^{TS} + \delta_t^{TS,ch} \cdot R^{TS,stor} - \delta_t^{TS,dis} \cdot R^{TS,stor} \qquad \forall t \tag{20}$$

$$\delta_t^{TS,ch} + \delta_t^{TS,dis} \leq 1 \qquad \forall t \tag{21}$$

$$0 \leq \delta_t^{TS,ch} \leq 1, 0 \leq \delta_t^{TS,dis} \leq 1 \qquad \forall t \tag{22}$$

$$0 \leq R_t^{TS} \leq R^{TS,max}, \qquad \forall t \tag{23}$$

District

Minimize $\boldsymbol{\alpha^D}$

s.t.

$$-S_t^D - V_t^{PV} - V_t^{WPP} + (R_t^D - R_{t-1}^D) + E_t^D \cdot x_t^{n+1} + z_t^{Power} \cdot \Gamma_t^{Power} + p_t^{E_t^D} \leq 0 \quad \forall t \tag{24}$$

$$z_t^{Power} + p_t^{E_t^D} \geq \hat{E}_t^D \cdot y_t^{E_t^D} \qquad \forall t \tag{25}$$

$$-y_t^{E_t^D} \leq x_t^{n+1} \leq y_t^{E_t^D} \qquad \forall t \tag{26}$$

$$\sum_{t=0}^{T} \left(c_t^p \cdot S_t^D + c_t^D \cdot V_t^{WPP} + c_t^D \cdot V_t^{PV} \right) + \sum_{t=0}^{T} \left(z_t^{Cost} \cdot \Gamma_t^{Cost} + p_t^{c_t^p} + p_t^{c_t^D} \right) \leq \alpha^D \tag{27}$$

$$z_t^{Cost} + p_t^{c_t^p} \geq \hat{c}_t^p \cdot y_t^{c_t^p}, z_t^{Cost} + p_t^{c_t^D} \geq \hat{c}_t^D \cdot y_t^{c_t^D} \quad \forall t \tag{28}$$

$$-y_t^{c_t^p} \leq S_t^D \leq y_t^{c_t^p}, -y_t^{c_t^D} \leq V_t^{WPP} + V_t^{PV} \leq y_t^{c_t^s} \quad \forall t \tag{29}$$

$$R_t^D \leq R_{t-1}^D + \delta_t^{D,ch} \cdot R^{D,stor} - \delta_t^{D,dis} \cdot R^{D,stor} \quad \forall t \tag{30}$$

$$\delta_t^{D,ch} + \delta_t^{D,dis} \leq 1 \quad \forall t \tag{31}$$

$$0 \leq \delta_t^{D,ch} \leq 1, 0 \leq \delta_t^{D,dis} \leq 1 \quad \forall t \tag{32}$$

$$0 \leq R_t^D \leq R^{D,max} \quad \forall t \tag{33}$$

$$S_t^D \geq 0 \quad \forall t \tag{34}$$

$$V_t^{PV} = \tilde{V}_t^{PV}, V_t^{WPP} = \tilde{V}_t^{WPP} \quad \forall t \tag{35}$$

Wind Power Plant

Maximize $\boldsymbol{\alpha^{WPP}}$

s.t.

$$L_t^{WPP} + V_t^{WPP} - P_t^{WPP} \cdot x_t^{n+1} + z_t^{Power} \cdot \Gamma_t^{Power} + p_t^{P_t^{WPP}} \leq 0 \quad \forall t \tag{36}$$

$$z_t^{Power} + p_t^{P_t^{WPP}} \geq \hat{P}_t^{WPP} \cdot y_t^{P_t^{WPP}} \quad \forall t \tag{37}$$

$$-y_t^{P_t^{WPP}} \leq x_t^{n+1} \leq y_t^{P_t^{WPP}} \quad \forall t \tag{38}$$

$$\sum_{t=0}^{T} (c_t^s \cdot L_t^{WPP} + c_t^D \cdot V_t^{WPP}) - \sum_{t=0}^{T} \left(z_t^{Cost} \cdot \Gamma_t^{Cost} + p_t^{c_t^s} + p_t^{c_t^D} \right) \geq \alpha^{WPP} \tag{39}$$

$$z_t^{Cost} + p_t^{c_t^s} \geq \hat{c}_t^s \cdot y_t^{c_t^s}, z_t^{Cost} + p_t^{c_t^D} \geq \hat{c}_t^D \cdot y_t^{c_t^D} \quad \forall t \tag{40}$$

$$-y_t^{c_t^s} \leq L_t^{WPP} \leq y_t^{c_t^s}, -y_t^{c_t^D} \leq V_t^{WPP} + V_t^{PV} \leq y_t^{c_t^s} \quad \forall t \tag{41}$$

$$\begin{cases} \gamma \cdot \tilde{E}_t^D \leq V_t^{WPP}, & if\ P_t^{WPP} \geq \gamma \cdot \tilde{E}_t^D \\ 0 \leq V_t^{WPP}, & otherwise \end{cases} \quad \forall t \tag{42}$$

$$L_t^{WPP} \geq 0, V_t^{WPP} \geq 0, V_t^{PV} \geq 0 \quad \forall t \tag{43}$$

where L_t^{TS} and L_t^{WPP} *(kWh)* are the portions of energy sold to the external grid by the TS and WPP, respectively, S_t^{TS} and S_t^D *(kWh)* are the portions of energy purchased from the external grid by the TS and D, respectively, V_t^{PV} and V_t^{WPP} *(kWh)* are the portions sold to the D and generated by the PV panels of the TS and WPP, respectively, β and γ are the coefficients defining the minimum amount of energy to be sold to D by TS and WPP, respectively, $\tilde{E}_t^D$ (kWh) is the expected energy demand for D (for the moment, considered without uncertainty) at time step *t*, predicted by TS and WPP, $\tilde{V}_t^{PV}$ and $\tilde{V}_t^{WPP}$ (kWh) are the energy portions, which TS and WPP are ready to sell to D at time step *t.* The variables $\delta_t^{TS,ch}$, $\delta_t^{TS,dis}$, $\delta_t^{D,ch}$ *and* $\delta_t^{D,dis}$ used in the formulas (20) – (22) and (30) – (32) are binary variables, which take values 0 or 1 to indicate that the battery can either only be charged or discharged at time t.

As mentioned earlier, the objective functions to be optimized are costs for the TS and D, and revenues for the WPP. The optimization problems account for the energy balance eqs. (10), (13), (24) and (36), and the costs and revenues eqs. (15), (27) and (39). The batteries charging and discharging dynamics is formulated with eqs. (20) - (23) for TS, and eqs. (30) - (33) for D. Eqs. (18), (34) and (43) are the decision variables constraints. The coefficients β and γ in eqs. (19) and (42) increase the regularity of energy exchanges between the microgrid agents, by imposing the minimum amount of energy that WPP and TS must supply to D under conditions of availability of wind and solar energy outputs and promoting the local energy exchanges among the microgrid agents.

i", "nonables z_t^{Power}, z_t^{Cost}, z_t^{Micro} $p_t^{P_t^{WPP}}$, $p_t^{P_t^{PV}}$, $p_t^{E_t^D}$, $p_t^{E_t^{TS}}$, $p_t^{c_t^p}$, $p_t^{c_t^s}$, $p_t^{c_t^D}$, $y_t^{P_t^{WPP}}$, $y_t^{P_t^{PV}}$, $y_t^{E_t^D}$, $y_t^{E_t^{TS}}$, $y_t^{c_t^p}$, $y_t^{c_t^s}$ and $y_t^{c_t^D}$ are the RO variables which are forced to be greater than or equal to zero, x_t^{n+1} and x_t^{n+2} are auxiliary variables that are forced to be equal to one. Γ_t^{Power} and Γ_t^{Cost} define the level of uncertainty considered in each optimization model (a zero value corresponds to the deterministic problem) and are such that $0 \leq \Gamma_t^{Power} \leq 1$ and $0 \leq \Gamma_t^{Cost} \leq 2$ for the D and WPP, and $0 \leq \Gamma_t^{Power} \leq 2$ and $0 \leq \Gamma_t^{Cost} \leq 3$ for the TS.

Note that the RO presents the advantage that it represents the uncertainty related to the variations of the operational or environmental conditions in terms of PIs without making any assumption about the probabilistic distribution of the uncertainty. For example, for the WPP in the robust formulation the level of uncertainty $\hat{P}_t^{WPP}$ is calculated as $\hat{P}_t^{WPP} = (P_t^{WPP,ub} - P_t^{WPP,lb})/2$,

where $P_t^{WPP,ub}$ and $P_t^{WPP,lb}$ *(kWh)* are the upper and lower prediction bounds at time *t*, respectively. In this work, we take the mean of the prediction interval as point estimate of the wind energy output P_t^{WPP} in eq. (36). The point estimates of the other uncertain variables are the values calculated with the models of Section 3, before the addition of the random noises.

Note that the values of the decision variables identified during the optimization phase are adjusted based on the real values of the uncertain parameters. In this view, we assume that the decision variables R_t^D, R_t^{TS}, V_t^{WPP} and V_t^{PV} stay unchanged and can be affected only by the large prediction error of the available power or the technical failures of generation units.

Figure 3 a,b illustrates the structure of the control algorithm and operation procedure of the microgrid. The outputs from the models of the individual components are used to forecast the energy demands of the TS and D, the wind power output of the WPP, as well as the energy prices. These forecasted quantities are used by the RO for the decision making to determine the optimal batteries scheduling actions and other decision variables, e.g., the energy portion to exchange between the agents and the upstream grid. In order to set up the price for the energy trading, the agents use 24-hours ahead predictions of the reference prices, i.e., c_t^p price for kWh from the upstream grid. Note that these predictions do not account for eventual upstream price variations.

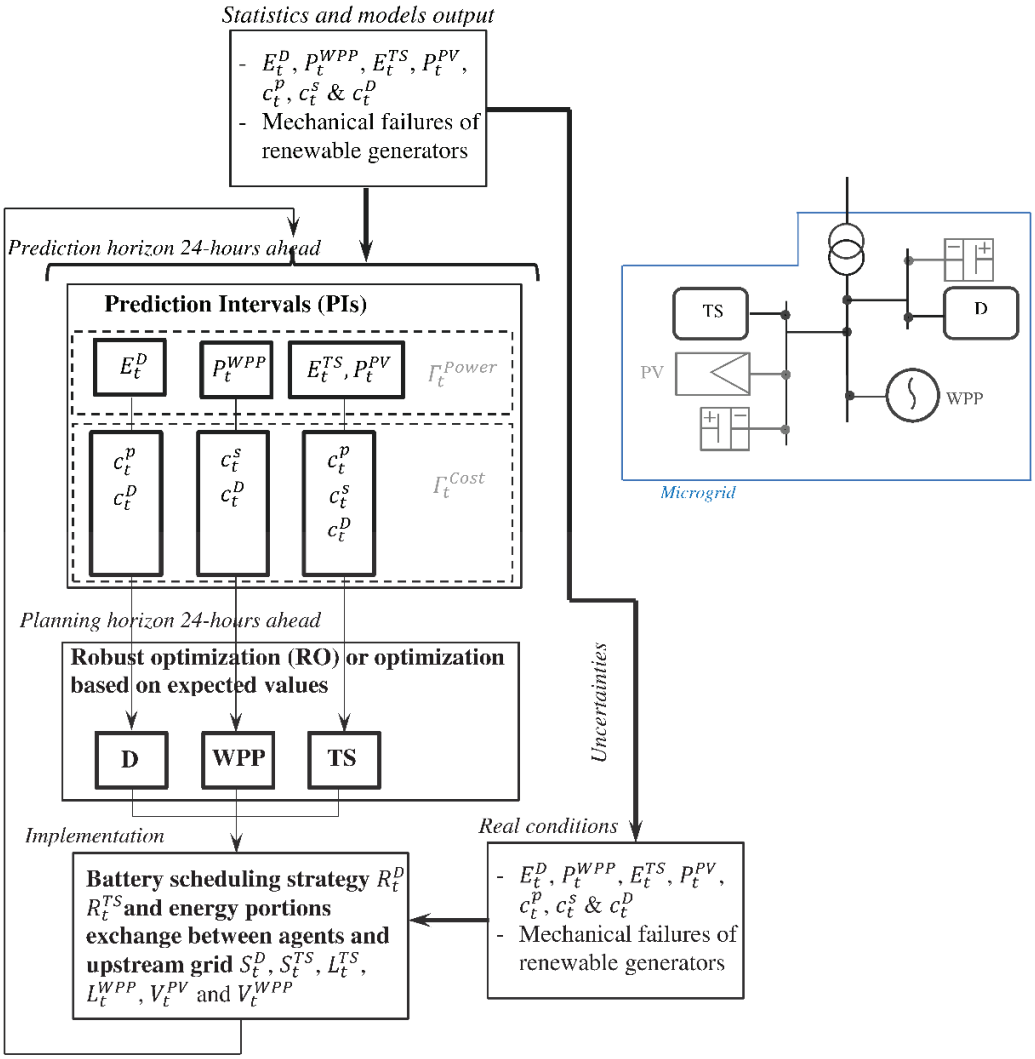

a)

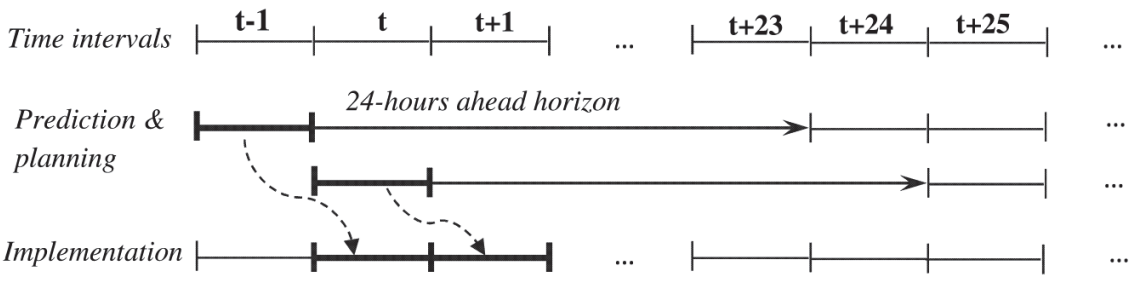

b)

Figure 3. Integrated framework: a) Structure of the control algorithm; b) Operation procedure.

The decision-making strategy for each agent, identified by using the RO approach, is based on the goal of cost functions minimization for the D and TS, and revenues function maximization for the WPP. These goals are achieved through the strategic battery scheduling and the selection of the optimal energy exchanges between the microgrid agents and the upstream electricity grid. Since the battery cannot be charged and discharged at the same time, only one of these actions can be executed at time t. Thus, the consumer aims to optimize its decision-making strategy on a time horizon of 24 time steps, each of one hour duration.

The RO problems are solved by using the optimization package CPLEX, implemented in Java code, which guaranty global optimality for mixed integer programming (MIP) problems (the iterative process of optimization in CPLEX is not illustrated in the paper: the interested reader may refer to [67] for further details). After optimization, the decisions are shared among the agents through the communication process indicated in the paper.

At each time *t*, the microgrid energy producers (WPP and TS) and consumer (D) have the possibility to negotiate the bilateral contracts of energy exchanges within the microgrid. The framework of this negotiation is discussed in Subsection 5.3. Note that in this paper demand-response mechanisms for the energy management are not considered.

5.2. Predictions

The PIs, estimated by NSGA – II trained NN, are optimized both in terms of coverage probability (CP) and prediction interval width (PIW). For this purpose, a multi-objective genetic algorithm (namely, non-dominated sorting genetic algorithm–II (NSGA-II)) is implemented to find the optimal parameters (weights and biases) of the NN. By using NSGA-II, Pareto-optimal solution sets, including several non-dominated solutions with respect to the two objectives (CP and PIW), are generated.

The computational complexity of the NSGA-II trained NN algorithm is explained by two time demanding sub-operations: non-dominated sorting and fitness evaluation. At first, the time complexity of the non-dominated sorting part depends on the number of objectives and the population size. At second, the complexity of the fitness evaluation phase is related to the number of input samples for each of which a fitness value is obtained through the training of a Neural Network (NN) by the NSGA-II. In this view, the complexity of one generation represents

the sum of the computational complexities of these two stages.

In [34], a comparison have been done between different optimization techniques: MOGA (Multi-Objective Genetic Algorithms), SOGA (Single-Objective Genetic Algorithms) and SOSA (Single-Objective Simulated Annealing) applied to PIs of time series prediction. Based on this comparison, the mean CPU times for training with MOGA, SOGA and SOSA are 258.84, 199.36 and 163.29 seconds, respectively. Note that the GA optimization techniques are population based algorithm, so their computational time is more than Simulated Annealing (SA). The required average CPU time for testing, i.e., for the online prediction of PIs, is very fast for all algorithms, which is about 0.05 s. From the user point of view, the computational burden of the training phase is relatively less important since the training phase is, usually, only performed once. In cases where online learning is implemented, the algorithms are usually not retrained, but their parameters are updated. This is, usually, computationally less expensive than a new training phase. Note that the computational burden is dependent on the complexity of the structure of the model (e.g. number of input neurons, hidden layers, and hidden neurons), the size of the dataset and the performance of the learning algorithm.

In addition, the existing techniques for estimating PIs for NN algorithm outputs such as Delta and Bayesian methods require the calculation of Jacobian and Hessian matrixes, respectively, and although they are capable of generating high quality PIs, they demand high computational time in the development stage [68]. Compared to Delta and Bayesian methods, NSGA-II is less demanding at the training phase.

5.3. Communication framework

Figure 4 depicts the communication interactions among the microgrid agents. It can be noted that the microgrid does not include an independent controller or operator, responsible for coordinating, controlling and operating the electric power system or/and market, as in the actual power grid. Indeed, we assume that all coordination procedures are done in a decentralized manner through direct negotiation among the agents, similar to [18], [19]. However, to facilitate the agents communications, an additional agent called Independent System Operator (ISO) is introduced in the model, similar to [69]. The role of the ISO agent is to collect the requests for

energy purchase from the *Consumers*, such as D, and the energy sale offers from the *Generators*, such as TS and WPP.

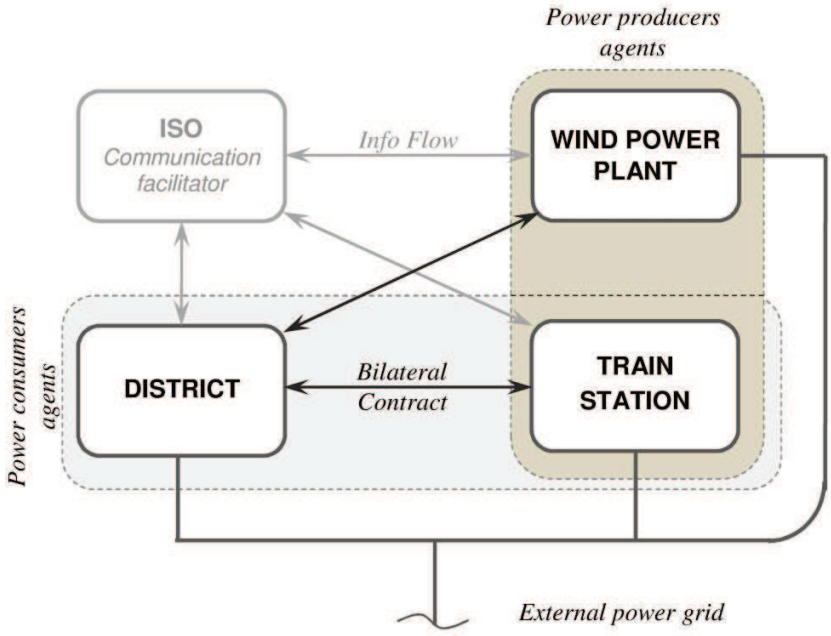

Figure 4. Multi-layered interaction between agents.

The microgrid agents participate in the decision-making framework as illustrated in Figure 5. Note that the hierarchy of decision considered in this work for exemplification, gives priority to the energy generators, i.e., TS and WPP, to decide the renewable energy V_t^{PV} and V_t^{WPP} that is available for sale to D, and L_t^{PV} and L_t^{WPP} for sale to the external grid at each time step t. These decisions are transmitted through the ISO agent to D, which considers these decisions as constant parameters (eq. (35)) for the costs optimization for D). After the determination of other energy scheduling variables, such as S_t^D and R_t^D, D sets a bilateral agreement with TS and WPP to purchase V_t^{PV} and V_t^{WPP}. The duration of the bilateral contract is assumed to be one hour.

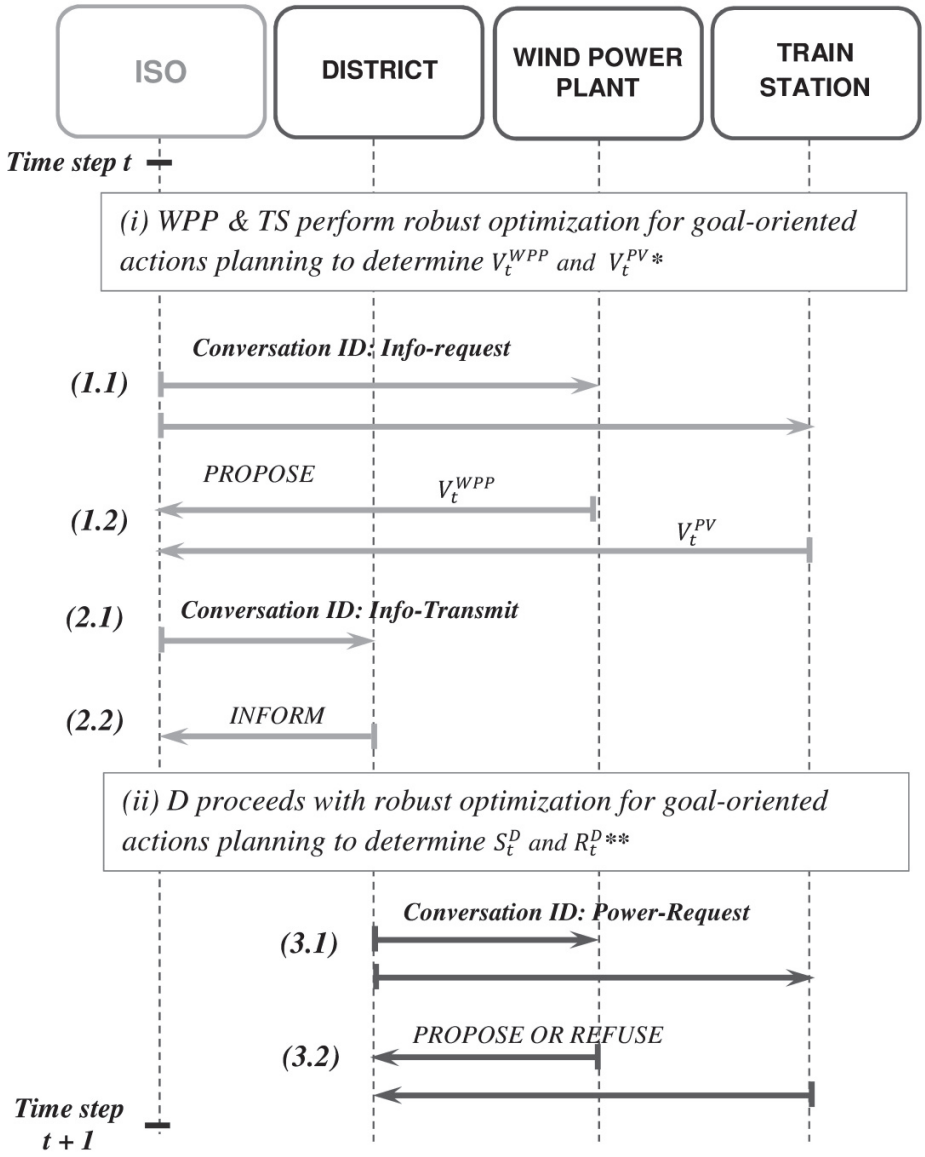

Figure 5. Example of agents communication at time step t.

Table 1 regroups the previsions of the operational conditions (i) made by the agents themselves and (ii) received from other agents through the ISO and (iii) the decision variables.

Table 1. Previsions and decision variables.

Previsions of the operational conditions	D	WWP	TS
(i) agent personal previsions*	$E_t^D;\ c_t^p;\ c_t^D$	$P_t^{WPP};\ c_t^s;\ c_t^D$	$E_t^{TS};\ P_t^{PV};\ c_t^p;\ c_t^D;\ c_t^s$
(ii) previsions received from other agents through *ISO*	$V_t^{PV};\ V_t^{WPP}$	-	-
(iii) decision variables based on the previsions	$S_t^D;\ R_t^D$	$V_t^{WPP};\ L_t^{WPP}$	$V_t^{PV};\ L_t^{TS};\ S_t^{TS};\ R_t^{TS}$

* Personal previsions of agents are represented by PIs for RO and point predictions for the deterministic optimization.

Note that the adopted hierarchical decision scheme allows, on the one hand to TS and WPP to increase their revenues by deciding which amount of energy to sell to D or to the external grid using the most profitable actions planning, on the other hand it gives the possibility to D to purchase emissions-free and less expensive energy, generated by TS and WPP in the microgrid.

6. OUTPUT INDICATORS

6.1. Reliability of the microgrid

As mentioned in Introduction, we focus on the grid-connected mode. In this case the power imbalances inside the microgrid and between the microgrid and the upstream grid can be produced by the technical failures of energy generators and/or forecast errors in the energy output of the renewable generators. Indeed, the energy from the upstream grid is always available and can be used to compensate the power imbalance generated by the unavailability of the energy producer. The reliability indicators are used to evaluate the performance of the optimal management and are calculated based on the optimal values of the decision variables.

The overall microgrid performance is evaluated in terms of classical adequacy assessment metrics, which characterize the ability of the distributed generation system energy capacity to meet system demand in presence of uncertainty [70]. Specifically, Loss of Load Expectation (LOLE) is used to characterize the probability of unsatisfied electricity demand and Loss of Expected Energy (LOEE) to quantify the expected amount of energy losses for *Ns* time steps of one hour:

$$LOLE = \sum_{t=0}^{Ns} Pr_t(P_t < E_t) \tag{44}$$

$$LOEE = \sum_{t=0}^{Ns} Pr_t(P_t < E_t) \cdot (E_t - P_t) \tag{45}$$

where $Pr_t(P_t < E_t)$ is the probability of loss of load at time step *t*, P_t *(kWh)* is the available capacity at time period *t*, E_t *(kWh)* is the energy demand at time step *t* and $E_t - P_t$ *(kWh)* is the energy that the system is not able to supply at time step *t*. The situation when the available capacity P_t is lower than the energy demand E_t at time step *t*, produces an electricity shortage in that time step *t*.

The available power capacity of the microgrid P_t represents the sum of the electricity produced by all generation units at time step *t*. In our case, P_t accounts for the amount of energy purchased from the external grid (i.e., S_t^D and S_t^{TS}), produced by the local generators (i.e., V_t^{PV} and V_t^{WPP}) and discharged from the batteries (i.e., $\delta_t^{D,dis} \cdot R^{D,stor}$ and $\delta_t^{TS,dis} \cdot R^{TS,stor}$):

$$P_t = S_t^D + S_t^{TS} + V_t^{PV} + V_t^{WPP} + \delta_t^{D,dis} \cdot R^{D,stor} + \delta_t^{TS,dis} \cdot R^{TS,stor} \qquad \forall t \quad (46)$$

Finally, the energy demand E_t in the microgrid is defined as follows:

$$E_t = E_t^D + E_t^{TS} + \delta_t^{D,ch} \cdot R^{D,stor} + \delta_t^{TS,ch} \cdot R^{TS,stor} \qquad \forall t \qquad (47)$$

The reliability indices considered in this work, i.e., LOLE and LOEE, are used to account for the impact of the failures of power generators; on the contrary, the within-hour variability of the energy output from the PV and wind generators is neglected, for simplicity. The time step of 1 hour is typical for power system reliability assessment [71], [72], based on the available data for wind and PV generators, and the failure data statistics, e.g., MTTF and MTTR.

6.2. Impact of wind power prediction errors and mechanical failures of wind power generator

In the end, it is important to quantify the effects of errors in the predictions resulting in the non-supply of the committed energy. Focusing on the impact of errors in the predictions of wind power and wind power generator technical failures, a penalty or imbalance cost is added to the revenue or cost functions of the WPP to quantify the deviation from the commitment.

It is important to note that the revenues are affected by predictions only in the case that they are generated from the market (through the submission of offers and bids). In case of application of feed-in tariff system, when all energy (*kWh*) from renewable generation is purchased by the

transmission company in exchange of a fix remuneration (e.g., like in France), predictions do not play any role in the revenues calculation [73].

On the one hand, the WPP participates in the microgrid energy market by committing to provide V_t^{WPP} to the D. The D optimizes its energy strategy based on the amount of the committed energy V_t^{WPP}, which if not-supplied can generate reliability problems to the whole microgrid. On the other hand, the amount of energy L_t^{WPP} is sold to the external grid, which does not impose particular constraints and purchases all amount of energy. In this view, the penalty based on [74] is applied only to the V_t^{WPP}. Note that the formulation of revenues accounting for the imbalance cost is done for a contract duration of one hour. By taking into account the prediction errors and/or technical failures of the wind generator, the revenues of the WPP for time step *t* are formulated as follows:

$$\alpha_t^{WPP} = L_t^{WPP,c} \cdot c_t^s + V_t^{WPP,c} \cdot c_t^D + T_t^{WPP} \qquad \forall t \qquad (48)$$

where $L_t^{WPP,c}$ and $V_t^{WPP,c}$ *(kWh)* are the contracted amounts of energy provided by the WPP to the external and microgrids, respectively, T_t^{WPP} *(€)* is the imbalance cost defined as follows:

$$T_t^{WPP} = \begin{cases} c_t^{D,+} \cdot d_t^{WPP,*}, & d_t^{WPP,*} \geq 0 \\ c_t^{D,-} \cdot d_t^{WPP,*}, & d_t^{WPP,*} < 0 \end{cases} \qquad \forall t \qquad (49)$$

where $d_t^{WPP,*} = V_t^{WPP,*} - V_t^{WPP,c}$ *(kWh)* is the imbalance for time step *t* calculated as the difference between $V_t^{WPP,*}$ *(kWh)* the actual amount of energy that WPP can supply and $V_t^{WPP,c}$ *(kWh)* the level of contracted energy, and $c_t^{D,+}$ and $c_t^{D,-}$ *(€/kWh)* are the imbalance prices for positive and negative imbalances, respectively, at time step *t*.

As it can be noticed, when the inequality $d_t^{WPP,*} < 0$, i.e., a negative imbalance, is satisfied, T_t^{WPP} takes a negative value, representing the penalty that WPP must pay for the non-supplied energy. On the contrary, for a positive imbalance $d_t^{WPP,*} \geq 0$, the WPP receives the payment T_t^{WPP} for the surplus of energy.

For the application of this paper, we have reviewed the existing imbalance tariff structures and regulation mechanism of some European countries [75], such as Belgium, Netherland, France and Spain, to define the formulation of the imbalance prices. Among the existing formulations, the definition of imbalance price in Spain is taken as the simplest, where the imbalance price is

equal to a certain proportion of the spot price [74], [76]. For the numerical application that follows (Section 7), we assume that deviations from the schedule are charged by 10% of the daily market price [76].

To evaluate the impact of the imbalance cost on the WPP revenues, we introduce the performance ratio γ, calculated over a simulation period of *Ns* hours by normalizing the actual revenue of the WPP by the revenue that would be obtained in the case of the perfect forecast [74]:

$$\gamma = \left(1 - \frac{\sum_{t=0}^{Ns} |T_t^{WPP}|}{\sum_{t=0}^{Ns} V_t^{WPP,c} \cdot c_t^D}\right) \cdot 100\% \qquad (50)$$

The proposed performance ratio is expressed in percentage and such that $\gamma \in (0,100]$. For perfect predictions, when deviations from committed energy are null, $\gamma = 100\%$.

In this paper, the indirect 'failure cost' resulting from failures or interruptions is partly accounted for in the cost or revenue objective functions of the microgrid stakeholders. In this view, if the failure of the renewable generator occurs, an energy producer, e.g., WPP, will be requested to pay the penalty (imbalanced cost) for the amount of energy not supplied and an energy consumer, e.g., D, will be obliged to purchase the needed energy amount from the external grid. Therefore, to reduce the cost due to failures or other interruptions (e.g., due to low wind), each stakeholder aims at optimizing its revenue or cost functions by using the available predictions – expected values or PIs of operational and environmental parameters. However, the direct 'failure cost' due to reparation or maintenance actions of the energy generators are not accounted in our research, but the modelling framework is general and these can be added in future work.

7. APPLICATION

The optimization framework is applied on a time horizon of 1680 hrs. This is sufficiently large to determine the converged indicators in presence of the variability due to the random technical failures. In addition, the results obtained in this paper are calculated by a large number of simulations to ensure convergence of the indicators in presence of the variability due to the random technical failures. For convergence, the difference between two successive values of the moving average of the indicators is considered, and a threshold value of 2% is used.

Moreover, the availability of the data, used to simulate the real conditions, i.e., wind energy output, energy demand of the TS and D, is also an important aspect of this work. Indeed, as it is discussed in Section 5, the PIs are estimated by a multi-perceptron neural network. For this purpose the available data was divided into two samples, i.e., training and testing samples. In this view, to simulate the real conditions of the microgrid operation the testing samples are used.

As it is highlighted in Subsection 6.2, the time step of 1 hour is typically used for power system reliability assessment [71], [72], based on the available data for wind and PV generators, and the failure data statistics, e.g., MTTF and MTTR. In addition, the focus of the work is not to model the fluctuations and make accurate predictions of wind speed and solar irradiation, but to illustrate an optimization framework capable of handling this aspect. Note, that the proposed architecture can handle the upscale to more complete and realistic models of the individual components in future research works.

In this view, different references from the literature use one hour time step to explore energy management in microgrids, e.g., the demand-side management in the residential sector incorporating local PV energy generation and energy storage [77], the energy management in the autonomous polygeneration microgrid [78] and the economic analysis for smart microgrid management [79]. Therefore, we believe that by reducing the model complexity, we have struck a balance between modelling accuracy and computational efficiency.

As discussed in Section 4, the PIs of the available wind energy output P_t^{WPP}, and energy demands E_t^{TS} and E_t^D have been estimated by a NN trained by a NSGA-II with respect to two objectives: the coverage of the prediction interval (to be maximized) and their width (to be minimize) [34]. This optimization gives rise to the Pareto fronts depicted in Figure 6, from which different solutions can be selected and used in the energy management by RO, differing in interval widths and coverage probability.

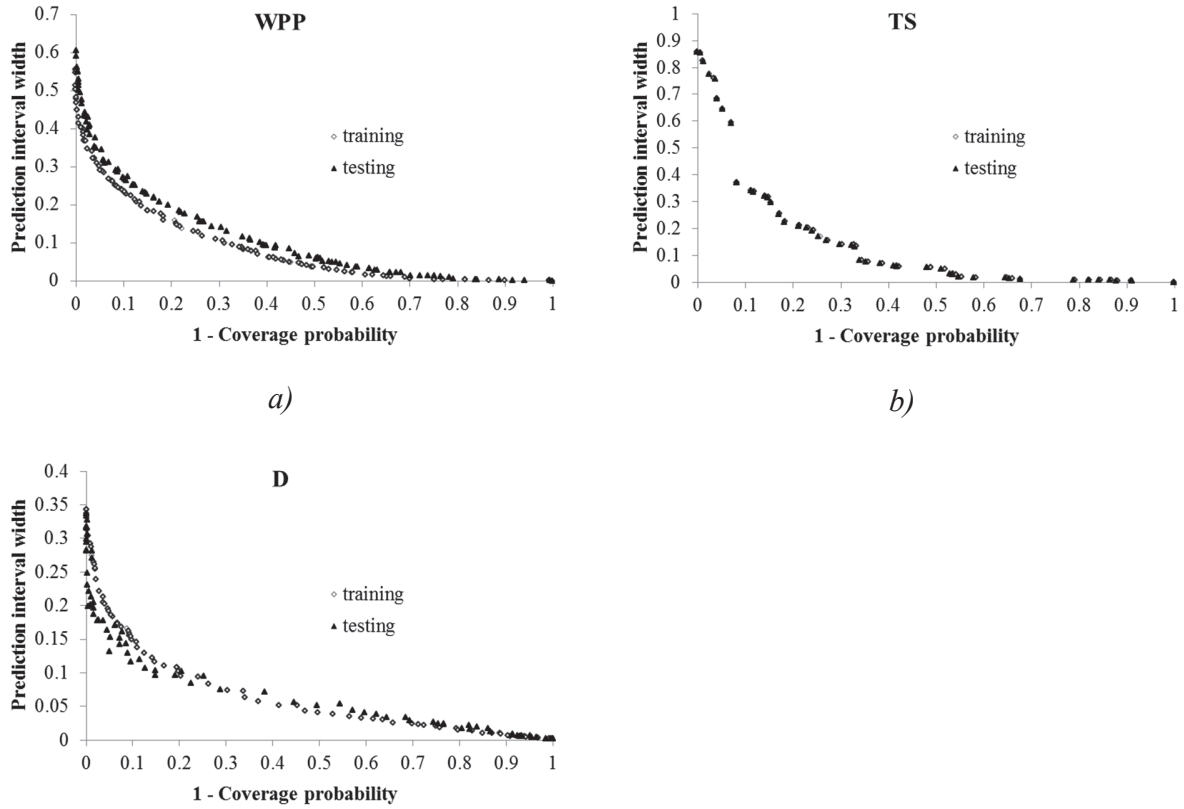

Figure 6. Pareto fronts of PIs: a) P_t^{WPP}, b) E_t^{TS} and c) E_t^D.

The developed optimization framework has been tested in the offline mode, i.e., the environmental and operational conditions of the microgrid have been modelled by using data driven models, i.e., beta distribution and time series to model solar irradiation and wind speed, respectively, and with statistical data. The possible uncertainties in these conditions have been accounted for by the microgrid stakeholders by using PIs. However, it is important to highlight that such a test can be also done in situ, when the developed optimization framework will be searching for the optimal energy management strategy under real operational and environmental conditions. In this case, the PIW can be calibrated in order to account not only for fluctuations of weather conditions, but also for some practical problems, which could be related to sensors malfunction and inaccuracy. Note that the RO approach is particularly useful for these cases - even when the realization of the uncertainty is not within the predicted intervals, the performance of the RO solutions is still good enough [25].

To account for the variations of the electricity prices c_t^p, c_t^s and c_t^D, the lower and upper bounds of their associated PIs were assumed to be the ±10% of their expected values. Similarly, the variations of P_t^{PV} were accounted for by setting the lower and upper bounds of the PIs to the ±5% of their expected values. Note that these width of the PIs were fixed based on the accuracy of a 24-hours ahead prediction for the electricity prices [80] and the PV energy output [81].

For comparison, a deterministic energy management optimization based on the mean values of the PIs has been performed as well.

To 'encourage' the energy exchanges among the microgrid agents, we deliberately decrease c_t^s to 0.06 €/kWh, thereby making profitable to the WPP and the TS selling energy to the D. In addition, for the numerical application we consider that D proposes to the microgrid energy producers a price $c_t^D = 0.7 \cdot c_t^p$. The coefficients β and γ, which are introduced in eqs. (19) and (42) to increase the regularity of energy exchanges between the microgrid agents through the increase of the minimum amount of exchanged energy, are assumed equal to 0.05. The peak energy consumption of the D was assumed to be 300 kWh. The maximum capacity of the D and TS batteries were assumed to be 360 kWh (with $R^{TS,stor} = 15kWh$) and 120 kWh (with $R^{D,stor} = 45kWh$), respectively.

7.1. Optimization results

This section presents and compares the results of the RO based on PIs and the optimization based on expected values for a period of 24 hours.

For the sake of simplicity, the results are first reported for the case of perfect prediction, i.e., exact forecast of the uncertain parameters. Figure 7 *(a, b, c)* gives an example of the variation of the energy management decision variables for the TS, the D and the WPP, as a function of their input parameters. As it can be observed, the TS tends to charge the battery (i.e., R_t^{TS} increases) during the periods of lower prices and lower energy demand in order to discharge it during the periods of peak prices and higher consumption levels, in order to decrease its expenses (Figure 7 a). This is possible because the lower electricity prices c_t^p, especially during the night period, allow the TS to increase the amount of energy imported from the external grid S_t^{TS}, which is used to charge the battery. According to the formulation of the optimization problem, i.e., eq. (13), the available PV energy output P_t^{PV} is used to sell the energy to the D (V_t^{PV}) and the external grid

(L_t^{TS}). Note that the optimization problem could be reformulated to allow the TS to use the available energy output P_t^{PV} to charge the battery.

The D behaviour for the battery charging is similar to the TS, especially when the amount of energy imported from the external grid during the periods of lower energy prices contributes to charge the battery (Figure 7 b). Note that in the case of the D, the amounts of energy purchased from the TS (V_t^{PV}) and WPP (V_t^{WPP}) are also used to charge the battery.

The WPP sells the available wind energy output to the external grid (L_t^{WPP}) and the D (V_t^{WPP}). According to the numerical values of prices assumed for this example, the price c_t^D proposed by the D is lower than the price of energy purchase by the external grid c_t^s. In this view, the amount of energy committed to the D by the WPP is equal to the minimum amount fixed by eq. (42).

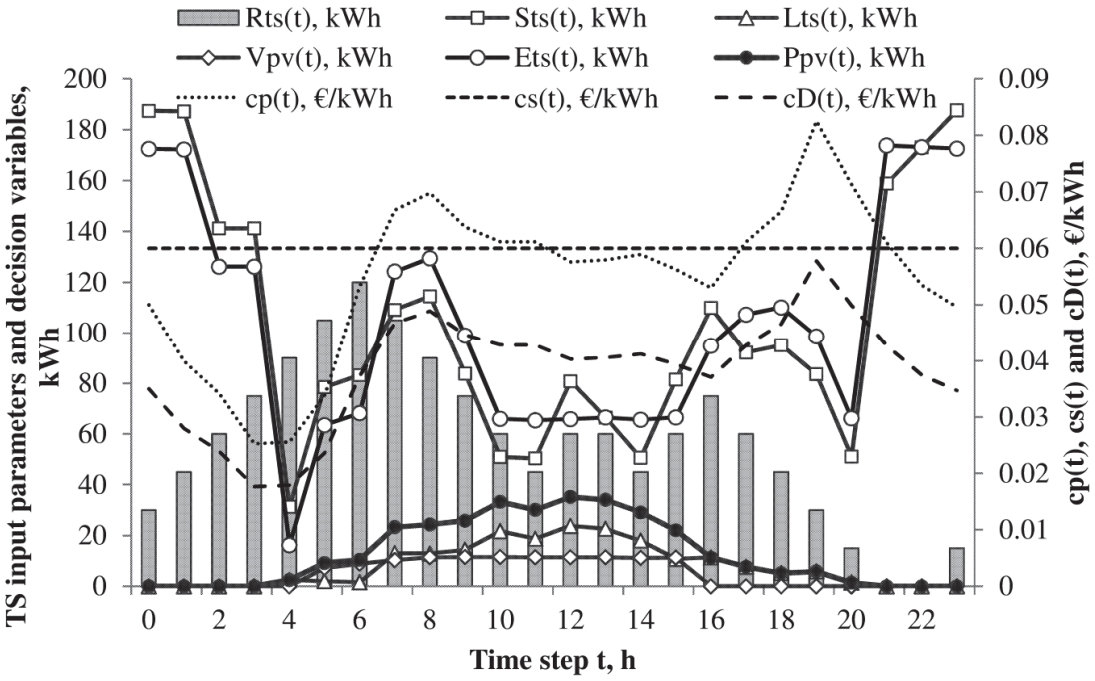

a)

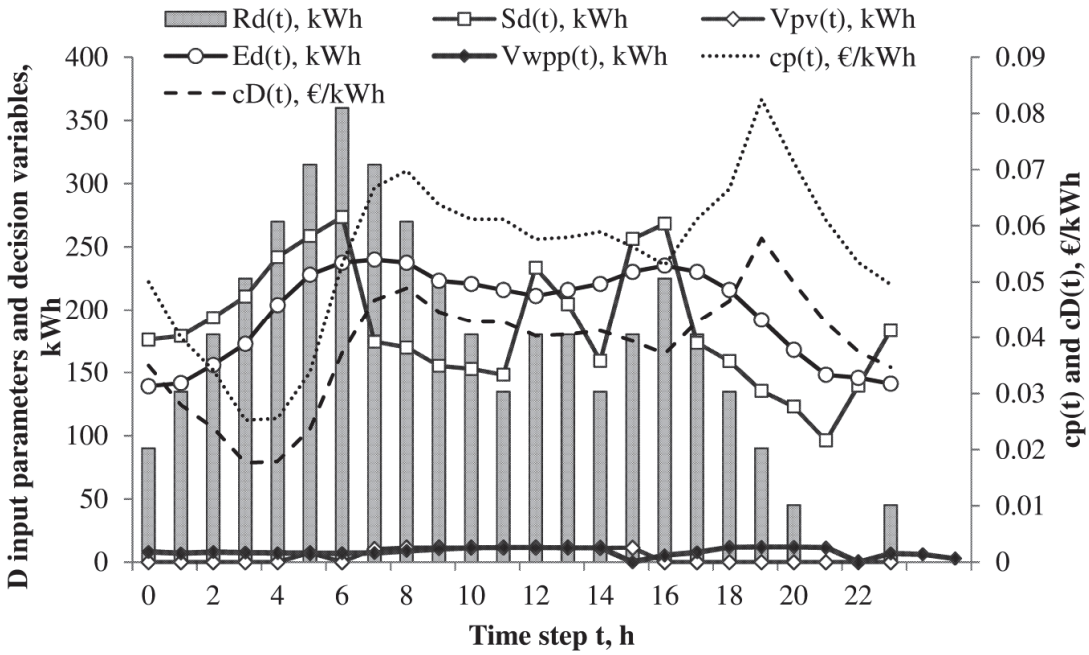

b)

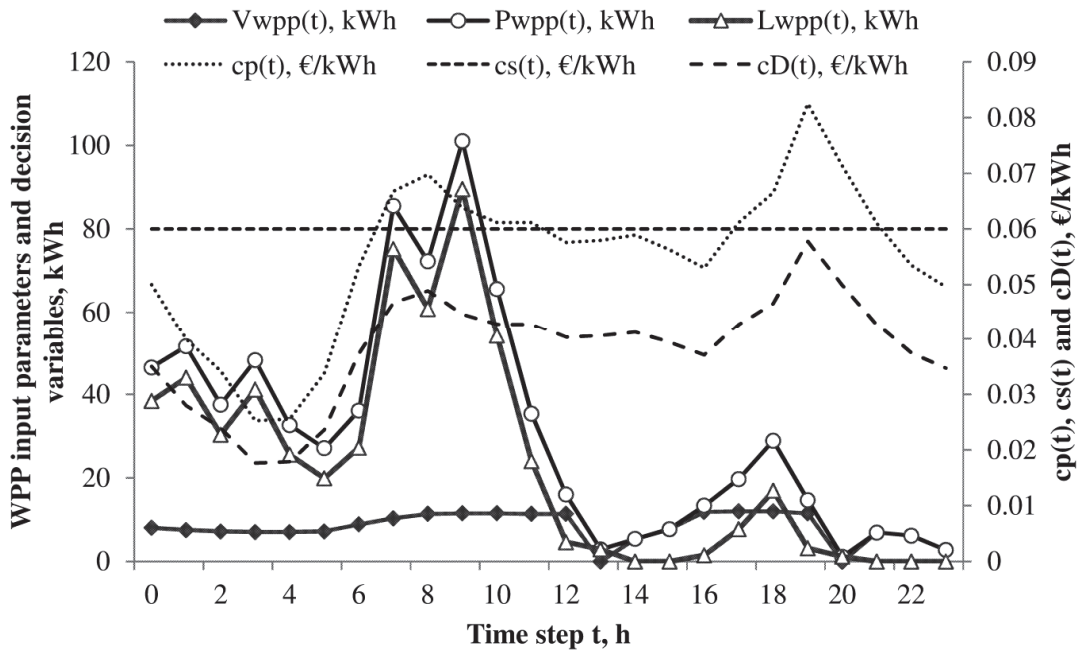

c)

Figure 7. Energy management for: a) TS, b) D, c) WPP.

For the sake of simplicity, to analyse the advantages of the RO based on PIs and to compare it with the optimization based on the expected values, we show and discuss the optimization results only for the TS with one uncertain parameter E_t^{TS}. Figure 8 gives, as an example, the PIs compared to the real energy demand of TS for the considered period of 24 hours.

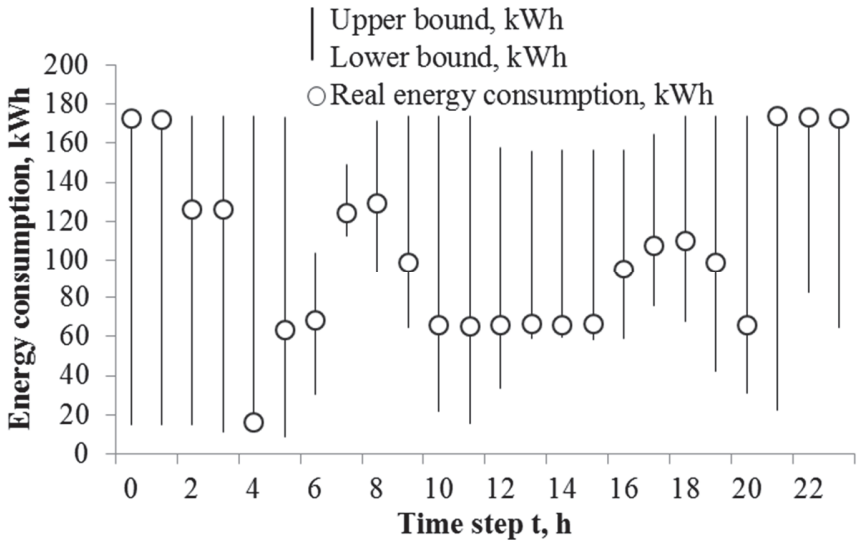

Figure 8. Predictions and real energy demand of TS.

Figure 9 provides the comparison between the decision variables, i.e., S_t^{TS} and L_t^{TS}, and the TS expenses at time step t (α_t^{WPP}), obtained with the RO (Figure 9 a, c, e) and the optimization based on the expected value (Figure 9 b, d, f), for the same $\tau = 24\ h$. For the reminder, in case of the optimization based on the expected values the level of uncertainty, e.g., Γ_t^{Power}, is equal to zero. The optimized values of the parameters are compared with the real values recalculated based on the real energy demand of the TS.

In case of RO, the amount of energy imported from the external grid S_t^{TS} is limited by the upper prediction bound, which determines the maximum energy demand E_t^{TS} (Figure 9 a). Therefore, the TS tends to buy more energy from the external grid to satisfy the energy balance eq. (10) of Subsection 5.1. In the deterministic case, the TS optimizes S_t^{TS} based on point predictions (interval means) of energy demand (Figure 9 b). Thus, the amount of S_t^{TS} is chosen to satisfy the energy balance of eq. (10) where $\Gamma_t^{Power} = 0$. The results show similar behaviours for the

decision variable L_t^{TS} (Figure 9 c, d) in both RO and deterministic cases. As it can be observed, the deterministic case does not allow accounting for the uncertainty in the energy demand E_t^{TS} and therefore the real TS expenses α_t^{TS} are higher than the optimized ones for some time steps (Figure 9 e, f).

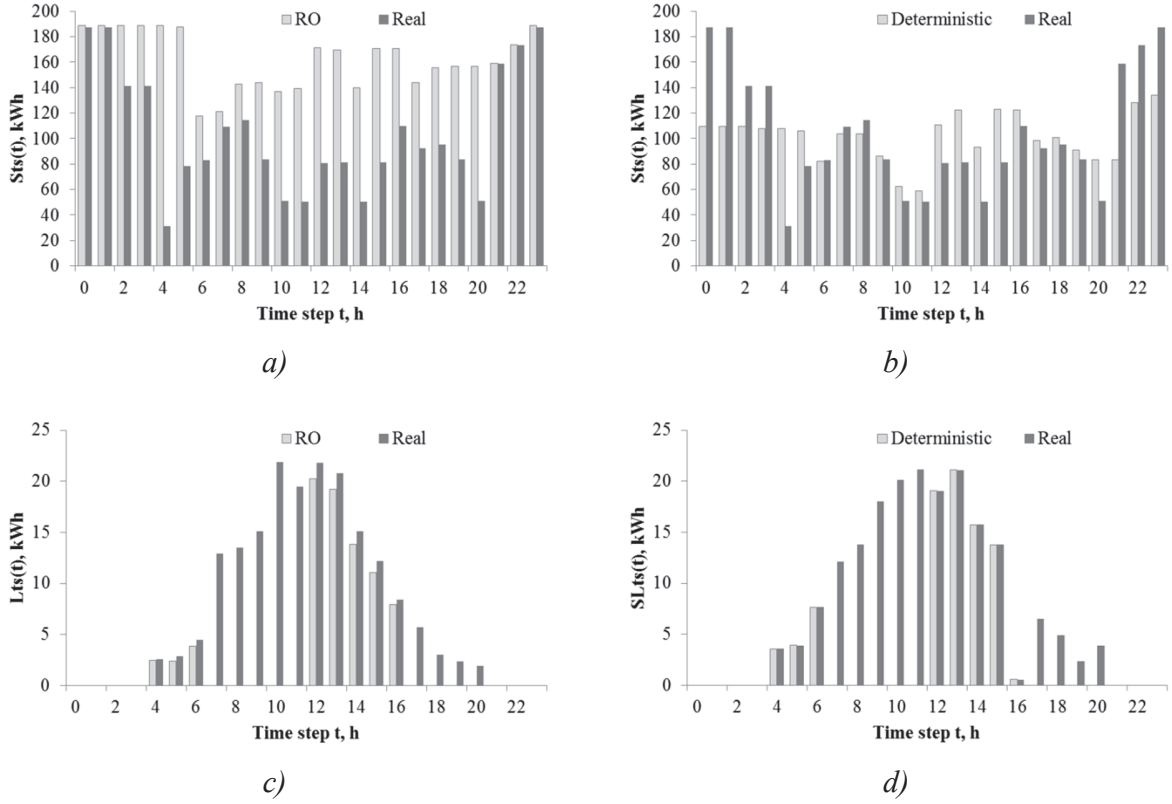

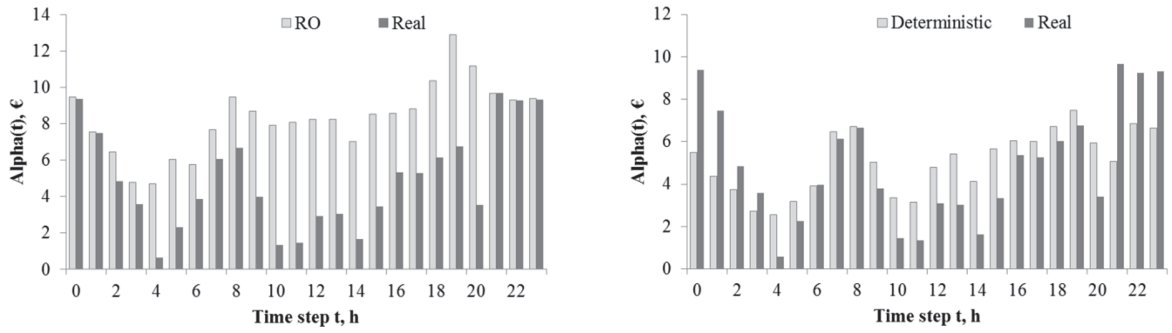

e) *f)*

Figure 9. Comparison of two optimization cases, i.e., RO based on PIs and optimization based on the expected values, and real results for: a-b) S_t^{TS}, c-d) L_t^{TS}, e-f) α_t^{TS}.

Note that we observe equivalent trends for the energy scheduling of the other agents as the RO bounds the worst case scenarios for the optimization (i.e., high energy demands, low energy outputs from renewables etc.). Robustly accounting for uncertainty during the optimization generates safety margins for the optimized expenses and revenues, which are respectively overestimated and underestimated in comparison with real expenses and revenues.

7.2. Influence of the energy imbalance on the microgrid

This section provides an analysis, based on different optimization approaches, of the energy imbalances within the microgrid that are generated by the failures of the wind power generator or by interruptions due to unavailability of wind. For this purpose, Table 2 reports the simulation results for (i) optimization based on expected values of P_t^{WPP} without accounting for technical failures, (ii) optimization based on expected values of P_t^{WPP} with presence of technical failures and (iii - vi) RO based on PIs with different CP with presence of technical failures. The output indicators are calculated as the average over Ns simulations, sufficient to determine the converged values of these indicators. The main indicators used to compare the performance of different approaches are the reliability indicators, i.e., LOLE and LOEE, the part of imbalance of committed energy and the performance ratio. This comparison is done to analyse the major trends in variation of the performance and reliability indicators and make the selection of the most promising optimization approaches.

Table 2. Influence of the energy imbalance in the microgrid.

#	(i)	(ii)	(iii)	(iv)	(v)	(vi)
CP of Pis, %	-	-	56.3	73.5	89.4	96
LOLE, h/τ	0.2452	0.2568	0.0048	0.0028	0.0012	0.002
LOEE, kWh/τ	1.2024	1.3834	0.0485	0.0275	0.0113	0.0202
Committed energy $V_t^{WPP,c}$, kWh	12219.67	12219.67	5076.17	3856.83	3319.81	2615.75
Shortage, kWh	2210.07	2290.76	116.94	77.24	37.85	37.08
Total revenue from the microgrid, €	391.14	387.79	194.67	148.30	128.33	101.12
Part of imbalance of committed energy, %	18.09	18.75	2.30	2.00	1.14	1.42
Performance ratio, %	82.99	82.28	97.53	97.87	98.91	98.58

(i – ii) Optimization based on expected values of P_t^{WPP}

- The reliability indicators LOLE and LOEE are lower in the case (i) without technical failures than in the case (ii) with technical failures. However, we can notice that the effect of technical failures is less important than the effect of the prediction errors of P_t^{WPP} variability.
- The amount of committed energy $V_t^{WPP,c}$ is the same for both cases (i) and (ii). Indeed, the committed energy is identified based on the same expected values of P_t^{WPP}.
- Similar to the reliability indicators, the shortage and the imbalances are lower in the case (i) without technical failures than in the case (ii) with technical failures.
- The revenues and performance ratio are higher in the case (i) without technical failures than in the case (ii) with technical failures.

(iii – vi) RO based on PIs

Note that using PIs characterized by large values of CP leads to the following effects:

- The indicators LOLE and LOEE decrease with a consequent increase in the system reliability.
- The amount of committed energy $V_t^{WPP,c}$ decreases due to the underestimation of the possible values of P_t^{WPP}.

- The shortage of energy decreases. For the cases (v) and (vi) the values of shortage are comparable. Indeed, even if most of the time the effect of failures is mitigated by the lower prediction bounds of PIs, their effect can be still sensible, especially when failures occur during the periods of high expected P_t^{WPP}. In this case, the PIs with high CP provide comparable results.
- Revenues of the WPP from the microgrid decrease. This indicates that even if the effect of prediction errors and failures is mitigated most of the time, the PIs underestimating the values of P_t^{WPP} results in a significant decrease of the amount of $V_t^{WPP,c}$ and, consequently, the revenues.
- Parts of the imbalances follow the behaviour of the shortage with a progressive decrease of its value, except for the case (vi). Indeed, the decrease of committed energy $V_t^{WPP,c}$ with the shortage, comparable to case (v), increases the part of imbalances for case (vi).
- The performance ratio increases, except for case (vi). This is due to the decrease of the revenues with the imbalance, comparable to case (v), which decreases the performance ratio for case (vi).

Based on these observations several conclusions can be highlighted:

- The optimization based on the PIs gives more reliable results in terms of decrease of LOLE and LOEE indicators, but at the expense of a decrease in the revenues from selling $V_t^{WPP,c}$. Revenues are higher for the case of optimization based on expected values of P_t^{WPP}, even in presence of a penalty for the non-supplied energy.
- Optimization based on large PIs, for example case (vi), penalizes the part of imbalance and performance ratio indicators. Indeed, the amount of committed energy $V_t^{WPP,c}$ decreases, in correspondence of almost the same amount of shortage.

Based on the analysis results, three representative cases from Table 2 were selected for a further detailed comparison with other optimization approaches, i.e., case (ii) of optimization based on expected values, case (iii) of RO based on PIs with CP = 56.3% and case (vi) of RO based on PIs with CP = 96% (i.e., two “extreme” cases, with low and high CP). Note that even if the case (ii) decreases the microgrid reliability, it provides promising results in terms of performance ratio. In this view, the optimization based on the expected values was also included for comparison with

the optimization approaches of [74], presented in Subsection 7.3. Note that the comparison, summarized in in Table 4, is done in terms of part of imbalance and performance ratio. The reliability indicators LOLE and LOEE have been not accounted in [74] and introduced in our paper as the additional indicators.

7.3. Influence of the positive and negative imbalance

The aim of this section is to compare the results of the part of imbalance and performance ratio obtained by the different prediction/optimization approaches, and reported in Table 2, with those in [74]. In this latter work, the authors considered the participation of a wind power producer in the Dutch electricity pool over the year 2002. The wind power data predictions (48 hours ahead point predictions) were obtained with a persistence prediction method in which the last measured value is applied for the look-ahead period, and a fuzzy-neural networks (Fuzzy-NN)-based approach is adopted to perform the prediction. In addition, the authors explored the methods of annual or quarterly trends estimation for regulation unit costs. The considered pool included a day-ahead market with a program time unit of 1 h, i.e., the period for energy quantity-price bids. The entrance or participant fees were not accounted for. The average spot and regulation prices on a monthly basis were accounted for following the market outcomes from 2002. It is important to note that possible positive and negative imbalances were accounted for.

For comparing the performance indicators, we must account not only for the negative imbalance between the WPP and the microgrid, but also for the imbalance between the WPP and the external grid (mainly positive). To do so, we consider imbalance prices that are equal to the average yearly imbalance prices of [74]: 36% of the average yearly spot price for the positive imbalance and 13% of the average yearly spot price for the negative imbalance. Equations (48) - (50) was extended to integrate the cost generated by the imbalance between the WPP and the external grid. For comparison, three representative cases from Table 2 were selected, i.e., case (ii) of optimization based on expected values, case (iii) of RO based on PIs with CP = 56.3% and case (vi) of RO based on PIs with CP = 96% (i.e., two “extreme” cases, with low and high CP).

Table 3 presents the results of committed energy, surplus, shortage and total revenues for the selected cases, accounting for their positive and negative imbalances.

Table 3. Influence of the positive and negative energy imbalances.

	Optimization based on expected values	RO based on PIs with CP = 56.3%	RO based on PIs with CP = 96%
Committed energy, kWh	41345.03	24766.33	7690.51
Surplus, kWh	2206.92	9611.80	25892.33
Shortage, kWh	12255.19	1382.44	98.24
Total revenues, €	2223.48	1596.86	974.82

It is observed that the ROs based on PIs decrease drastically the amount of committed energy. More precisely, due to the significant underestimation of the expected P_t^{WPP}, the surplus of the sold energy for the case with CP = 96% is almost 3.4 times higher than the amount of committed energy, whereas the surplus for the case with CP = 56.3% is reasonable compared to the amount of committed energy. As it is expected, the observed energy shortage for the RO based on large PIs (CP = 96%) is smaller than for the RO based on PIs with CP = 56.3%. As a consequence, the total revenues for the case with CP = 56.3% are almost twice higher than the revenues obtained with the RO based on PIs with CP = 96%.

The optimization based on expected values makes it possible to commit large amounts of energy. In comparison with the cases of RO, the amount of surplus is smaller, but the energy shortage is more significant. Nevertheless, the total revenues are higher for the case of the optimization based on expected values.

To highlight the advantages of the optimization approach presented in this paper the comparison is done with the approaches from [74]: Persistence, Fuzzy – NN and Probabilistic Choice (PC) models. The Persistence prediction method consists in using the last measured power value (in [74] at 10:00) as a prediction for all look-ahead times. The use of Persistence and perfect forecasts can be seen as the most pessimistic and optimistic cases for trading wind power, respectively. Fuzzy-NN gives the possibility to generate the interval forecasts for several nominal coverage rates by using triangular fuzzy sets for modelling the different uncertainty regimes as a function of the level of predicted power [74], [82]. Fuzzy NN prediction model is regarded to provide a good alternative to statistical and other artificial intelligent prediction models since it is easy to construct, understand and calibrate. It also gives an ability to explain the relationship between response and input variables and, in some cases, handles ambiguity in the relations between variables. However, this prediction model is highly sensible to outliers, to the number of fuzzy rules and to the expert subjective opinion. Similar to Fuzzy NN,

Probabilistic Choice (PC) models can be easy constructed and calibrated [83]. In this view, the calibrations of PC with loss functions for different time periods, accounted in [74], gives the possibility to improve the optimization results in terms of the performance ratio. However, as in the case of Fuzzy NN this can reinforce the model sensitivity to outliers.

These approaches have been selected for comparison, because they have been widely explored in the field of energy management in recent publications, e.g., NN based forecast of the environmental conditions ensemble with Fuzzy Logic based optimization of battery scheduling in the microgrid [82], Fuzzy NN for prediction of solar irradiation and long-term ahead PV power output correction [84] and probabilistic models for predictive monitoring and energy management [11], [85]. The persistence technique is usually considered as a simple technique used as a reference to evaluate advanced approaches, which must be able to "outperform naïve techniques resulting from simple considerations without special modelling efforts" [86]. In this view, different papers are using the persistence approach to highlight the efficiency of the developed approaches, e.g., model for predictive control and weather forecast for the efficient building climate control [87] and prediction approach of global solar irradiance [88].

In comparison with these approaches the optimization framework presented in this paper provides good performance regarding both the prediction and optimization modules. Indeed, a NSGA – II trained NN allows to generate, by using statistical data, a high range of PIs classified in the Pareto front by their width and coverage probability. This gives the decision-makers a large variety of PIs, which can be selected to feed the RO. The choice of the appropriate PIs can be done depending on the reliability constraints: when to increase system reliability the PIs with large width will be selected, when to decrease energy imbalances the PIs with small width are more suitable.

Table 4 provides the comparison of results obtained with optimization based on PIs and the results from prediction and optimization approaches from [74].

Table 4. Comparison with results from other approaches.

#	From our case study			From [74]			
	Expected values	PIs with CP=56.3%	PIs with CP = 96%	Persistence	Fuzzy-NN	PC1	PC2
Part of imbalance, %	34.98	44.39	337.96	73.69	40.55	45.72	55.46
Performance ratio, %	74.80	86.03	-37.24	79.1	86.99	89.14	92.1

PC1 – Method of trends estimation with Probabilistic Choice based on single loss function for the whole year [74].
PC2 – Method of trends estimations with Probabilistic Choice based on four different loss functions for the four quarters of year [74].

For the optimization based on PIs with CP = 96%, the part of imbalance is almost three times higher than the committed energy. The performance ratio for this case study, i.e., -36.63%, indicates that the total revenues are highly affected by the imbalances (large positive).

For the optimization based on PIs with CP = 56.3% the part of imbalance and performance ratio are comparable with the results obtained with different approaches in [74].

An important observation is that the performance indicators for the case of optimization based on expected values are comparable with the case of RO based on PIs with CP = 56.3%.

The drawbacks of the developed optimization framework can be the following. Similar to all data driven prediction model, a NSGA – II trained NN is sensible to the high data variability between training and unseen testing patterns, which can decrease the prediction accuracy. This problem can be avoided by using pattern recognition techniques or online learning. Another limitation lies in the way of accounting uncertainty by the RO, which is done at the cost of possible lower revenues for the energy generators and higher expenses for the energy consumers than those that could be obtained by optimizing over the expected values of the uncertain parameters. Future work will consist of investigating the influence of uncertain events on the microgrid performance and identifying the conditions under which the application of RO or optimization based on expected values is most advantageous.

Based on the results comparison, provided in Subsections 7.2 and 7.3, it is shown that the proposed framework of RO based on PIs leads to a high system reliability, but at the expense of conservative results regarding the system revenues or expenses. In fact, the proposed framework allows the decision maker anticipating the worst possible realization of the uncertain parameters and to choose the best solution with respect to such a case. By so doing, the producer can plan its

energy scheduling strategy by committing less energy for sale while the consumer can purchase more energy than it is likely to require. Indeed, among PIs selected for comparison, those with smaller width characterized by CP=56.3% provide the best solution regarding the part of imbalance and performance ratio. However, the values of these indicators remain close to the ones obtained with an optimization based on expected values. Therefore, the fair question "what are the operational and environmental conditions for whose the results obtained from the RO based on PIs are suitable?" can be risen.

To address this question a further analysis, aiming at evaluating the system performance for different levels of uncertainty affecting both operational and environmental conditions, has been started. These uncertainties can be broadly classified into two types: (i) uncertainty related to fluctuations of the operational and environmental conditions within expected and acceptable limits, which are typical conditions within a microgrid operation, and (ii) uncertainty related to extreme events. In the first case, the fluctuations of the operational and environmental conditions can be managed by optimization based on expected parameters values without particular performance degradation, as it can be observed in Subsections 7.2 and 7.3. In the second case, RO is expected to lead to management actions that guarantee the operation within safety margins.

8. CONCLUSIONS

We have extended a framework for microgrid energy management based on agent-based modelling, by introducing robust optimization (RO). The extension of the framework involves multiple agents and includes communication among the agents and handles uncertainties, e.g., in wind power output and components failures. For exemplification purposes, we have considered a microgrid connected to the external grid via a transformer, and which includes a middle-size train station with an integrated photovoltaic power production system, a small energy production plant composed of urban wind turbines and its surrounding district that includes residences and small businesses. Each of these components is modelled as an individual intelligent agent, which makes decisions guided by specific goals formulated in terms of cost or revenue functions. RO of these individual objectives has been performed under stochastic operational and environmental parameters. The prediction of the uncertainty associated to wind energy output and energy

demands of the train station and the district has been quantitatively accounted for by a Non-dominated Sorting Genetic Algorithm (NSGA-II) trained Neural Network (NN) which provides prediction intervals (PIs). The proposed optimization framework allows evaluating the impact of different levels of uncertainty quantification on the prediction accuracy of the cost and revenue functions, and overall microgrid reliability. The imbalance cost was introduced to quantify the effect of prediction errors and failure occurrences of the wind generator.

The reliability analysis performed for energy scheduling under different levels of wind power output uncertainty shows the strong improvement of the reliability indicators and decrease of energy shortage and surplus for the case of RO based on the PIs. However, the overall effect of the improved reliability is a decrease in the revenues of the energy producer by decreasing the amount of the committed energy. In this view, the optimization based on expected values of the wind energy output provides better results in terms of the part of imbalance and performance ratio indicators. Finally, the results obtained with the RO based on PIs are comparable with those from other prediction and optimization approaches.

In summary, the original contributions of the work are:

- the extension of the original agent-based model of the microgrid for integrating multiple energy generators and consumers with conflicting energy management objectives and limited access to information;
- the use of RO based on data-driven estimated PIs for the quantification of the uncertain parameters.

A strong point of the proposed framework is its flexibility to accommodate more complex models of the individual agents, e.g., to account for variations of charging and discharging efficiencies and energy losses due to battery degradations, or the refinement of the time step to account for short-term variations.

ACKNOWLEDGMENTS

The authors acknowledge the support of the Chair on Systems Science and the Energetic Challenge, European Foundation for New Energy - Electricité de France (EDF) at Ecole Centrale Paris and Supelec and Econoving International Chair of University of Versailles Saint-Quentin-

en-Yvelines. They also wish to thank for the collaboration the "Programme Gare" project, of the National Society of French Railways (SNCF) and Econoving International Chair of University of Versailles Saint-Quentin-en-Yvelines, and supported by the French National Research Agency (ANR).

The authors also wish to thank the anonymous referees for their scrupulous review work and the comments provided to us, which have helped improving the paper significantly.

APPENDIX

This section describes the models and assumptions made for the operational and environmental conditions of the microgrid.

A.1. Passenger flow

The passenger flow F_t^{pas} *(number/h)* through TS at time *t* is the most important factor influencing the energy consumption of the lifting equipment, i.e., elevators and escalators. The passengers' flow is provided by the TS operator, who takes in-situ real time records of the passengers flow during the opening periods of the TS , i.e., from 5 a.m. to 1 a.m. of the next day, with a time step of one hour. The typical passengers flow in the TS during week day and week day and week end is presented in Figure A.1. The two characteristic peaks during the working days related to the periods of high affluence of passengers going to work and coming back home can be noticed. The passengers' flow during the week-end days is almost constant throughout the day, at a level which is around 15% of that of peak during working days.

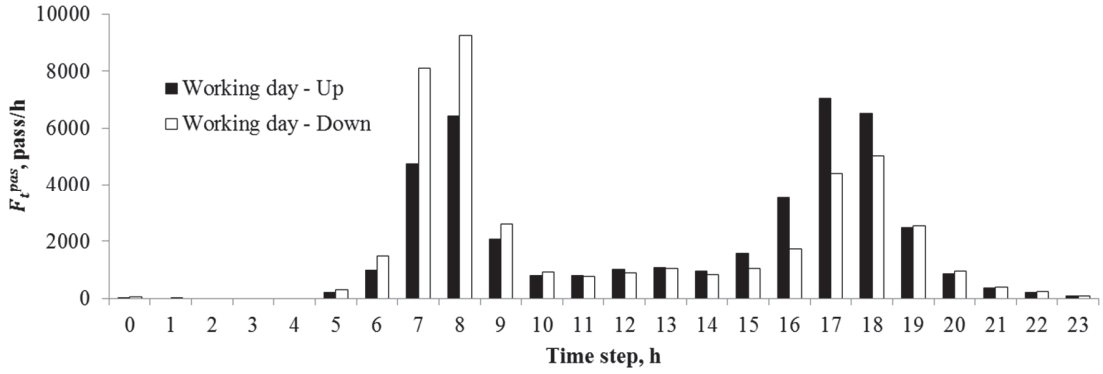

a)

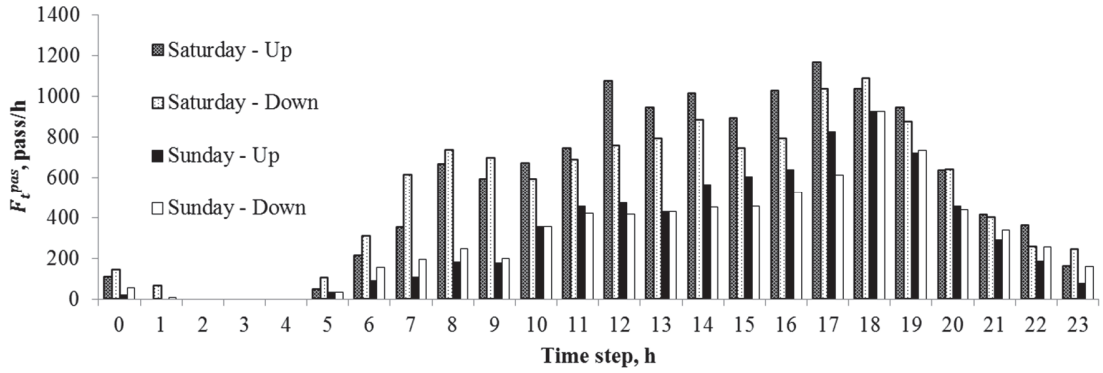

b)

Figure. A.1. Up and down passenger flow through the TS: a) working days; b) Saturday and Sunday.

A.2. Solar irradiation

The solar irradiation s_t *(W/m²)* at time *t* affects the amount of energy required by the consumers, e.g., the inside and outside lighting of the TS, and also the energy output of PV panels. Different approaches have been proposed to model the behaviour of solar irradiation, e.g., probability density functions (PDFs), times series [89] and artificial neural networks [90].

In the present work, we use the beta distribution to model solar irradiation. The beta distribution for describing solar irradiation for PV energy generation has been used in several scientific

papers [60], [89], [91] and shown to be a sufficiently flexible two-parameter distribution that can fit well empirical data under different conditions.

Also, in general note that some assumptions (simplifications) in the modelling of the individual components have been guided by the interest of keeping the models, but physically meaningful, in order to concentrate on the development of the optimization framework and is verification.

In the application of this paper, the average hourly solar irradiation data from [59] has been used to estimate the beta parameters.

A.3. Wind speed

The wind speed v_t *(m/s)* at time *t* influences the energy output from the WPP. There are numerous approaches for modelling the wind energy source [92]. Among the most used are: the ARMA (auto regressive moving average) models [61], special correlation models [93] and NNs [34], [94], [95].

In the application of this paper, to model the WPP we proceed as follows. The hourly wind speed data is obtained from [61], representative of an urban area equipped with a wind generator with a capacity factor of about 13%, i.e., the ratio between the actual wind energy output and the potential wind energy output if the wind turbine operates constantly at its nominal capacity. The wind speed data is transformed into wind energy output data using the cubic correlation of [62]. To account for the uncertainties, PIs for the wind energy output are estimated (Subsection 1.1) by a NN trained by a GA [34].

A.4. Electricity prices

The electricity prices are key operational variables for the expenses and revenues of the microgrid agents. In this work, the market electricity price c_t^p (€/kWh) is assumed variable in a way similar to the trend of the wholesale market price in France [96] lead to hourly electricity market prices higher during working days than during weekends, which is situation is typical for most electricity systems. However, in countries with strong electricity markets, which include producers, consumers and transmission companies, the correlation between electricity consumption and price decreases significantly (e.g., only 0.58 for UK). Moreover, the electricity

price of the individual regional market can be highly affected by other factors, e.g., fuel availability and transmission constraints. In this view, the existing speculations in the fuel markets can artificially increase the electricity price during the periods of low electricity demand (the case of some regions in UK). That is why, it is important to highlight this assumption in our paper.

We assume that the grid offers fixed electricity price c_t^s *(€/kWh)* to purchase the energy from the agents. The electricity price c_t^D *(€/kWh)* is the price offered by the D to purchase the energy from the microgrid energy producers. A random noise is introduced to simulate the uncertainty in electricity prices.

REFERENCES

[1] J. C. Glenn, T. J. Gordon, and E. Florescu, "2009 State of the Future," 2009.

[2] B. J. Owen, "The planet 's future : Climate change ' will cause civilisation to collapse '," *The Independent*, London, 2009.

[3] M. Jung and P. Yeung, "Connecting smart grid and climate change," 2009.

[4] R. Hledik, "How Green Is the Smart Grid?," *Electr. J.*, vol. 22, no. 3, pp. 29–41, Apr. 2009.

[5] N. D. Hatziargyriou, *European Transactions on Electrical Power. Special Issue: Microgrids and Energy Management*, no. December 2010. 2011.

[6] F. Katiraei and M. R. Iravani, "Power Management Strategies for a Microgrid With Multiple Distributed Generation Units," *Power Systems, IEEE Transactions on*, vol. 21, no. 4. pp. 1821–1831, 2006.

[7] J. M. Carrasco, L. G. Franquelo, J. T. Bialasiewicz, E. Galvan, R. C. P. Guisado, M. A. M. Prats, J. I. Leon, and N. Moreno-Alfonso, "Power-Electronic Systems for the Grid Integration of Renewable Energy Sources: A Survey," *Industrial Electronics, IEEE Transactions on*, vol. 53, no. 4. pp. 1002–1016, 2006.

[8] M. Manfren, P. Caputo, and G. Costa, "Paradigm shift in urban energy systems through distributed generation: Methods and models," *Appl. Energy*, vol. 88, no. 4, pp. 1032–1048, Apr. 2011.

[9] C. Chen, S. Duan, T. Cai, B. Liu, and G. Hu, "Smart energy management system for optimal microgrid economic operation," *Renewable Power Generation, IET*, vol. 5, no. 3. pp. 258–267, 2011.

[10] T. Niknam, R. Azizipanah-Abarghooee, and M. R. Narimani, "An efficient scenario-based stochastic programming framework for multi-objective optimal micro-grid operation," *Appl. Energy*, pp. 455 – 470, Jul. 2012.

[11] T. Niknam, F. Golestaneh, and A. Malekpour, "Probabilistic energy and operation management of a microgrid containing wind/photovoltaic/fuel cell generation and energy storage devices based on point estimate method and self-adaptive gravitational search algorithm," *Energy*, vol. 43, no. 1, pp. 427–437, Jul. 2012.

[12] A. G. De Muro, J. Jimeno, and J. Anduaga, "Architecture of a microgrid energy management system," *Eur. Trans. Electr. Power*, vol. 21, pp. 1142–1158, 2011.

[13] E. Kuznetsova, K. Culver, and E. Zio, "Complexity and vulnerability of Smartgrid systems," in *European Safety and Reliability Conference (ESREL 2011)*, 2011, pp. 1–8.

[14] M. H. Colson, C. M. Nehrir, and R. W. Gunderson, "Multi-agent Microgrid Power Management," in *18th IFAC World Congress*, 2011, pp. 3678–3683.

[15] P. P. Reddy and M. M. Veloso, "Strategy Learning for Autonomous Agents in Smart Grid Markets," in *Twenty-Second International Joint Conference on Artificial Intelligence*, 2005, pp. 1446–1451.

[16] T. Krause, E. Beck, R. Cherkaoui, A. Germond, G. Andersson, and D. Ernst, "A comparison of Nash equilibria analysis and agent-based modelling for power markets," *Int. J. Electr. Power Energy Syst.*, vol. 28, no. 9, pp. 599–607, Nov. 2006.

[17] A. Weidlich and D. Veit, "A critical survey of agent-based wholesale electricity market models," *Energy Econ.*, vol. 30, no. 4, pp. 1728–1759, Jul. 2008.

[18] S. Yousefi, M. P. Moghaddam, and V. J. Majd, "Optimal real time pricing in an agent-based retail market using a comprehensive demand response model," *Energy*, vol. 36, no. 9, pp. 5716–5727, Sep. 2011.
[19] Z. Jun, L. Junfeng, W. Jie, and H. W. Ngan, "A multi-agent solution to energy management in hybrid renewable energy generation system," *Renew. Energy*, vol. 36, no. 5, pp. 1352–1363, May 2011.
[20] E. Kuznetsova, C. Ruiz, Y. F. Li, E. Zio, G. Ault, and K. Bell, "Reinforcement learning for microgrid energy management," *Energy*, vol. 59, pp. 133–146, 2013.
[21] Y. Zeng, Y. Cai, G. Huang, and J. Dai, "A Review on Optimization Modeling of Energy Systems Planning and GHG Emission Mitigation under Uncertainty," *Energies*, vol. 4, no. 12, pp. 1624–1656, Oct. 2011.
[22] J. Lagorse, M. G. Simoes, and A. Miraoui, "A Multiagent Fuzzy-Logic-Based Energy Management of Hybrid Systems," *Ind. Appl. IEEE Trans.*, vol. 45, no. 6, pp. 2123–2129, 2009.
[23] J. Solano Martínez, R. I. John, D. Hissel, and M.-C. Péra, "A survey-based type-2 fuzzy logic system for energy management in hybrid electrical vehicles," *Inf. Sci. (Ny).*, vol. 190, pp. 192–207, May 2012.
[24] A. Ben-Tal and A. Nemirovski, "Robust solutions of uncertain linear programs," *Oper. Res. Lett.*, vol. 25, no. 1, pp. 1–13, Aug. 1999.
[25] D. Bertsimas and M. Sim, "The Price of Robustness," *Oper. Res.*, vol. 52, no. 1, pp. 35–53, 2004.
[26] V. Krey, D. Martinsen, and H.-J. Wagner, "Effects of stochastic energy prices on long-term energy-economic scenarios," *Energy*, vol. 32, no. 12, pp. 2340–2349, Dec. 2007.
[27] Y. P. Cai, G. H. Huang, Z. F. Yang, Q. G. Lin, and Q. Tan, "Community-scale renewable energy systems planning under uncertainty—An interval chance-constrained programming approach," *Renew. Sustain. Energy Rev.*, vol. 13, no. 4, pp. 721–735, May 2009.
[28] M. Liu, "An Interval-parameter Fuzzy Robust Nonlinear Programming Model for Water Quality Management," *J. Water Resour. Prot.*, vol. 05, no. 01, pp. 12–16, 2013.
[29] Y. Li and G. Huang, "Robust interval quadratic programming and its application to waste management under uncertainty," *Environ. Syst. Res.*, vol. 1, no. 1, p. 7, 2012.
[30] A. Parisio, C. Del Vecchio, and A. Vaccaro, "Electrical Power and Energy Systems A robust optimization approach to energy hub management," *Int. J. Electr. Power Energy Syst.*, vol. 42, no. 1, pp. 98–104, 2012.
[31] C. Chen, Y. P. Li, G. H. Huang, and Y. F. Li, "A robust optimization method for planning regional-scale electric power systems and managing carbon dioxide," *Electr. Power Energy Syst.*, vol. 40, pp. 70–84, 2012.
[32] C. Chen, Y. P. Li, G. H. Huang, and Y. Zhu, "An inexact robust nonlinear optimization method for energy systems planning under uncertainty," *Renew. Energy*, vol. 47, pp. 55–66, 2012.
[33] C. Dong, G. H. Huang, Y. P. Cai, and Y. Liu, "Robust planning of energy management systems with environmental and constraint-conservative considerations under multiple uncertainties," *Energy Convers. Manag.*, vol. 65, pp. 471–486, 2013.
[34] R. Ak, Y. F. Li, V. Vitelli, and E. Zio, "Multi-objective Generic Algorithm Optimization of a Neural Network for Estimating Wind Speed Prediction Intervals," *Submitt. to Appl. Soft Comput.*, 2013.

[35] A. Khosravi, S. Nahavandi, D. Creighton, and F. A. Amir, "A Comprehensive Review of Neural Network-based Prediction Intervals and New Advances," *IEEE Trans. Neural Net.*, vol. 22, no. 9, pp. 1341–1356, 2011.
[36] Econoving, "Programme Gare," *Econoving*, 2011. [Online]. Available: http://www.econoving.uvsq.fr/econoving/langue-fr/recherche/projets/programme-gare/programme-gare-236018.kjsp. [Accessed: 13-Feb-2013].
[37] K. Culver, R. Guilloteau, and C. Hue, "Hard Nodes in Soft Surroundings: A 'dream of islands' strategy for urban sustainability," *Development*, vol. 54, pp. 336–342, 2011.
[38] European Commission, "Photovoltaic Solar Energy Best Practice Stroies," 2002.
[39] E. Fischer and C. Lo, "Back to the future : Top trends in railway station design," *railway-technology.com*, 2011. [Online]. Available: http://www.railway-technology.com/features/featureback-to-the-future-top-trends-in-railway-station-design. [Accessed: 24-Sep-2013].
[40] RTE, "Bilan électrique 2012," 2012.
[41] A. L. Saint Girons, "Des incertitudes juridiques croissantes dans le secteur du photovoltaïque: vers un blocage de la filière?," *Actu-Environnement*, 2010. [Online]. Available: http://www.actu-environnement.com/ae/news/anne-laure-saint-girons-incertitudes-juridiques-photovoltaique-11077.php4. [Accessed: 24-Sep-2013].
[42] C. Traub, "Autolib': Rent an Electric Car in Paris," *About.com Guide*, 2013. [Online]. Available: http://goparis.about.com/od/transportation/a/Autolib-electric-cars-Paris.htm. [Accessed: 04-Oct-2013].
[43] T. Niknam, R. Azizipanah-Abarghooee, and M. R. Narimani, "An efficient scenario-based stochastic programming framework for multi-objective optimal micro-grid operation," *Appl. Energy*, vol. 99, pp. 455–470, Nov. 2012.
[44] H.-M. Kim, Y. Lim, and T. Kinoshita, "An Intelligent Multiagent System for Autonomous Microgrid Operation," *Energies*, vol. 5, no. 12, pp. 3347–3362, Sep. 2012.
[45] A. D. Hawkes and M. A. Leach, "Modelling high level system design and unit commitment for a microgrid," *Appl. Energy*, vol. 86, no. 7–8, pp. 1253–1265, Jul. 2009.
[46] H. Ren and W. Gao, "A MILP model for integrated plan and evaluation of distributed energy systems," *Appl. Energy*, vol. 87, no. 3, pp. 1001–1014, 2010.
[47] D. Liu, J. Guo, Y. Huang, and W. Wang, "An active power control strategy for wind farm based on predictions of wind turbine's maximum generation capacity," *J. Renew. Sustain. Energy*, vol. 5, no. 1, p. 013121, 2013.
[48] R. S. Chandra, Y. Liu, S. Bose, and J. M. Bedout, "Hybrid Robust Predictive Optimization Method of Power System Dispatch," 2011.
[49] M. M. Mahmoud and I. H. Imad, "Field experience on solar electric power systems and their potential in Palestine," *Renew. Sustain. Energy Rev.*, vol. 7, pp. 531–543, 2003.
[50] F. A. Mohamed and H. N. Koivo, "Electrical Power and Energy Systems System modelling and online optimal management of MicroGrid using Mesh Adaptive Direct Search," *Int. J. Electr. Power Energy Syst.*, vol. 32, no. 5, pp. 398–407, 2010.
[51] F. A. Mohamed and H. N. Koivo, "Online management genetic algorithms of microgrid for residential application," *Energy Convers. Manag.*, 2012.
[52] C. Dong, G. H. Huang, Y. P. Cai, and Y. Liu, "Robust planning of energy management systems with environmental and constraint-conservative considerations under multiple uncertainties," *Energy Convers. Manag.*, vol. 65, pp. 471–486, Jan. 2013.

[53] Y. P. Cai, G. H. Huang, Z. F. Yang, and Q. Tan, "Identification of optimal strategies for energy management systems planning under multiple uncertainties," *Appl. Energy*, vol. 86, no. 4, pp. 480–495, Apr. 2009.
[54] Y. P. Li, G. H. Huang, and M. W. Li, "An integrated optimization modeling approach for planning emission trading and clean-energy development under uncertainty," *Renew. Energy*, vol. 62, pp. 31–46, Feb. 2014.
[55] L. Al-Sharif, "Modelling of escalator energy consumption," *Energy Build.*, vol. 43, no. 6, pp. 1382–1391, Jun. 2011.
[56] Ademe, "Eclairage public: routier, urban, grands espaces, illuminations et cadre de vie," 2002.
[57] Safety Time Inc., "Automatic Fare Collection System," 2010.
[58] B. Roux Dit Riche, "Les distributeurs automatiques devront réduire leur consommation d ' énergie," *Cleantech Republic*, 2011. [Online]. Available: http://www.cleantechrepublic.com/2009/06/09/les-distributeurs-automatiques-devront-reduire-leur-consommation-denergie/. [Accessed: 12-Apr-2011].
[59] F. A. Mohamed and H. N. Koivo, "System modelling and online optimal management of MicroGrid using mesh adaptive direct search," *Int. J. Electr. Power Energy Syst.*, vol. 32, no. 5, pp. 398–407, 2010.
[60] Y. M. Atwa, M. M. A. Salama, and R. Seethapathy, "Optimal renewable resources mix for distribution system energy loss minimization," *IEEE Trans. Power Syst.*, vol. 25, no. 1, pp. 360–370, 2010.
[61] D. C. Hill, D. Mcmillan, K. R. W. Bell, and D. Infield, "Application of auto-regressive models to UK wind speed data for power system impact studies," *IEEE Trans. Sustain. Energy*, vol. 3, no. 1, 2012.
[62] E. N. Dialynas and A. V. Machias, "Reliability modelling interactive techniques of power systems including wind generating units," *Arch. fur Elektrotechnik*, vol. 72, pp. 33 – 41, 1989.
[63] C. Fong, S. Haddad, and D. Patton, "The IEEE reliability test system - 1996," *IEEE Trans. Power Syst.*, vol. 14, no. 3, 1999.
[64] G. M. J. Herbert, S. Iniyan, and R. Goic, "Performance , reliability and failure analysis of wind farm in a developing country," *Renew. Energy*, vol. 35, no. 12, pp. 2739–2751, 2010.
[65] R. Karki and R. Billinton, "Reliability/cost implications of PV and wind energy utilization in small isolated power systems," *IEEE Trans. Energy Convers.*, vol. 16, no. 4, pp. 368–373, 2001.
[66] B. Hahn, M. Durstewitz, and K. Rohrig, "Reliability of Wind Turbines Break down of Wind Turbines," in *Wind Energy*, Springer B., 2007, pp. 329–332.
[67] E. Zio, *The Monte Carlo Simulation Method for System Reliability and Risk Analysis*. Springer, 2013.
[68] IBM, "IBM ILOG CPLEX Optimization Studio, CPLEX User's Manual," 2011.
[69] Z. Zhi, C. Wai Kin, and C. Joe H, "Agent-based simulation of electricity markets : a survey of tools," *Artif. Intell. Rev.*, vol. 28, pp. 305–342, 2009.
[70] Y. G. Hegazy, M. M. A. Salama, and A. Y. Chikhani, "Adequacy assessment of distributed generation systems using Monte Carlo simulation," *IEEE Trans. Power Syst.*, vol. 18, no. 1, pp. 48–52, 2003.

[71] N. Chaudhry and L. Hughes, "Forecasting the reliability of wind-energy systems: A new approach using the RL technique," *Appl. Energy*, vol. 96, pp. 422–430, Aug. 2012.
[72] P. Zhang, W. Li, S. Li, Y. Wang, and W. Xiao, "Reliability assessment of photovoltaic power systems: Review of current status and future perspectives," *Appl. Energy*, vol. 104, pp. 822–833, Apr. 2013.
[73] R. Girard, K. Laquaine, and G. Kariniotakis, "Assessment of wind power predictability as a decision factor in the investment phase of wind farms," *Appl. Energy*, vol. 101, pp. 609–617, 2013.
[74] P. Pinson, C. Chevallier, and G. N. Kariniotakis, "Trading Wind Generation From Short-Term Probabilistic Forecasts of Wind Power," *IEEE Trans. Power Syst.*, pp. 1–9, 2007.
[75] P. J. Luickx, P. S. Pérez, J. Driesen, and W. D. D'haeseleer, "Imbalance Tariff Systems In European Countries And The Cost Effect Of Wind Power," WP EN2009-002, 2009.
[76] J. Usaola, O. Ravelo, G. González, F. Soto, M. C. Dávila, and B. Díaz-Guerra, "Benefits for Wind Energy in Electricity Markets from Using Short Term Wind Power Prediction Tools - a Simulation Study," *Wind Eng.*, vol. 28, no. 1, pp. 119–127, Jan. 2004.
[77] E. Matallanas, M. Castillo-Cagigal, a. Gutiérrez, F. Monasterio-Huelin, E. Caamaño-Martín, D. Masa, and J. Jiménez-Leube, "Neural network controller for Active Demand-Side Management with PV energy in the residential sector," *Appl. Energy*, vol. 91, no. 1, pp. 90–97, Mar. 2012.
[78] G. Kyriakarakos, D. D. Piromalis, A. I. Dounis, K. G. Arvanitis, and G. Papadakis, "Intelligent demand side energy management system for autonomous polygeneration microgrids," *Appl. Energy*, vol. 103, pp. 39–51, Mar. 2013.
[79] Y.-H. Chen, S.-Y. Lu, Y.-R. Chang, T.-T. Lee, and M.-C. Hu, "Economic analysis and optimal energy management models for microgrid systems: A case study in Taiwan," *Appl. Energy*, vol. 103, pp. 145–154, Mar. 2013.
[80] R. C. Garcia, J. Contreras, M. Van Akkeren, and J. B. C. Garcia, "A GARCH Forecasting Model to Predict Day-Ahead Electricity Prices," *IEEE Trans. Power Syst.*, vol. 20, no. 2, pp. 867–874, 2005.
[81] M. Cococcioni, E. D'Andrea, and B. Lazzerini, "24-hour-ahead forecasting of energy production in solar PV systems," in *Intelligent Systems Design and Applications (ISDA), 2011 11th International Conference on*, 2011, pp. 1276–1281.
[82] N. Dalili, A. Edrisy, and R. Carriveau, "A review of surface engineering issues critical to wind turbine performance," *Renew. Sustain. Energy Rev.*, vol. 13, pp. 428–438, 2009.
[83] F. Y. Ettoumi, A. Mefti, A. Adane, and M. Y. Bouroubi, "Statistical analysis of solar measurements in Algeria using beta distributions," *Renew. Energy*, vol. 26, pp. 47–67, 2002.
[84] L. Martin, L. F. Zarzalejo, J. Polo, A. Navarro, R. Marchante, and M. Cony, "Prediction of global solar irradiance based on time series analysis: Application to solar thermal power plants energy production planning," *Sol. Energy*, vol. 84, pp. 1772–1781, 2010.
[85] M. Y. Sulaiman, W. M. H. Oo, and M. A. Wahab, "Application of beta distribution model to Malaysian sunshine data," *Renew. Energy*, vol. 18, pp. 573–579, 1999.
[86] S. Mohammadi, B. Mozafari, S. Solimani, and T. Niknam, "An Adaptive Modified Firefly Optimisation Algorithm based on Hong's Point Estimate Method to optimal operation management in a microgrid with consideration of uncertainties," *Energy*, vol. 51, pp. 339–348, Mar. 2013.

[87] M. Lei, L. Shiyan, J. Chuanwen, L. Hongling, and Z. Yan, "A review on the forecasting of wind speed and generated power," *Renew. Sustain. Energy Rev.*, vol. 13, pp. 915–920, 2009.

[88] F. Pimenta, W. Kempton, and R. Garvine, "Combining meteorological stations and satellite data to evaluate the offshore wind power resource of Southeastern Brazil," *Renew. Energy*, vol. 33, pp. 2375–2387, 2008.

[89] G. Grassi and P. Vecchio, "Commun Nonlinear Sci Numer Simulat Wind energy prediction using a two-hidden layer neural network," *Commun. Nonlinear Sci. Numer. Simul.*, vol. 15, no. 9, pp. 2262–2266, 2010.

[90] A. Khosravi, S. Nahavandi, D. Creighton, and A. F. Atiya, "Lower Upper Bound Estimation Method for Construction of Neural Network-Based Prediction Intervals," *IEEE Trans. Neural Net.*, vol. 22, no. 2, pp. 337–346, 2011.

[91] EEX, "Hour Contracts - France," *European Energy Exchange*, 2013. [Online]. Available: http://www.eex.com/en/Market Data/Trading Data/Power/Hour Contracts | Spot Hourly Auction/spot-hours-table/2013-02-14/FRANCE. [Accessed: 13-Feb-2013].

Paper 3

Analysis of robust optimization for decentralized microgrid energy management under uncertainty

Elizaveta Kuznetsova, Yan Fu Li, Carlos Ruiz and Enrico Zio

Submitted to Electrical Power and Energy Systems

Analysis of robust optimization for decentralized microgrid energy management under uncertainty

Elizaveta Kuznetsova[1,2], Carlos Ruiz[3], Yan-Fu Li[2], Enrico Zio[2,4]

[1] REEDS International Centre for Research in Ecological Economics, Eco-Innovation and Tool Development for Sustainability, University of Versailles Saint Quentin-en-Yvelines, 5-7 Boulevard d'Alembert, bâtiment d'Alembert - room A301, 78047 Guyancourt, France.
[2] Chair on Systems Science and the Energetic Challenge, European Foundation for New Energy-Electricité de France, Ecole Centrale Paris, Grande Voie des Vignes 92295 Châtenay-Malabry, Supelec, 91190 Gif-sur-Yvette, France.
[3] Department of Statistics, Universidad Carlos III de Madrid, Avda. de la Universidad, 30, 28911-Leganes (Madrid), Spain.
[4] Dipartimento di Energia, Politecnico di Milano, Via Lambruschini 4, 20156 Milano, Italy.

ABSTRACT

The present paper provides an extended analysis of a microgrid energy management framework based on Robust Optimization (RO). Uncertainties in wind power generation and energy consumption are described in the form of Prediction Intervals (PIs), estimated by a Non-dominated Sorting Genetic Algorithm (NSGA-II) – trained Neural Network (NN). The framework is tested and exemplified in a microgrid formed by a middle-size train station (TS) with integrated photovoltaic power production system (PV), an urban wind power plant (WPP) and a surrounding residential district (D). The system is described by Agent-Based Modelling (ABM): each stakeholder is modelled as an individual agent, which aims at a specific goal, either of decreasing its expenses from power purchasing or increasing its revenues from power selling. The aim of this paper is to identify which is the uncertainty level associated to the "extreme" conditions upon which robust management decisions perform better than a microgrid management based on expected values. This work shows how the probability of occurrence of some specific uncertain events, e.g., failures of electrical lines and electricity demand and price peaks, highly conditions the reliability and performance indicators of the microgrid under the two optimization approaches: (i) RO based on the PIs of the uncertain parameters and (ii) optimization based on expected values.

Keywords: microgrid, agent-based model, uncertain scenarios, robust optimization, power imbalance.

NOMENCLATURE

t	time step *(h)*,
F_t^{pas}	passengers flow through TS at time *t (number/h)*,
s_t	average solar irradiation at time *t* (W/m^2),
v_t	average wind speed at time *t (m/s)*,
E_t^l	energy required for inside and outside lighting in the TS at time *t (kWh)*,
E_t^{elev}	energy required for passengers lifting in the TS at time *t (kWh)*,
E_t^{elec}	energy required for electronic equipment in the TS at time *t (kWh)*,
E_t^{TS}	total hourly required energy in the TS at time *t (kWh)*,
E_t^D	total hourly required energy in the D at time *t (kWh)*,
P_t^{PV}	available energy output from the PV generators installed in the TS at time *t (kWh)*,
P_t^{WPP}	available energy output from the WPP at time *t (kWh)*,
S_t^{TS} and S_t^D	portions of energy purchased from the external grid by the TS and D, respectively (*kWh),*
L_t^{TS} and L_t^{WPP}	portions of energy sold to the external grid by the TS and WPP, respectively *(kWh)*,
V_t^{PV} and V_t^{WPP}	portions of energy sold to the D and generated by the PV panels of the TS and WPP, respectively *(kWh),*
R_t^{TS} and R_{t-1}^{TS}	energy levels in the TS battery at time *t* and *t-1*, respectively *(kWh),*
R_t^D and R_{t-1}^D	energy levels in the D battery at time *t* and *t-1*, respectively *(kWh),*
$R^{TS,stor}$	energy portion that the TS battery is capable of charging or discharging during time *t (kWh)*,
$R^{D,stor}$	energy portion that the D battery is capable of charging or discharging during time *t (kWh)*,

$\delta_t^{TS,ch}$ and $\delta_t^{TS,dis}$	binary variables which model that the TS battery can either only be charged or discharged at time *t*,
$\delta_t^{D,ch}$ and $\delta_t^{D,dis}$	binary variables which model that the D battery can either only be charged or discharged at time *t*,
$R^{TS,max}$	the maximum TS battery charge *(kWh)*,
$R^{D,max}$	the maximum D battery charge *(kWh)*,
T	time horizon considered for the optimization *(h)*,
α^{TS} and α^{D}	total costs for TS and D, respectively, for time period *T (€)*,
α^{WPP}	total revenue for WPP in time period *T (€),*
c_t^p and c_t^s	average hourly costs of purchasing and selling *1 kWh* from the external grid, respectively, at time *t* (*€kWh*),
c_t^D	average hourly cost per *kWh* from the bilateral contract agreed with D at time *t (€kWh)*.
β and γ	coefficients defining the minimum amount of energy to be sold to D by TS and WPP, respectively,
$\tilde{E}_t^D$	expected energy demand for D (for the moment, considered without uncertainty) at time step *t*, predicted by TS and WPP (*kWh*),
$\tilde{V}_t^{PV}$ and $\tilde{V}_t^{WPP}$	energy portions, which TS and WPP are ready to sell to D at time step *t* (*kWh*),
$\hat{P}_t^{WPP}$	level of uncertainty quantified for the RO at time *t (kWh)*,
$P_t^{WPP,ub}$ and $P_t^{WPP,lb}$	upper and lower prediction bounds of WPP power output at time *t*, respectively *(kWh)*,
τ	simulation time period composed of *Ns* time steps of one hour *(h)*,
LOLE	Loss of Load Expectation, characterizing the probability of unsatisfied electricity demand during τ,
LOEE	Loss of Expected Energy, quantifying the expected amount of energy losses during τ,

P_t	available capacity in the microgrid at time step *t (kWh)*,
E_t	energy demand in the microgrid at time step *t* (*kWh)*,
$Pr_t(P_t < E_t)$	probability of loss of load at time step *t,*
$E_t - P_t$	energy portion that the system is not able to supply at time step *t* (*kWh)*,
$L_t^{WPP,c}$ and $V_t^{WPP,c}$	portions of energy contracted by the WPP to the external grid and microgrid, respectively *(kWh)*,
$L_t^{WPP,*}$ and $V_t^{WPP,*}$	actual portions of energy provided by the WPP to the external grid and microgrid, respectively *(kWh)*,
T_t^{WPP}	imbalance cost generated by WPP at time step *t (€),*
$d_t^{WPP,*}$	energy imbalance generated by WPP at time step *t (kWh)*,
$c_t^{D,+}$ and $c_t^{D,-}$	prices for positive and negative imbalances, respectively, at time step *t (€/kWh)*,
γ^C and γ^P	performance ratio calculated over a simulation period of *Ns* hours by normalizing the imbalance cost by the actual expenses / revenues calculated in the case of perfect forecast (%),
T^{hw} and T^n	constants denoting the average annual duration of high and normal wind conditions, respectively, over the time period T^{tot} *(h)*,
$\lambda^{wind}(v_t)$ and λ^{norm}	failure rates at high and normal wind conditions *(occur./y)*, respectively,
$f_v(v_t)$	weight factor caused by severe weather,
f_t^d and f_t^h	weight factors for hourly and daily variations, respectively,
r^{norm}	reference restoration time during normal weather conditions, modelled as a random variable with lognormal distribution.

1. INTRODUCTION

Renewable energies are promising solutions to the energetic and environmental challenges of the 21st century [1], [2]. Their integration into the existing grids generates technical and social challenges related to their efficient and secure management.

From this point of view, a closer location of generation and consumption sources in decentralized microgrids is expected to increase service quality for the consumers by decreasing transmission losses and the time needed to manage fault restoration and congestions. However, energy management can become critical in the microgrid, due to possible conflicting requirements or poor communication between the different microgrids elements [3]. Therefore, there is a need of frameworks for efficient microgrid energy management.

A way to model microgrids and the related individual goal-oriented decision-making of the microgrid elements is that of Agent-Based Modelling (ABM) [4–6], which allows analysing by simulating the interactions among individual intelligent decision makers (the agents). The most widespread application of this modelling approach concerns the bidding strategies among individual agents, who want to increase their immediate profits through mutual negotiations and by participating in a dynamic energy market [7–10]. Recent studies show the extension of the ABM approach to more complex interactions in the energy management of hybrid renewable energy generation systems [6], [11], [12]. In these works, the long-term goals are focused on the efficient use of electricity within microgrids, e.g., the planning of battery scheduling to locally store the electricity generated by renewable sources and reuse it during periods of high electricity demand [11]. However, the decision framework is commonly developed under deterministic conditions, e.g., those of a typical day in summer.

To account for the variability and randomness of the operational and environmental parameters of the energy systems, several optimization techniques have been progressively introduced for handling uncertainty [13]. Fuzzy mathematical programming models and their extensions have been developed for optimal management of hybrid energy systems [14], [15]. Stochastic programming models, where the uncertain parameters are described by probability distributions, and interval programming models, where the uncertainty is described by intervals [16], [17], have been used to deal with different sources of uncertainty in optimization problems, like

economic-energy scenarios planning [18], design of renewable systems for community energy management [19], and water quality and waste management [20], [21].

In this paper, we propose an analysis of a microgrid energy management framework based on Robust Optimization (RO) previously proposed by the authors [22]. The analysis is intended to identify the conditions required for an optimal microgrid operation in presence of several sources of uncertainty, affecting the power output from renewable generators [23], the production costs [24], the electricity demand [25]. The uncertainty in the parameters is represented by Prediction Intervals (PIs), which are estimated by a Non-dominated Sorting Genetic Algorithm (NSGA-II) – trained Neural Network (NN) to provide lower and upper prediction bounds between which the uncertain values of the parameters are expected to lie for a given confidence level [26], [27].

The RO framework improves the reliability of the microgrid operation by selecting energy management actions that are optimal under the worst realization of the uncertainty conditions. However, this is done at the cost of possible lower revenues for the energy generators and higher expenses for the energy consumers than those that could be obtained by optimizing over the expected values of the uncertain parameters. The proposed analysis investigates the influence of uncertain events on the microgrid performance and identifies the conditions under which the application of RO or optimization based on expected values is most advantageous.

The paper is organized as follows. Section 2 motivates for the analysis carried out. Section 3 describes the models of the individual agents in the microgrid and the way that the uncertainties in the energy management parameters are accounted for. The procedure for the simulation of the uncertain scenarios and the definitions of the output quantities are discussed in Section 4 and Section 5, respectively. Section 6 applies the presented methodology to a reference microgrid system. Finally, the last section draws conclusions and gives an outlook on future research.

2. MOTIVATION

Two optimization approaches are considered: (i) optimization based on the expected values of the uncertain quantities (also called “deterministic” optimization) and (ii) RO based on PIs with a given Coverage Probability (CP).

In a previous work [22], the authors have shown that the proposed framework of RO based on PIs leads to high system reliability, but at the expense of conservative results regarding system

revenues or expenses. In fact, the proposed framework leads the decision maker to anticipate the worst possible realization of the uncertain parameters and choose the best solution with respect to such a case. By so doing, the producer plans its energy scheduling strategy by committing less energy for sale while the consumer purchases more energy than it is likely required.

The analysis proposed in this paper, aims at evaluating the system performance for different levels of uncertainty affecting both operational and environmental conditions. These uncertainties can be broadly classified in two types: (i) uncertainty related to fluctuations of the operational and environmental conditions within expected and acceptable limits. These are typical conditions for the microgrid operation, and (ii) uncertainty related to extreme events. In the first case, the fluctuations of the operational and environmental conditions can be managed by optimization based on expected parameters values without particular performance degradation [22]. In the second case RO is expected to lead to management actions that guarantee the operation within safety margins. This paper proposes methodology to simulate the uncertainty related to extreme events and to evaluate microgrid reliability and performance under different optimization approaches.

To evaluate the performance of the proposed methodology, we adopt classical reliability indicators and the so called performance ratio to quantify negative / positive imbalances caused by the prediction errors. This analysis allows showing how the probability of occurrence of an uncertain event can influence the microgrid performance indicators. Thus, this analysis provides a way of identifying the level of uncertainty in the system upon which RO performs better versus an optimization based on expected values.

3. MICROGRID ENERGY MANAGEMENT: THE PRACTICAL SETTING

The reference system considered in this paper is the same as in [22]. It includes a middle-size train station (TS), which can play the role of power producer and consumer, the surrounding district (D) with residences and small businesses, and a small urban wind power plant (WPP). The goal of TS is to decrease its electricity expenses while satisfying its demand. To achieve this, the TS strategy includes the integration of renewable generators and energy exchanges with the local community to increase the power flexibility of the microgrid. Photovoltaic panels (PV)

have been shown to be an adapted and efficient technology for its implementation on large commercial, public buildings and transportation hubs [28], [29]. For the energy exchanges with local community, we consider only the possibility of exchange between the TS and the D. This is done to keep the model simple but also complete in order to properly illustrate the optimization analysis. Future work includes the modelling of the energy exchanges between the TS and the WPP.

The goal of WPP is to increase its revenues from selling the electricity to the external grid and to the D. The latter is considered only as an energy consumer, with the goal of decreasing its electricity purchase from the external grid by prioritizing the purchase of electricity from local sources, i.e., the TS and the WPP. In addition, we assume that the TS and the D have the capacity to store electricity in batteries.

For our current D model, we assume that the effect of locally installed renewable generators, in our case PV panels, can be neglected. The energy generated with PV panels is around 0.8% of the annual energy consumption in 2012 for the considered area [30].

Only a synthetic description of the models of the individual agents of the microgrid is presented below; for more detailed information, the interested author can refer to [22]. Additionally, a detailed description of the optimization problems, the agents' negotiation framework and the uncertainty model are provided in Appendix A.

TS: The energy consumption E_t^{TS} *(kWh)* in the main passengers building is divided into a variable consumption, i.e. lighting and lifting depending on the solar irradiation and passengers flow, respectively, and a fixed consumption represented by plug-in electronic devices. The power required by the lifting equipment is calculated by using the methodology in [31], which is based on in-situ real time records of passengers flow. The electrical energy consumed by the lighting equipment is calculated based on the inside and outside luminosity (e.g., EN13272:2001 UK) [32]. The total energy produced by PV P_t^{PV} *(kWh)* is calculated based on the solar irradiation and technical specification of PV module [33], [34].

WPP: The total energy produced by the WPP P_t^{WPP} *(kWh)* is calculated based on the wind speed data from [35], by using the cubic correlation described in [36].

D: To simulate the energy consumption of the D, we use a top-down approach based on available statistical collections of electricity consumptions [37]. Models for the batteries charging/discharging are presented in Appendix A, i.e., eqs. (A.11) – (A.14) and eqs. (A.21) – (A.24) for the TS and D, respectively.

In this work, the market electricity price c_t^p (€/kWh) is assumed to vary following a similar trend to the wholesale market price in France [38]. Moreover, we assume that the grid offers an electricity price c_t^s *(€/kWh)* to purchase the energy from the agents. Finally, the electricity price c_t^D *(€/kWh)* is the one offered by the D to purchase the energy from the other microgrid energy producers.

Figure 1 a,b illustrates the structure of the management scheme and operation procedure of the microgrid. The outputs from the models of the individual components are used to forecast the energy demands of the TS and D, i.e., E_t^{TS} and E_t^D, the energy outputs of the WPP and PV, i.e., P_t^{WPP} and P_t^{PV}, and the electricity prices c_t^p. These forecasted quantities feed the optimization models of the different decision-makers to determine their optimal decision variables, e.g., the battery scheduling and the energy portion to exchange between the agents and the upstream grid. In order to set up the price for the energy trading, the agents use 24-hours ahead predictions of the reference prices (c_t^p). Note that these predictions may not account for unexpected price variations.

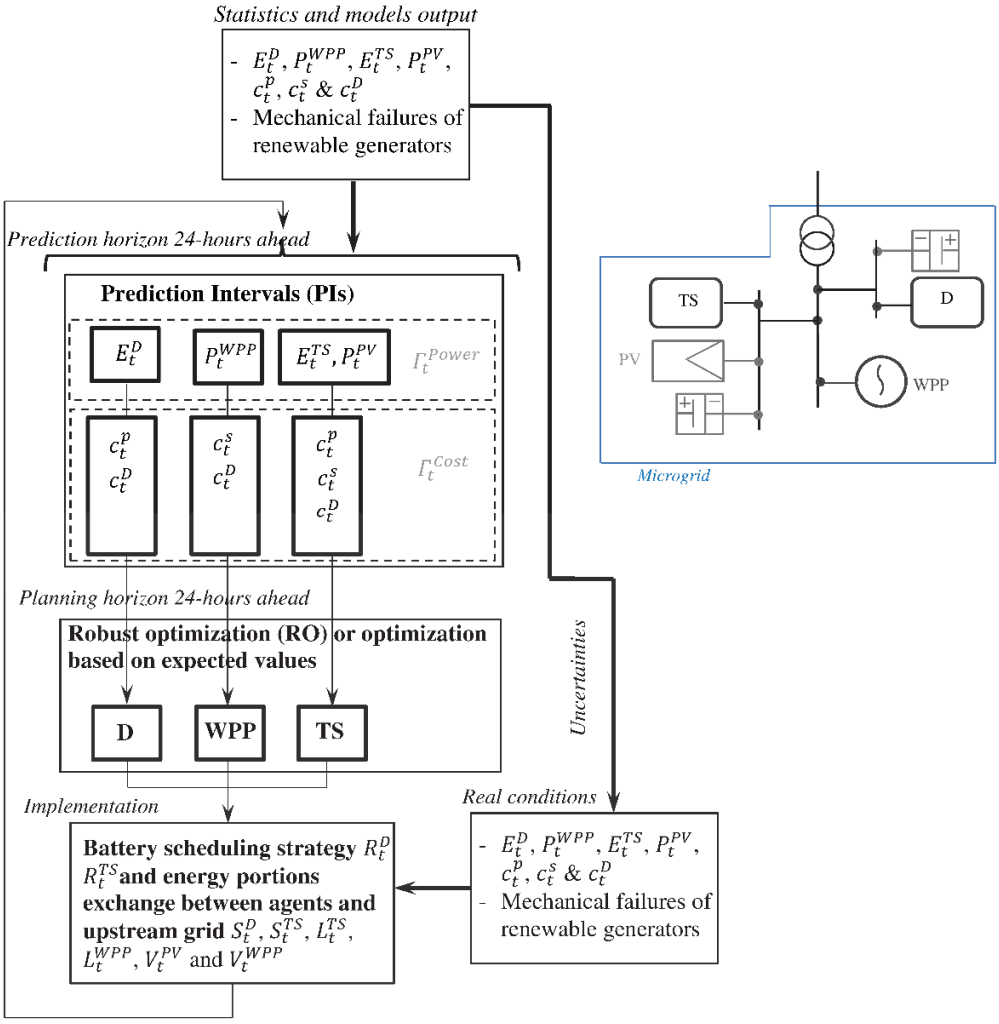

a)

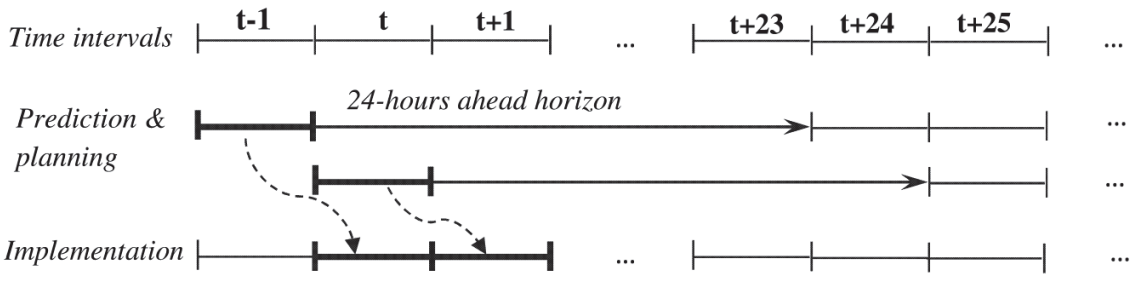

b)

Figure 1. Integrated framework: a) Structure of the management scheme; b) Operation procedure [39].

The decision-making strategy for each agent is obtained by an optimization approach so that the expenses are minimized for the D and the TS, while the revenues are maximized for the WPP. These goals are achieved through strategic battery scheduling and the optimal selection of energy exchanges between the microgrid agents and the upstream electricity grid. Thus, the consumer aims to optimize its strategy considering a time horizon of 24 time steps, each of one hour duration. Similarly, at each time *t*, the microgrid energy producers (WPP and TS) and consumer (D) have the possibility to negotiate bilateral contracts of energy exchanges to achieve their goals. Note that in this paper demand-response mechanisms for the energy management are not considered.

4. SIMULATION OF UNCERTAIN SCENARIOS

In order to analyse the RO framework developed in [39], we have adopted the framework illustrated in Figure 2 that allows integrating uncertain events.

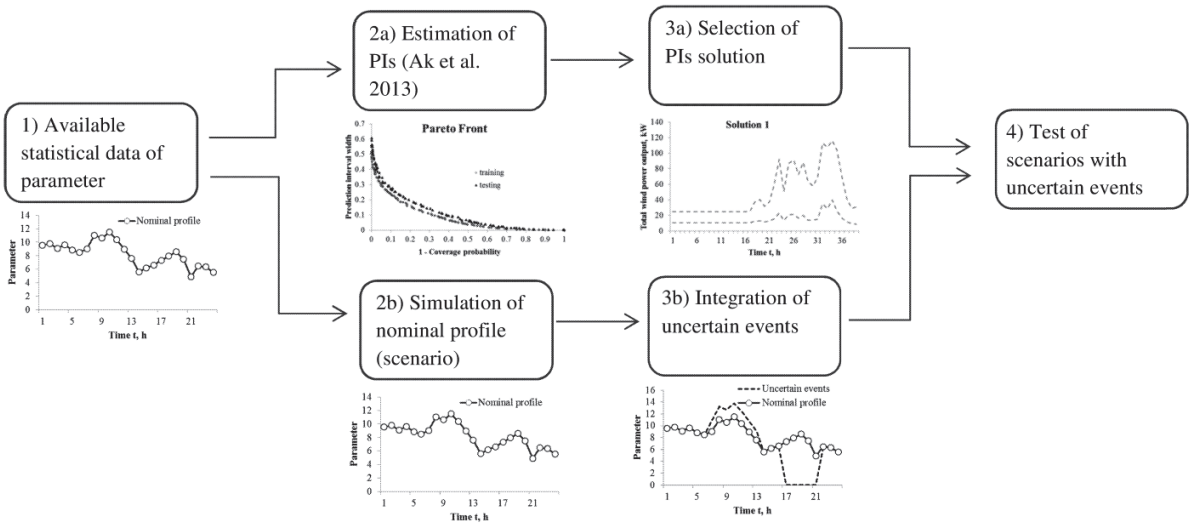

Figure 2. Procedure for construction and test of scenarios with uncertain events.

The step-by-step procedure is described in the following. The available statistical data of the parameters, such as wind power output of WPP or electricity demand for D and TS, is divided into two data sets: the first data set feeds a NSGA-II – trained NN for the estimation of the PIs; this provides a Pareto front of prediction solutions in terms of PIs with lower and upper prediction bounds between which the uncertain parameters are expected to lie with a given

confidence level [27]. The second data set is used to simulate the nominal variations of the considered parameter. From the Pareto front of the available solutions, one solution of PIs can be selected according to two characteristics, i.e., Coverage Probability (CP) and Prediction Interval Width (PIW), and be used to characterize the uncertainty feasible region in the RO (eqs. (A.1) – (A.34)). In parallel, the second data set representing the nominal profile of the considered parameter is updated with uncertain events. Note that the reference to the nominal profile of the parameter indicates that it is based on historical data and does not account for any uncertain events which can arise in the future. Finally, the updated nominal profile is tested to explore the effects that the level of uncertain events may have on the microgrid performance. This is done by comparing the two management strategies for the microgrid described in Section 3, i.e., optimization based on the expected values and RO based on PIs.

The procedure for simulation of the uncertain events is briefly described in this section.

4.1. Wind storms and associated failures of the electrical lines

We consider failures/repairs of the wind power generator and its auxiliary equipment, which are correlated with the wind speed intensity. In order to generate different profiles of wind speed, the procedure of Figure 2 is used:

1) The initial profile of wind speed is used to sample storms with different probabilities of occurrence. The continuous increase of the storms probability allows generating wind speed profiles representing different levels of uncertain conditions.
2) Each wind speed profile is analysed and the total expected failure rate and restoration time are computed.
3) The obtained failure/restoration rates are used to simulate different scenarios of uncertain events.

There are several statistical studies that provide detailed information about the annual downtime and failure frequencies of wind turbine components [40]. However, the reliability models describing wind correlated failures of wind turbines components are rare or inexistent. We should mention that there are a few examples that treat the influence of wind turbulence on rotor and pitch mechanism [41], and demonstrate that the wind turbine failure rates can be learnt by monitoring the wind characteristics [42].

As described in [43], our work focuses on the simulation of wind speed-correlated failures in the overhead lines. This allows accounting for the increase of failures frequency and repair durations in presence of extreme environmental conditions [43]. The following equation defines the expected total failure rate $E\big(\lambda(v_t)\big)$:

$$E\big(\lambda(v_t)\big) = \frac{T^{hw}}{T^{tot}} \cdot \lambda^{wind}(v_t) + \frac{T^{n}}{T^{tot}} \cdot \lambda^{norm} \tag{1}$$

where T^{hw} and T^{n} are constants which denote the average annual duration (h) of high and normal wind conditions, respectively, T^{tot} is the total duration of the simulation period (h), $\lambda^{wind}(v_t)$ and λ^{norm} are the failure rates (occur./y) at high and normal wind conditions, respectively, and α is a scaling parameter. Note that contrary to [43], we do not consider possible failures due to lightning events: therefore, eq. (1) accounts only for the increase of wind speed above a critical value. To describe the failure rate at high wind conditions, we use an exponential relationship between the failure rates of lines and wind speed:

$$\lambda^{wind}(v_t) = (\gamma_1 \cdot e^{\gamma_2 v_t} - \gamma_3) \cdot \lambda^{norm} \tag{2}$$

where v_t is the wind speed (m/s) at time *t*, $\alpha, \gamma_2, \gamma_3$ are scaling parameters and λ^{norm} is the constant failure rate during normal weather conditions. The restoration time for the overhead lines is defined as follows:

$$r_t = f_v(v_t) \cdot f_t^d \cdot f_t^h \cdot r^{norm} \tag{3}$$

where $f_v(v_t)$ is a weighting factor caused by the severe weather, f_t^d and f_t^h are weighting factors for hourly and daily variations, respectively, and r^{norm} is the reference restoration time during normal weather conditions modelled as a random variable with a lognormal distribution:

$$f_v(v_t) = \begin{cases} 1, & if\ v_t < v^{crit} \\ 1 + \frac{k \cdot (v_t - v^{crit})}{\bar{r}^{norm}}, & if\ v_t \geq v^{crit} \end{cases} \tag{4}$$

For this model, the scaling parameters and weight factors were defined through the analysis of real data in [43].

The drastic increase of the wind-caused failure rate is simulated and validated with real data for wind speeds higher than the critical one [44]. According to different studies, the critical wind

speed above which the expected failure rate of the electrical lines increases is around 8 m/s [43], [44]. Based on this indication, Figure 3 *a, b* illustrates the occurrence and duration rates of discretized wind speeds for the nominal profile. The grey bars indicate normal wind speed conditions, while the black ones are related to severe wind speeds (storms) conditions.

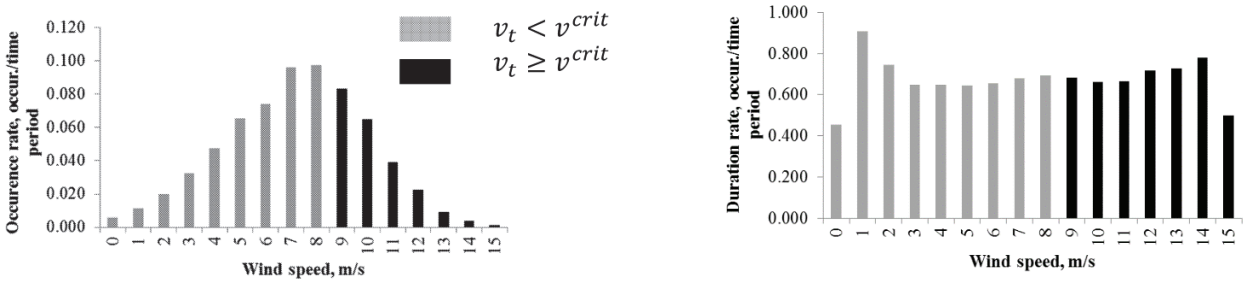

a) *b)*

Figure 3. Analysis of nominal wind speed profile: a) occurrence rate and b) duration rate of discretized wind speeds.

To inject the increase in the frequency of lines failures due to wind storms, the level of wind speed in the nominal profile is artificially raised. To simulate the wind 'peaks', we focus on the maximum wind speed magnitude of the profile of Figure 3 a, i.e., 15 m/s. The initial occurrence rate of such wind speed magnitude has been progressively increased, as reported in Table 1. The exponential distribution is used to model the time between storms occurrence, which are considered statistically independent events [45]. The mean duration of maximum wind speed magnitude is fixed.

Table 1. Failure and repair rates of overhead lines for different wind speed conditions.

# of wind speed profile	Wind storms		Overhead line failures	
	Occurrence rate, occur./time period	Duration rate, occur./time period	Total expected failure rate (MTTF, h), occur./time period	MTTR, h
a. Initial wind speed profile	0.001	0.5	0.5619 (3097)	2.15
b.	0.01		0.8369 (2086)	2.31
c.	0.1		3.4982 (499)	3.95
d.	1		10.3420 (168)	8.18
e.	10		11.6372 (154)	9.01

As seen in *Table 1*, the increase of the wind storms occurrence rate generates the decrease of the MTTF and the increase of the MTTR of overhead line failures.

4.2. Energy demand and price peaks

4.2.1. Energy demand peaks

The importance to forecast the energy demand peaks and evaluate their impact on the performance and reliability of energy systems was initially emphasized in [46], and explored in other reports and scientific works for various reasons, i.e., (i) the increasing concern about electric system reliability and growing trend towards energy efficiency as a resource [47]; (ii) emergence of new market structures and opportunities for monetary compensation of sources of system reliability [47], [48]; and (iii) increased adoption of advanced metering and communication technologies that make it easier and less costly to evaluate peak demand impacts [49].

Energy demand is primarily influenced by weather conditions, i.e., temperature and hours of daylight, as well as other consumption patterns such as number of business hours and school holidays. In this view, the temperature typically drives electric demand especially among residential consumers, who can use more than half of the electricity during the peak hours of the coldest or hottest days (regulation of household temperature). However, the consumption peak can also be influenced by other parameters, e.g., special calendar events and demographics. Moreover, peaks' shifting during the day is possible during the day due to the adoption of smart grid technologies, e.g., massive plug-in of the electrical cars. Therefore, the prediction of the energy consumption patterns remains an important challenge, mainly because of the absence of sufficient amount of statistical data. For these reasons, the increase of the consumption peak occurrence and intensity are difficult to forecast with statistical models. Different works develop numerical tools to forecast the increase in energy demand peaks, e.g., statistical tools capable to capture unexpected extreme intraday increases by using available statistical records of energy demand [50], parametric models to predict long-term peaks correlated with weather, economic and demographic parameters of a particular area [51] or Bayesian estimation techniques to predict energy consumption peaks in transportation systems [52].The statistical forecast approaches are based on the so-called normal profiles of the statistical parameter, e.g., energy

consumption or temperature, which do not account for a possible increase of the peak occurrence and magnitude in the future [53]. Moreover, the multi-parameters time series models accounting for weather-induced effects, daily/weekly/yearly seasonality, special calendar events and in some cases, the variation of GDP and demographics of the geographical areas, provide a more accurate forecast for peak occurrence and magnitude [54–56]. Different research papers and reports [57], [58] situate the main energy demand peak timing period from noon to 6 p.m. Off-peak occurs from 9:30 p.m. to 8:30 a.m. and the rest of hours are considered to be the partial peak.

In our case, the prediction of electricity demand, which is done by using the nominal profile of the consumption, does not allow using the forecast model to simulate the increase of energy consumption peaks. The uncertainty in variations of the energy demand is, thus, artificially simulated by increasing the daily peaks during the peak hours. For this purpose, we assign the probability of peak occurrence to each day during a week by using the probabilistic approach described in [54]. According to this approach, which is validated with real statistical data, the working days, i.e., from Monday to Thursday, hold the highest probability of peak occurrence, which can vary from 0.05 to 0.15 depending on the season (Figure 1 *a*). It also provides the pdfs of the magnitude of peak electricity demand (*Figure 4 b*).

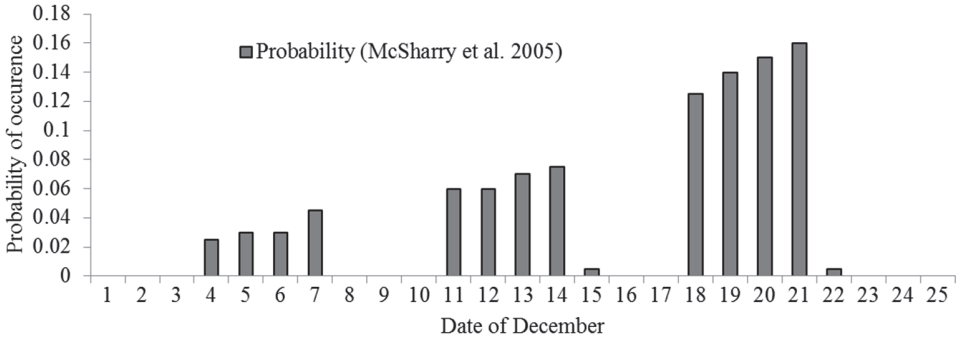

a)

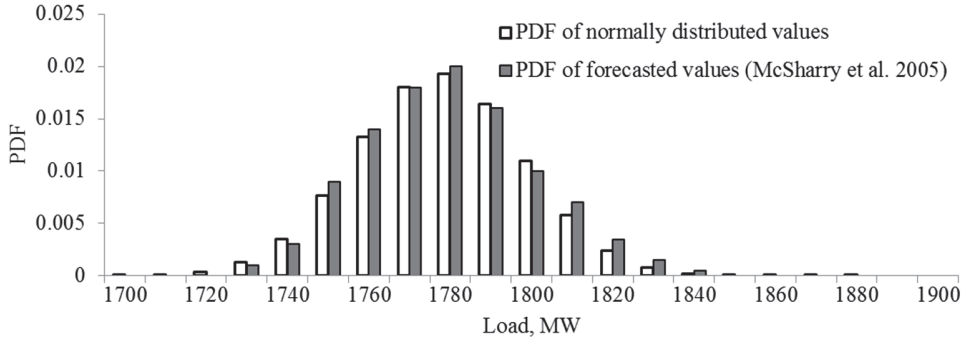

b)

Figure 4. Example of the probabilistic forecast of the load peak year 2000 [54]: a) Occurrence probability on various dates in December; b)pdf for forecasted values of load peak.

Based on the conclusions presented in [54], we account for the possibility of peak occurrence only from Monday to Thursday. To generate scenarios with different level of uncertainty in energy demand, we assign a constant probability of peak occurrence from Monday to Thursday which we progressively increase, i.e., the scenarios tested here have 0.1, 0.2, 0.4, 0.6 and 0.8 probability of peak occurrence. Given the particular characteristics of the presented distribution, we assume that the peaking values of energy demand are normally distributed. In this view, the nominal value of each peak is calculated by assuming the same proportional standard deviation and a maximum value for the load peak of about 4% [54].

4.2.2. Energy price

The analysis of recent trends related to household energy bills shows a significant increase of electricity prices. For example, in the UK the increase of the energy bill is estimated to be around 20% since 2007 [59]. Moreover, the particular geographical location, implying sometimes particular microclimate conditions, as well as different electricity network configurations or energy generation portfolios, are able to generate important variations on the energy prices as it is already the case of the different UK regions [60]. In addition, the further development of Smart grids is regarded to be a main driver of the increase of the household energy bills [59].

However, even in countries with strong electricity markets, where producers, consumers and transmission companies are involved in the price formulation, the correlation between energy demand and price remains important (e.g., 0.58 for UK). Indeed, important investments, that are

directed to upgrade the existing infrastructure to help the network support demand during peak times and to avoid power outages, are one of the causes of the increase of electricity prices. Therefore, in this paper the increase of the energy demand peaks is explored jointly with the increase of the electricity market price especially when the variations in market electricity prices allow following the trend of the energy demand curve, i.e., during working days rather than during weekends.

This increase of the energy demand peaks is assumed to be followed by an increase in the electricity price from the upstream grid. The electricity tariff from the external grid adopted for this case study is a tariff structure for commercial utilization, which is made up of a basic charge, a daytime unit rate, a night unit rate and a peak charge. This tariff is introduced in [57] and adopted in [61]. By assuming that the energy demand of the D E_t^D follows the same trend than the energy demand profile in the upstream grid, we can adopt a similar assumption regarding the proportional correlation between the daily electricity market price and the daily energy demand [57], [61], [62].This is done to simulate the variations in the upstream market price. However, it is important to highlight that during the peaks of electricity demand, the electricity price can be no longer proportional to demand, but rise drastically. This Critical Peak Price (CPP) represents a dynamic rate that is dispatched for the utilities based on real-time capacity conditions. The value of the critical peak price is several times higher than the usual price applied during the off-peak periods, e.g., CPP rate is 6 - 7 for [63], [64]. The objective of this price increase can be to reduce the electricity consumption during critical times [63], [65].

In this paper, we are not focussing on demand-response management techniques, but on evaluating the expenses paid by the consumers in case of an inaccurate prediction of the energy consumption. For this, we have tested different values of the critical peak price, applied during the peak period from noon to 6 p.m.

5. OUTPUT INDICATORS

In this section we present the indicators used to evaluate microgrid performance and reliability.

5.1. Microgrid reliability

The overall microgrid performance is evaluated in terms of classical adequacy assessment metrics, which characterize the ability of the DG system energy capacity to meet system demand

in presence of uncertainty [66]. Specifically, Loss of Load Expectation (LOLE) is used to characterize the probability of unsatisfied electricity demand and Loss of Expected Energy (LOEE) to quantify the expected amount of energy losses for *Ns* time steps of one hour:

$$LOLE = \sum_{t=0}^{Ns} Pr_t(P_t < E_t) \tag{5}$$

$$LOEE = \sum_{t=0}^{Ns} Pr_t(P_t < E_t) \cdot (E_t - P_t) \tag{6}$$

where $Pr_t(P_t < E_t)$ is the probability of loss of load at time step *t*, P_t *(kWh)* is the available capacity at time period *t*, E_t *(kWh)* is the energy demand at time step *t*, in our case defined as follows:

$$P_t = S_t^D + S_t^{TS} + V_t^{PV} + V_t^{WPP} + \delta_t^{D,dis} \cdot R^{D,stor} + \delta_t^{TS,dis} \cdot R^{TS,stor} \qquad \forall t \tag{7}$$

$$E_t = E_t^D + E_t^{TS} + \delta_t^{D,ch} \cdot R^{D,stor} + \delta_t^{TS,ch} \cdot R^{TS,stor} \qquad \forall t \tag{8}$$

The available power capacity of the microgrid P_t (eq. 7) represents the sum of the electricity produced by all generation units at time step *t*. In our case, P_t accounts for the amount of energy purchased from the external grid (i.e., S_t^D and S_t^{TS}), produced by the local generators (i.e., V_t^{PV} and V_t^{WPP}) and discharged from the batteries (i.e., $\delta_t^{D,dis} \cdot R^{D,stor}$ and $\delta_t^{TS,dis} \cdot R^{TS,stor}$).

5.2. Microgrid imbalance

The renewable generators installed in the microgrid, i.e., WPP and PV power production in TS, are committed to provide V_t^{WPP} and V_t^{PV} to the D, and L_t^{WPP} and L_t^{PV} to the upstream grid. The non-supplied energy can generate reliability problems for the microgrid and the upstream grid. By taking into account the prediction errors and/or the mechanical failures of the renewable generators, their common revenues for time step *t* are formulated as:

$$\alpha_t^{\Sigma,\mathrm{P}} = (L_t^{WPP,c} + L_t^{PV,c}) \cdot c_t^s + (V_t^{WPP,c} + V_t^{PV,c}) \cdot c_t^D + T_t^{\Sigma,\mathrm{P}} \qquad \forall t \tag{9}$$

where $L_t^{WPP,c}$, $L_t^{PV,c}$, $V_t^{WPP,c}$ and $V_t^{PV,c}$ *(kWh)* are the contracted amounts of energy provided by the WPP and PV to the external grid and microgrid, respectively, $T_t^{\Sigma,\mathrm{P}}$ *(€)* is the imbalance cost of the renewable generators defined as follows:

$$T_t^{\Sigma,\mathrm{P}} = (d_t^{L_t^{WPP,*}} + d_t^{L_t^{PV,*}}) \cdot c_t^{s,+/-} + (d_t^{V_t^{WPP,*}} + d_t^{V_t^{PV,*}}) \cdot c_t^{D,+/-} \tag{10}$$

where $d_t^{V_t^{WPP,*}}$, $d_t^{V_t^{PV,*}}$, $d_t^{L_t^{WPP,*}}$ and $d_t^{L_t^{PV,*}}$ *(kWh)* are the imbalances for time step *t* calculated as the difference between the actual amount of energy *(kWh)* that the renewable generator can supply and the level of contracted energy *(kWh)*. The prices $c_t^{D,+/-}$ and $c_t^{s,+/-}$ *(€/kWh)* are the imbalance prices for positive and negative imbalances, respectively, at time step *t*.

Note that the expenses of D are defined similar to the revenues of the renewable generators:

$$\alpha_t^{\Sigma,\mathrm{C}} = S_t^{D,c} \cdot c_t^p + (V_t^{WPP,c} + V_t^{PV,c}) \cdot c_t^D + T_t^{\Sigma,\mathrm{C}} \qquad \forall t \qquad (11)$$

where $S_t^{D,c}$, $V_t^{WPP,c}$ and $V_t^{PV,c}$ *(kWh)* are the contracted amounts of energy from the external grid and local renewable generators, respectively, and $T_t^{\Sigma,\mathrm{C}}$ *(€)* is the cost paid to supply the peak electricity demand.

Again, note that the formulation of revenues accounting for the imbalance cost is done for contract durations of one hour.

To define the formulation of the imbalance prices, we have reviewed the existing imbalance tariff structures and regulation mechanism of European countries [67] such as Belgium, Netherland, France and Spain. Among the existing formulations, the definition of imbalance price in Spain is taken as example because of its simplicity, whereby the imbalance price is equal to a certain proportion of the spot price [68], [69]. In the numerical application that follows (Section 6), we have tested different imbalance prices to analyse the influence on the performance.

To evaluate the impact of the imbalance cost on the renewable generators revenues, we introduce the performance ratio γ^P (eq. 12), which is calculated over a simulation period of *Ns* hours. Note that γ^P is computed by normalizing the total imbalance cost generated by the renewable generators by the revenues that would be obtained in the case of a perfect forecast [68]. To evaluate the impact of the load and price peaks, the coefficient γ^C (eq. 13) is calculated similar to γ^P, i.e., normalizing the imbalance cost generated during the peaking periods by the expenses that D would pay in case of a perfect forecast:

$$\gamma^P = \left(1 - \frac{\sum_{t=0}^{Ns} \left|T_t^{\Sigma,\mathrm{P}}\right|}{\sum_{t=0}^{Ns} \left[(L_t^{WPP,c} + L_t^{PV,c}) \cdot c_t^s + (V_t^{WPP,c} + V_t^{PV,c}) \cdot c_t^D\right]}\right) \cdot 100\% \qquad (12)$$

$$\gamma^C = \left(1 - \frac{\sum_{t=0}^{Ns} \left|T_t^{\Sigma,C}\right|}{\sum_{t=0}^{Ns} \left[S_t^{D,c} \cdot c_t^p + (V_t^{WPP,c} + V_t^{PV,c}) \cdot c_t^D\right]}\right) \cdot 100\% \quad (13)$$

The proposed performance ratios are expressed in percentage, i.e., $\gamma^P, \gamma^C \in (0,100]$. For perfect predictions, i.e., when deviations from committed energy are null, performance ratios are 100%.

In general, microgrids can operated in two modes: the grid-connected mode and the islanded mode. In the grid-connected mode, the microgrid can trade power with the upstream power grid to solve the power imbalance. On the other hand, power imbalances in the islanded mode can be solved by decreasing the total output of the distributed generators (DGs), or by load-shedding, which is an intentional load reduction [70]. In our paper, we focus on the grid-connected mode. Therefore, the power imbalances are accounted inside the microgrid and between the microgrid power producers and the upstream external grid.

6. NUMERICAL CASE STUDY

As discussed in Subsection 3.3, the PIs of the available wind energy output P_t^{WPP}, and energy demands E_t^{TS} and E_t^D are estimated by a NN trained by a NSGA-II with respect to two objectives: the coverage of the PIs (to be maximized) and their width (to be minimized) [27]. This optimization gives rise to the Pareto fronts depicted in Figure 5, from which different solutions can be selected and used in the energy management by RO. Note that these solutions differs on the PIW and on their corresponding coverage probability and were also used in paper [39].

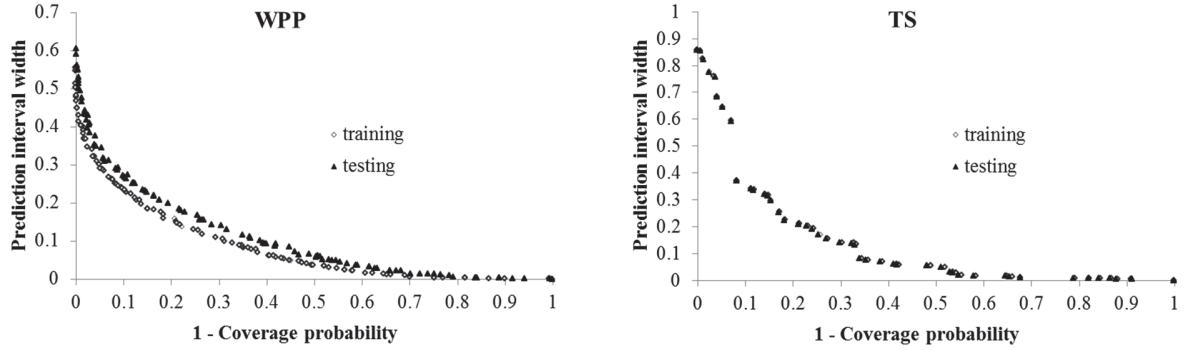

a) *b)*

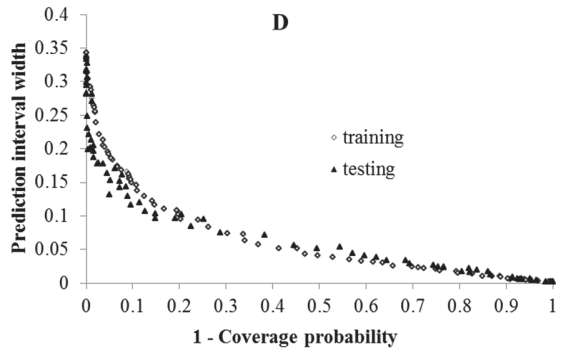

c)

Figure 5. Pareto fronts of PIs: a) P_t^{WPP}, b) E_t^{TS} and c) E_t^D.

The comparison of the optimization results obtained with the RO based on PIs with (i) CP = 96% and (ii) CP = 56.3% shows that PIs with high CP decrease drastically the amount of committed energy [39]. This is due to the large width of the PIs characterized by high CP, i.e., 96%, which forces the RO to provide a very conservative solution. As a consequence, the producer plans its energy scheduling strategy based on the worst possible realization of the available power production and thus commits less energy for sale; at the opposite, the consumer anticipates the worst possible realization of its uncertain consumption and, thus, it purchases more energy than it will probably be required in the future. As a consequence the performance ratio of the RO based on the PIs with high CP = 96% is very low. On the contrary, the optimization based on the PIs with low CP = 56.3% considers "less extreme" worst realizations and, thus, provides adequate results in terms of performance ratio, comparable with results of other optimization techniques [68], and achieves satisfactory values of the reliability indicators, i.e., LOLE and LOEE, in comparison with these achieved by the optimization based on expected values.

In this view, for the following we consider and analyse the performance of the RO based on the PIs with moderate CP in the range of 50 – 60%. The PIs used for the prediction of the electricity power output are selected from the Pareto front (Figure 5 *a*) of the available solutions, with PIW and CP equal to 0.0535 and 56%, respectively. The PIs used for the electricity demand prediction are selected from the Pareto front (Figure 5 *c*) of the available solutions with similar characteristics than the PIs used for the wind power output prediction, i.e., PIW = 0.0518 and CP = 50.5%.

To account for the variations of the electricity prices c_t^p, c_t^s and c_t^D, the lower and upper bounds of their associated PIs have been assumed to be the ±10% of their expected values. Similarly, the variations of P_t^{PV} have been accounted for by setting the lower and upper bounds of the PIs to ±5% of their expected values. Note that these PIs widths have been fixed based on the accuracy of a 24-hours ahead prediction for the electricity prices [71] and the PV energy output [72].
The optimization based on the expected values has been performed also; as it was discussed in Appendix A.1, by considering the mean of the PIs as a point estimate of the uncertain quantity of interest. Note that the effect of the electrical lines failures and the increase of the energy demand and prices peaks will be explored separately from each other.

6.1. Impact of wind storms and associated lines failures

Based on Table 1, five case studies are considered under the following assumptions:

- Failures of the electrical lines are considered to occur within the microgrid.
- The same initial wind speed profile was used for the sampling of overhead line failures with different MTTF and MTTR. Indeed, the use of the wind speed profiles with the artificially increased wind speeds for the different case studies, renders a higher wind power output and, consequently, the performance ratio over the simulation period is increased. This disturbs the output indicators, such as the performance ratio, by hiding the effect of the overhead lines failures.
- The failures/repair rates of the generation units inside the microgrid, i.e., PV and WPP, are considered constant and of the same values as in [39].

For the point estimation of the wind energy output P_t^{WPP}, which is used for the optimization based on the expected values, we use the mean of the considered PIs with CP = 56.3%. The results obtained by the simulation of the agents dynamics on a period of $\tau = 1680\,h$ have been calculated as the average over *Ns = 20* simulations, which is a sufficiently large number of simulations to efficiently determine the convergence of the different indicators. The convergence is evaluated by considering the difference between two successive values of the indicators moving average where a threshold value of 2% is used.

Figure 6 a,b shows the variations of the shortage and surplus in percentage of the total amount of committed energy under different conditions of failures and repairs using the RO and the optimization based on expected values.

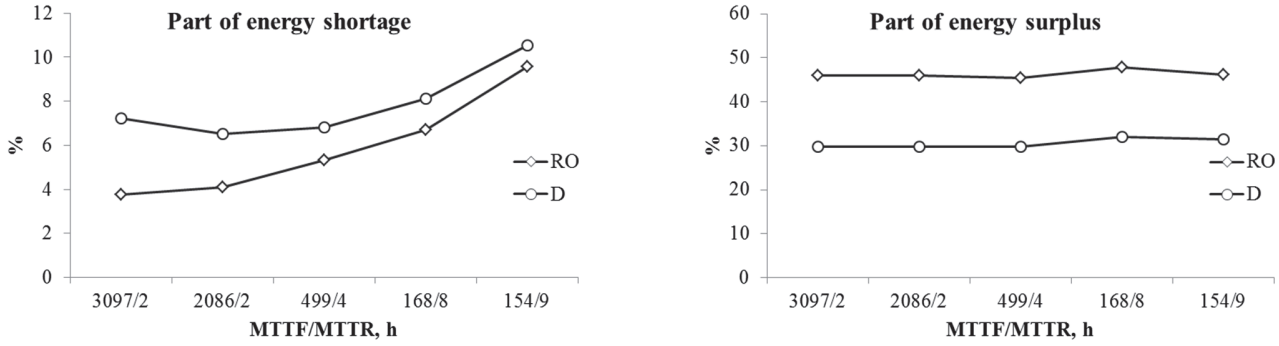

a) *b)*

Figure 6. Variations of shortage and surplus proportions in percentage of the total amount of committed energy using RO based on the PIs and deterministic optimization based on the expected values: a) Shortage; b) Surplus.

As it can be observed in *Figure 6 a,b*, the increase of the MTTF associated to the electrical lines increases the number of shortages in the grid, and this is common to both optimization approaches. With the increase of the probability of electrical lines failure, i.e., of the ratio MTTF/MTTR, the proportions of shortage tend to the values 9.59% and 10.54% for RO based on the PIs and optimization based on the expected values, respectively. This indicates that the RO based on the PIs with moderate CP efficiently account for shortage up to a certain level of the probability of the uncertain events occurrence. Note that the energy shortage due to large failure rates of the electrical lines optimized by RO based on PIs tends to the results provided by the optimization based on expected values. In order to increase the robustness to failures, PIs with higher CP would have to be used.

At the same time, the surplus caused by the low available wind power used by the RO remains almost the same, with a minor increase of about 1% between a MTTF/MTTR of 3097/2 and 154/9, respectively. This increase is due to the increase of the electrical line failures between D and the other microgrid players, which results in the rise of the energy surplus in the microgrid.

It is important to highlight that the RO based on the PIs is generally characterized by smaller shortages and a higher surpluses than the optimization based on the expected values.

Due to the particular characteristics and data of the case study considered in this paper, the negative imbalance is smaller than the positive imbalance. In this view, the variations in the negative imbalance generate a small impact on the performance ratios (12) and (13), which show a decrease of 0.66 and 1.02% between a MTTF/MTTR of 3097/2 and 154/9, for the RO based on the PIs and the optimization based on the expected values, respectively. Note that the surplus and shortage values depend on different microgrid parameters, i.e., the microgrid structure and characteristics, strategy of the agents, optimization constraints, etc. In this view, the higher the shortage the higher impact on the performance ratios, especially for the optimization based on the expected values, which is more sensible to the negative imbalances.

Table 2. Performance ratios γ^P of the RO based on PIs and the optimization based on the expected values.

%		10	20	40	60	80	100	120	140	160	180	200	220	240
3097/2	RO	97	96.6	**95.7**	**94.9**	**94.1**	**93.2**	**92.4**	**91.6**	**90.7**	**89.9**	**89.0**	**88.2**	**87.4**
	D	97.5	96.7	95.2	93.6	92	90.4	88.8	87.2	85.6	84	82.4	80.8	79.2
154/9	RO	96.4	95.2	93.3	91.2	**89.2**	**87.1**	**85**	**83**	**80.9**	**78.9**	**76.8**	**74.7**	**73.1**
	D	97.1	95.7	93.7	91.4	89.1	86.8	84.6	82.3	80	77.7	75.4	73.2	70.9

Table 2 provides the information about the values of the performance ratios γ^P of the RO based on the PIs and the optimization based on the expected values obtained for the two extreme scenarios presented in Table 2, i.e., MTTF/MTTR of 3097/2 and 154/9, respectively. As it can be observed, both optimization approaches provide good performance, which is comparable to the performances of different approaches tested in [68]. The RO based on the PIs becomes more advantageous with the increase of the negative imbalance price (bold values).

Based on the results in Table 2, the variation of the performance ratio γ^P depends not only on the energy shortage and surplus, but also on the spot and upstream electricity prices. Figure 7 illustrates the variation of the difference between the performance ratios obtained for the RO based on the PIs and the optimization based on the expected value for two extreme scenarios, i.e., MTTF/MTTR of 3097/2 and 154/9, respectively. Note that in Figure 7 the percentage of the price for the positive imbalance is considered to be 5% of the spot price. The Standard Deviation

(SD) is used to quantify the uncertainty of the performance ratios in the *Ns = 20* scenarios summarized in Table 1.

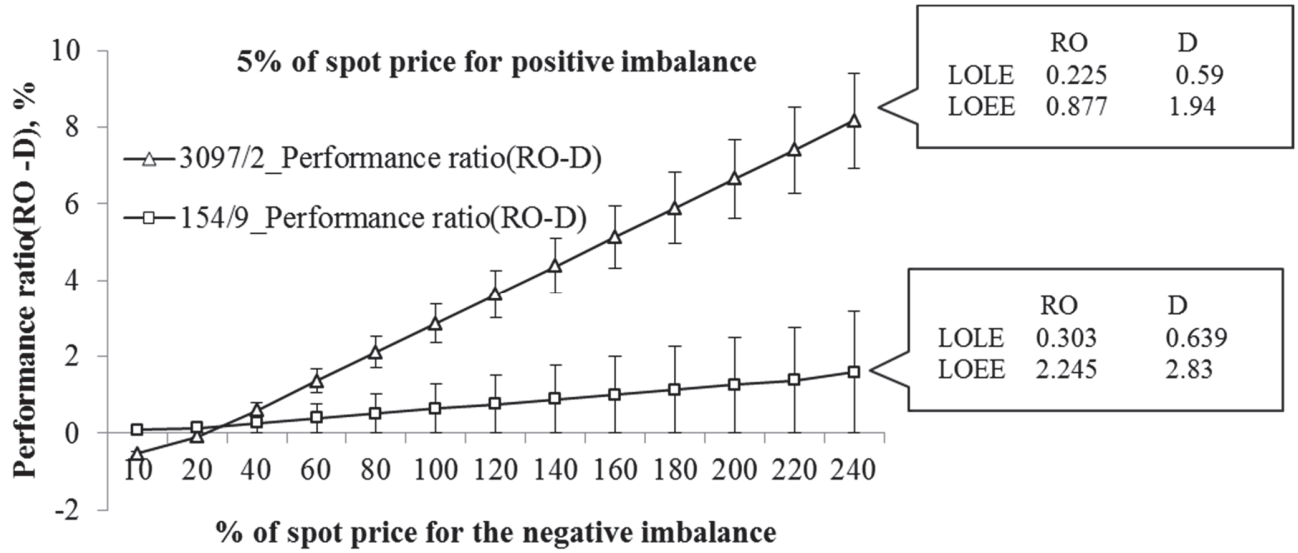

Figure 7. Performance ratio γ^P differences for RO based on PIs and optimization based on the expected values.

It can be observed that with the increase of the negative imbalance price, the network optimized by RO based on the PIs gains in profitability in terms of performance ratio. This profitability is even more evident for the case of MTTF/MTTR = 3097/2. For the case of MTTF/MTTR = 154/9, the performance ratio of the RO based on the PIs shows a small increase and remains close to the performance ratio obtained with the optimization based on the expected values. According to the reliability indicators, shown for the two considered scenarios in the right part of Figure 7, the RO based on the PIs holds the lowest LOLE and LOEE for both scenarios. The increase of MTTF from 3097 to 154 h decreases the reliability indicators for both optimization approaches. However, the RO based on the PIs is more reliable in comparison with the optimization based on the expected values.

Figure 8 a-d shows the variation of the performance ratio in a three-dimensional coordinate system defined by the following axes: percentage of the negative imbalance price (%), MTTF/MTTR (h) and the difference between the performance ratio values calculated for the RO based on the PIs and the optimization based on the expected values (%). The performance ratio difference provides a visual illustration of the profitability for the two approaches: the white bars

(negative values) show the advantage to use the optimization based on the expected values over the RO based on the PIs and the grey bars (positive values) indicates a better performance of the RO based on the PIs. Each figure plots different values for the positive imbalance prices.

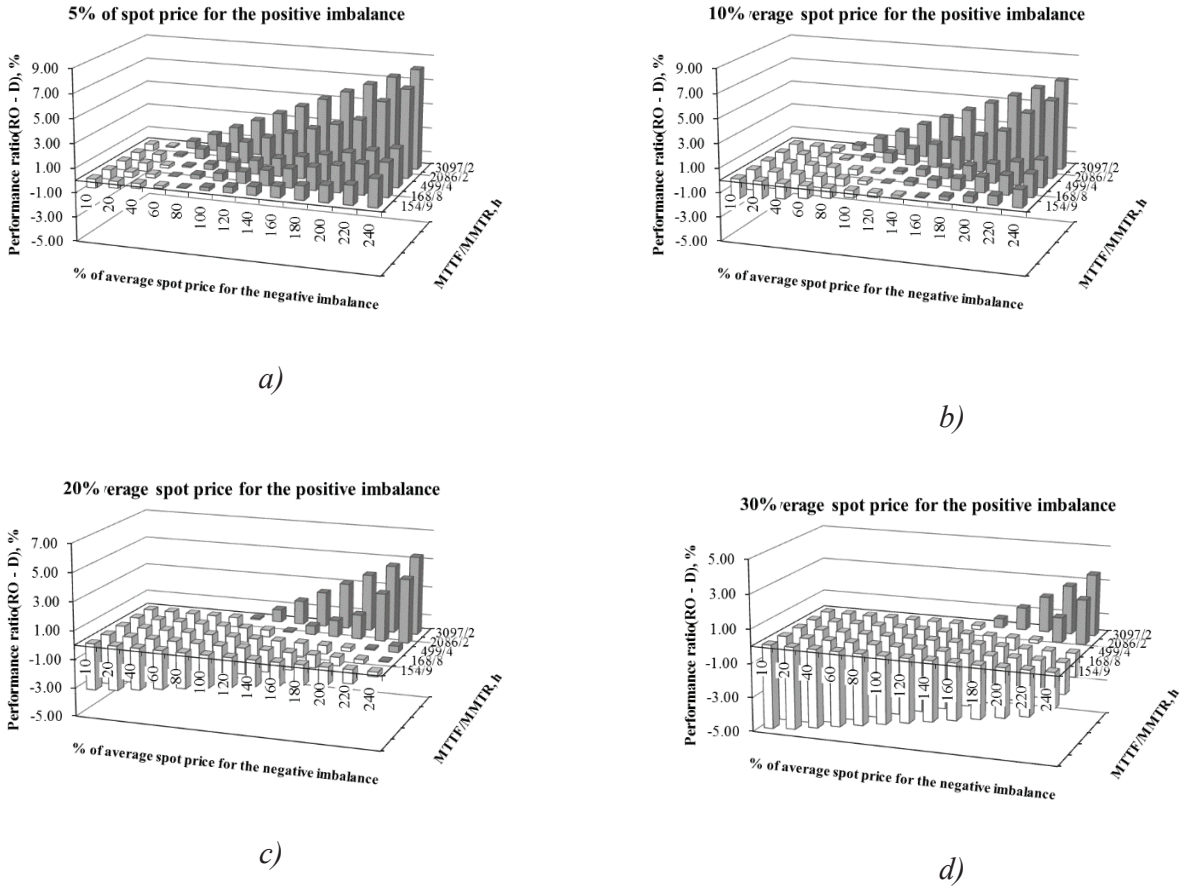

Figure 8. Performance ratio differences for RO based on PIs and the optimization based on the expected values depending on the negative imbalance price and MTTF/MTTR for different percentages of spot price for the positive imbalance: a) 5%; b) 10%; c) 20%; d) 30%.

As it can be observed in *Figure 8 a*, the increase of the negative imbalance price makes the use of the RO based on the PIs more profitable in terms of the performance ratio (starting with 40% of average spot price for the negative imbalance). This profitability becomes significant as the rates of failures occurrence are lower, i.e., MTTF/MTTR = 3097/2 h. Note that the advantage of RO slightly decreases with the increase of the MTTF of the electrical lines due to the increase of

the negative imbalance part (cf. *Figure 8 a*). The increase of the positive imbalance price compensates progressively the penalty paid for the negative imbalance and reduces the advantage of the RO based on the PIs.

We have to underline once again that the performance ratio characterizes the microgrid revenues in presence of negative and positive imbalances. However, these results highly depend on the election on the model parameters, i.e., the microgrid structure and characteristics, strategy of the agents, optimization constraints, etc.

6.2. Energy demand and prices peaks

We tested different values of the peak price applied during the peak periods, i.e., from noon to 6 p.m. Table 3 recalls the performance ratios γ^C of the RO based on the PIs and the optimization based on expected values obtained for two extreme peak occurrence probability scenarios: 0.1 and 0.8.

Table 3. Performance ratios and reliability indicators for the RO based on PIs and the optimization based on expected values.

%/ CPP rate			1	2	4	6	8
Probability of peak occurrence	0.1	RO	94.56	94.35	93.94	**93.54**	**93.16**
		D	95.74	95.23	94.29	93.44	92.66
	0.8	RO	92.3	**90.33**	**87.7**	**86.02**	**84.85**
		D	92.51	89.87	86.57	84.58	83.25

As it can the observed, the increase of the probability of peak occurrence generates a decrease of the performance ratio γ^C. Additionally, the increase of the CPP rate degrades the performance ratio for both RO based on the PIs and the optimization based on the expected values. It can be noticed that the RO based on the PIs becomes more advantageous with the increase of the CPP rate (bold values).

Figure 9 illustrates the influence of the progressive increase of the probability of the load peak occurrence on the output indicators.

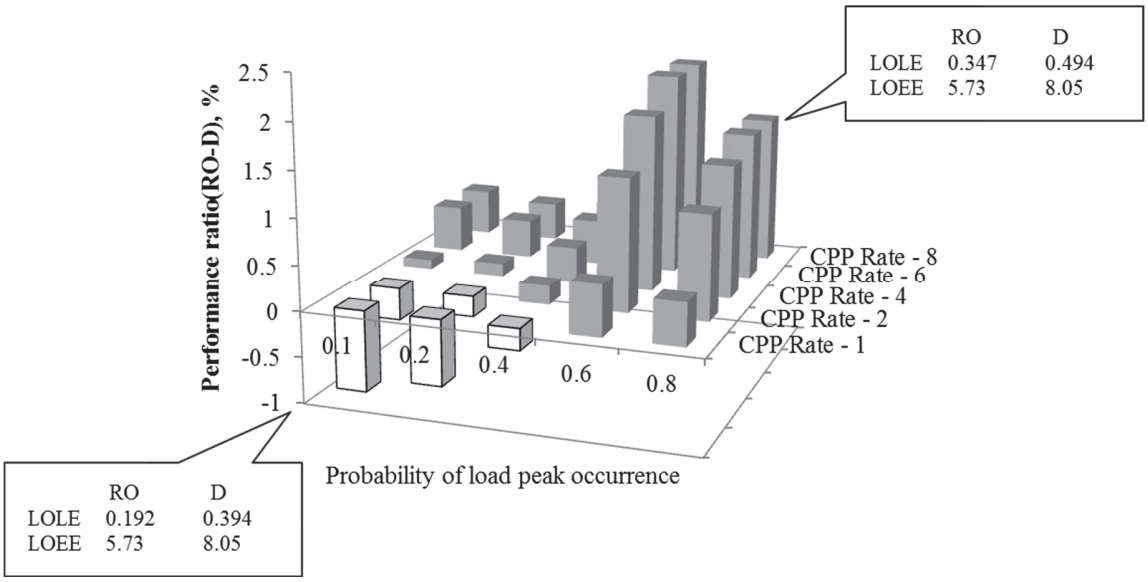

Figure 9. Performance ratio γ^C differences for RO based on PIs and optimization based on the expected value.

It can be observed, that with the increase of the probability of peak occurrence, the RO based on the PIs performs better in terms of the performance ratio γ^C. This profitability is even more evident for the case of a maximum CPP rate. Moreover, the peak of profitability for the RO is situated at a probability of peak occurrence of 0.6. The progressive increase of the probability of peak occurrence will decrease the performance ratio γ^C obtained with the RO. According to the reliability indicators, shown for two extreme scenarios of 0.1 and 0.8 of probability of peak occurrence, the RO based on the PIs holds the lowest LOLE and LOEE for both scenarios. The increase of probability of peak occurrence from 0.1 to 0.8 degrades the reliability indicators for both optimization approaches. However, the RO based on the PIs is more reliable in comparison with the optimization based on the expected values.

7. CONCLUSIONS

The present paper provides an extended analysis of microgrid energy management under two optimization frameworks: Robust Optimization (RO) based on Prediction Intervals (PIs) and optimization based on expected values. The considered frameworks are exemplified on a microgrid including the following stakeholders: a middle-size train station (TS) with integrated

PV power production system (PV), a urban wind power plant (WPP), and a surrounding residential district (D). The system is described by Agent-Based Modelling (ABM), in which each stakeholder, modelled as an individual agent, aims at a particular goal, i.e., decreasing its expenses from power purchases or increasing its revenues from power selling.

The proposed analysis allows evaluating the impact of different levels of uncertainty on the agent expense and revenue functions, as well as on the overall microgrid reliability. Furthermore, the imbalance cost has been introduced to quantify the effect of prediction errors and failure occurrences. The analysis shows how the probability of occurrence of some specific uncertain events, e.g. failures of electrical lines and electricity demand and price peaks, highly conditions the reliability and the performance indicators of the microgrid under the two optimization approaches: RO based on the PIs and optimization based on expected values.

In particular, the proposed methodology allows identifying the level of uncertainty in the operational and environmental conditions upon which RO performs better than an optimization based on expected values.

This analysis is intended to assist decision-makers to select microgrid energy management actions that provide an adequate trade-off between system reliability and economic performance.

Regarding the results obtained in the numerical case study considered, the following conclusions have been drawn:

- The reliability analysis performed for different levels of wind power output uncertainty shows a strong improvement on the reliability indicators if RO based on the PIs is used
- As it was expected, the increase of the probabilities of uncertain events, i.e., failure of electrical lines, frequency of electricity peaks and increase of electricity price during peak-hours, shows the advantage of RO based on the PIs in comparison with an optimization based on the expected values.
- The price variations play a significant role in the system's performance. In particular, with an increase of either the price for the negative imbalance or the peak-hours price, the RO shows a clear advantage in comparison with the optimization based on expected values. Thus, there is a threshold probability of uncertain events occurrence above which RO based on PIs performs better, which strongly depends on the price variations.

- In addition, there is a second threshold probability that indicates some limitations of the RO based on the PIs. In particular, the PIs considered in this paper, which are obtained from a CP of about 50% , efficient up to certain level of the probability of the uncertain events occurrence.

The adoption of RO based on the PIs or optimization based on expected values must be guided by the knowledge on the environmental and operational conditions of the microgrid under study. Future research will consider the development of hybrid optimization frameworks, for switching between different optimization techniques by considering the different environmental and operational conditions of the microgrid that may be expected at different times.

ACKNOWLEDGMENTS

The authors acknowledge the support of the Chair on Systems Science and the Energetic Challenge, European Foundation for New Energy - Electricite de France (EDF) at Ecole Centrale Paris and Supelec.

APPENDIX A

A.1. Optimization framework

For completeness of the paper, we present the optimization framework as considered in [22] and here taken for our analysis. The decision-making strategy for each agent, identified by the use of RO, is based on the expenses minimization for the D and TS and the revenues maximization for the WPP. The approach adopted in this paper allows the linear formulation of the robust counterpart of an optimization problem [17]. The RO of energy scheduling for the TS, WPP and D, where the objective functions to be optimized are formulated in terms of expenses for the TS (eq.(A.6)) and D (eq.(A.18)), and revenues for the WPP (eq.(A.30)), are posed as follows.

Train Station

Minimize $\boldsymbol{\alpha^{TS}}$

s.t.

$$-S_t^{TS} + L_t^{TS} + \delta_t^{TS,ch} \cdot R^{TS,stor} - \delta_t^{TS,dis} \cdot R^{TS,stor} + V_t^{PV} - P_t^{PV} \cdot x_t^{n+1} + E_t^{TS} \cdot x_t^{n+2} + z_t^{Power} \cdot \Gamma_t^{Power} + p_t^{P_t^{PV}} + p_t^{E_t^{TS}} \leq 0 \qquad \forall t \tag{A.1}$$

$$z_t^{Power} + p_t^{P_t^{PV}} \geq \hat{P}_t^{PV} \cdot y_t^{P_t^{PV}},\ z_t^{Power} + p_t^{E_t^{TS}} \geq \hat{E}_t^{TS} \cdot y_t^{E_t^{TS}} \qquad \forall t \tag{A.2}$$

$$-y_t^{P_t^{PV}} \leq x_t^{n+1} \leq y_t^{P_t^{PV}}, -y_t^{E_t^{TS}} \leq x_t^{n+2} \leq y_t^{E_t^{TS}} \qquad \forall t \tag{A.3}$$

$$L_t^{TS} + V_t^{PV} - P_t^{PV} \cdot x_t^{n+1} + z_t^{Micro} \cdot \Gamma_t^{Micro} + p_t^{P_t^{PV}} \leq 0 \qquad \forall t \tag{A.4}$$

$$z_t^{Micro} + p_t^{P_t^{PV}} \geq \hat{P}_t^{PV} \cdot y_t^{P_t^{PV}} \qquad \forall t \tag{A.5}$$

$$\sum_{t=0}^{T} (c_t^p \cdot S_t^{TS} - c_t^s \cdot L_t^{TS} - c_t^D \cdot V_t^{PV}) + \sum_{t=0}^{T} \left(z_t^{Cost} \cdot \Gamma_t^{Cost} + p_t^{c_t^p} + p_t^{c_t^s} + p_t^{c_t^D} \right) \leq \alpha^{TS} \tag{A.6}$$

$$z_t^{Cost} + p_t^{c_t^p} \geq \hat{c}_t^p \cdot y_t^{c_t^p}, z_t^{Cost} + p_t^{c_t^s} \geq \hat{c}_t^s \cdot y_t^{c_t^s}, z_t^{Cost} + p_t^{c_t^D} \geq \hat{c}_t^D \cdot y_t^{c_t^D} \qquad \forall t \tag{A.7}$$

$$-y_t^{c_t^p} \leq S_t^{TS} \leq y_t^{c_t^p}, -y_t^{c_t^s} \leq L_t^{TS} \leq y_t^{c_t^s}, -y_t^{c_t^D} \leq V_t^{PV} \leq y_t^{c_t^D} \qquad \forall t \tag{A.8}$$

$$S_t^{TS} \geq 0, L_t^{TS} \geq 0, V_t^{PV} \geq 0 \qquad \forall t \tag{A.9}$$

$$\begin{cases} \beta \cdot \tilde{E}_t^D \leq V_t^{PV}, & if\ P_t^{PV} \geq \beta \cdot \tilde{E}_t^D \\ 0 \leq V_t^{PV}, & otherwise \end{cases} \qquad \forall t \tag{A.10}$$

$$R_t^{TS} \leq R_{t-1}^{TS} + \delta_t^{TS,ch} \cdot R^{TS,stor} - \delta_t^{TS,dis} \cdot R^{TS,stor} \qquad \forall t \tag{A.11}$$

$$\delta_t^{TS,ch} + \delta_t^{TS,dis} \leq 1 \qquad \forall t \tag{A.12}$$

$$0 \leq \delta_t^{TS,ch} \leq 1, 0 \leq \delta_t^{TS,dis} \leq 1 \qquad \forall t \tag{A.13}$$

$$0 \leq R_t^{TS} \leq R^{TS,max}, \qquad \forall t \tag{A.14}$$

District

Minimize $\boldsymbol{\alpha^D}$

s.t.

$$-S_t^D - V_t^{PV} - V_t^{WPP} + (R_t^D - R_{t-1}^D) + E_t^D \cdot x_t^{n+1} + z_t^{Power} \cdot \Gamma_t^{Power} + p_t^{E_t^D} \leq 0 \quad \forall t \tag{A.15}$$

$$z_t^{Power} + p_t^{E_t^D} \geq \hat{E}_t^D \cdot y_t^{E_t^D} \quad \forall t \tag{A.16}$$

$$-y_t^{E_t^D} \leq x_t^{n+1} \leq y_t^{E_t^D} \quad \forall t \tag{A.17}$$

$$\sum_{t=0}^{T} \left(c_t^p \cdot S_t^D + c_t^D \cdot V_t^{WPP} + c_t^D \cdot V_t^{PV}\right) + \sum_{t=0}^{T} \left(z_t^{Cost} \cdot \Gamma_t^{Cost} + p_t^{c_t^p} + p_t^{c_t^D}\right) \leq \alpha^D \tag{A.18}$$

$$z_t^{Cost} + p_t^{c_t^p} \geq \hat{c}_t^p \cdot y_t^{c_t^p}, z_t^{Cost} + p_t^{c_t^D} \geq \hat{c}_t^D \cdot y_t^{c_t^D} \quad \forall t \tag{A.19}$$

$$-y_t^{c_t^p} \leq S_t^D \leq y_t^{c_t^p}, -y_t^{c_t^D} \leq V_t^{WPP} + V_t^{PV} \leq y_t^{c_t^s} \quad \forall t \tag{A.20}$$

$$R_t^D \leq R_{t-1}^D + \delta_t^{D,ch} \cdot R^{D,stor} - \delta_t^{D,dis} \cdot R^{D,stor} \quad \forall t \tag{A.21}$$

$$\delta_t^{D,ch} + \delta_t^{D,dis} \leq 1 \quad \forall t \tag{A.22}$$

$$0 \leq \delta_t^{D,ch} \leq 1, 0 \leq \delta_t^{D,dis} \leq 1 \quad \forall t \tag{A.23}$$

$$0 \leq R_t^D \leq R^{D,max} \quad \forall t \tag{A.24}$$

$$S_t^D \geq 0 \quad \forall t \tag{A.25}$$

$$V_t^{PV} = \tilde{V}_t^{PV}, V_t^{WPP} = \tilde{V}_t^{WPP} \quad \forall t \tag{A.26}$$

Wind Power Plant

Maximize $\boldsymbol{\alpha^{WPP}}$

s.t.

$$L_t^{WPP} + V_t^{WPP} - P_t^{WPP} \cdot x_t^{n+1} + z_t^{Power} \cdot \Gamma_t^{Power} + p_t^{P_t^{WPP}} \leq 0 \quad \forall t \tag{A.27}$$

$$z_t^{Power} + p_t^{P_t^{WPP}} \geq \hat{P}_t^{WPP} \cdot y_t^{P_t^{WPP}} \quad \forall t \tag{A.28}$$

$$-y_t^{P_t^{WPP}} \leq x_t^{n+1} \leq y_t^{P_t^{WPP}} \quad \forall t \tag{A.29}$$

$$\sum_{t=0}^{T}(c_t^S \cdot L_t^{WPP} + c_t^D \cdot V_t^{WPP}) - \sum_{t=0}^{T}\left(z_t^{Cost} \cdot \Gamma_t^{Cost} + p_t^{c_t^S} + p_t^{c_t^D}\right) \geq \alpha^{WPP} \quad \text{(A.30)}$$

$$z_t^{Cost} + p_t^{c_t^S} \geq \hat{c}_t^S \cdot y_t^{c_t^S}, z_t^{Cost} + p_t^{c_t^D} \geq \hat{c}_t^D \cdot y_t^{c_t^D} \qquad \forall t \quad \text{(A.31)}$$

$$-y_t^{c_t^S} \leq L_t^{WPP} \leq y_t^{c_t^S}, -y_t^{c_t^D} \leq V_t^{WPP} + V_t^{PV} \leq y_t^{c_t^S} \qquad \forall t \quad \text{(A.32)}$$

$$\begin{cases} \gamma \cdot \tilde{E}_t^D \leq V_t^{WPP}, & if\ P_t^{WPP} \geq \gamma \cdot \tilde{E}_t^D \\ 0 \leq V_t^{WPP}, & otherwise \end{cases} \qquad \forall t \quad \text{(A.33)}$$

$$L_t^{WPP} \geq 0, V_t^{WPP} \geq 0, V_t^{PV} \geq 0 \qquad \forall t \quad \text{(A.34)}$$

where L_t^{TS} and L_t^{WPP} *(kWh)* are the portions of energy sold to the external grid by the TS and WPP, respectively, S_t^{TS} and S_t^D *(kWh)* are the portions of energy purchased from the external grid by the TS and D, respectively, V_t^{PV} and V_t^{WPP} *(kWh)* are the portions sold to the D and generated by the PV panels of the TS and WPP, respectively, β and γ are the coefficients defining the minimum amount of energy to be sold to D by TS and WPP, respectively, $\tilde{E}_t^D$ (kWh) is the expected energy demand for D (for the moment, considered without uncertainty) at time step *t*, predicted by TS and WPP, $\tilde{V}_t^{PV}$ and $\tilde{V}_t^{WPP}$ (kWh) are the energy portions, which TS and WPP are ready to sell to D at time step *t*. The variables $\delta_t^{TS,ch}$, $\delta_t^{TS,dis}$, $\delta_t^{D,ch}$ *and* $\delta_t^{D,dis}$ are binary variables, which take values 0 or 1 to indicate that the battery can either only be charged or discharged at time t.

The coefficients β and γ in eqs. (A.10) and (A.33) allow regulating the energy exchanges between the microgrid agents, by imposing the minimum amount of energy that WPP and TS can supply to D under conditions of availability of wind and solar energy outputs, and promoting the local energy exchanges among the microgrid agents.

The variables z_t^{Power}, z_t^{Cost}, z_t^{Micro} $p_t^{P_t^{WPP}}$, $p_t^{P_t^{PV}}$, $p_t^{E_t^D}$, $p_t^{E_t^{TS}}$, $p_t^{c_t^p}$, $p_t^{c_t^S}$, $p_t^{c_t^D}$, $y_t^{P_t^{WPP}}$, $y_t^{P_t^{PV}}$, $y_t^{E_t^D}$, $y_t^{E_t^{TS}}$, $y_t^{c_t^p}$, $y_t^{c_t^S}$ and $y_t^{c_t^D}$ are dual or auxiliary variables needed to formulate the linear counterpart of the RO problem [17]. These are forced to be greater than or equal to zero, similarly, x_t^{n+1} and x_t^{n+2} are auxiliary variables that are forced to be equal to one. Γ_t^{Power} and Γ_t^{Cost} define the level of uncertainty considered in each optimization model (a zero value corresponds to the deterministic problem) and are such that $0 \leq \Gamma_t^{Power} \leq 1$ and $0 \leq \Gamma_t^{Cost} \leq 2$ for the D and WPP,

and $0 \leq \Gamma_t^{Power} \leq 2$ and $0 \leq \Gamma_t^{Cost} \leq 3$ for the TS. The upper limits of Γ_t^{Power} and Γ_t^{Cost} indicate the maximum number of uncertain parameters handled by the RO formulated here above. The value of the uncertainty levels can be fixed and adjusted independently by each agent depending on the uncertainty related to different numerical case studies, i.e., $\Gamma_t^{Power} = 1$ for the D and TS to account for the uncertainty in wind and PV power output in case of wind storms and associated lines failures, and $\Gamma_t^{Cost} = 2$ for D and WPP and $\Gamma_t^{Power} = 3$ for TS to account for the uncertainty in energy demands and electricity prices.

Note that the RO presents the advantage that it represents the uncertainty related to the variations of the operational or environmental conditions in terms of PI without making any assumption about the probabilistic distribution of the uncertainty. For example, for the WPP in the robust formulation the level of uncertainty $\hat{P}_t^{WPP}$ can be defined as $\hat{P}_t^{WPP} = (P_t^{WPP,ub} - P_t^{WPP,lb})/2$, where $P_t^{WPP,ub}$ and $P_t^{WPP,lb}$ (kWh) are the upper and lower prediction bounds at time t, respectively. In this work, we take the mean of the PIs as point estimate of the wind energy output P_t^{WPP} in eq. (A.27). The point estimates of the other uncertain variables are the values calculated with the models of the individual components or other statistical data described in [22].

The RO problems are solved by using the optimization package CPLEX, implemented in Java code, which guaranty global optimality for mixed integer linear programming (MIP) problems (the iterative process of optimization in CPLEX is not illustrated in the paper: the interested reader may refer to [73] for further details). After optimization, the decisions are shared among the agents through the communication process indicated in the paper.

A.2. Communication framework

Figure. A1 depicts the communication interactions among the microgrid agents. It can be noted that the microgrid does not include an independent operator, responsible for coordinating, controlling and operating the electric power system or/and market, as in most of the actual power grids. Indeed, we assume that all coordination procedures are done in a decentralized manner through direct negotiation among the agents, similar to [10], [11]. However, to facilitate the

agents communications, an additional agent called Independent System Operator (ISO) is introduced in the model, similar to [74], assisting communication between microgrid agents.

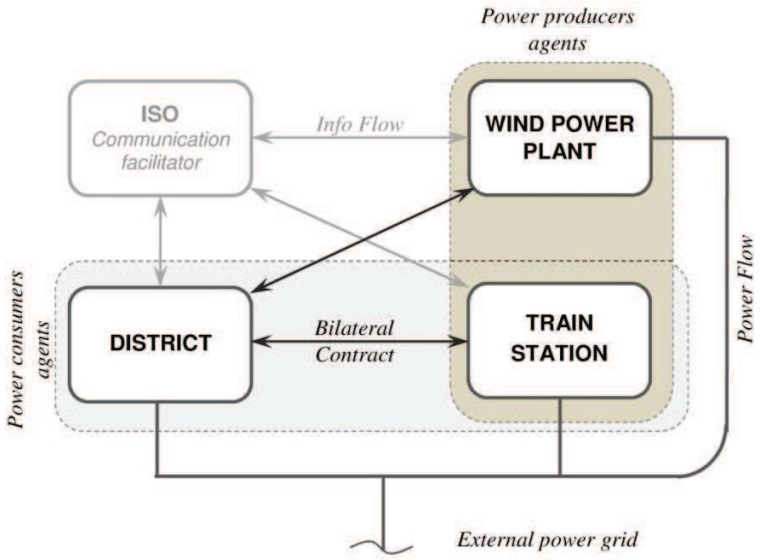

Figure. A1. Multi-layered interaction between agents [22].

The microgrid agents participate in the decision-making framework as illustrated in Figure. A2. For the sake of clarity, the hierarchy of decisions considered in this work gives priority to the energy producers, i.e., the TS and the WPP, to decide the renewable energy V_t^{PV} and V_t^{WPP} that is available to be sold to the D, and the energy quantities L_t^{PV} and L_t^{WPP} that are sold to the external grid at each time step *t*. These decisions are transmitted through the ISO agent to the D, which considers these decisions as constant parameters for its optimization problem (eqs. (A.15) and (A.18) in the expenses optimization for D). After the determination of other energy scheduling variables, such as S_t^D and R_t^D, the D sets a bilateral agreement with the TS and the WPP in order to purchase V_t^{PV} and V_t^{WPP}, respectively. The duration of the bilateral contract is assumed to be one hour.

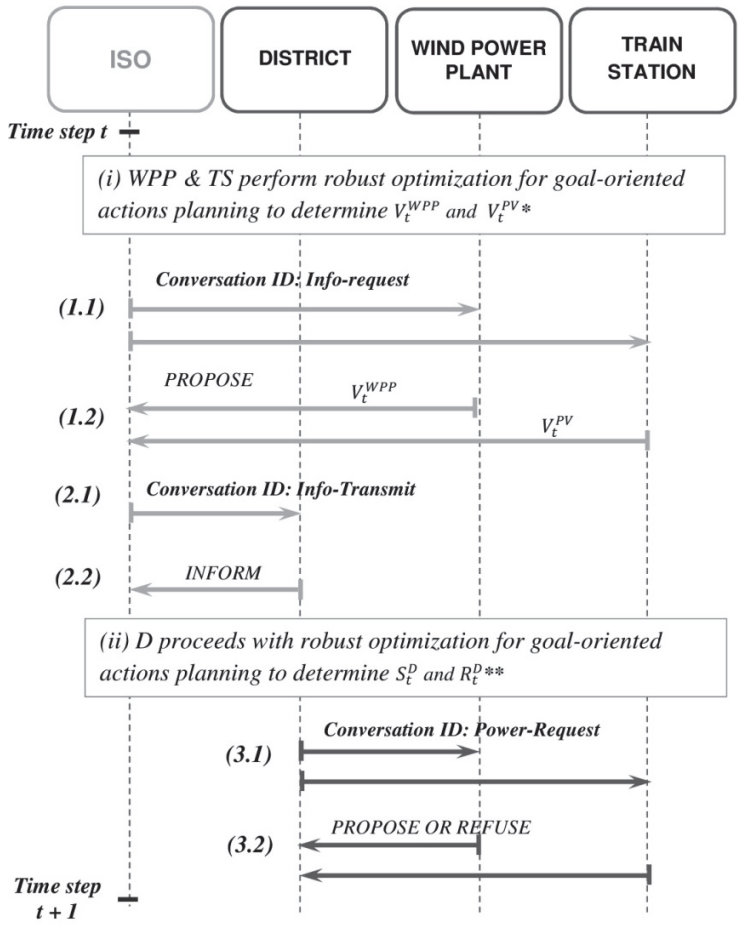

Figure. A2. Example of agents communication at time step t [22].

Table A1 gathers the previsions of the operational conditions (i) made by the agents themselves and (ii) received from other agents through the ISO and (iii) the decision variables.

Table A1. Previsions and decision variables.

Previsions of the operational conditions	D	WWP	TS
(i) agent personal previsions*	$E_t^D;\ c_t^p;\ c_t^D$	$P_t^{WPP};\ c_t^s;\ c_t^D$	$E_t^{TS};\ P_t^{PV};\ c_t^p;\ c_t^D;\ c_t^s$
(ii) previsions received from other agents through *ISO*	$V_t^{PV};\ V_t^{WPP}$	-	-
(iii) decision variables based on the above previsions	$S_t^D;\ R_t^D$	$V_t^{WPP};\ L_t^{WPP}$	$V_t^{PV};\ L_t^{TS};\ S_t^{TS};\ R_t^{TS}$

* Personal previsions of agents are represented by PIs for RO and point predictions for the deterministic optimization.

Note that the adopted hierarchical decision scheme allows, on the one hand, the TS and the WPP increasing their revenues by deciding which amount of energy to sell to the D or to the external grid using the most profitable actions planning; on the other hand, it gives the possibility to the D

to purchase the emissions-free and less expensive energy generated by the TS and WPP in the microgrid.

A.3. Uncertainties in energy management

The expenses and revenues of each agent, and the global reliability of the microgrid are affected by uncertain parameters, such as the energy outputs from renewable generators P_t^{PV} and P_t^{WPP}, the energy demands of the consumers E_t^{TS} and E_t^{D}, and the electricity prices c_t^{p}, c_t^{s} and c_t^{D}. This section illustrates the procedure used to account for these uncertainties.

A.3.1. Energy output of renewable energy generators

The energy outputs from the renewable generators are affected by the variability of the renewable sources of energy, i.e., wind for WPP and solar irradiation for PV.

As discussed previously, the uncertainty related to the availability of the wind energy output P_t^{WPP} is described by PIs, estimated by a multi-perceptron NN [27]. The PIs are optimized in terms of maximum CP and minimum PIW. A multi-objective genetic algorithm (namely, NSGA-II) is used to find the optimal parameters (weights and biases) of the NN. Pareto-optimal solution sets of several non-dominated solutions with respect to the two objectives (CP and PIW), are generated.

As presented in Section 3, the expected value of PV energy output P_t^{PV} is simulated based on the solar irradiation and technical specification of PV module [33], [34]. In absence of a prediction model for the PV energy output, the related uncertainty is described by intervals, whose lower and upper bounds are symmetric around the expected value of PV energy output. The width of the interval is selected to account for the variability of the PV energy output in the time period considered.

The actual energy output of renewable generators is also affected by mechanical failures, which may lead to periods of production unavailability during the subsequent repairs. A description of this effect is given by the compound quantitative indicator called technical unavailability [75]. Mechanical failures of generation units of the same type are, for simplicity, assumed to be independent from each other: no common causes for failures are considered. Moreover, no particular reduction of energy production due to units degradation has been considered: only two states are possible, i.e., 100% of technical availability and 0% during the repair upon a failure.

Failure and repair times are assumed to follow exponential distributions, considering the useful life of the components. For the numerical application of this paper, the Mean Time To Failure (MTTF) and Mean Time To Repair (MTTR) of the wind energy generation units have been taken equal to 1920 h and 25 h, respectively [76]. The failures of the power electronics parts are major contributors to the reliability problem and represent about 40% of the annual failure frequency for the wind turbines, based on long-term feedback experience [40], which is almost two times higher than the annual frequency of other wind turbine components. For the sake of simplicity, in this research we used the term 'mechanical failure' to represent all types of failures of the wind turbines and the generators.

Failure times and repair durations are simulated by sampling from the exponential distribution of failure and repair times for the given MTTF and MTTR values, with the inverse transform technique [77].

A.3.2. Energy demand

Similar to the wind energy output, PIs accounting for the variability of the energy demands E_t^{TS} and E_t^D, are used as estimated a NSGA – trained NN [27].

A.3.3. Electricity prices

Similar to the PV energy output, the uncertainty related to the variability of electricity prices c_t^p, c_t^s and c_t^D is accounted for in the form of intervals, whose lower and upper bounds are symmetric around the expected value of each variable. The width of the intervals is selected to account for the fluctuations of these variables in the time period considered.

REFERENCES

[1] J. C. Glenn, T. J. Gordon, and E. Florescu, "2009 State of the Future," 2009.

[2] B. J. Owen, "The planet 's future : Climate change ' will cause civilisation to collapse '," *The Independent*, London, 2009.

[3] N. D. Hatziargyriou, *European Transactions on Electrical Power. Special Issue: Microgrids and Energy Management*, no. December 2010. 2011, pp. 1139–1342.

[4] A. G. De Muro, J. Jimeno, and J. Anduaga, "Architecture of a microgrid energy management system," *European Transactions on Electrical Power*, vol. 21, pp. 1142–1158, 2011.

[5] E. Kuznetsova, K. Culver, and E. Zio, "Complexity and vulnerability of Smartgrid systems," in *Advances in Safety, Reliability and Risk Management, European Safety and Reliability Conference (ESREL 2011)*, 2011, pp. 2474–2482.

[6] M. H. Colson, C. M. Nehrir, and R. W. Gunderson, "Multi-agent Microgrid Power Management," in *18th IFAC World Congress*, 2011, pp. 3678–3683.

[7] P. P. Reddy and M. M. Veloso, "Strategy Learning for Autonomous Agents in Smart Grid Markets," in *Twenty-Second International Joint Conference on Artificial Intelligence*, 2005, pp. 1446–1451.

[8] T. Krause, E. Beck, R. Cherkaoui, A. Germond, G. Andersson, and D. Ernst, "A comparison of Nash equilibria analysis and agent-based modelling for power markets," *International Journal of Electrical Power & Energy Systems*, vol. 28, no. 9, pp. 599–607, Nov. 2006.

[9] A. Weidlich and D. Veit, "A critical survey of agent-based wholesale electricity market models," *Energy Economics*, vol. 30, no. 4, pp. 1728–1759, Jul. 2008.

[10] S. Yousefi, M. P. Moghaddam, and V. J. Majd, "Optimal real time pricing in an agent-based retail market using a comprehensive demand response model," *Energy*, vol. 36, no. 9, pp. 5716–5727, Sep. 2011.

[11] Z. Jun, L. Junfeng, W. Jie, and H. W. Ngan, "A multi-agent solution to energy management in hybrid renewable energy generation system," *Renew. Energ.*, vol. 36, no. 5, pp. 1352–1363, May 2011.

[12] E. Kuznetsova, C. Ruiz, Y. F. Li, E. Zio, G. Ault, and K. Bell, "Reinforcement learning for microgrid energy management," *Energy*, vol. 59, pp. 133–146, 2013.

[13] Y. Zeng, Y. Cai, G. Huang, and J. Dai, "A Review on Optimization Modeling of Energy Systems Planning and GHG Emission Mitigation under Uncertainty," *Energies*, vol. 4, no. 12, pp. 1624–1656, Oct. 2011.

[14] J. Lagorse, M. G. Simoes, and A. Miraoui, "A Multiagent Fuzzy-Logic-Based Energy Management of Hybrid Systems," *Industry Applications, IEEE Transactions on*, vol. 45, no. 6, pp. 2123–2129, 2009.

[15] J. Solano Martínez, R. I. John, D. Hissel, and M.-C. Péra, "A survey-based type-2 fuzzy logic system for energy management in hybrid electrical vehicles," *Information Sciences*, vol. 190, pp. 192–207, May 2012.

[16] a. Ben-Tal and a. Nemirovski, "Robust solutions of uncertain linear programs," *Operations Research Letters*, vol. 25, no. 1, pp. 1–13, Aug. 1999.

[17] D. Bertsimas and M. Sim, "The Price of Robustness," *Operations Research*, vol. 52, no. 1, pp. 35–53, 2004.
[18] V. Krey, D. Martinsen, and H.-J. Wagner, "Effects of stochastic energy prices on long-term energy-economic scenarios," *Energy*, vol. 32, no. 12, pp. 2340–2349, Dec. 2007.
[19] Y. P. Cai, G. H. Huang, Z. F. Yang, Q. G. Lin, and Q. Tan, "Community-scale renewable energy systems planning under uncertainty—An interval chance-constrained programming approach," *Renewable and Sustainable Energy Reviews*, vol. 13, no. 4, pp. 721–735, May 2009.
[20] M. Liu, "An Interval-parameter Fuzzy Robust Nonlinear Programming Model for Water Quality Management," *Journal of Water Resource and Protection*, vol. 05, no. 01, pp. 12–16, 2013.
[21] Y. Li and G. Huang, "Robust interval quadratic programming and its application to waste management under uncertainty," *Environmental Systems Research*, vol. 1, no. 1, p. 7, 2012.
[22] E. Kuznetsova, C. Ruiz, Y. F. Li, and E. Zio, "Reliable microgrid energy management under environmental uncertainty and mechanical failures: an agent-based modeling and robust optimization," in *Safety, Reliability and Risk Analysis: Beyond the Horizon (ESREL 2013)*, 2013, pp. 2873 – 2882.
[23] A. Parisio, C. Del Vecchio, and A. Vaccaro, "Electrical Power and Energy Systems A robust optimization approach to energy hub management," *International Journal of Electrical Power and Energy Systems*, vol. 42, no. 1, pp. 98–104, 2012.
[24] C. Chen, Y. P. Li, G. H. Huang, and Y. F. Li, "A robust optimization method for planning regional-scale electric power systems and managing carbon dioxide," *Electrical Power and Energy Systems*, vol. 40, pp. 70–84, 2012.
[25] C. Chen, Y. P. Li, G. H. Huang, and Y. Zhu, "An inexact robust nonlinear optimization method for energy systems planning under uncertainty," *Renew. Energ.*, vol. 47, pp. 55–66, 2012.
[26] A. Khosravi, S. Nahavandi, D. Creighton, and F. A. Amir, "A Comprehensive Review of Neural Network-based Prediction Intervals and New Advances," *IEEE Trans. on Neural Net.*, vol. 22, no. 9, pp. 1341–1356, 2011.
[27] R. Ak, Y. F. Li, V. Vitelli, and E. Zio, "Multi-objective Generic Algorithm Optimization of a Neural Network for Estimating Wind Speed Prediction Intervals," *submitted to Applied Soft Computing*, 2013.
[28] E. Commission, "Photovoltaic Solar Energy Best Practice Stroies," 2002.
[29] E. Fischer and C. Lo, "Back to the future : Top trends in railway station design," *railway-technology.com*, 2011. [Online]. Available: http://www.railway-technology.com/features/featureback-to-the-future-top-trends-in-railway-station-design. [Accessed: 24-Sep-2013].
[30] RTE, "Bilan électrique 2012," 2012.
[31] L. Al-Sharif, "Modelling of escalator energy consumption," *Energy and Buildings*, vol. 43, no. 6, pp. 1382–1391, Jun. 2011.
[32] Ademe, "Eclairage public: routier, urban, grands espaces, illuminations et cadre de vie," 2002.
[33] F. A. Mohamed and H. N. Koivo, "System modelling and online optimal management of MicroGrid using mesh adaptive direct search," *Int. J. of Electr. Power and Energy Syst.*, vol. 32, no. 5, pp. 398–407, 2010.

[34] Y. M. Atwa, M. M. A. Salama, and R. Seethapathy, "Optimal renewable resources mix for distribution system energy loss minimization," *IEEE Trans. on Power Syst.*, vol. 25, no. 1, pp. 360–370, 2010.

[35] D. C. Hill, D. Mcmillan, K. R. W. Bell, and D. Infield, "Application of auto-regressive models to UK wind speed data for power system impact studies," *IEEE Trans. on Sustain. Energy*, vol. 3, no. 1, 2012.

[36] E. N. Dialynas and A. V. Machias, "Reliability modelling interactive techniques of power systems including wind generating units," *Archiv fur Elektrotechnik*, vol. 72, pp. 33 – 41, 1989.

[37] C. Fong, S. Haddad, and D. Patton, "The IEEE reliability test system - 1996," *IEEE Trans. on Power Syst.*, vol. 14, no. 3, 1999.

[38] EEX, "Hour Contracts - France," *European Energy Exchange*, 2013. [Online]. Available: http://www.eex.com/en/Market Data/Trading Data/Power/Hour Contracts | Spot Hourly Auction/spot-hours-table/2013-02-14/FRANCE. [Accessed: 13-Feb-2013].

[39] E. Kuznetsova, Y.-F. Li, C. Ruiz, and E. Zio, "An integrated framework of agent-based modelling and robust optimization for microgrid energy management," *submitted to Applied Energy*, 2013.

[40] B. Hahn, M. Durstewitz, and K. Rohrig, "Reliability of Wind Turbines Break down of Wind Turbines," in *Wind Energy*, Springer B., 2007, pp. 329–332.

[41] P. Tavner, Y. Qiu, A. Korogiannos, and Y. Feng, "The correlation between wind turbine turbulence and pitch failure," UK, 2010.

[42] C. Su, Q. Jin, and Y. Fu, "Correlation analysis for wind speed and failure rate of wind turbines using time series approach," *Journal of Renewable and Sustainable Energy*, vol. 4, no. 3, p. 032301, 2012.

[43] K. Alvehag and L. Söder, "A Reliability Model for Distribution Systems Incorporating Seasonal Variations in Severe Weather," *IEEE Transactions on Power Delivery*, vol. 26, no. 2, pp. 910–919, 2011.

[44] C. Lallemand, "Methodology for a Risk Based Asset Management," Royal Institute of Technology, 2008.

[45] B. B. Brabson and J. P. Palutikof, "Tests of the Generalized Pareto Distribution for Predicting Extreme Wind Speeds," *Journal of Applied Meteorology and Climatology*, vol. 39, no. 9, pp. 1627–1640, 2000.

[46] D. York, M. Kushler, and P. Witte, "Examining the Peak Demand Impacts of Energy Efficiency: A Review of Program Experience and Industry Practices," Washington, USA, 2007.

[47] F. Stern, "Chapter 10: Peak Demand and Time-Differentiated Energy Savings Cross-Cutting Protocols," in *The Uniform Methods Project: Methods for Determining Energy Efficiency Savings for Specific Measures*, no. April, 2013, pp. 1 – 13.

[48] J. Protasiewicz and P. S. Czczepaniak, "Neural Models of Demands for Electricity - Prediction and Risk Assessment," *Electrical Review*, vol. 88, no. 6, pp. 272–279, 2012.

[49] S. Heiken, D. Elzinga, S.-K. Kim, and Y. Ikeda, "Impact of Smart Grid Technologies on Peak Load to 2050," Paris, France, 2011.

[50] C. Sigauke, A. Verster, and D. Chikobvu, "Tail Quantile Estimation of Heteroskedastic Intraday Increases in Peak Electricity Demand," *Open Journal of Statistics*, vol. 02, no. 04, pp. 435–442, 2012.

[51] R. J. Hyndman and S. Fan, "Forecasting long-term electricity demand for," Melbourne, Australia, 2009.
[52] E. Chiodo and D. Lauria, "Probabilistic description and prediction of electric peak power demand," *Electrical Systems for Aircraft, Railway and Ship Propulsion (ESARS), 2012*. pp. 1–7, 2012.
[53] ERCOT, "2013 ERCOT Planning Long-Term Hourly Peak Demand and Energy Forecast," 2013.
[54] P. E. McSharry, S. Bouwman, and G. Bloemhof, "Probabilistic Forecasts of the Magnitude and Timing of Peak Electricity Demand," *IEEE Transactions on Power Systems*, vol. 20, no. 2, pp. 1166–1172, May 2005.
[55] C. J. Ziser, Z. Y. Dong, and T. Saha, "Investigation of Weather Dependency and Load Diversity on Queensland Electricity Demand," in *Australasian Universities Power Engineering Conference*, 2005, pp. 25–28.
[56] Y. Yu and L. Zhang, "An empirical study on seasonal fluctuations in electricity demand in China," *Journal of Renewable and Sustainable Energy*, vol. 4, no. 3, p. 031803, 2012.
[57] H. Ren and W. Gao, "A MILP model for integrated plan and evaluation of distributed energy systems," *Applied Energy*, vol. 87, no. 3, pp. 1001–1014, 2010.
[58] W. Saman and E. Halawa, "NATHERS - Peak Load Performance Module Research," Canberra, Australia, 2009.
[59] DECC, "Estimated impacts of energy and climate change policies on energy prices and bills," London, England, 2013.
[60] J. Faith, "Regional variations in energy prices revealed," *YourMoney.com*, 2013. .
[61] R. Mena, M. Hennebel, Y.-F. Li, C. Ruiz, and E. Zio, "A Risk-Based Simulation and Multi-Objective Optimization Framework for the Integration of Distributed Renewable Generation and Storage," *submitted to Renew. and Sustain. Energy Rev.*, pp. 1–33, 2013.
[62] H. Falaghi, C. Singh, M.-R. Haghifam, and M. Ramezani, "DG integrated multistage distribution system expansion planning," *International Journal of Electrical Power & Energy Systems*, vol. 33, no. 8, pp. 1489–1497, Oct. 2011.
[63] Smartgrid.gouv, "Critical Peak Pricing Lowers Peak Demands and Electric Bills in South Dakota and Minnesota," 2013. [Online]. Available: http://www.smartgrid.gov/case_study/news/critical_peak_pricing_lowers_peak_demands_and_electric_bills_south_dakota_and_minnesota. [Accessed: 29-Nov-2013].
[64] K. Herter, P. McAuliffe, and A. Rosenfeld, "An exploratory analysis of California residential customer response to critical peak pricing of electricity," *Energy*, vol. 32, no. 1, pp. 25–34, Jan. 2007.
[65] A. Bego, L. Li, and Z. Sun, "Identification of reservation capacity in critical peak pricing electricity demand response program for sustainable manufacturing systems," *International Journal of Energy Research*, p. n/a–n/a, 2013.
[66] Y. G. Hegazy, M. M. A. Salama, and A. Y. Chikhani, "Adequacy assessment of distributed generation systems using Monte Carlo simulation," *IEEE Trans. on Power Syst.*, vol. 18, no. 1, pp. 48–52, 2003.
[67] N. Chaudhry and L. Hughes, "Forecasting the reliability of wind-energy systems: A new approach using the RL technique," *Applied Energy*, vol. 96, pp. 422–430, Aug. 2012.
[68] P. Zhang, W. Li, S. Li, Y. Wang, and W. Xiao, "Reliability assessment of photovoltaic power systems: Review of current status and future perspectives," *Applied Energy*, vol. 104, pp. 822–833, Apr. 2013.

[69] P. J. Luickx, P. S. Pérez, J. Driesen, and W. D. D'haeseleer, "Imbalance Tariff Systems In European Countries And The Cost Effect Of Wind Power," no. March. pp. 1–23, 2009.
[70] P. Pinson, C. Chevallier, and G. N. Kariniotakis, "Trading Wind Generation From Short-Term Probabilistic Forecasts of Wind Power," *IEEE Transactions on Power Systems*, pp. 1–9, 2007.
[71] J. Usaola, O. Ravelo, G. González, F. Soto, M. C. Dávila, and B. Díaz-Guerra, "Benefits for Wind Energy in Electricity Markets from Using Short Term Wind Power Prediction Tools - a Simulation Study," *Wind Engineering*, vol. 28, no. 1, pp. 119–127, Jan. 2004.
[72] H.-M. Kim, Y. Lim, and T. Kinoshita, "An Intelligent Multiagent System for Autonomous Microgrid Operation," *Energies*, vol. 5, no. 12, pp. 3347–3362, Sep. 2012.
[73] R. C. Garcia, J. Contreras, M. Van Akkeren, and J. B. C. Garcia, "A GARCH Forecasting Model to Predict Day-Ahead Electricity Prices," *IEEE Transactions on Power Systems*, vol. 20, no. 2, pp. 867–874, 2005.
[74] M. Cococcioni, E. D'Andrea, and B. Lazzerini, "24-hour-ahead forecasting of energy production in solar PV systems," in *Intelligent Systems Design and Applications (ISDA), 2011 11th International Conference on*, 2011, pp. 1276–1281.
[75] IBM, "IBM ILOG CPLEX Optimization Studio, CPLEX User's Manual," 2011.
[76] Z. Zhi, C. Wai Kin, and C. Joe H, "Agent-based simulation of electricity markets : a survey of tools," *Artificial Intelligence Review*, vol. 28, pp. 305–342, 2009.
[77] G. M. J. Herbert, S. Iniyan, and R. Goic, "Performance , reliability and failure analysis of wind farm in a developing country," *Renew. Energ.*, vol. 35, no. 12, pp. 2739–2751, 2010.
[78] R. Karki and R. Billinton, "Reliability/cost implications of PV and wind energy utilization in small isolated power systems," *IEEE Trans. on Energy Convers.*, vol. 16, no. 4, pp. 368–373, 2001.
[79] E. Zio, *The Monte Carlo Simulation Method for System Reliability and Risk Analysis*. Springer, 2013.